

LIBRARY
COPY

TURBULENT FLOW OF PSEUDOPLASTIC FLUIDS
IN STRAIGHT, CYLINDRICAL TUBES

by

Robert G. Shaver

S.B., M.I.T. (1952)

S.M., M.I.T. (1953)

Submitted in Partial Fulfillment
of the Requirements for the
Degree of Doctor of Science

at the

MASSACHUSETTS INSTITUTE OF TECHNOLOGY

September 1957

Signature of Author:

Department of Chemical Engineering,
September 30, 1957

Certified by:

.....
Thesis Supervisor

Accepted by:

.....
Chairman, Departmental Committee on
Graduate Theses

31 Upland Road
West Concord, Massachusetts

September 30, 1957

Mr. L. F. Hamilton
Secretary of the Faculty
Massachusetts Institute of Technology
Cambridge, Massachusetts

Dear Sir:

The thesis entitled "Turbulent Flow of Pseudoplastic
Fluids in Straight Cylindrical Tubes" is hereby submitted in partial
fulfillment of the requirements for the Degree of Doctor of Science.

Respectfully submitted,

Robert G. Shaver

Acknowledgments

The author wishes to express his gratitude to Professor E. W. Merrill for his inspiration and guidance, to Professor T. K. Sherwood for his advice on fluid-flow, to Mr. Donald Brookfield for the use of viscometric apparatus, to Professor J. Kaye for his advice on impact probes, and to Messrs. H. H. Carter, Henry Chasen, Schuyler Holbrook, and Al Merrill for their aid in equipping the experimental work. Also, the financial aid by the Esso Research and Engineering Corporation and by the Humble Oil and Refining Company was greatly appreciated.

ABSTRACT

TURBULENT FLOW OF PSEUDOPLASTIC FLUIDS IN STRAIGHT CYLINDRICAL TUBES

Robert G. Shaver

Submitted to the Department of Chemical Engineering on September 30, 1957 in partial fulfillment of the requirements for the degree of Doctor of Science.

This work dealt with the fluid dynamics, particularly in the turbulent region, of pseudoplastic fluids; that is, fluids whose viscosity decreases reversibly with increasing shear rate, which have no "yield value", and which undergo no time-dependent change in consistency. These were dilute solutions of free-draining, non-associating, linear polymers -- sodium carboxymethylcellulose, ammonium alginate, polyisobutylene, carboxypolymethylene. The rheological properties of these solutions (the relations between shear stress, τ , and shear rate, du/dy , were determined with the Merrill-Brookfield coaxial-cylinder viscometer and with a modified Brookfield Syncoelectric viscometer (for low shear rates). The rheology was then expressed mathematically by fitting to the power-law model: $\tau = b(du/dy)^s$, where s expresses the degree of pseudoplasticity.

These fluids were then run in laminar, transition and turbulent flow in a pipeline flow apparatus, designed to permit measurement of dynamic pressure drop and also impact pressure by radial traverse. Dimensional analysis and laminar calculations had led to the expectation of friction factors and velocity profiles being some function of the exponent, s , and the dimensionless group, $(D^s v^{2-s} \rho / b) \cdot 8 [2(3-1/s)]^{-s}$, which was called the pseudoplastic Reynolds Number. Previous work showed that in laminar flow the data follow the conventional expression for the Fanning friction factor: $f = 16/N_{Re}$, using the pseudoplastic N_{Re} defined above.

The experimental studies on the particular pseudoplastic fluids described in this thesis have shown that: (1) velocity profiles for laminar flow follow closely the theoretically anticipated relation, $u/u_{max} = 1 - (1-y/R)^{1+1/s}$; (2) for conditions of turbulent flow the relation of the Fanning friction factor, f , to Reynolds Number, N_{Re} , for hydrodynamically smooth tubes is not expressible by a single curve, as in the case of Newtonian fluids in turbulent flow, but instead is given by a family of curves, such that at any value of the pseudoplastic Reynolds Number, the value of f is lower, the greater the degree of pseudoplasticity (the lower the value of s); (3) velocity profiles in pseudoplastic turbulent flow do not follow the classic generalized turbulent profiles for Newtonians, but rather are progressively less

blunt as pseudoplasticity is increased. The turbulent friction factor data has been empirically generalized by the expression: $f = 0.079/(s^5 \cdot N_{Re}^\gamma)$ where $\gamma = 2.63/(10.5)^s$.

Photographic studies using dye injection at the tube wall and at the tube center showed that turbulent pseudoplastic flow has the following characteristics compared to the Newtonian case: (1) poor overall radial mixing, (2) thicker non-turbulent layer at the wall, and (3) decreased formation of horseshoe vortices at the wall.

The proposed mechanistic hypothesis to explain the foregoing phenomena was, briefly, a decreasing frequency of vortex formation in turbulent flow as pseudoplasticity is increased, due to an increasingly steep radial gradient of viscosity -- the latter due to the rheological peculiarity of pseudoplastics as described by the viscometric studies.

Thesis Supervisor: Edward W. Merrill
Title: Assistant Professor
of Chemical Engineering.

CONTENTS

I.	SUMMARY	1
II.	INTRODUCTION	8
III.	PROCEDURE	38
IV.	RESULTS.	43
	A. Rheological Curves	43
	B. Pipe-line Flow	44
V.	DISCUSSION OF RESULTS.	52
	A. Rheological Curves	52
	B. Pipe-line Flow	56
VI.	CONCLUSIONS.	79
VII.	RECOMMENDATIONS.	80
VIII.	APPENDIX	81
	A. Supplementary Details.	82
	1. Discussion of Change of Degree of Pseudo- plasticity with Shear Rate.	82
	2. Merrill-Brookfield Viscometer Details . . .	88
	3. Low Shear Rate Viscometer Details	89
	4. Details of Moyno Pumps.	90
	5. Details of Traversing Impact Probe.	91
	B. Sample Calculations	92
	C. Summary of Data and Calculated Values.	96
	D. Location of Original Data145
	E. Nomenclature.146
	F. Literature Citations.147

FIGURES AND GRAPHS

Figure 1.	Typical Rheological Curves	8
	2. Influence of Velocity Gradient on Coiled Molecule.11
	3. Slug of Fluid Flowing in a Tube.19
	4. Pipeline Flow Apparatus.38
	5. High Shear Range Rheology of Aqueous Sodium Carboxymethylcellulose, CMC-70, 72°F43
	6. High Shear Range Rheology of Aqueous Ammonium Alginate, 71°F.43
	7. High Shear Range Rheology of Aqueous Sodium Carboxymethylcellulose, CMC-70S, 75° F.43
	8. High Shear Range Rheology of Aqueous Carbopol 934, 72°F43
	9. Effect of Shear on the Rheology of 0.52% Vistanex.43
	10. Low Shear Rate Rheology, CMC-70, 72°F.43
	11. Low Shear Rate Rheology, Ammonium Alginate 71°F.43
	12. Low Shear Rate Rheology, Carbopol, CMC-70S & Vistanex.43
	13. Friction Factors for Pseudoplastic Liquids45
	14. Pseudoplastic Friction Factors in Laminar Flow45
	15. Friction Factors, Newtonian & $s = 0.95$45
	16. Friction Factors, $s = 0.85, 0.84, 0.83$45
	17. Friction Factors, $s = 0.82, 0.78, 0.74$45
	18. Friction Factors, $s = 0.73, 0.71, 0.70$45
	19. Friction Factors, $s = 0.66, 0.64, 0.62$45
	20. Friction Factors, $s = 0.61, 0.60, 0.59$45
	21. Friction Factors, $s = 0.57, 0.54, 0.53$45
	22. Effect of Tube on Transition45
	23. Laminar Velocity Profiles, CMC-70, $s = 0.53$ & 0.5446
	24. Laminar Velocity Profiles, $s = 0.59, 0.60$46
	25. Laminar Velocity Profiles, $s = 0.74, 0.95$46
	26. Newtonian Velocity Deficiency Curve.46
	27. Pseudoplastic ($s = 0.85$) Velocity Deficiency46
	28. Pseudoplastic ($s = 0.75$) Velocity Deficiency46
	29. Pseudoplastic ($s = 0.65$) Velocity Deficiency46
	30. Pseudoplastic ($s = 0.60$) Velocity Deficiency46
	31. Pseudoplastic ($s = 0.54$) Velocity Deficiency46
	32. Logarithmic Distribution of Deficiencies46
	33. Mixing Lengths, Newtonian and $s = 0.85$46
	34. Mixing Lengths, $s = 0.75$ and 0.6546
	35. Mixing Lengths, $s = 0.60$ and 0.5446
	36. Comparison of Newtonian and Pseudoplastic Eddy Viscosities at Constant N_{Re} Based on48
	37. Comparison of Newtonian and Pseudoplastic Eddy Viscosities at Constant N_{Re} Based on du/dr48
	38. Laminar Flow, Dye Injection at Tube Center49
	39. Laminar Flow, Dye Injection at Tube Wall49
	40. Newtonian Turbulent Flow, Dye Injection at Tube Center.49
	41. Pseudoplastic Turbulent Flow, Dye Injection at Tube Center.49

Figure 42. Pseudoplastic Turbulent Flow, Higher N_{Re} , Dye In-	
jection at Tube Center.	49
43. Newtonian Turbulent Flow, Dye Injection at Tube Wall.	49
44. Pseudoplastic Turbulent Flow, Dye Injection at Tube	
Wall.	49
45. Correlation of Pseudoplastic Friction Factors in Tur-	
bulent Flow	58
46. Composite Diagram of Turbulent Velocity Deficiencies.	65
47. Conversion of Laminar to Turbulent Profiles	77
48. Molecular Structures of Ammonium Alginate and CMC	84
49. Merrill Viscometer Head	88
50. Merrill Viscometer System	88
51. Rotor and Stator of Low Shear Rate Viscometer	89
52. 6M4 Moyno Pump Curves	90
53. 3L2 Moyno Pump Curve.	90
54. Details of Traversing Impact Probe.	91

TABLES

Table 1. Mixing Length Constants (k).47.

Table 2. Summary of Differences in Pseudoplasticity between Low
and High Shear Rate Ranges53.

I. SUMMARY

This work dealt with the dynamics of pseudoplastic fluids as determined by (1) viscometric studies and (2) pipe-line flow studies, with particular emphasis on the turbulent flow regime. This type of fluid is defined as one whose viscosity decreases reversibly with shear rate, which has no "yield value", and which undergoes no time-dependent change in consistency. In general, dilute solutions of free-draining, non-associating polymers and also bulk polymer melts fall into this category.

Fluids Used in Experimentation. The fluids used in this experimentation were dilute aqueous solutions of sodium carboxymethylcellulose, ammonium alginate, carboxypolymethylene, and polyvinyl alcohol, and dilute cyclohexane solutions of polyisobutylene.

Determination of Rheological Curves. Due to the variation in the viscosities of these fluids with shear rate, it was necessary to determine their rheological (shear stress - shear rate) curves over a very large range in order to include any region of behavior that could reasonably be expected to be of importance in the subsequent pipeline flow experiments. This was done with the Merrill-Brookfield coaxial-cylinder viscometer (28, 30) to 20,000 reciprocal seconds of shear rate. A Brookfield Synchroelectric viscometer modified with a coaxial-cylinder rotor and stator was used for accurate determinations in the low shear rate range (0.1 to 42 sec.⁻¹). The rheology thus determined was expressed

mathematically by fitting to it the power-law model: $\tau = b(du/dy)^s$, where τ = shear stress and du/dy = shear rate. Obviously, s expresses the degree of curvature of the mathematical curve, and since this curvature is an indication of the departure from Newtonian behavior, the exponent, s , is a measure of the pseudoplasticity of a fluid in question.

Power-law Expressions. Since the shear stress distribution in a tube flowing in laminar flow is known explicitly, the flow equations for pseudoplastics in laminar flow can be derived by assuming the power-law rheology. The resultant expressions are:

$$\text{friction factor: } f = [16b/(D^s v^{2-s} \rho)] \cdot [2(3+1/s)]^s / 8 \quad (20)$$

$$\text{Poiseuille's law: } Q = (\Delta p / 2Lb)^{1/s} \cdot \pi / (3+1/s) \cdot R^{3+1/s} \quad (17)$$

$$\text{Velocity distribution: } u/u_{\max} = 1 - (1-y/R)^{1/s+1} \quad (15)$$

Examination of equation 20 showed it to be analogous to the Newtonian expression:

$$f = 16/N_{Re} \quad (21)$$

if the Reynolds Number was defined as $(D^s v^{2-s} \rho / b) \cdot 8 [2(3+1/s)]^{-s}$.

This was called the pseudoplastic Reynolds Number. Previous work (13, 31, 33) had shown that the above expressions for the Fanning friction factor and Poiseuille's law were followed with a high degree of precision in laminar flow by experimental data. However such data in turbulent flow were meager and open to question, so the flow relations for pseudoplastics in turbulent flow were essentially unknown, previous to this work.

Pipeline Flow Experimentation. The pipeline flow experimentation in this work was carried out in a recirculating system that could be fitted with smooth-bore test sections varying in diameter from 3/8 inch ID to 3/4 inch ID. These test sections were fitted so that frictional pressure drop could be measured at various locations along the tubes and so that impact pressure could be measured as a function of radial position. This system was pumped by either of two Moyno pumps in parallel which provided essentially pulse-free, positive-displacement pumping up to 40 GPM.

In laminar flow the results obtained with this system and with the independent viscometric studies confirmed the foregoing Fanning friction factor and Poiseuille's law expressions, and in addition confirmed the laminar velocity distribution expression.

Turbulent Flow Results. In turbulent flow, the friction factor-Reynolds Number relationship was found to consist of a series of curves differing from each other in the value of the rheological exponent, s , (see Figure 13) if the pseudoplastic Reynolds Number as defined above was used. It is interesting to note that increasing the degree of pseudoplasticity (decreasing s) results in lowering the friction factor in turbulent flow at a given Reynolds Number.

Figure 32 contains the velocity profile data collected in turbulent flow, expressed as velocity deficiencies and collected on one plot. In Newtonian turbulent flow, it has been found (5) that this type of correlation brings together the profiles for all conditions of Reynolds Number and tube roughness onto a single curve. However, it can be seen

that this correlation did not bring the pseudoplastic turbulent velocity profiles onto a single curve, but rather presented a series of curves, again depending on the value of s . In addition it can be seen that there is a region in the vicinity of the center of the tube in which all the curves coincide, but this region gets progressively smaller as pseudoplasticity is increased. In general it can be said that, at a given Reynolds Number in turbulent flow in a smooth tube, a pseudoplastic fluid will have a lower friction factor and a less blunt velocity profile than a Newtonian fluid.

In addition it was found that the "mixing length" distribution curves calculated from the velocity profiles did not coincide with the classical curves obtained with Newtonian fluids, but also deviated systematically with the value of s .

In view of the apparent dependence of turbulent flow behavior upon the Reynolds Number and the rheological exponent, s , the following empirical expression was proposed to generalize the friction factor data in turbulent flow:

$$f = 0.079 / (s^5 \cdot N_{Re}^\delta) \quad (39)$$

where:

$$\delta = 2.63 / (10.5)^s \quad (40)$$

In Figure 45 it can be seen that this expression correlated the experimental data with behaviors from Newtonian to a pseudoplasticity of $s = 0.53$ with a precision of about $\pm 12\%$. This correlation cannot be used with fluids having an s value less than about 0.4, since the pre-

dicted friction factor would then be less than in laminar flow, but possibly true pseudoplastic fluids with an s value lower than 0.4 may not exist. The author has not worked with any nor have any been reported in the literature that are unmistakably true pseudoplastic solutions. It is possible to attribute a very low s value to a fluid with a yield value, but this is a plastic and not a pseudoplastic fluid. It has been the experience of the author that the polymers that were used to make pseudoplastic solutions will make plastic suspensions at higher concentrations, and using higher concentrations is the common method of decreasing the value of s . It is felt by the author that if pseudoplastics exist with s values less than 0.4, the observed trend suggests that the turbulent flow characteristics of such fluids would closely resemble laminar flow conditions -- at least to 100,000 Reynolds Number.

Dye Injection. Photographic studies using injection of dyed fluid at (1) the tube wall through a wall tap and (2) the center of the tube through a hypodermic tubing probe are shown in Figures 38 to 44. A 40 microsecond exposure was obtained by strobe flash. Examination of the photos of injection at the center show that the effect of turbulence on the fluid in the core of the flow is much different in the pseudoplastic than in the Newtonian case. That is, the Newtonian turbulence produced complete mixing of the dye stream across the diameter of the tube, but the pseudoplastic turbulence had merely distorted the dye stream in a gross fashion. Examination of the wall injection photos showed the formation of turbulent eddies at the wall as "horseshoe vortices",

which have been reported elsewhere for Newtonian flow (55). The following characteristics of turbulent flow of pseudoplastics can be seen, relative to Newtonian behavior: (1) poor overall radial mixing, (2) thicker non-turbulent layer at the wall, and (3) decreased formation of the horseshoe vortices at the wall.

Mechanistic Hypothesis. Experiments reported by Richardson (44) have shown that stable laminar flow velocity profiles can be converted to profiles that are identical with the logarithmic type of turbulent flow simply by superimposing a periodic oscillation on the flow. The explanation proposed by Richardson involves an "alternating" form of flow in which most of the flow occurs near the wall of the tube -- a hydrodynamic analogy to the "skin effect" in alternating electric current. The turbulent profile would be therefore the time-average of the laminar profile and the superimposed alternating profile. It was proposed in this study that the explanation for the decreased friction factors and less blunt profiles in natural turbulent flow of pseudoplastic fluids lies in a decreased natural frequency of occurrence of the "alternating" form of flow with pseudoplastic fluids. In turn this decreased frequency of alternation can be explained as due to the extraordinary damping effect upon any random eddy of the radial gradient of viscosity present in a tube flowing with a pseudoplastic fluid in unstable laminar flow. That is, because of the decrease of viscosity with increase in shear stress with pseudoplastics, there would be a condition of minimum viscosity at the wall of a tube and maximum viscosity at its center, where the shear stress is zero. Since the tur-

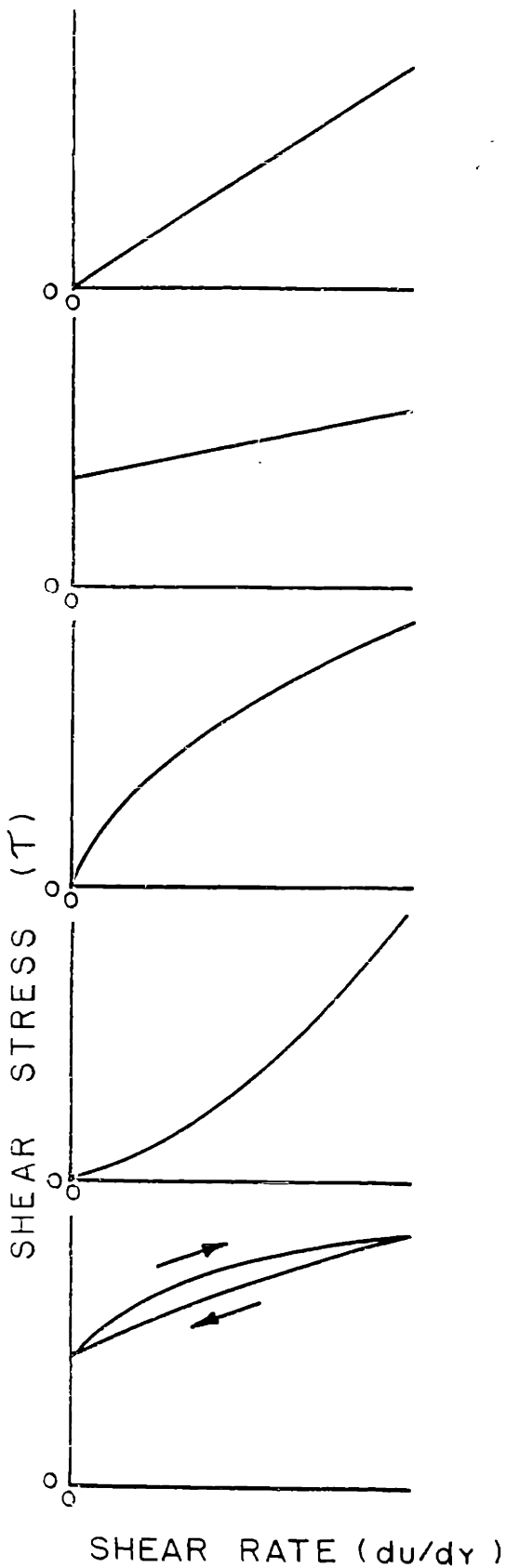
bulent vortex in forming at the wall and travelling inward toward the center of the tube would be encountering a positive gradient of viscosity, it is to be expected that an additional damping tendency on such a vortex would exist beyond that for the Newtonian case. This would result in decreased frequency of formation of vortices (comparable to decreased frequency of alternation in the Richardson theory) which would lead in turn to decreased friction factors and less blunt velocity distribution. Thus the variation of turbulent flow characteristics with the degree of pseudoplasticity, s , follows, because the radial gradient of viscosity would be a function of the value of s .

I. INTRODUCTION

Pseudoplasticity. The term "pseudoplastic" is used herein to denote those fluids whose viscosity (the ratio of shear force to shear rate) decreases reversibly with increasing shear rate and which have no yield value or time dependency. The term "thixotropic" is sometimes used to denote these fluids (19), but it is felt that "pseudoplastic" is the more explicit term since it excludes yield values and time dependency, which thixotropy can include. See Figure 1 for typical shear stress - shear rate curves of Newtonian and various non-Newtonian fluids, together with the appropriate terminology.

Pseudoplasticity is found chiefly in most polymer solutions and in bulk polymer melts. Industrially, it is encountered in certain crude oils, liquids thickened with natural or synthetic resins or gums, and in high-polymer melts.

The Conceptual Difficulty. When one is considering Newtonian fluids -- that is, those fluids whose shear stress - shear rate ratio is constant, except chiefly for the variables of temperature and pressure -- one can speak of a parameter, viscosity, which possesses a high degree of constancy, or order, and hence is an extremely valuable parameter in scientific and engineering work. Indeed, in the case of liquids in the range of pressures ordinarily of interest, the pressure coefficient of viscosity is negligible. But, when viscosity is variable with shear rate, the most pressing problem is to decide what characterizing factors



NEWTONIAN

$\tau = \mu (du/dy)$, WHERE μ IS VISCOSITY

BINGHAM PLASTIC

$\tau - \tau_0 = B (du/dy)$,

WHERE τ_0 IS THE YIELD VALUE AND B IS AN EXPERIMENTAL COEFFICIENT

PSEUDOPLASTIC

DILATANT

TIME-DEPENDENT
(OFTEN CALLED "THIXOTROPIC")

FIGURE I
TYPICAL RHEOLOGICAL
CURVES

should be substituted for the Newtonian viscosity, μ , in for instance the Reynolds Number, $DV\rho/\mu$. There is a corresponding loss of physical significance in both the term "viscosity" and the expressions containing it. It was therefore a prime purpose of this work to attempt to generalize the characteristics of pseudoplastic fluid flow to the greatest possible extent in order to gain a valid physical concept of the processes by which the flow phenomena of pseudoplastic fluids take place. Theories on the cause of the pseudoplastic rheological phenomenon (decreasing viscosity with increasing shear) are presented in the subsequent sections.

Theories of Pseudoplasticity. It seems to be a good generalization to say that to have pseudoplastic behavior there must be present, in the fluid, bodies of extraordinary anisometry and of considerable flexibility. Those fluids having anisometric bodies of considerable rigidity are generally Bingham plastics such as clay or pulp suspensions. The types of substances which seem to best fit into the category for pseudoplastics are high molecular weight polymers of the linear or branched-chain type in roughly the colloidal range of dimensions. When dissolved, these large molecules, dissociated from each other to a greater or lesser degree, are free to flex or rotate as circumstances dictate.

A number of theories with varying sophistication attempt to explain the pseudoplastic type of behavior on the basis of either mechanics or energy considerations.

One of the simplest and most appealing theories is exemplified by

that of Lewis, Squires and Broughton (24). The long molecules, randomly oriented in the fluid at rest, are aligned in the direction of flow by the viscous forces of shear and disrupted from this alignment by the randomizing influence of thermal agitation. The balance between these two effects results in progressively greater alignment with increasing shear, and progressively lower viscosity because of the progressively less tumbling of the long molecules across successive layers of flow. This effect has been evaluated quantitatively by Staudinger (53) by considering the long molecules as tumbling long rods whose effective volume is proportional to the volume swept out by the rod rotating about its center point, this effective volume corresponding to the volume term of the Einstein equation of viscosity.

Molecular Coil with Hydrodynamic Interaction. In this theory, the long-chain molecules are envisioned as forming loose coils in solution, hence sometimes called the "necklace model" (41). The solvent in which these molecules are dispersed is then able to pass freely through the polymer coil. Under a velocity gradient the coil would be caused to rotate by the effect of viscous forces. As seen in the accompanying diagram (Figure 2) the coil would be compressed and extended along axes at right angles to each other, and, because of the rotation, the compression and extension zones would move around the circumference of the coil.

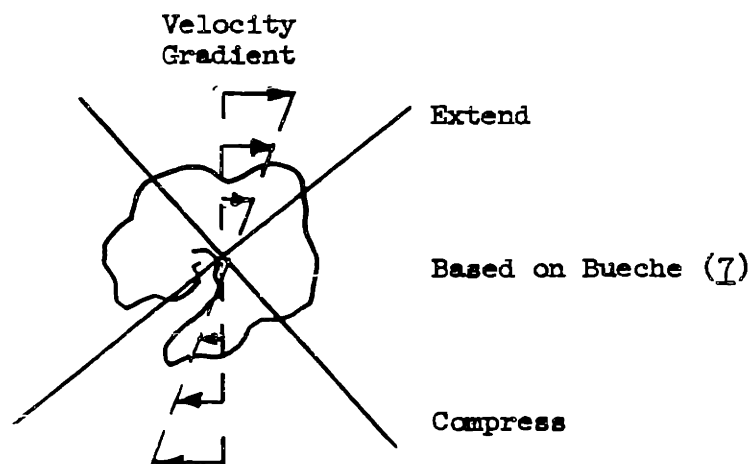


Figure 2: Influence of Velocity Gradient on Coiled Molecule.

This would cause any given segment of the coil to be exposed to a periodically varying force, so that the coil would then resemble a tank tread in motion.

As Bueche (9) points out, if the polymer coil were completely flexible (no resistance to deformation between its links) the extension and compression of the coil would in itself not lead to pseudo-plasticity. However, most polymers are not completely flexible. Owing to bond angles, steric effects of side groups, the presence of solvating sheath, and so on, the polymer chain usually acts "somewhat stiff" when exposed to a deforming stress. In other words it does not instantaneously respond to the stress by assuming a new configuration. Consequently the compression and extension of the polymer coil is somewhat out of phase with the shear stress communicated by the solvent and therefore the solvent surges through the coil leading to hydrodynamic friction. The greatest extension and

compression of the polymer coil occurs at the lowest shear rate. As the rate of rotation is increased, the time of rotation becomes comparable with, and then exceeds, the relaxation time of the polymer coil. In other words the polymer coil can respond less and less effectively to the shear stress by extension and compression as the shear rate increases. Therefore, there is less viscous loss owing to the surge of solvent through the coil. This would account, in theory, for the decrease of viscosity with increasing shear rate.

Consideration of this mechanism led to the following type of expression (41) for the dependence of viscosity upon shear rate:

$$\mu = (\mu)_0 \left[1 - B(\dot{\gamma})^n + \dots \right] \quad (1)$$

where $(\mu)_0$ is the viscosity at zero shear rate, B is a positive constant, and n is a constant power. Due to limited accuracy of the data used and various other difficulties, there is some disagreement on the power to use in this expression -- Bueche (9) uses a power of 1/2 whereas others use powers of 1 or 2 (41). However, Bueche formulates his expression with shear stress instead of shear rate.

The confusion regarding the mathematical details of this type of expression make its use of doubtful value in the extension of limited rheological data, for example, but the mechanistic picture behind it seems to be a very fruitful one in terms of visualizing the mechanism of pseudoplasticity, quantitatively at least.

Goodeve Theory. Goodeve (19) explains the pseudoplastic decrease in viscosity by means of an "impulse theory". He conceives of a "scaffolding" structure within the solution and of interference occurring when particles touch one another. When they touch, they stick together and shearing the system distorts the resultant links until they are broken. The resultant impulse is the mechanism for the transfer of momentum, and obviously the amount of momentum transferred will depend on the length of time the force has been applied -- that is, the life of the link. The strength of such a link is independent of shear rate, but the rate of link breakages (rate of impulses) is proportional to the shear rate.

However, there is also the possibility of reduction of particle size with shear -- an effect which would reduce the total force transmitted.

In the case of pseudoplastics, the net result of the multiplication of the impulse rate by the average impulse, taking into account any breakdown in particle size, must be a less than proportional increase in the shear force with shear rate. This can be visualized as a disentanglement of long molecules by the shearing action. Thus the chief difference between Newtonian and non-Newtonian fluids is attributed to shear influencing the average life of a link in the latter case.

The Goodeve theory gives mathematical results that will describe the rheology of molecules which associate (by hydrogen bonding) in

solution. It does not give an accurate representation for molecules like polystyrene, polyisobutylene, and the polyelectrolytes which do not associate.

Absolute Reaction Rates. An interesting treatment of liquid viscosity in general is that involving the theory of absolute reaction rates, as proposed by Eyring (18). It involves the conception of a liquid as matter made up of molecules bound together and of holes moving about through this system. Since flow of a liquid is a rate process, the concept of absolute reaction rates should apply.

In the process of flow, a molecule will move from one equilibrium position to another if there is a hole for it to move into. The production of such a "hole" requires the expenditure of energy in pushing back surrounding molecules. Hence the movement of a molecule from one equilibrium position to another can be thought of as movement through a potential energy barrier, since any intermediate position would possess more free energy than either equilibrium position. In a static liquid this potential energy barrier is a symmetrical one, and there would be no greater tendency for a random molecule to move in one direction than in another. However, if flow were imposed on the system the potential energy barrier would be so distorted as to produce a lower free energy state in a site farther downstream. In all cases, however, there would be involved an energy of activation in going through the potential energy barrier. This sort of consideration leads to a viscosity - temperature relationship of the sort:

$$\mu = B e^{E/kT} \quad (2)$$

where B and k are constants, E is an energy term and T is absolute temperature. This fits the known experimental facts well.

Also developed from this line of reasoning is the following general relationship between viscosity and shearing force:

$$\mu = (\lambda_1 f) / [2 \lambda K \sinh (f \lambda_2 \lambda_3 \lambda / 2kT)] \quad (3)$$

in which the lambdas are distances involved in the molecular movement and f is the shear force.

In the case of ordinary viscous Newtonian flow at shear forces of the order of 1 dyne per sq. cm. or less, the term $2 kT$ is much greater than the term $f \lambda_2 \lambda_3 \lambda$. making possible the simplification:

$$\mu = (\lambda_1 kT) / (\lambda_2 \lambda_3 \lambda^2 K) \quad (4)$$

in which there is no dependence of viscosity on shear force.

However, in the case of non-Newtonian fluids, the value of f is very large due to the relative rigidity of the system and so $f \lambda_2 \lambda_3 \lambda$ is approximately equal to, or greater than, $2kT$. This leads to an expression of the form:

$$\mu = A f \cdot e^{(a-bf)/T} \quad (5)$$

in which A, a and b are constants. This expression now predicts that the viscosity is a function of shear force, as is required by

non-Newtonian fluids. Also this expression predicts that the viscosity should decrease with increasing shear force. Limited experimental evidence with solutions of milled rubber, polystyrene and polyisobutylene tends to confirm this expression (18, 43, 48).

Since the rheological equation based on the above development:

$$\text{shear rate} = (\lambda/\lambda_1) 2k^n \sinh a_n f_n \quad (6)$$

is quite complex and has the additional disadvantage of having no term with the dimensions of viscosity, it is felt that the application of it to engineering correlations would be too cumbersome to yield much information.

Power Model of Rheology. Empirically, the shear stress - shear rate curves for pseudoplastics have been found to fit the mathematical model:

$$\tau = b (du/dy)^s \quad (7)$$

over large ranges to very good precision (2, 3, 6, 11, 13, 15, 31, 33, 34, 35, 60). In form it is strictly analogous to the Newtonian equation:

$$\tau = \mu (du/dy) \quad (8)$$

and reduces to it when s is unity. For the pseudoplastic type of fluid, s would be expected to lie in the range from one to zero in order to effect a decrease in consistency with increase in shear rate.

This has been experimentally verified (2, 6, 11, 13, 15, 33, 34, 35). However, in the range of s values greater than one, the consistency would increase with increasing shear rate -- a type of behavior that is called dilatant. This is completely different phenomenon and is not included in the present investigation.

One very convenient feature of this empirical expression is the dimensionless exponent, s , which sets mathematically the curvature of the shear stress - shear rate curve. Since the curvature of the curve is a measure of the degree of pseudoplastic behavior (Newtonian is straight, highly pseudoplastic is highly curved), s is then a measure of the degree of pseudoplasticity in dimensionless form. As s decreases from unity, one would expect pseudoplastic behavior to increase.

Criticism has been directed at this type of expression on several accounts (20): that it is empirical; that there is no parameter in it with the dimensions of viscosity when s is different from unity, and that it gives no mechanical picture of the cause of pseudoplasticity. It is felt by the author that the lack of a parameter with the dimensions of viscosity may be a blessing in disguise, since the term "viscosity" implies a degree of order (constancy) that is not present with pseudoplastic fluids. Therefore, there is some justification for the power model from the negative point of not introducing a viscosity term that could be misinterpreted by casual treatment.

Even though the power model gives no picture of the mechanics of pseudoplastic behavior, this is only an academic disadvantage at the present state of the art since all expressions, theoretical or not, presently require rheological studies to determine the factors involved. None can use strictly non-rheological data (e.g. molecular weight, refractive index) to predict a rheological curve that is useful even for engineering purposes. Thus the theoretical expressions suffer the same disadvantage as the empirical ones -- need for explicit rheological data -- but the resultant simplicity of the empirical power-law expression seems to hold the greatest promise for practical application.

Therefore, the analyses of pseudoplastic fluid-flow behavior carried out in this work were based on the power model of rheology.

Dimensional Analysis. Since there is no parameter in the power model of rheology with the dimensions of viscosity, it is not immediately obvious what expression should be used, for instance, in the place of the Reynolds Number in attempting to generalize fluid flow conditions. However, by applying the techniques of dimensional analysis to the case of pipe-line flow and realizing that the same factors would probably affect pseudoplastic flow as Newtonian flow, the conclusion is reached that the dimensionless pressure drop (Fanning friction factor, f) should be some function of the rheological exponent, s , and the dimensionless group, $D^s v^{2-s} \rho / b$. Expressed symbolically:

$$f = f(s, D^s V^{2-s} \rho / b) \quad (9)$$

for any steady mode of flow.

Inspection of the above dimensionless group shows it to be analogous to the Newtonian Reynolds Number, and reduces to it when $s = 1$.

Similarly, when dimension analysis is carried out with respect to the velocity distribution, the following conclusion is reached:

$$u_R = u_R(s, D^s V^{2-s} \rho / b, y/R) \quad (10)$$

where u_R is some reduced local velocity such as u/u_{maximum} , and y/R is the dimensionless distance from the wall. The next step is, therefore, to define these functions explicitly for the laminar case, where the shear stress conditions are known explicitly.

Laminar Pseudoplastic Flow. In the case of laminar flow, the energy dissipation is all by the mechanism of viscous shear and transient eddy effects are not present. Setting up a force balance on a cylindrical plug of fluid flowing concentrically in a tube (see Figure 3) results in:

$$\Delta p \cdot \pi r^2 = \tau \cdot 2\pi r \cdot L \quad (11)$$

which defines the radial shear stress distribution. Bringing

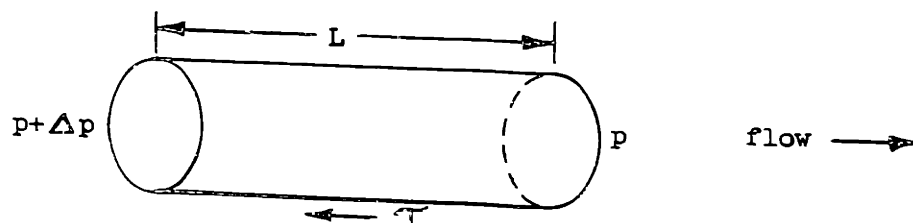


Figure 3: Slug of Fluid Flowing in a Tube

in the rheological power-law model results in:

$$\tau = (\Delta p/2L) \cdot r = b (du/dr)^s \quad (12)$$

Therefore the radial distribution of velocity gradient is:

$$du/dr = (\Delta p/2Lb)^{1/s} \cdot r^{1/s} \quad (13)$$

Integration yields the following velocity distribution:

$$u = (\Delta p/2Lb)^{1/s} \cdot (1 + 1/s)^{-1} \cdot (R^{1/s+1} - r^{1/s+1}) \quad (14)$$

Reduced to dimensionless form it becomes:

$$u/u_{\max} = 1 - (1-y/R)^{1/s+1} \quad (15)$$

Evidently, in laminar flow, the function is dependent on s and y/R and independent of $D^s v^2 - \rho/b$; this is analogous to the Newtonian case in which the laminar velocity distribution is a function of y/R only and independent of Reynolds Number.

Of course, the above velocity distribution reduces to the Newtonian distribution when s is unity, and of interest is the fact that the predicted velocity distribution for a pseudoplastic condition is a higher power than 2 of the radial position, leading to a more blunt profile than in the Newtonian case. For example, if $s = 0.5$, then the profile is a cubic instead of a parabolic one.

Laminar Friction Factors. In order to find the expression for the pressure drop as a function of the average velocity, the following

relates the local velocity with the average velocity:

$$\pi R^2 V = \int_0^R (u \cdot 2\pi r) dr \quad (16)$$

Substituting equation (14) into the above expression and subsequent integration yields:

$$\pi R^2 V = (\Delta p / 2Lb)^{1/s} \cdot \pi / (3+1/s) \cdot R^{3+1/s} \quad (17)$$

which is the pseudoplastic form of Poiseuille's Law, and reduces to the conventional one when $s = 1$. The following expression defines the Fanning friction factor (f):

$$\Delta p / L = f \rho V^2 / R \quad (18)$$

Substituting the above into equation (17) yields:

$$f = (2R)^{-s} (V)^{s-2} (\rho)^{-1} (3+1/s)^s (b)(2)^{s+1} \quad (19)$$

Rearranging:

$$f = \left[16b / (D^s V^{2-s} \rho) \right] \cdot 2^s / s \cdot (3+1/s)^s \quad (20)$$

which is analogous to the Newtonian friction factor curve:

$$f = 16 / N_{Re} \quad (21)$$

if the pseudoplastic Reynolds Number is defined as follows:

$$N_{Re} = (D^s V^{2-s} \rho / b) \cdot 8 \left[2(3+1/s) \right]^{-s} \quad (22)$$

The latter half of the pseudoplastic Reynolds Number, which is a

function of s only, is hereafter called $\phi(s)$ for the sake of simplicity.

Thus:

$$\phi(s) = 8 \left[2(3+1/s) \right]^{-s} \quad (23)$$

Turbulent Pseudoplastic Flow. In the case of laminar flow, explicit expressions for pressure drop and velocity profile as functions of s and a Reynolds Number or radial position were obtained because the flow equation is known explicitly. However, turbulent flow involves transient effects that prohibit rigorous mathematical treatment beyond the stage of setting up differential equations even in the Newtonian case. However the conclusions arrived at by dimensional analysis are still valid in turbulent flow:

$$f = f(s, D^s v^{2-s} \rho / b) \quad (9)$$

$$u_R = u_R(s, D^s v^{2-s} \rho / b, y/R) \quad (10)$$

Since the mathematical treatment of laminar flow has yielded a dimensionless group, $D^s v^{2-s} \rho / b \cdot \phi(s)$, that can easily be called a Reynolds Number in laminar flow, it seems reasonable to continue using this same group in the turbulent regime even though the dimensional analysis does not imply that the same function of s will apply in both flow regimes. Indeed it would be very extraordinary if such were the case, and it was one purpose of this work to find out how friction factors and velocity profiles vary in the turbulent regime with variation in s .

Since the flow conditions derived from the power-law model in

laminar pseudoplastic flow resemble, by analogy, the flow conditions for Newtonian laminar flow, and since the expression for friction factor vs. Reynolds Number and the one for Poiseuille's Law have been experimentally verified (13, 31, 33), it seems that this type of analysis applied to systematic data taken in the turbulent pseudoplastic regime should constitute a good test for the generality of the classical correlations of turbulent flow conditions that have been developed with Newtonian fluids (e.g., the turbulent f vs. N_{Re} curves, "universal" turbulent velocity profiles, velocity deficiencies, and mixing lengths). Therefore, another purpose of this work was to test these classical means of generalizing turbulent flow by systematic experimentation with pressure drops and velocity profiles in the turbulent regime with fluids of a variety of degrees of pseudoplasticity.

Classical Turbulent Flow Correlations. The first empirical mathematical expression for the friction factor, Reynolds Number data for smooth tubes in turbulent flow with Newtonian fluids was proposed by Blasius after collecting all available data (5, 42). This expression was:

$$f = 0.079 / (N_{Re})^{0.25} \quad (24)$$

The data that Blasius used extended to 100,000 Reynolds Number and is still used for smooth tubes in region of 10,000 to 100,000.

Upon the attainment of data to the region of 1,000,000 N_{Re} , Nikuadse proposed the following empirical correlation (5):

$$f = 0.00080 + 0.0552 / (N_{Re})^{0.237} \quad (25)$$

It is to be emphasized that these correlations are empirical and have been arrived at on the basis of data on Newtonian systems.

Universal Velocity Profile. In following the fruitful path of dealing with dimensionless ratios and thus abstracting the physical phenomena from absolute values (dimensional quantities), Prandtl suggested two ratios that have been of great value in Newtonian systems (5):

$$u^+ = u/u_* \quad (26)$$

$$y^+ = yu_*\rho/\mu \quad (27)$$

The former is the dimensionless local velocity involving the concept of "friction velocity", defined as:

$$u_* = \sqrt{\tau_w/\rho} \quad (28)$$

The second expression is a "friction distance Reynolds Number," involving the distance from the wall and the friction velocity. Experiments by Nikuradse show that the velocity profile in the core of turbulent flow in tubes follows the expression (5, 21):

$$u^+ = 5.5 + 5.75 \log y^+ \quad (29)$$

This verifies the semi-logarithmic shape commonly associated with turbulent velocity profiles. At values of y^+ less than about 40, the data deviate from the above expression, and this is generally taken to be the region of the buffer and laminar layers that are hypothesized to be in the vicinity of the wall in turbulent flow.

Velocity Deficiencies. On the basis of data of velocity distribution in turbulent flow, it came to light that the shape of the velocity curve in the core of the flow seemed to be the same for a given condition of shear (e.g. constant wall shear stress) and, with this restriction, independent of the throughput rate, roughness, etc. (5). The effect of roughness seemed to be limited to the region in the vicinity of the wall, affecting the laminar layer thickness, but the gradient remained constant. Von Karman deduced from these observations that a "deficiency velocity", defined as $u_{\max.} - u$, should be a function of the friction velocity, $\sqrt{\tau_w/\rho}$, and of the relative distance, y/R , only. If this were so, then there should be some function:

$$(u_{\max.} - u)/u_* = \text{function}(y/R) \quad (30)$$

This assumption was confirmed by Nikuradze's experimentation which found a unique curve of relative velocity deficiency vs. y/R under variable conditions of roughness and flow (5), with fluids of Newtonian properties.

An interesting feature of this type of correlation is the fact that, calculationally, it does not involve the use of viscosity in any form. Hence the possibility exists that it can be useful in correlating pseudo-plastic turbulent profiles without making any assumption or approximation with regard to the rheology.

Mixing Lengths. Since the local situation in turbulent flow is that of fluctuating velocity components, both radial and axial, it is clear

that radial transport of momentum can be accomplished by a particle of fluid moving from a lamina of a certain momentum level and embedding itself in another lamina of differing momentum level by means of the radial fluctuating velocity component. On the average, the radial velocity is zero in normal tube flow, but the intensity of the fluctuation about this mean clearly influences the degree of energy dissipation and diffusion of mass by the turbulent process. In an attempt to express this quantitatively, Prandtl introduced a length parameter, l , called the "mixing length", which represents the radial distance traveled by a particle moving in a transient fashion before it becomes embedded in another layer and loses its identity (5, 20). Mathematically, it is expressed:

$$l = u' / (du/dy) \quad (31)$$

where u' is the axial velocity component transported by the radial movement and du/dy is the local velocity gradient.

Reasoning that this axial velocity component is of the same order of magnitude as the fluctuating radial velocity component led to the "Prandtl equation":

$$\tau = \rho l^2 (dy/dy)^2 \quad (32)$$

and since shear stress is linearly distributed:

$$l \cdot du/dy = u_* \sqrt{1-y/R} \quad (33)$$

fixing the interdependence of the velocity distribution curve and the

distribution of mixing lengths.

Applying this relation to the data of Nikuradse led to a series of curves of mixing length radial distribution that appeared to approach a limiting curve with increasing Reynolds Number (5) suggesting a concept of "fully developed turbulence" in which there is a constant mixing length distribution. By making the mixing length relative, l/R , the curves were generalized for tubes of varying diameters.

Subsequent reasoning by von Karman (5, 20) led to the conclusion that the ratio of consecutive derivatives of the velocity should be proportional to the mixing length, e.g.:

$$l = k(du/dy)/(d^2u/dy^2) \quad (34)$$

This factor, k , was considered to be a universal constant for fully developed turbulence and to have a value of about 0.4. In the region near the wall of the tube, the values of y and dy nearly coincide. Since the ratio $(du/dy)/(d^2u/dy^2)$ is equivalent to dy , the equation (34) becomes, in the vicinity of the wall:

$$l = ky \quad (35)$$

Thus the value of the constant, k , can be easily determined as the slope at the wall of the radial mixing length distribution curve.

Hence an obvious course to follow in this work was to determine if the constant, k , also had the same value in the turbulent flow of pseudoplastic fluids, and also to see if the whole mixing length dis-

tribution curve for a pseudoplastic case coincided with that for Newtonians.

Prior-Art Correlations with the Power Model. Friction factor data in laminar flow for pseudoplastics have been correlated in different ways by Weltmann (60) and Metzner and Reed (33) using as a basis the power-law expression of rheology. Generality of the correlation was claimed for both laminar and turbulent flow regimes and for non-Newtonian fluids in general, but the meager amount of data available in the turbulent regime and the uncertainty of the rheological character of some of the liquids tested (i.e. whether plastic or pseudoplastic), throw doubt on the accuracy with which the proposed correlations (33, 60) can be extrapolated into the turbulent regime.

Weltmann Correlation. In this correlation, the friction factors were plotted against a Reynolds Number, $DV \rho / \text{viscosity}$, in which the viscosity is an "apparent" viscosity for pseudoplastics determined "at the flow condition that exists in the pipeline". Since there are an infinite number of flow conditions present in a pipeline from wall to axis, it is not at all obvious how this "apparent" viscosity is determined in a consistent and justifiable manner. Nevertheless, the resultant correlation is a series of curves parallel to the Newtonian laminar flow curve which vary with a "structure number", N , which is actually the inverse of the exponent in the power-law model, equation (7).

In this correlation the pseudoplastic turbulent flow friction factor curve is the same one as the Newtonian friction factor curve,

but begins at the point where the appropriate laminar friction factor curve intersects it. This results in an increasing Reynolds Number of transition with increasing pseudoplasticity, a multiplicity of curves in the laminar region, and a single curve in the turbulent region based on a limited amount of data of other workers in the turbulent region (60).

Metzner and Reed Correlation. After exploring the possibilities of correlations by means of apparent viscosities (32), Metzner, together with Reed, (33) concluded that the most fruitful approach was the use of the pseudoplastic Reynolds Number based on the power-law model, $D^s v^{2-s} \rho / b \cdot \phi(s)$. By reworking the data collected from various sources in the literature on not only pseudoplastic but also true plastic fluids, the single curve of:

$$f = 16/N_{Re} \quad (21)$$

in laminar flow was confirmed, the Reynolds Number being substantially the one defined in this thesis (equation 22).

In turbulent flow, the data did not contain any points made with recognizably pseudoplastic fluids (33) and the conclusion was reached, in spite of this, that the end of the laminar region was attained at a friction factor of 0.008 ($N_{Re} = 2000$) and that the transition region extended from 2000 to 70,000 Reynolds Number!

While the confirmation of the laminar flow pseudoplastic correlation based on the power-law model was gratifying, the complete lack of data

on true pseudoplastic fluids in the turbulent regime indicated the desirability of the investigation reported in this thesis.

The Rheological Problem. Since the viscosity of a pseudoplastic fluid varies with shear rate, there is a practical problem involved in arriving at the rheological curve, and the problem becomes increasingly acute with increasing curvature of the curve. This is due to the difficulty in getting a single value of shear rate in the viscometric apparatus under a given set of conditions. For example, in the capillary viscometer, the shear rate varies from zero at the center of the tube to some maximum at the wall, there are end effects and, with certain types, the flow varies with time. All of these factors make the analysis of the data from a capillary viscometer difficult at best and puts a dependence on approximation and the assumption of the rheological form of the fluid being studied (29).

Another common type of viscometer, the coaxial, rotational type exemplified by the Stormer, Couette and MacMichael viscometers (29, 52) have a shearing annulus of substantial width which necessarily involves a variation of shearing rate across the annulus. In addition there is an end effect in that the annulus is not bottomless and there is shear taking place on the bottom surfaces of the rotor and stator. This, too, places a practical difficulty in the way of determining the true rheological curve of a given pseudoplastic fluid. Further, the upper limit of shear rate measurable by these instruments is relatively low because, owing to the wide gap, turbulence is readily established at low rotational speeds.

A third common method of measuring viscosity is with a falling-ball instrument. The terminal velocity of the descending ball is measured and, from this, the dimensions of the apparatus and the densities involved, the viscosity is calculated by the application of Stokes' Law. The difficulty here with respect to non-Newtonian systems is that the shear rate varies within the instrument from zero in the main body of the fluid to some maximum at the surface of the ball.

Unfortunately those types of viscometers in which the problems of variation in shear rate are the most acute, namely the capillary and falling-ball viscometers, are the ones most often used in industrial practice to determine the viscosity of non-Newtonian fluids. In effect what is happening is that a "viscosity" is calculated which, if the fluid were Newtonian, would be the true viscosity, but which actually is some value averaged by some means over a very large and uncontrolled range of shear conditions. Any change in these shear conditions, such as changing an instrumental dimension, would result in the calculation of a different value for the "viscosity" of the fluid. Hence any rheological curve determined by one of these instruments would necessarily vary with the dimensions of the instrument unless some very great liberties were taken in interpreting the, as yet unknown, final form of the rheology.

Modifications of the Classical Coaxial Viscometers. The shortcomings of the classical forms of the coaxial cylinder viscometer when used with pseudoplastic fluids are:

- (1) variation in shear conditions across the annulus due to its finite width,
- (2) end effects due to the necessity of containing the fluid being tested, and
- (3) an upper limit on the range of shear rates possible due to the onset of turbulent flow, usually in the range of 50 to 200 sec.⁻¹ (26).

It is possible to minimize these shortcomings by the simple expedient of minimizing the annular width, with the exception of the end effects. To eliminate this defect, the annulus must be made bottomless.

A problem introduced by the production of very high shear rates is that of maintaining isothermal conditions. Clearly the reduction in the annular width of a coaxial cylinder viscometer must then be accompanied by some form of temperature control, since high shear rates infers high energy dissipation.

The advantages of this form of viscometer lie mainly in its potentials of (1) producing nearly unique shear conditions in the instrument and (2) controlling the shear rate over a wide range simply by varying the speed of the rotor.

NACA Automatic Viscometer. One viscometer built for the NACA to overcome the difficulties encountered in non-Newtonian viscometry has been reported by Weltmann and Kuhns (59). The features of this viscometer are: less than 15% variation in shearing stress across the

annulus, rates of shear up to 4000 sec.^{-1} , automatic programming and recording of the shear stress - shear rate curve, constant-temperature bath to minimize temperature increase due to shear, and precise alignment of the rotor and stator. This machine tends to minimize the end-effect but does not eliminate it altogether.

The Merrill-Brookfield Viscometer. The viscometer to be used in this study is the coaxial-cylinder viscometer designed by E.W. Merrill and built by the Brookfield Engineering Co. (28, 30). It, too, is designed to overcome the difficulties involved in non-Newtonian viscometry. The features of this apparatus are:

- (1) less than 0.5% variation of shear stress across the annulus,
- (2) bottomless annulus, shear occurring only between the cylindrical surfaces,
- (3) water jacketed stator and cored rotor, providing temperature control of both shearing surfaces,
- (4) rates of shear up to $20,000 \text{ sec.}^{-1}$, with no turbulence,
- (5) automatic variable programming and recording of the resultant shear stress - shear rate curve,
- (6) air bearings to minimize bearing drag and make possible the testing of fluids of low viscosity.

Since the annulus is 0.006 inches wide, the bottomless annulus is possible, the fluid being held up by capillary action. Fluids with viscosities as low as that of water can be run in this apparatus with

careful technique. See APPENDIX A for details of this apparatus.

Modified Brookfield Synchroelectric Viscometer. Another viscometer was used in this work to obtain rheological data at very low shear rates (0.1 to 40 sec.⁻¹). With the fluids studied, the background noise signal would make reliable interpretation of the Merrill viscometer data at very low shear rates impossible. Therefore a coaxial cylinder viscometer was furnished by the Brookfield Engineering Co. which consisted of the standard Synchroelectric viscometer head with an attached rotor bob immersed in an annular cup. The result was a double annulus with practically no end effect. The viscometer necessarily produced stepwise changes of shear rate, giving discreet point values on the rheological curve. The details of the construction of this viscometer are given in APPENDIX A.

The main purpose of this viscometer was to determine whether or not pseudoplastic materials become Newtonian at very low shear rates.

"Slip" at the Wall. There was an additional topic of interest that was borne in mind during this investigation, that of "slip" of the fluid at the wall of the tube. Behind this is the pioneering work of Bingham in the field of plastic fluids (20). He developed the concept of "yield value" for these materials to explain the anomalous results that had been obtained in capillary tubes, and as a consequence these materials were named for him -- Bingham plastics. The natural consequence of a material with a yield value flowing in a tube is the formation of a layer of mobile material in the vicinity of the wall where

the shear stress is high, and the remainder of the material in the core of the tube acting as a solid -- so-called "plug flow". This situation results in all the velocity gradient being carried in the layer near the wall -- hence a very blunt velocity profile is the case.

Further work by R.J. Richardson (45) has shown that with paper pulp slurries, which are plastic fluids, that there is formed a layer at the wall which is deficient in pulp particles -- essentially a layer of pure water -- and that most of the gradient occurs in this layer, resulting in very unusual flow characteristics. Since it seems reasonable that the effect is that of the presence of the wall preventing the relatively large pulp particles from being at the wall in main-stream concentration; others -- notably Toms (56) and Oldroyd (38) -- have rationalized that the same effect could occur with pseudoplastic fluids since they contain rather large molecules. Therefore, they set up mathematical expressions by which they felt this effect could be demonstrated in laminar and turbulent flow. Experiments (38, 56) were conducted and the results interpreted to show that such a "slip" layer does exist. In both cases the anomalous character of the flow characteristics of pseudoplastic fluids supported their theory. For instance, in the case of turbulent flow, the reasoning was, in effect, that the presence of a slip layer would lead to lower pressure drops than would be expected from the normal degree of turbulent energy dissipation found with Newtonian systems. Since lower pressure drops in turbulent flow were found, the theory was supposedly justified.

Dakekian and Engelken (13) carried out a test of their own in laminar flow to detect the presence of a slip layer, and they came to the conclusion that no such effect existed appreciably. Rather, the flow rate - pressure drop relationship was closely that to be expected on the basis of the power-law model of rheology (equations 7, 17). Unfortunately, no such independent test of the contention of slip at the wall in turbulent flow had been reported up to this present work, so one of the objects of this experimentation was the confirming or the denying of the contention of slip at the wall in pseudoplastic turbulent flow. A very simple method of determining this was to compare the pseudoplastic turbulent velocity profiles with the corresponding Newtonian ones -- slip at the wall would necessarily result in a more blunt profile than Newtonian, as was demonstrated above.

Problem Restated. On the basis of the work done in prior studies and the deficiencies revealed, the following problems were investigated in this work:

- (1) the form of the friction factor vs. pseudoplastic Reynolds Number curve(s) in turbulent flow,
- (2) the accuracy of the theoretical laminar pseudoplastic velocity profile,
- (3) the form of the turbulent pseudoplastic velocity profiles,
- (4) the generality of the classical turbulent flow correlations, such as mixing length, velocity deficiency,

- and universal velocity profile,
- (5) the determination of reliable rheological curves for these fluids, with which to obtain the desired generalizations, and
 - (6) the determination of the presence or absence of an anisotropic "slip" layer at the wall of the tube with pseudoplastic fluids.

II. PROCEDURE

Apparatus. There were two main types of apparatus involved in this experimentation: the viscometric apparatus to determine the shear stress - shear rate curves, and the pipeline flow apparatus to determine friction factors, velocity profiles and dye stream behavior as functions of flow rate and tube diameter.

The chief viscometric apparatus was the Merrill-Brookfield viscometer (described in detail in APPENDIX A), a bottomless, coaxial-cylinder, rotational viscometer producing a continuous plot of shear stress versus shear rate from 0 to 20,000 reciprocal seconds. A second viscometer, a modified Brookfield Synchroelectric with annular cup and cylindrical bob (also described in detail in APPENDIX A), was used to obtain accurate data in the low shear rate range of 0.1 to 40 reciprocal seconds, stepwise.

The pipeline flow apparatus (Figure 4) consisted of a recirculating system containing: replaceable test section, reservoir, heat exchanger, bypass and positive displacement pumping. The pumps were 6M4 and 3L2 Moyno pumps which were driven by a 7.5 HP shunt-wound DC motor with shunt field control and an AC U.S. Varidrive, respectively. The input speed to each of the pumps was monitored continuously by means of DC tachometer generators driven off the pump shafts and delivering voltage signals to voltmeters. The pumps were joined in parallel in the recirculating system, providing calibrated flow rates

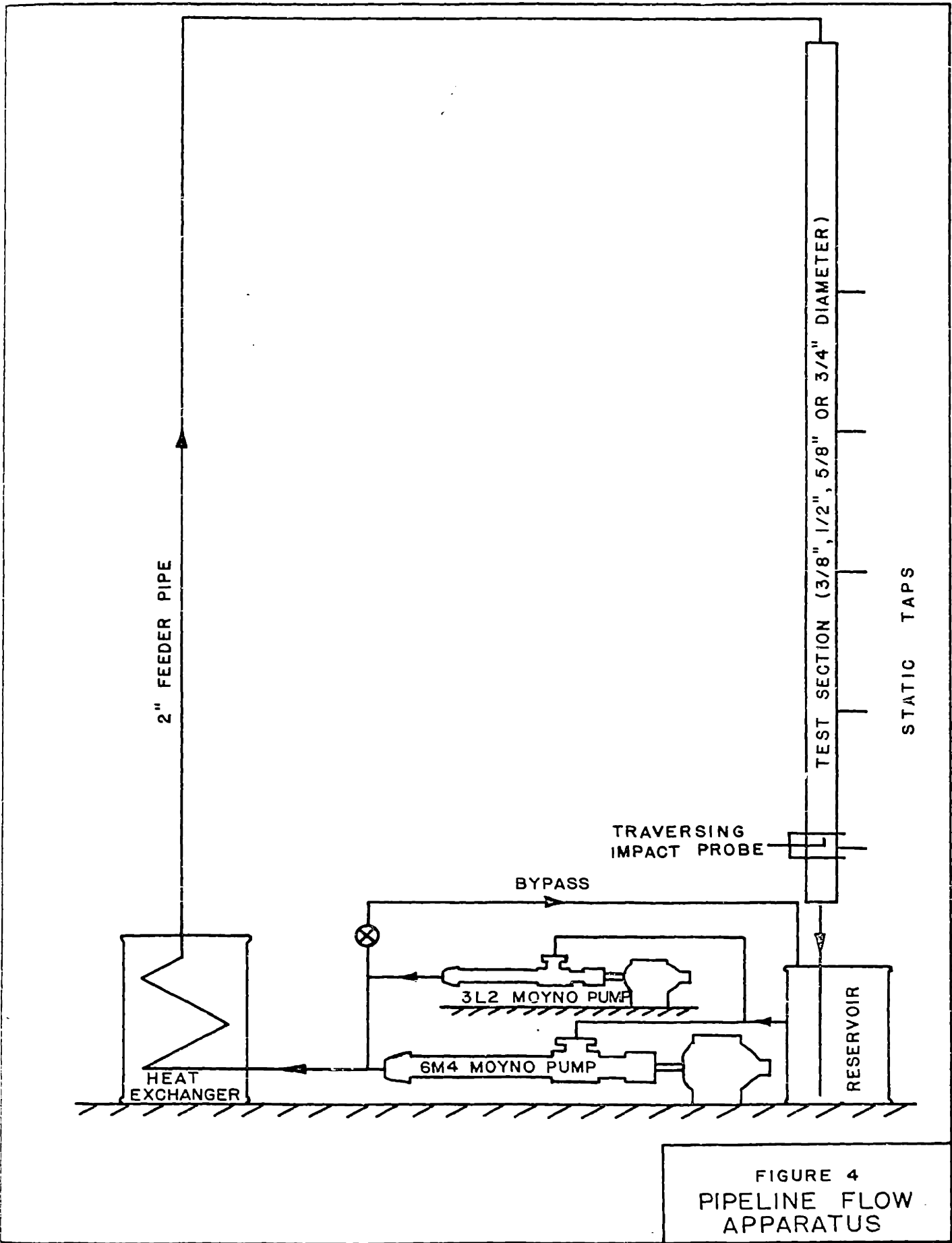


FIGURE 4
PIPELINE FLOW
APPARATUS

that were continuously variable up to 40 GPM.

Static pressure taps were carefully machined into the walls of the various test section tubes at intervals of 30 inches, the closest one to the entrance being 8.5 feet downstream. This provided a series of five pressure taps, across any combination of which the pressure differential could be measured. The taps were in no instance larger than $1/10$ the diameter of the tube they were in, and the largest tap used was $1/16$ of an inch. The tubes were stainless steel and sections of $1/4$ inch copper tubing was silver-soldered over each tap to connect it with the manometer system.

The impact-pressure traversing mechanism was designed and built by the author (see APPENDIX A for details). Its main features were:

- (1) positive continuous location of the probe in the tube by means of a micrometer mechanism,
- (2) detection of wall position by means of an electrical circuit and an insulated probe,
- (3) great structural rigidity in the probe, together with small diameter of the probe tip -- accomplished by the "nesting" of sections of successively smaller diameter hypodermic tubing, the tip being 0.025 OD and 0.013 ID, and,
- (4) minimum disturbance of flow using a simple impact tube and a wall tap.

Viscometric Data. The fluid to be tested was injected into the Merrill viscometer and several plots of shear stress vs. shear rate were obtained from zero to maximum shear rate and back again. Then where applicable, the fluid was tested in the modified Brookfield viscometer at the same temperature and the data from both viscometers put on a composite rheological plot.

Friction Factor Runs. With the appropriate test section in place, the fluid was circulated until the proper temperature was attained. The run was then made by proceeding stepwise from the lowest to the highest flow rate and then back again. Manometer displacements, temperature, pump RPM and observations of the stability of the flow were made at each flow rate.

Velocity Profile Runs. With the appropriate test section in place and the impact pressure traversing device affixed thereto, the fluid was circulated at the chosen flow rate until the proper temperature was attained. The position of electrical contact of the probe tip with the tube wall was noted. The run was then conducted by traversing stepwise from the approximate tube center toward the tube wall until the wall was contacted by the probe tip. Generally this was done in steps of 0.025 inch. Then the probe was returned to the center and traversed as far as possible toward the opposite side of the tube. At each position the manometer was allowed to come to rest and the displacement noted. Periodically, the displacement of the friction manometers were noted. The technique developed to prevent fouling of

the probe tip by the entry of the high polymer slurry was as follows:

The manometer line from the probe tip to the manometer was maintained full of pure solvent (water or cyclohexane). Because the solutions were so dilute, there was no appreciable density difference between solution and solvent. To maintain pure solvent in the line, solvent was injected into this line before taking a reading, and the manometer displacement therefore always decreased to the steady reading. By this expedient the probe tip was kept clear of fouling by the flow of pure solvent through it up to the moment of the steady reading.

It was found early in this investigation that any attempt to obtain an impact pressure reading by the usual method of allowing the fluid to enter the probe tip would result in almost instantaneous plugging of the probe, despite the fact that these fluids have no discernible gel point of macroscopic particle size.

Coincident with the impact pressure reading, temperature and pump RPM were noted. The temperature and pump RPM were, of course, held as constant as possible during the course of one run, generally less than one percent variation was encountered.

Dye Injection Runs. The dye injection experiments consisted of injecting a small amount of pigmented test fluid at one of several positions in a 3/4" ID Lucite tube and the dye stream observed visually and photo-

graphically by means of a short-duration flash. The two main points of injection used were:

1. centrally located at the entrance of the Lucite test section by means of an 0.025 inch O.D. hypodermic tube, 185 diameters upstream of the point of observation.
2. through a wall tap located at, or slightly above, the point of observation.

The injection was controlled by a hypodermic syringe compressed by a crank and screw-thread mechanism.

The purposes of the two above injection positions were to observe the effect of turbulence on (1) the fluid in the core of the tube and (2) the fluid at the boundary of the tube.

The photographic equipment used was a Leica model IIIc with 50 mm. Summar lens or 135 mm. Hektor lens fitted with an appropriate amount of extension tubes on a Focaslide attachment. The shutter of this camera was synchronized to the flash of a General Radio Corporation Strobolume of 40 micro-second flash duration.

III. RESULTS

The problem of determining the characteristics of pseudoplastic turbulent flow fell into two areas: (1) the determination of the rheological curve for the fluid in question by means of the Merrill and the modified Brookfield viscometers, and (2) the pipe-line flow experimentation. Therefore, for clarity, the results presented in this section will be grouped into these two main categories.

A. Rheological Curves

Figures 5 to 9 present the high shear range rheological curves for the fluids studied as determined by the Merrill viscometer. Since this machine gives a curve rather than discrete data points, these results have been plotted as continuous curves with the limits of the spread of successive curves indicated. The curves are cut off at the lower shear rate of 1000 sec.^{-1} since reliable reading of the original curves could not be done with these fluids due to size of the random fluctuations relative to the data at low shear rates.

Figures 10 to 12 present the low shear range rheological behavior for several of the fluids as determined by the modified Brookfield viscometer. Since this machine gives discrete data points, these points have been indicated on the plots.

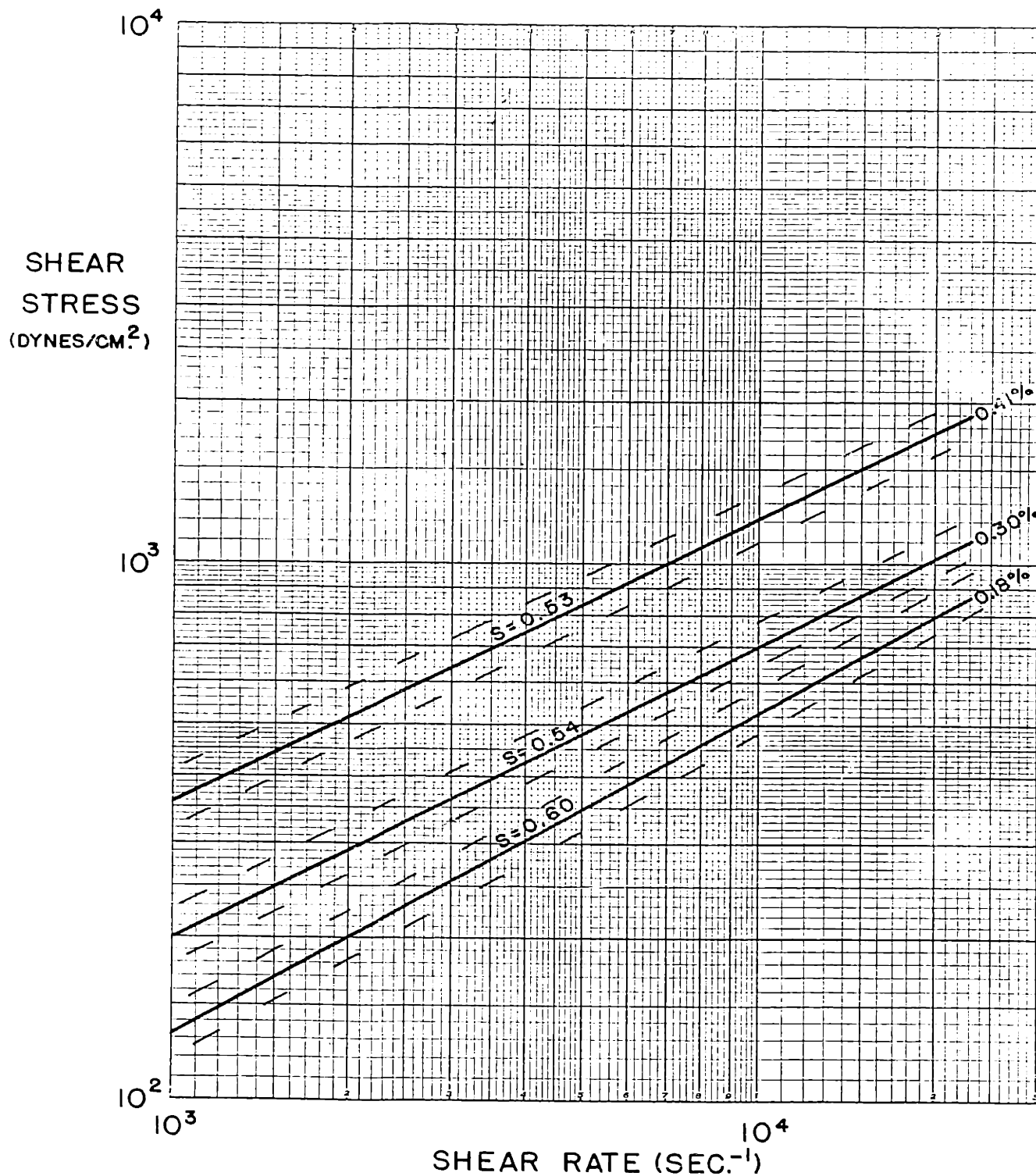


FIGURE 5
 HIGH SHEAR RANGE
 RHEOLOGY OF AQUEOUS
 SODIUM CARBOXYMETHYL-
 CELLULOSE, CMC-70
 72° F.

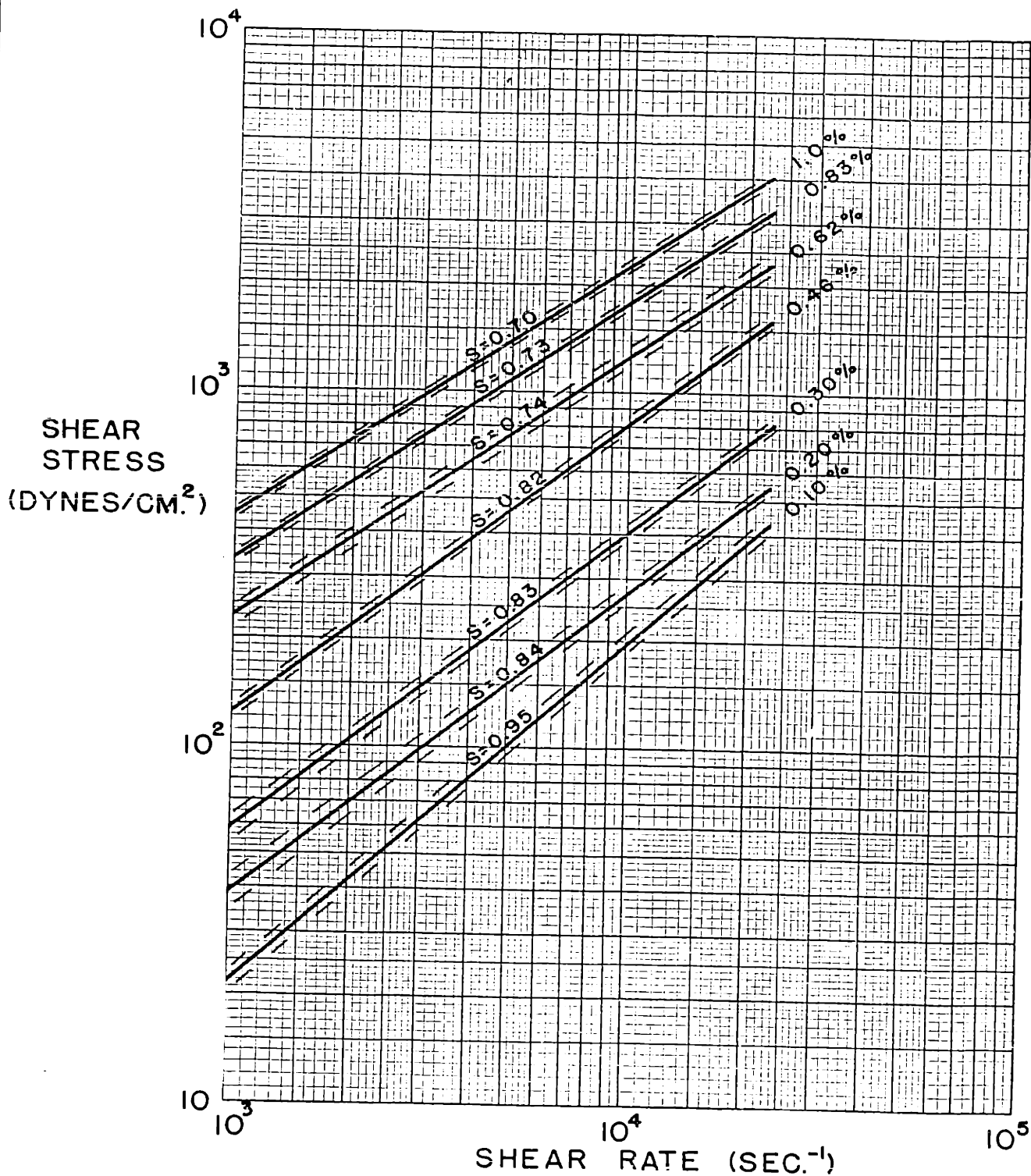


FIGURE 6
 HIGH SHEAR RANGE
 RHEOLOGY OF
 AQUEOUS AMMONIUM
 ALGINATE, 71°F.

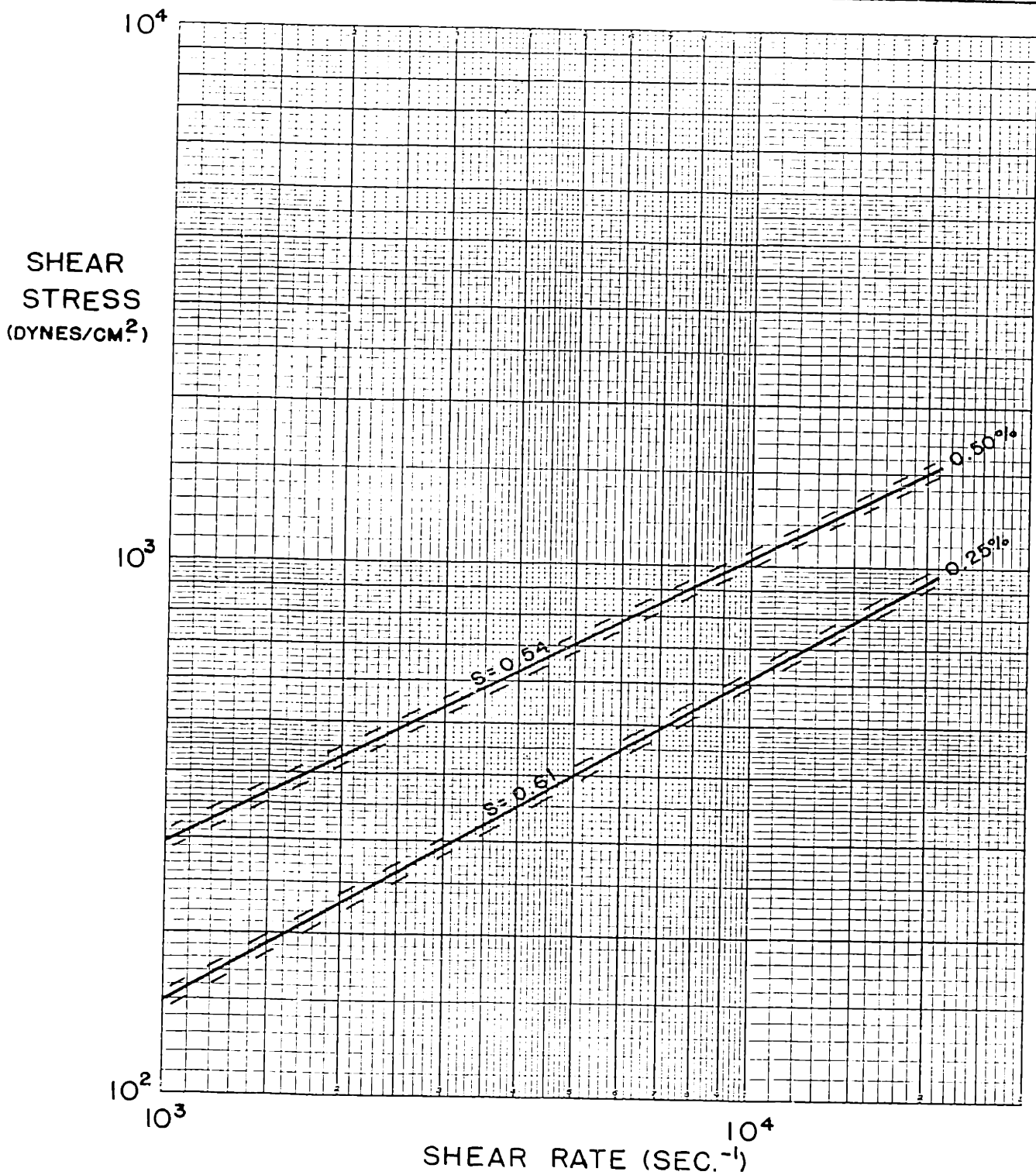


FIGURE 7
 HIGH SHEAR RANGE
 RHEOLOGY OF AQUEOUS
 SODIUM CARBOXYMETHYL-
 CELLULOSE, CMC-70S
 75° F.

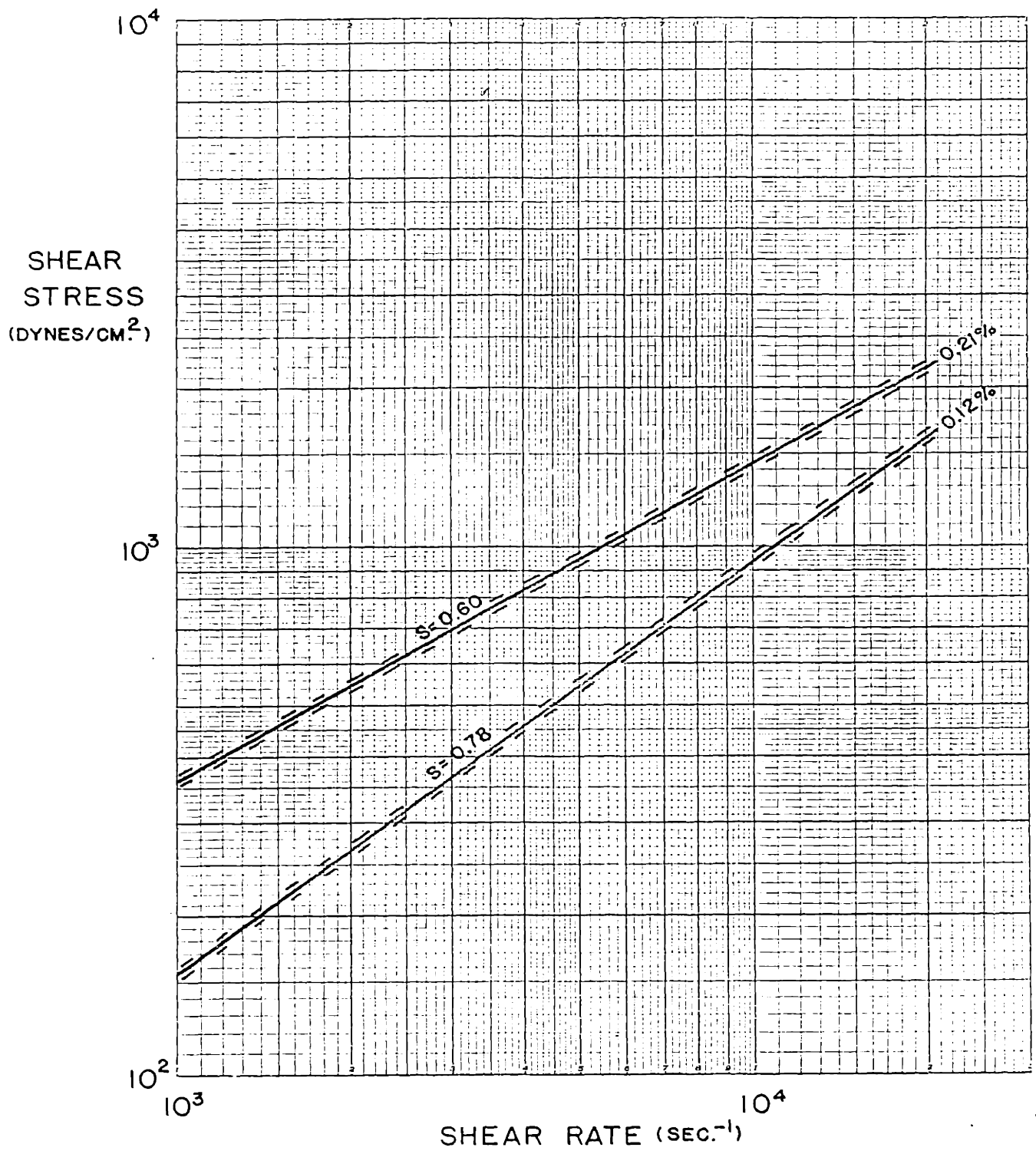


FIGURE 8
 HIGH SHEAR RANGE
 RHEOLOGY OF AQUEOUS
 CARBOPOL 934
 72° F.

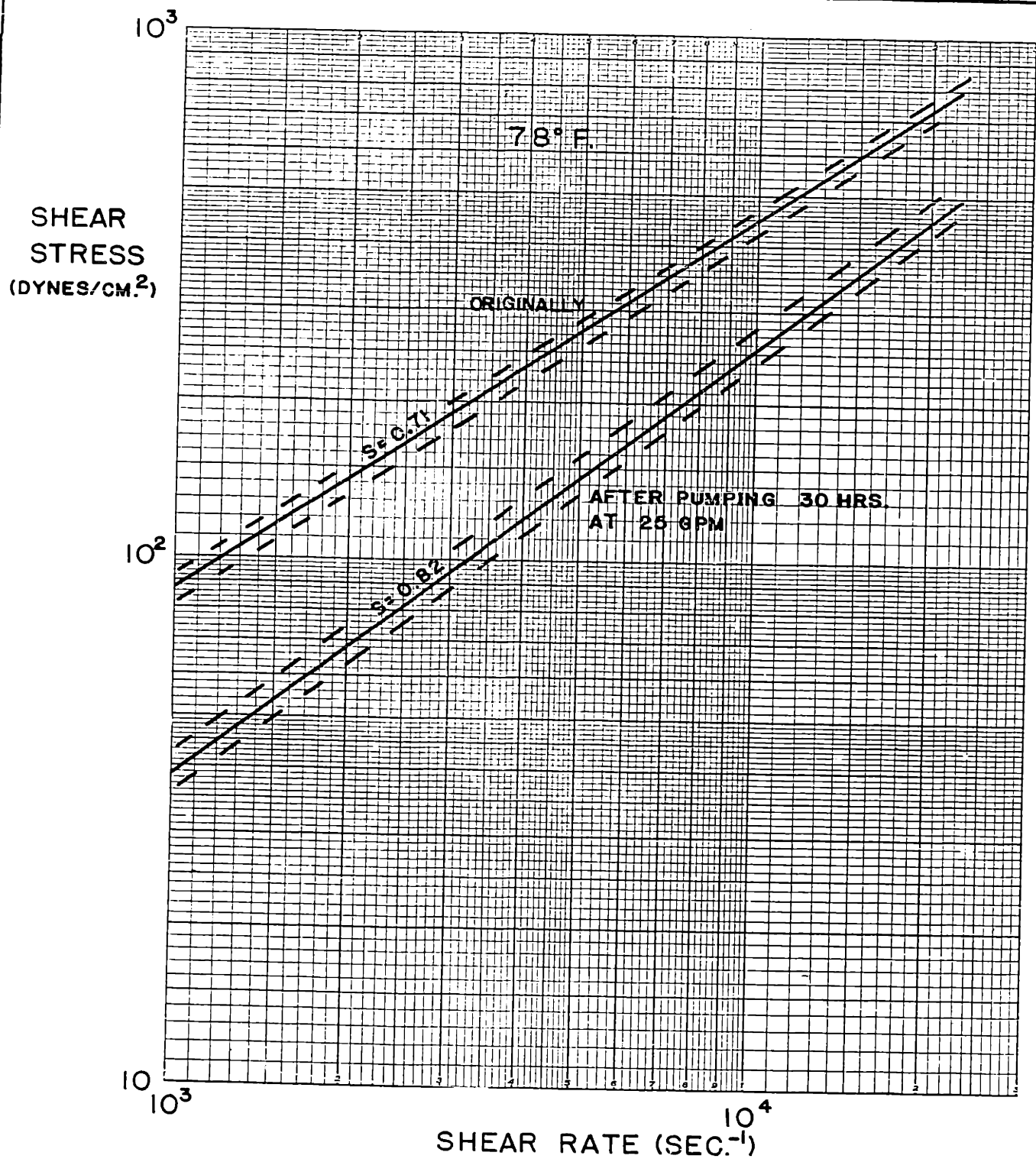


FIGURE 9
EFFECT OF SHEAR
ON THE RHEOLOGY
OF 0.52% VISTANEX

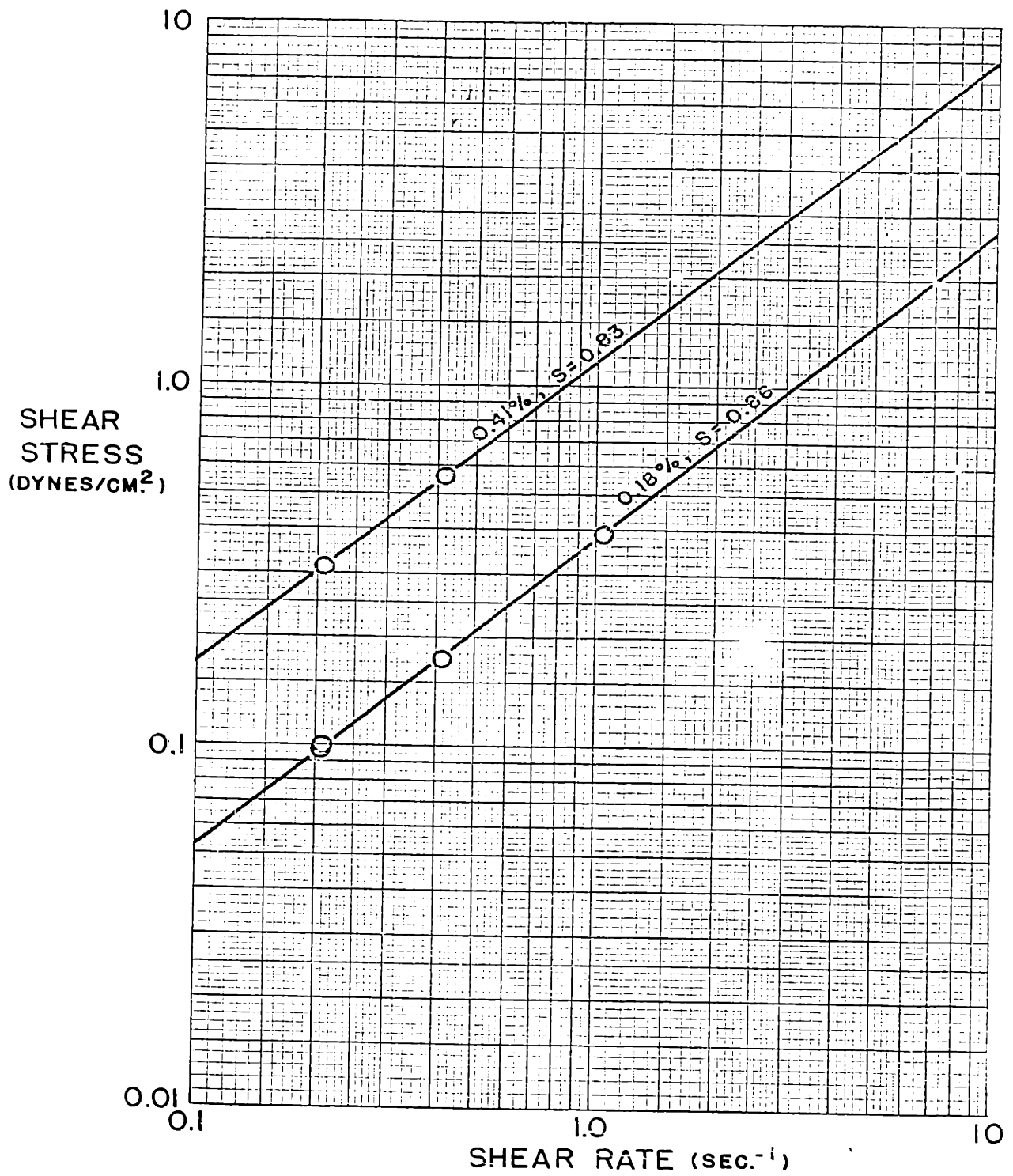


FIGURE 10
 LOW SHEAR RATE
 RHEOLOGY, CMC-70
 72° F.

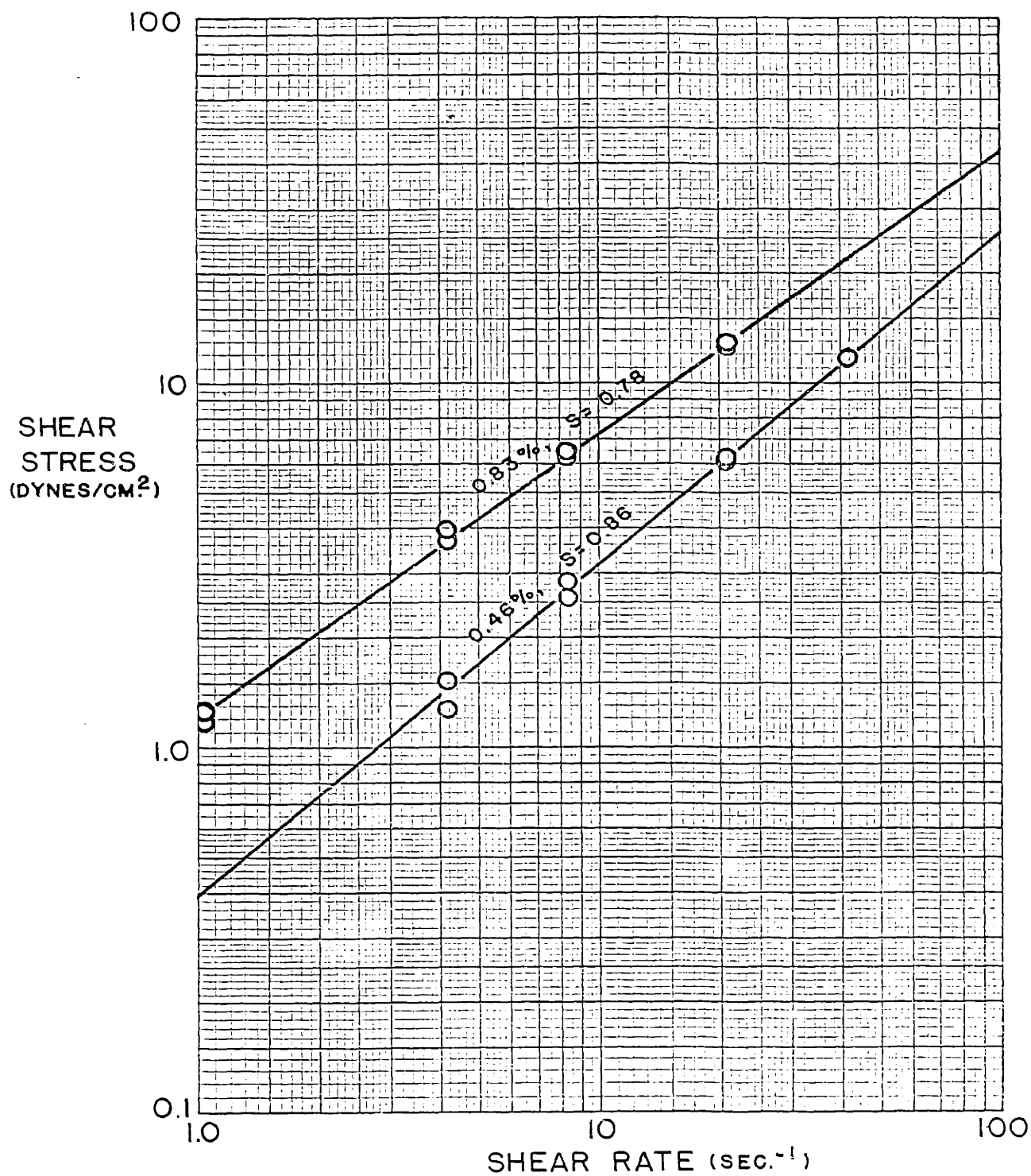


FIGURE II
 LOW SHEAR RATE
 RHEOLOGY,
 AMMONIUM ALGINATE, 71°F.

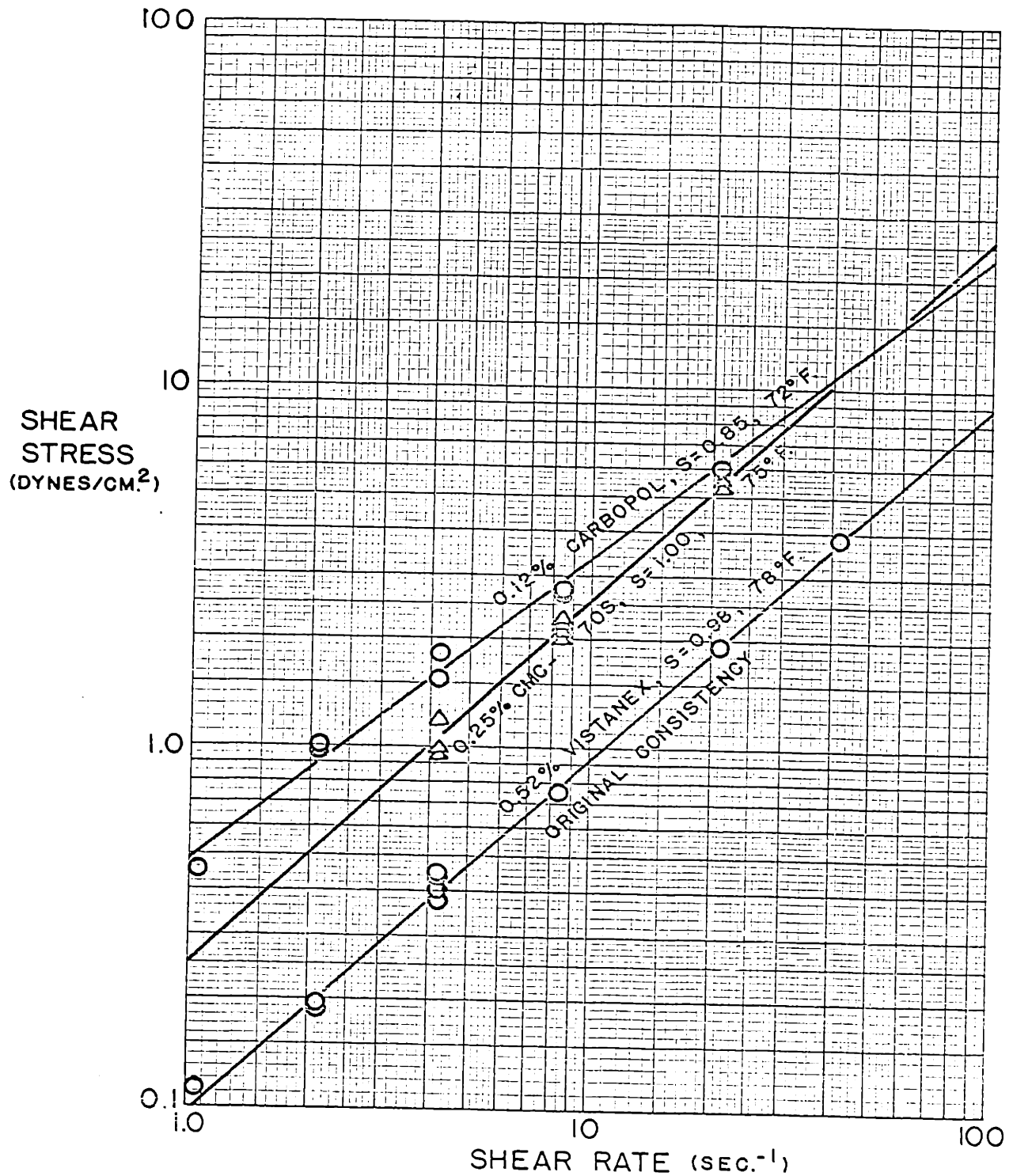


FIGURE 12
 LOW SHEAR RATE
 RHEOLOGY; CARBOPOL,
 CMC-70S & VISTANEX

III. RESULTS (Cont.) B. Pipe-line Flow

Friction Factors. The following polymers were tested in solution for dynamic pressure drop in straight, cylindrical tubes: sodium carboxymethylcellulose (Hercules Powder Co., CMC-70 and CMC-70S, a highly refined product), ammonium alginate (Kelco Co. Superloid), carboxypolyethylene (Goodrich Chemical Co. Carbopol 934), polyvinyl alcohol (DuPont Elvanol 50-42), and polyisobutylene (Enjay Co., Inc. Vistanex B-100). All were dispersed in water, except the polyisobutylene, which was dispersed in cyclohexane. With the exception of polyvinyl alcohol, they were solutions of free-draining, non-associating molecules. According to information supplied by the Hercules Powder Co., CMC-70 has areas of unreacted cellulose which do not go into solution, but remain in colloidal suspension. The CMC-70S product, on the other hand, has been processed to eliminate these areas, and is a homogeneous product.

In determining the Reynolds Number, the rheological constants were taken in that viscometric range in which the wall shear stress lay.

The friction factors and Reynolds Numbers thus obtained are generalized in Figure 13 for the laminar and turbulent regions between 100 and 100,000 Reynolds Numbers. Figure 14 shows the data points in laminar flow for all the pseudoplastic and Newtonian fluids tested. Figures 15 to 21 show the data points obtained at each s value in laminar, transition and turbulent regions.

Figure 22 shows the effect of varying the test section tube dia-

meter on the region of transition for typical set of highly pseudo-plastic runs.

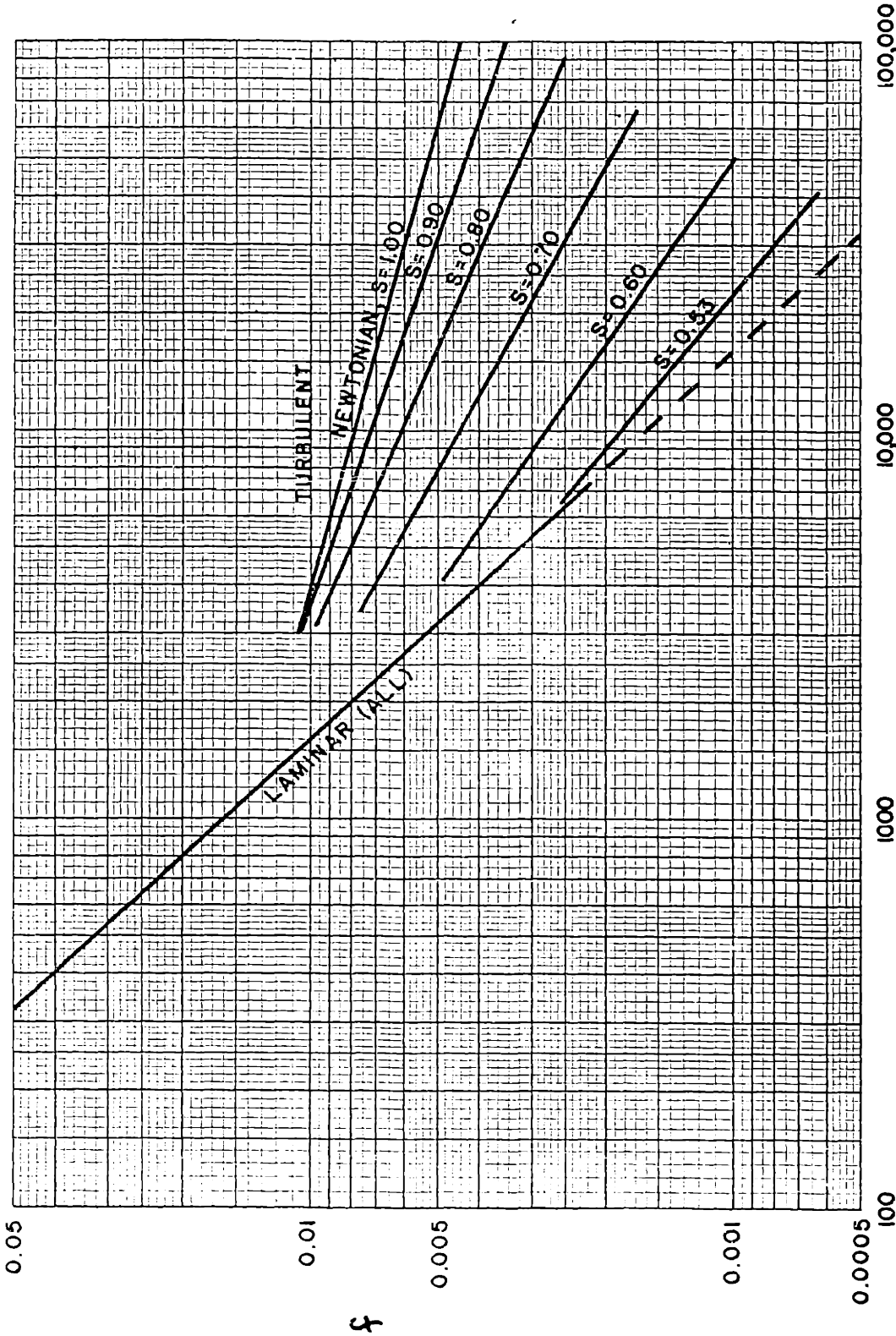
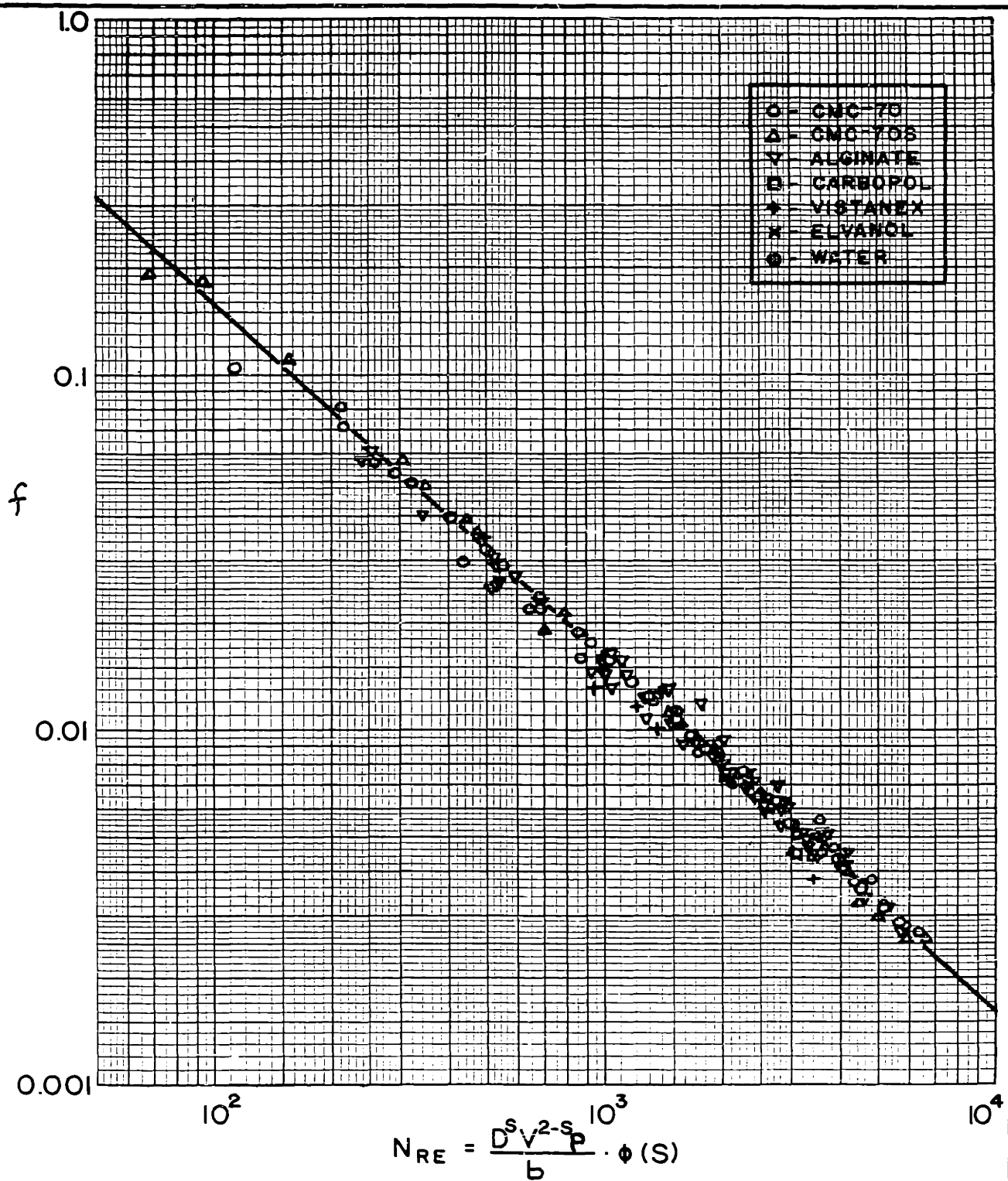


FIGURE 13

FRICITION FACTORS FOR PSEUDOPLASTIC LIQUIDS

$$N_{RE} = \frac{D^S V^{2-S} \rho}{b} \cdot \phi(S)$$

WHERE $\phi(S) = 8 \cdot \left(\frac{1}{2(3+1/S)} \right)^S$



WHERE $\phi(S) = 8 \cdot \left(\frac{1}{2(3+1/S)} \right)^S$

FIGURE 14
PSEUDOPLASTIC
FRICTION FACTORS
IN LAMINAR FLOW

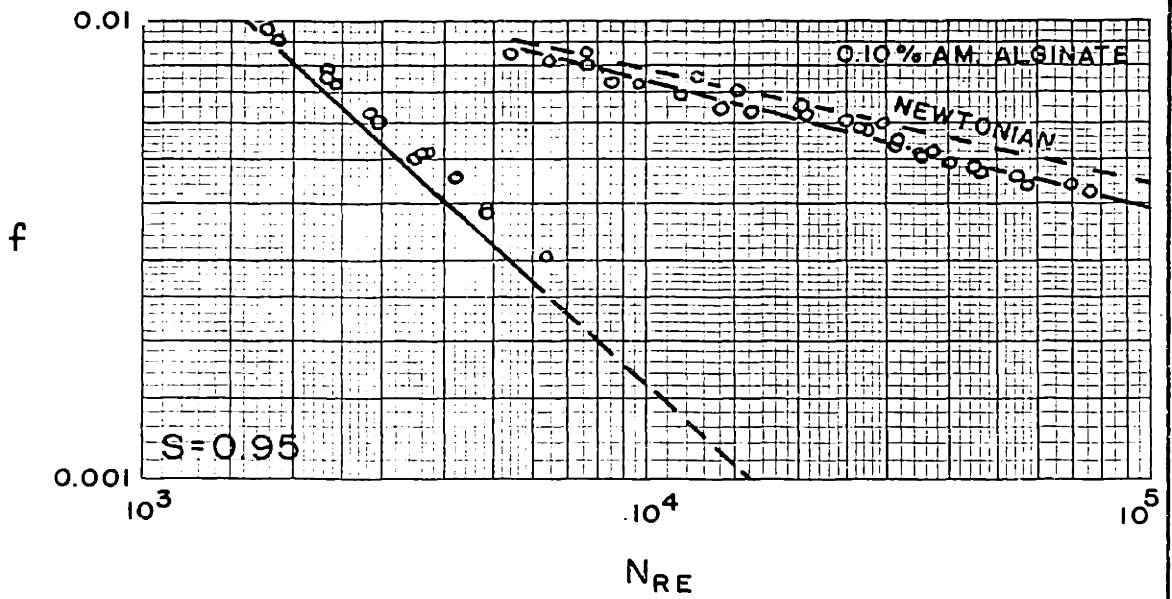
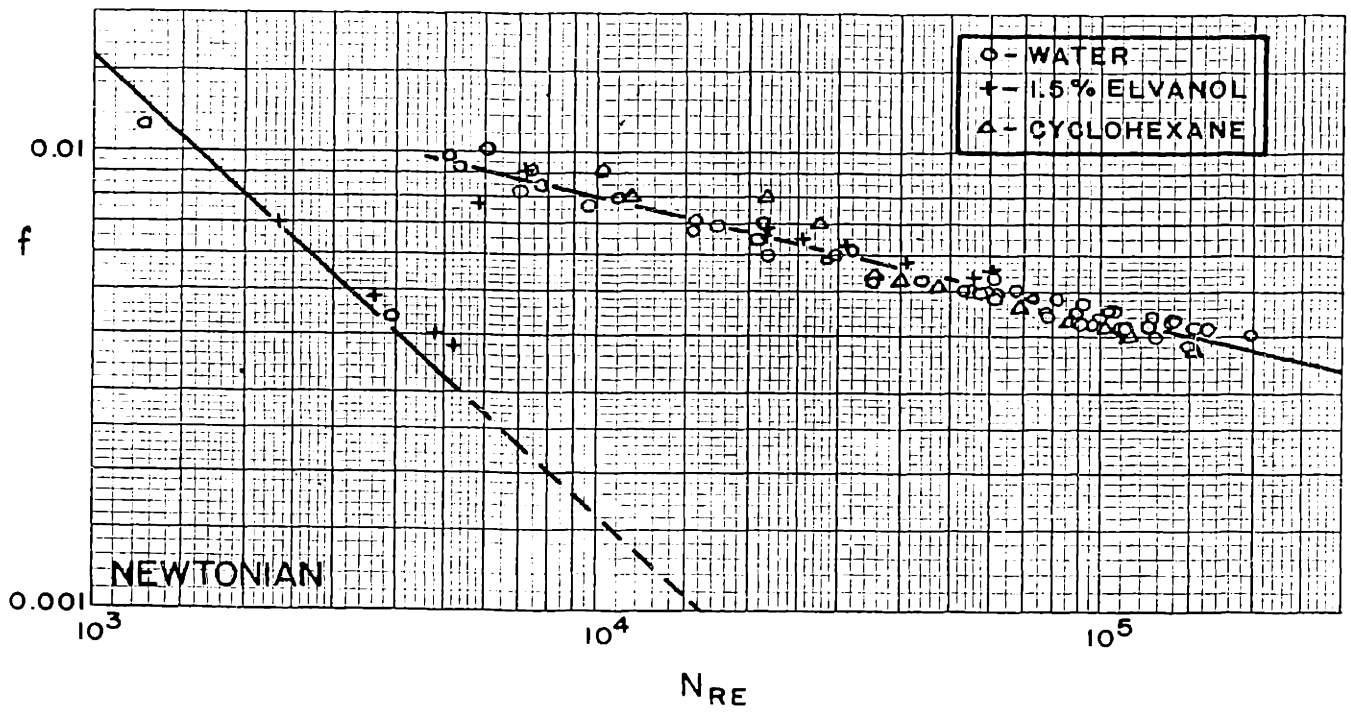
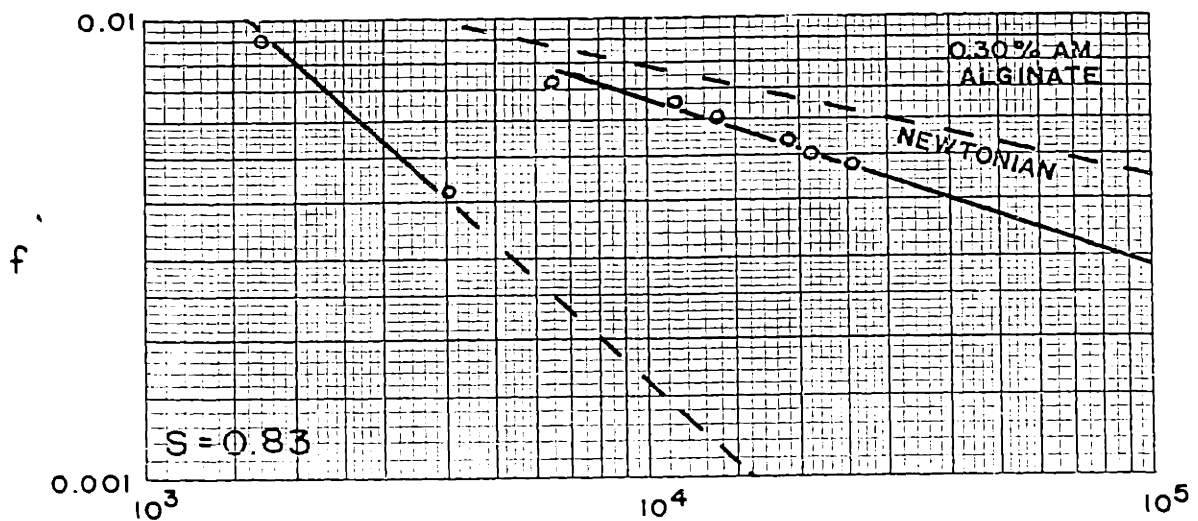
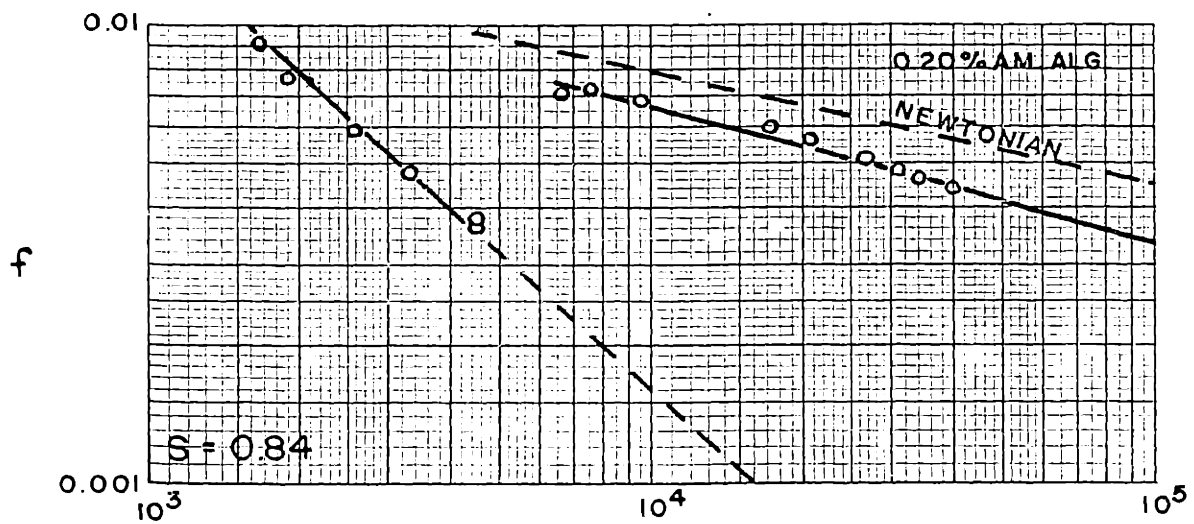
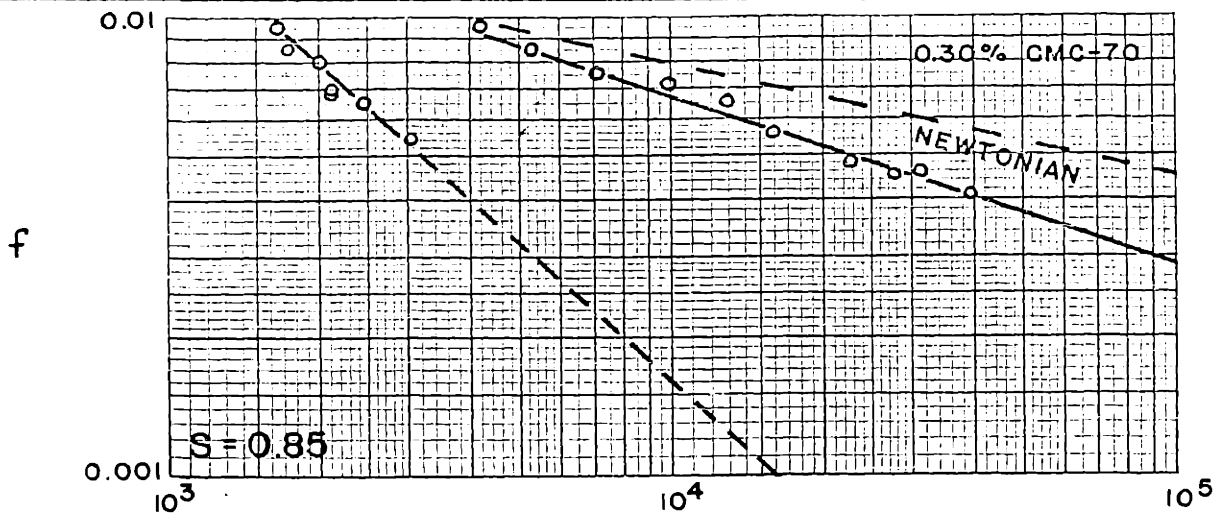
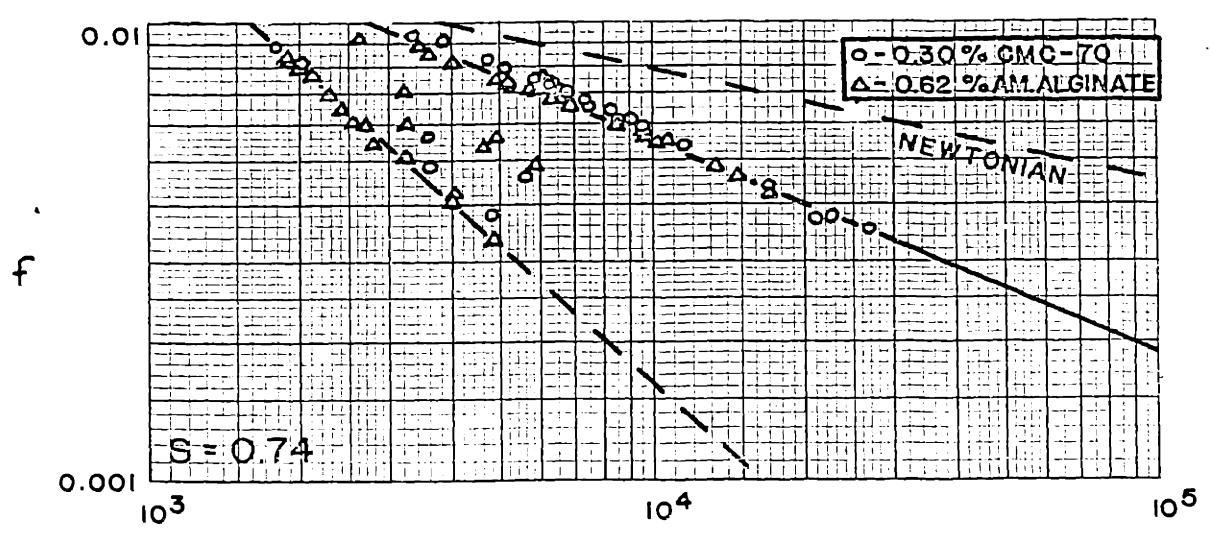
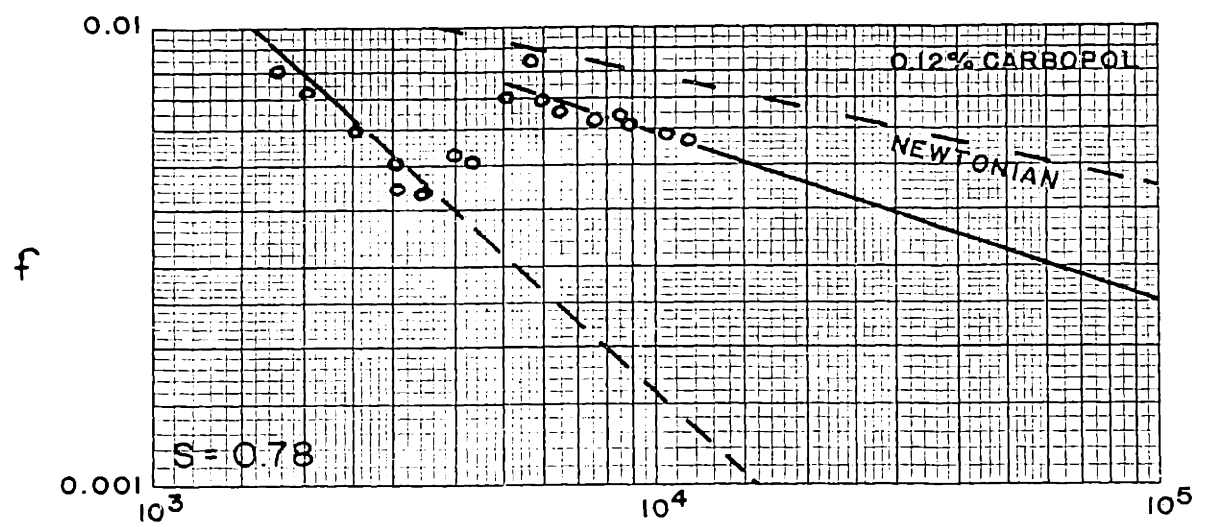
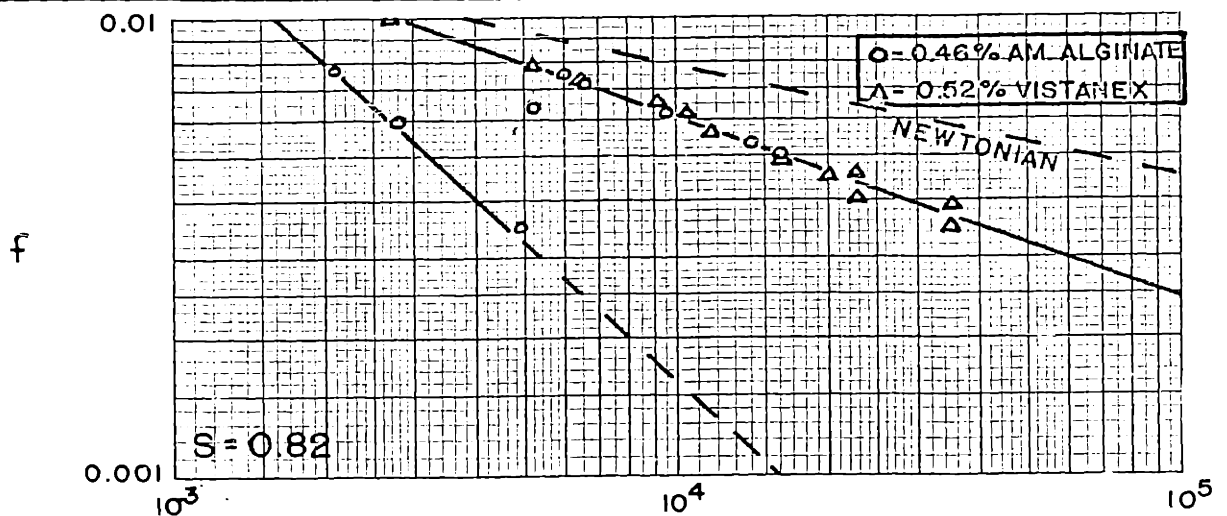


FIGURE 15
 FRICTION FACTORS,
 NEWTONIAN &
 S = 0.95



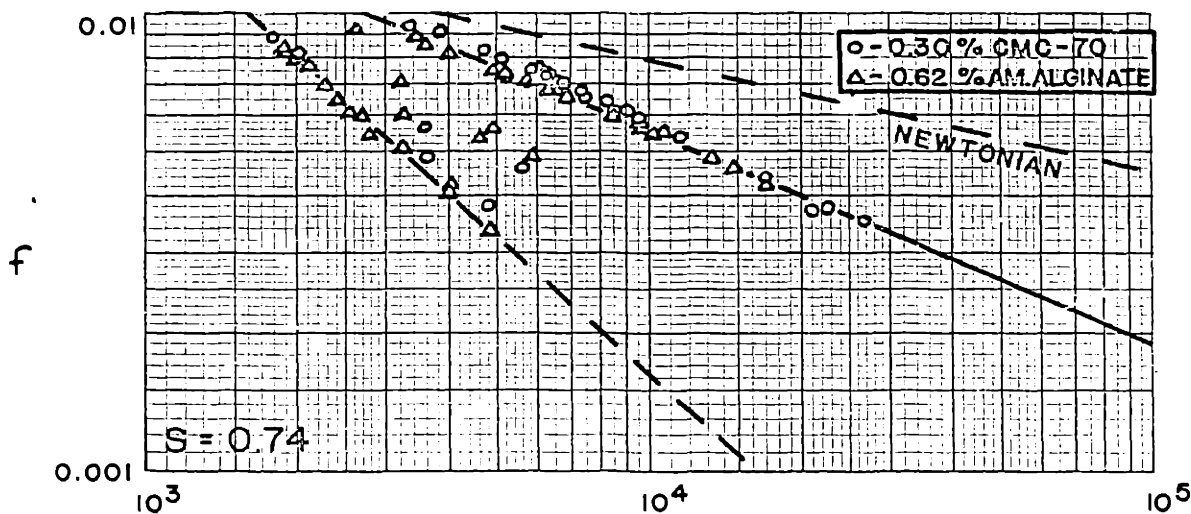
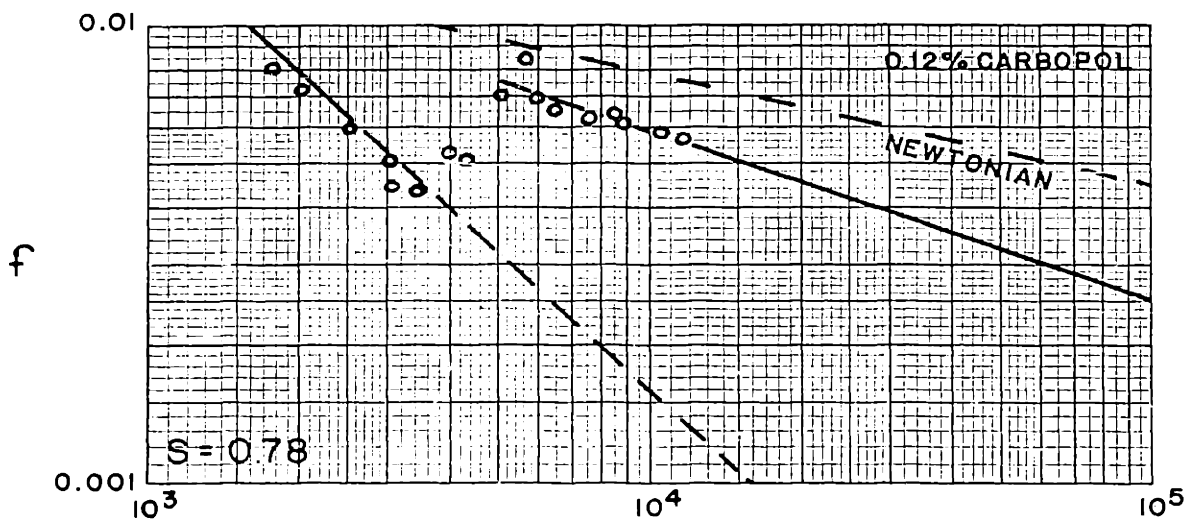
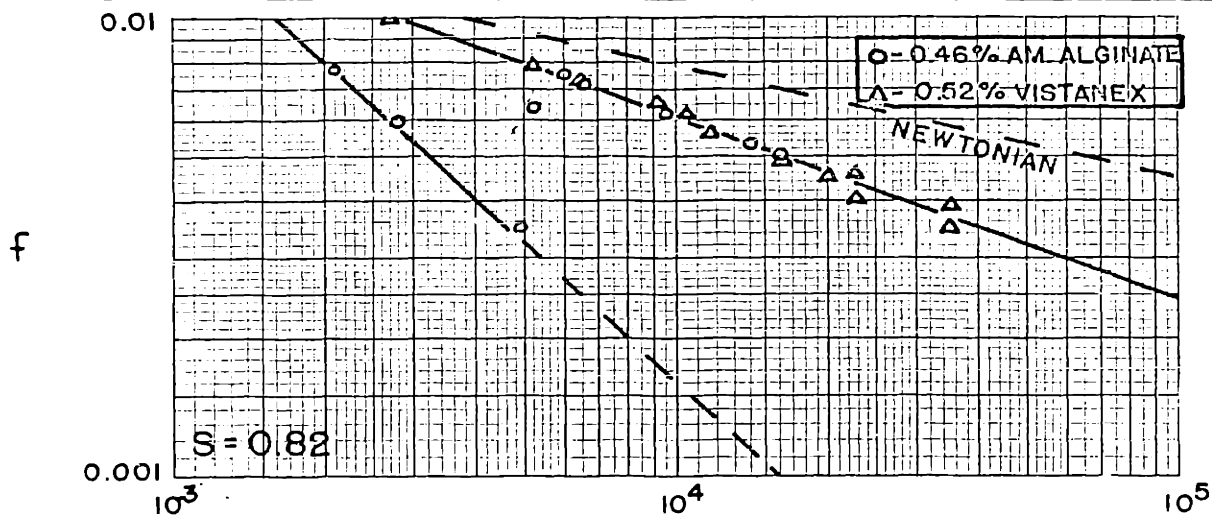
N_{RE}

FIGURE 16
FRICTION FACTORS,
 $S = 0.85, 0.84, 0.83$



N_{Re}

FIGURE 17
 FRICTION FACTORS,
 $S = 0.82, 0.78, 0.74$



N_{RE}

FIGURE 17
 FRICTION FACTORS,
 $S = 0.82, 0.78, 0.74$

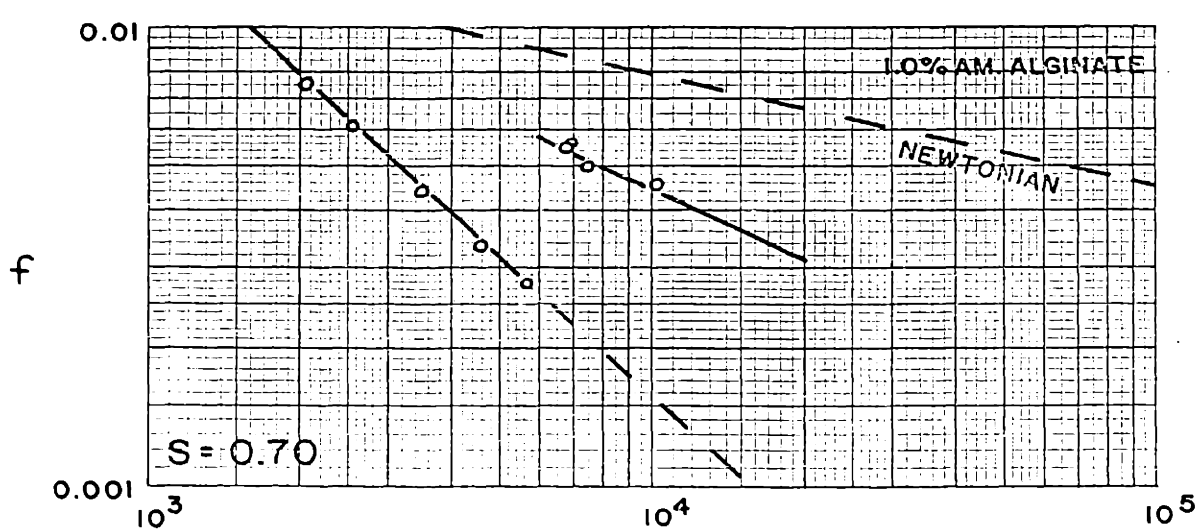
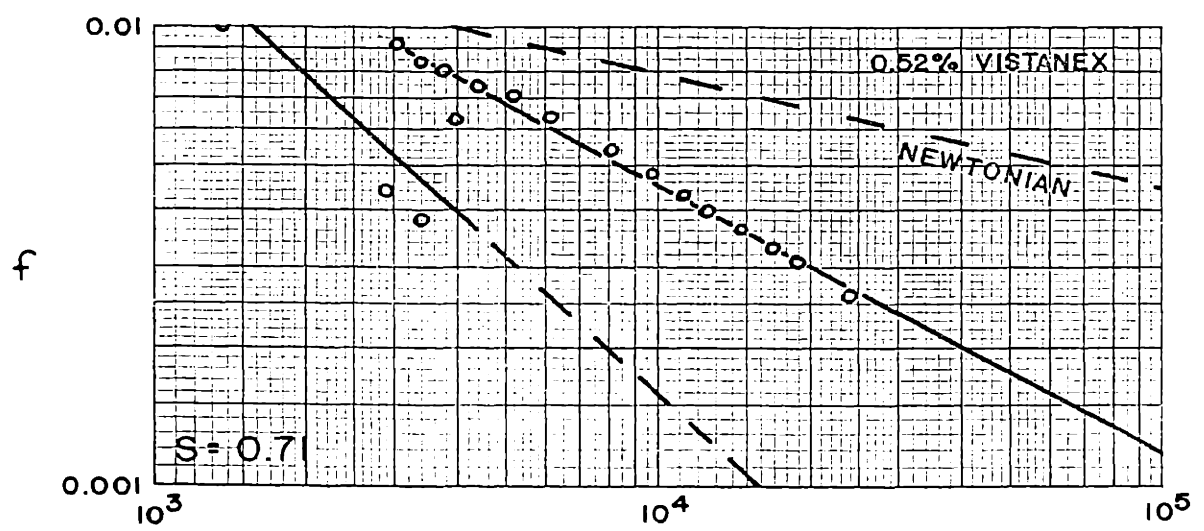
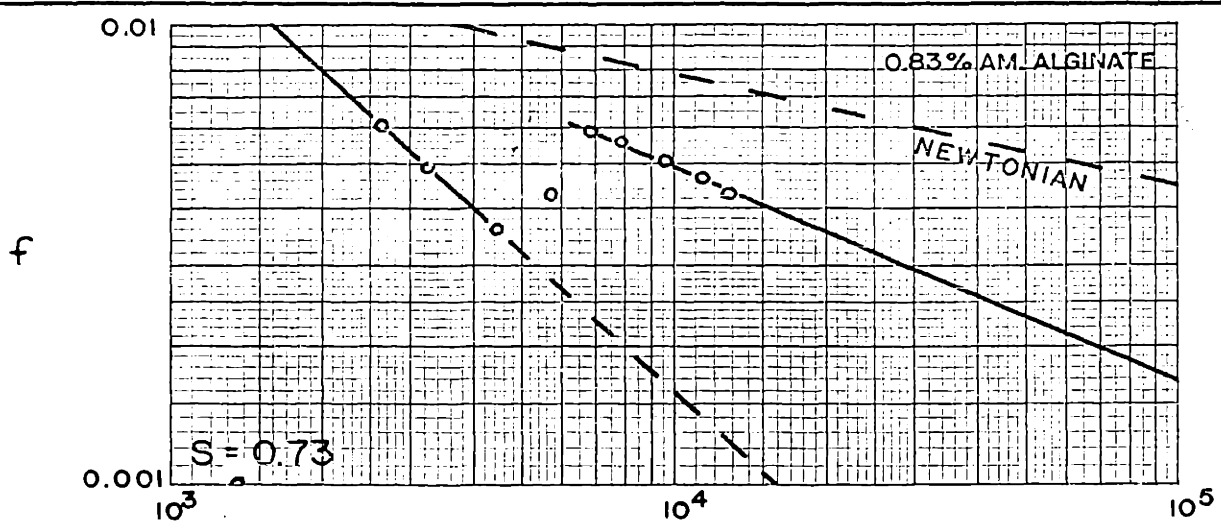
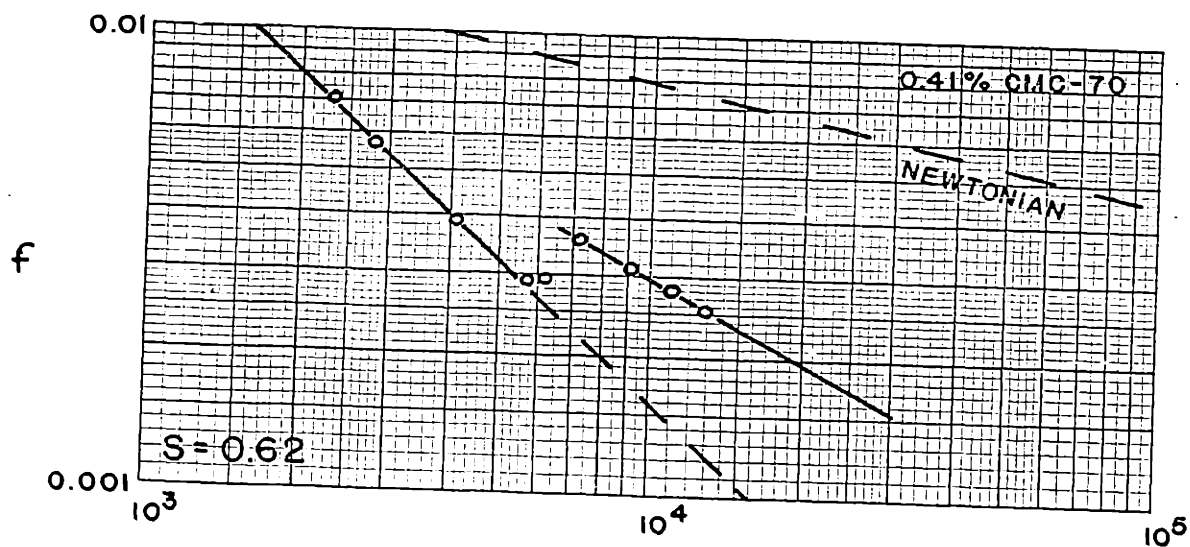
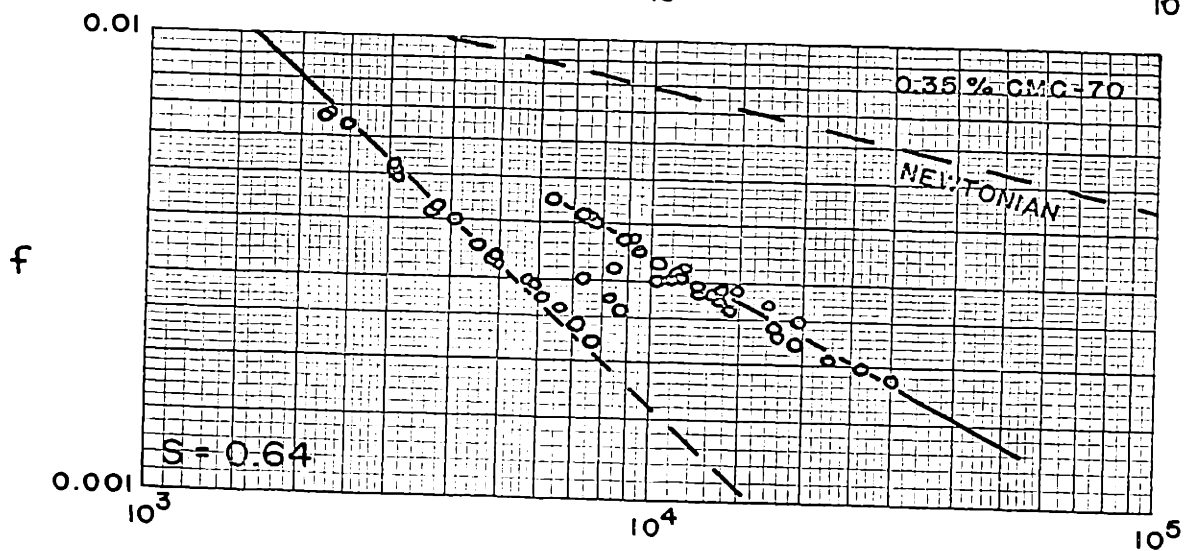
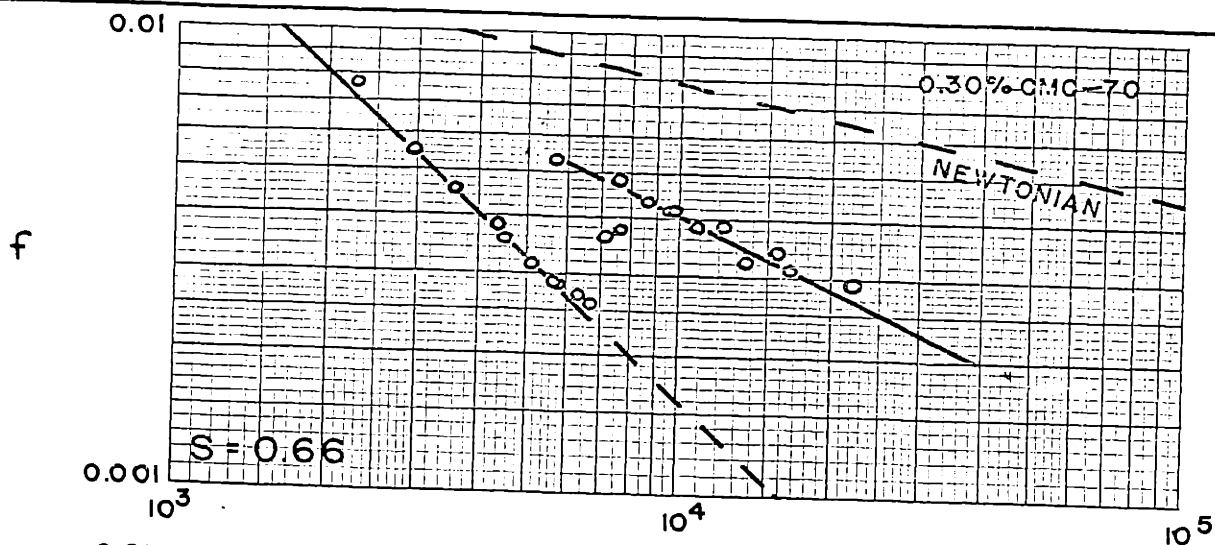
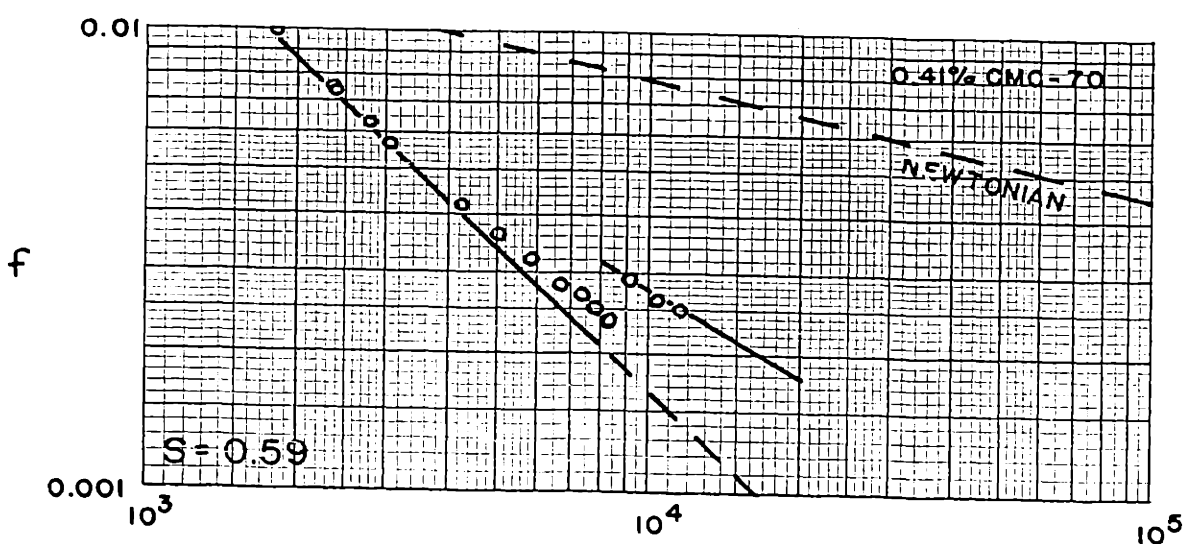
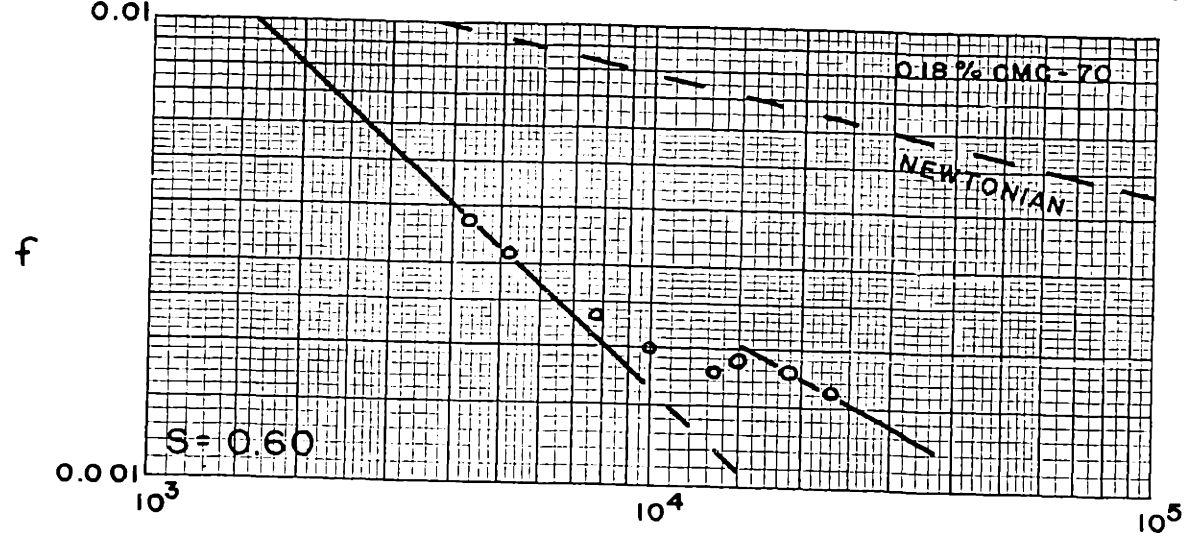
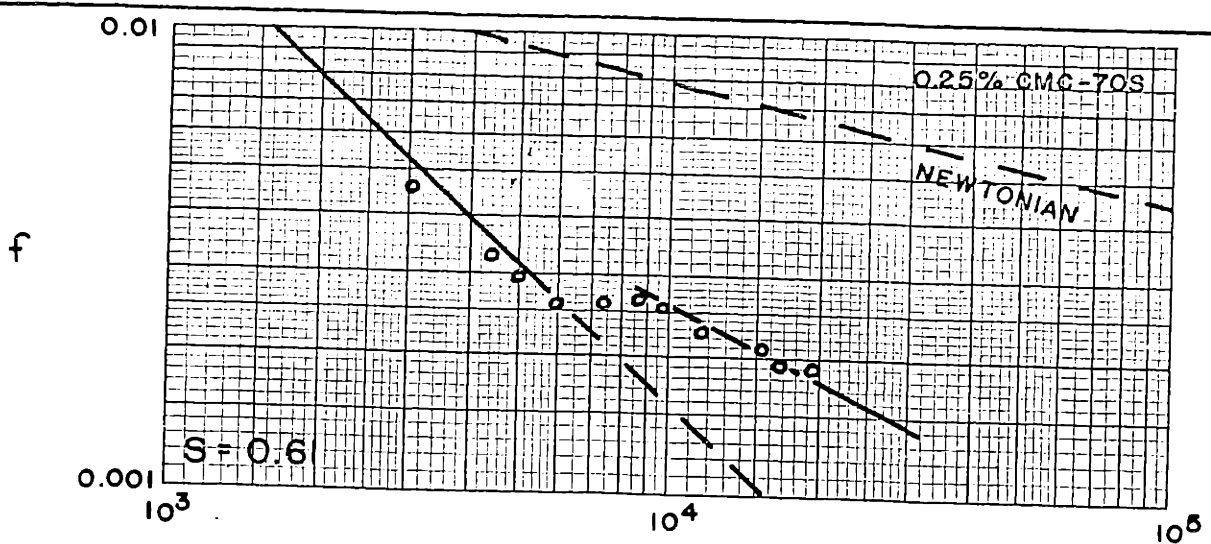


FIGURE 18
 FRICTION FACTORS,
 $S = 0.73, 0.71, 0.70$



N_{RE}

FIGURE 19
FRICTION FACTORS,
S = 0.66, 0.64, 0.62



N_{RE}

FIGURE 20
FRICTION FACTORS,
S = 0.61, 0.60, 0.59

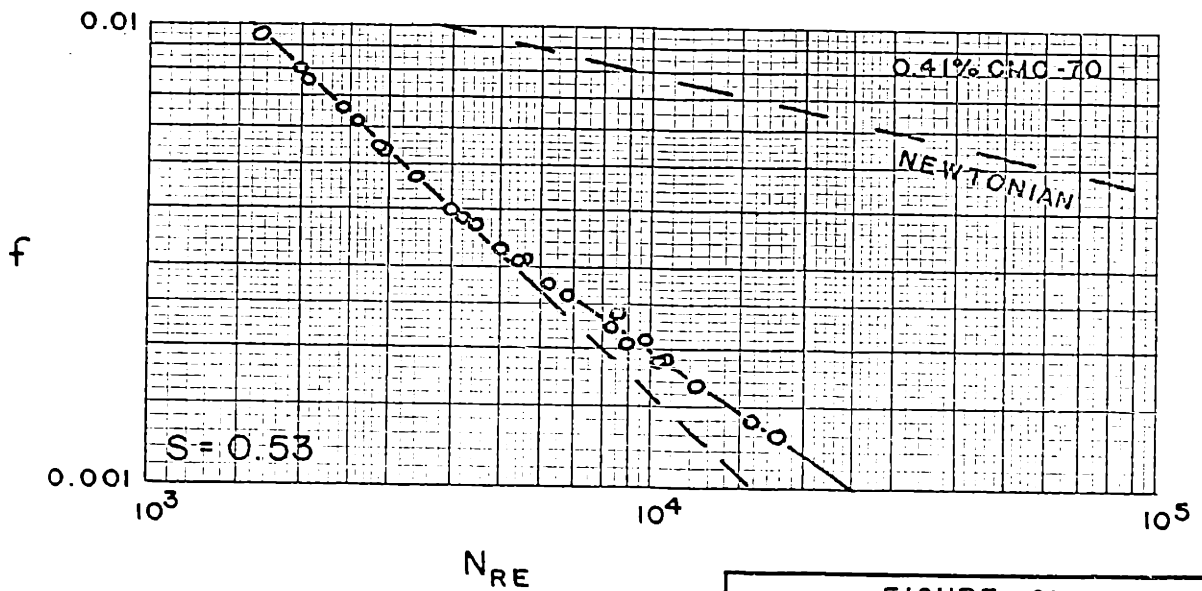
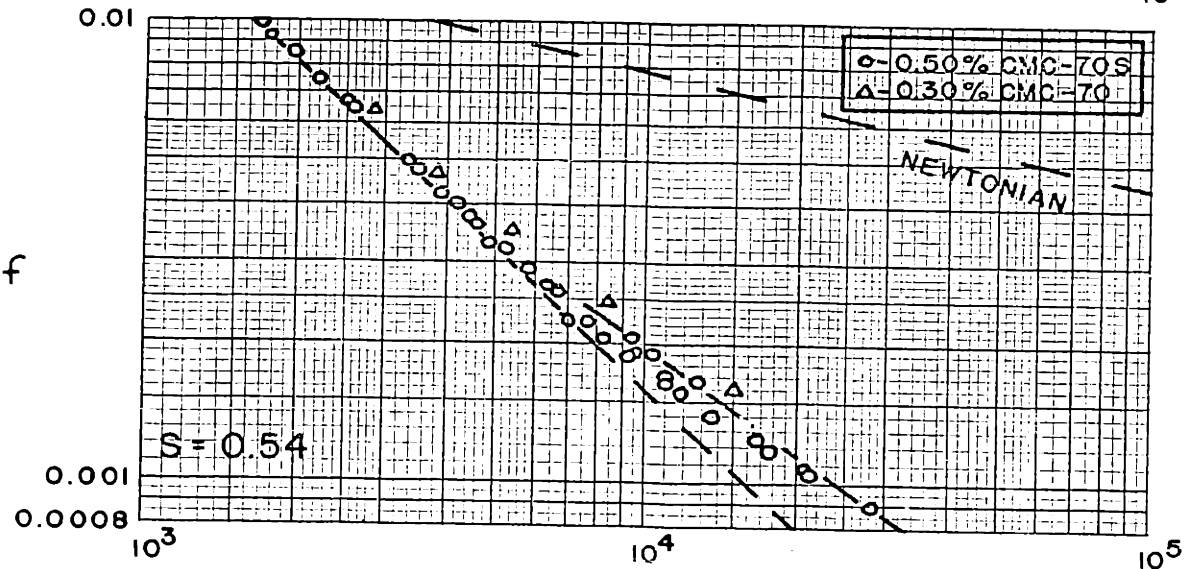
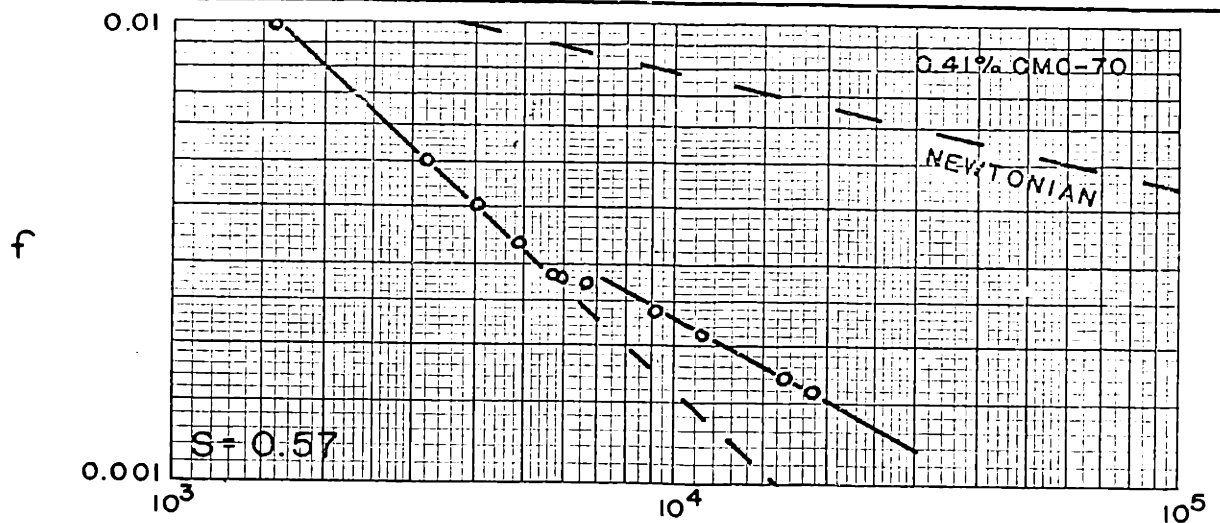
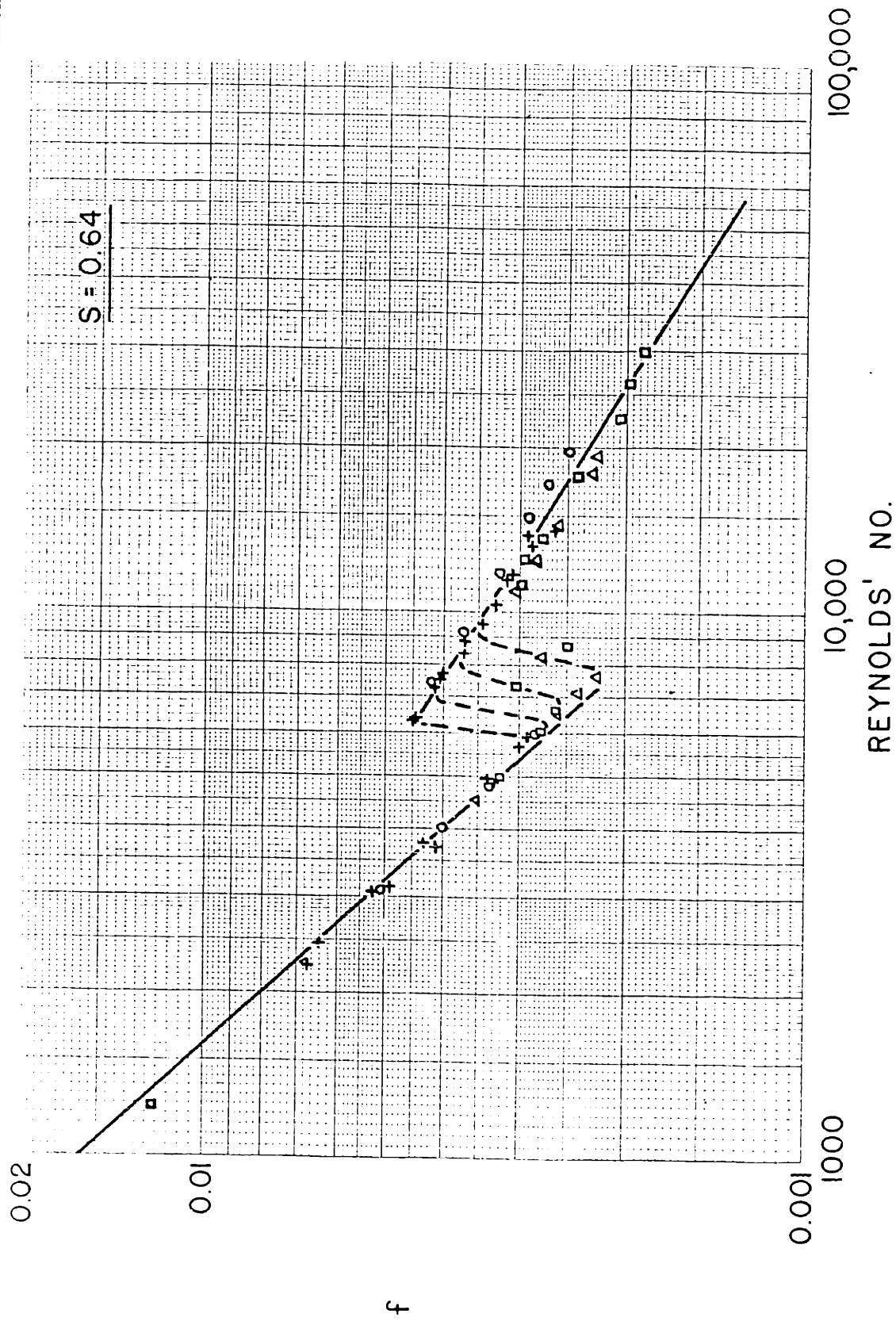


FIGURE 21
FRICTION FACTORS,
 $S = 0.57, 0.54, 0.53$



- Δ - 3/8" DIAM., RUN F4
- \square - 1/2" DIAM., RUN F3
- \circ - 5/8" DIAM., RUN F5
- $+$ - 3/4" DIAM., RUNS F1 & 2

FIGURE 22
EFFECT OF TUBE
ON TRANSITION

Velocity Profiles. Laminar and turbulent velocity profiles were obtained on most of the previously mentioned liquids. No velocity profile data was obtained with the Carbopol 934 solution because of plugging of the impact probe tip, or with the Vistanex in cyclohexane because of the rapid breakdown of the solution, presumably due to scission of the molecules under shear.

In Figures 23 to 25 the laminar profiles are presented as $u/u_{\max.}$ vs. y/R with the theoretical curve drawn according to:

$$u/u_{\max.} = 1 - (1-y/R)^{1/s + 1} \quad (15)$$

In Figures 26 to 31 the turbulent velocity profiles are presented as velocity deficiencies, $(\frac{u_{\max.} - u}{u_*})$, vs. $1-y/R$, with the curve for Newtonian deficiencies drawn.

Figure 32 is a composite plot of all the velocity deficiencies, the radial distance scale being logarithmic. This diagram is meant to demonstrate the logarithmic quality of the velocity distributions of pseudoplastics in turbulent flow.

In Figures 33 to 35 the turbulent velocity profile data is further presented as mixing lengths, l/R , vs. y/R , with the Newtonian mixing length curve drawn. Table 1 summarizes the values of k obtained from the mixing length curves for the various values of s .

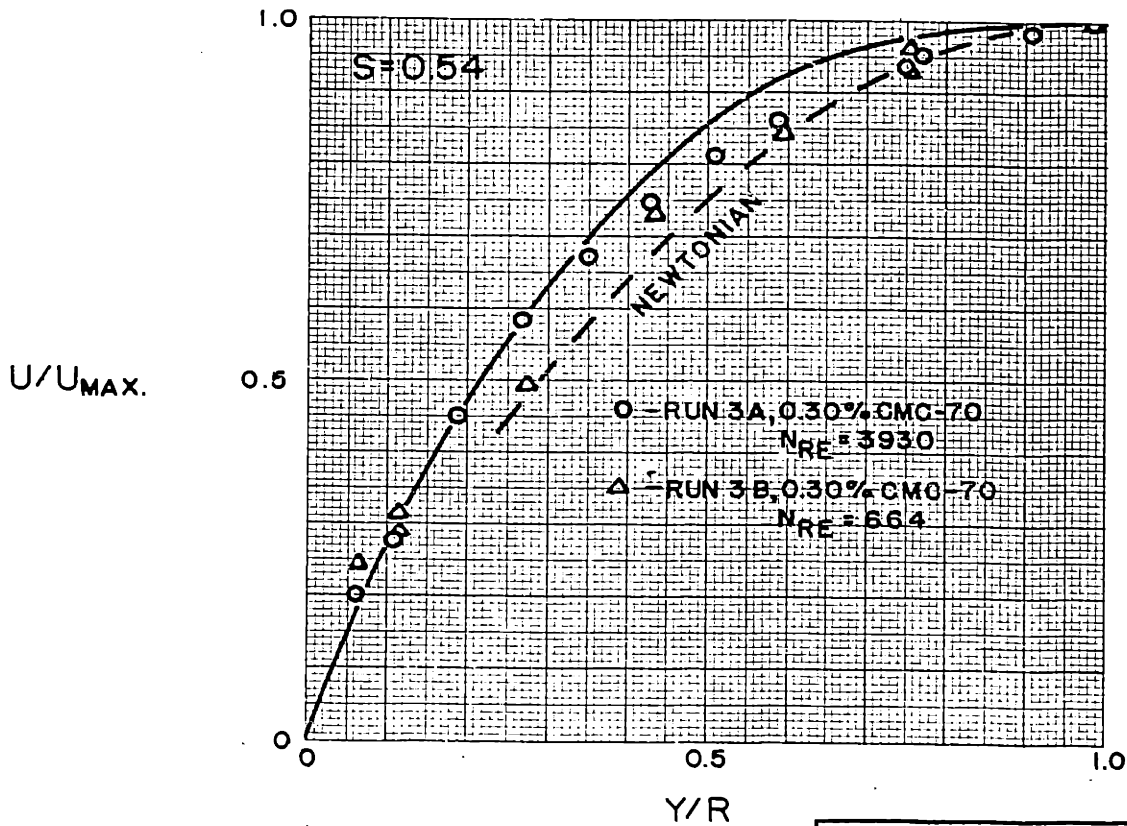
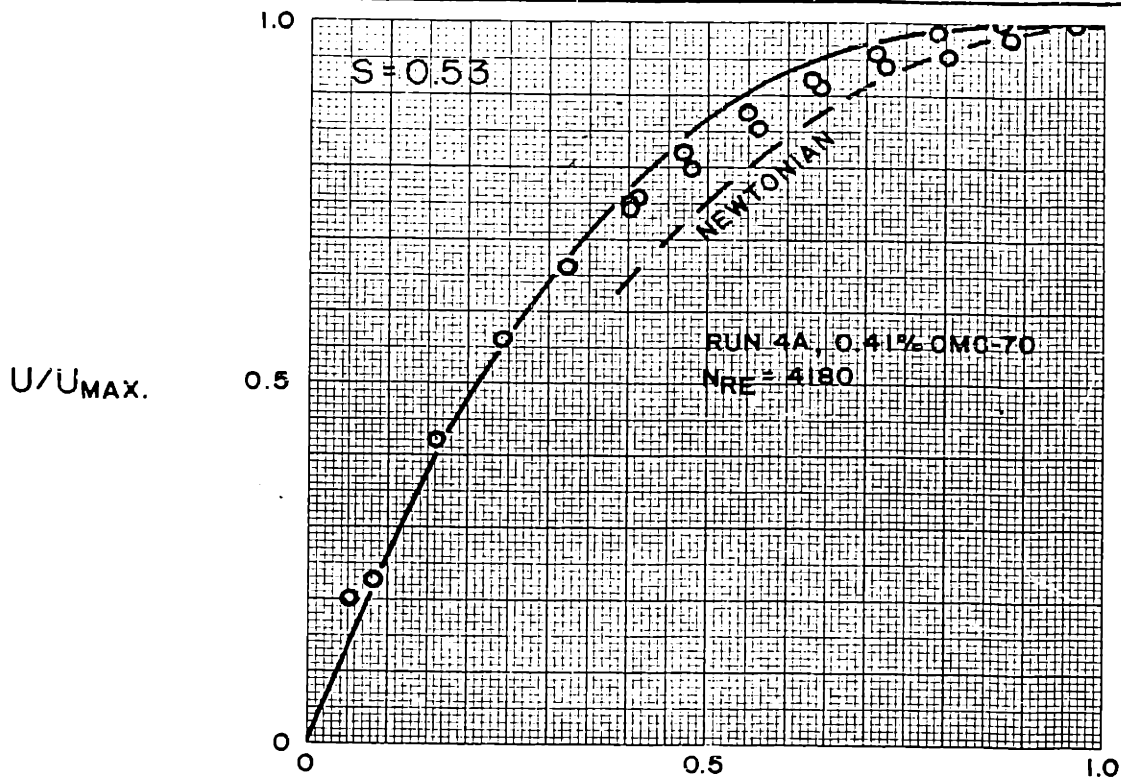


FIGURE 23
 LAMINAR VELOCITY
 PROFILES, CMC-70,
 $S=0.53$ & 0.54

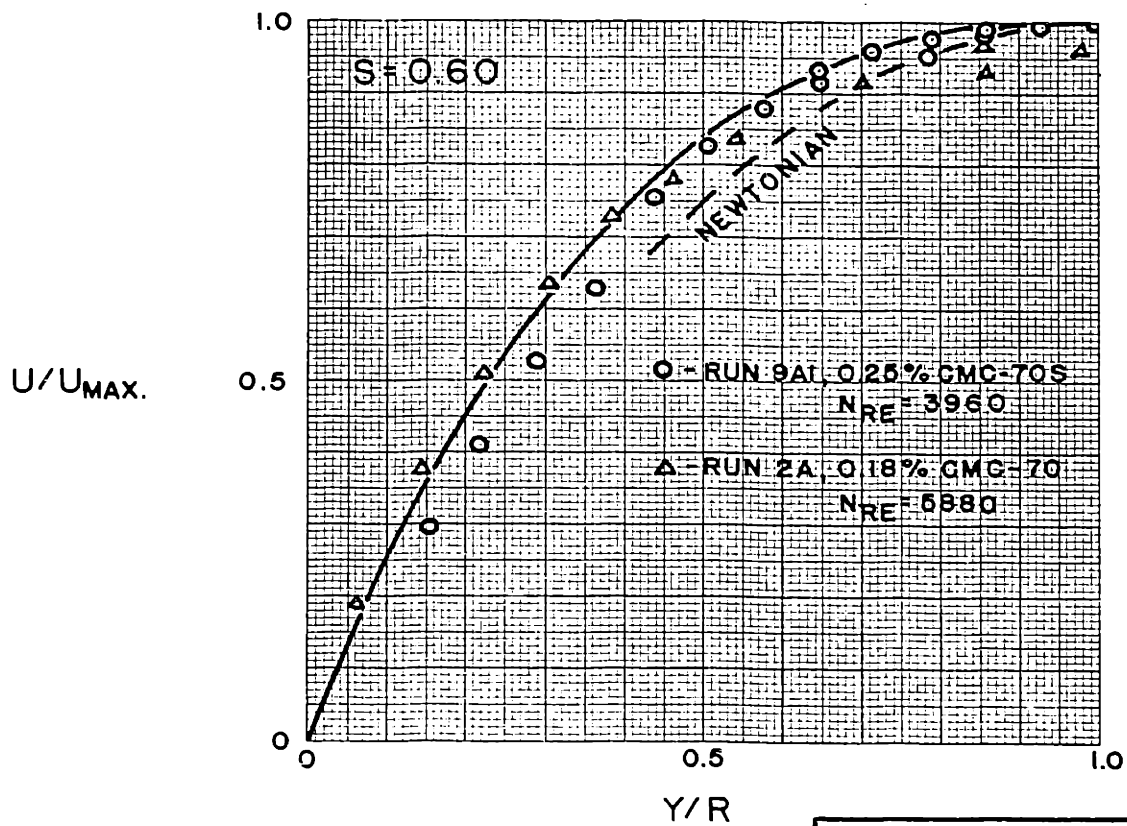
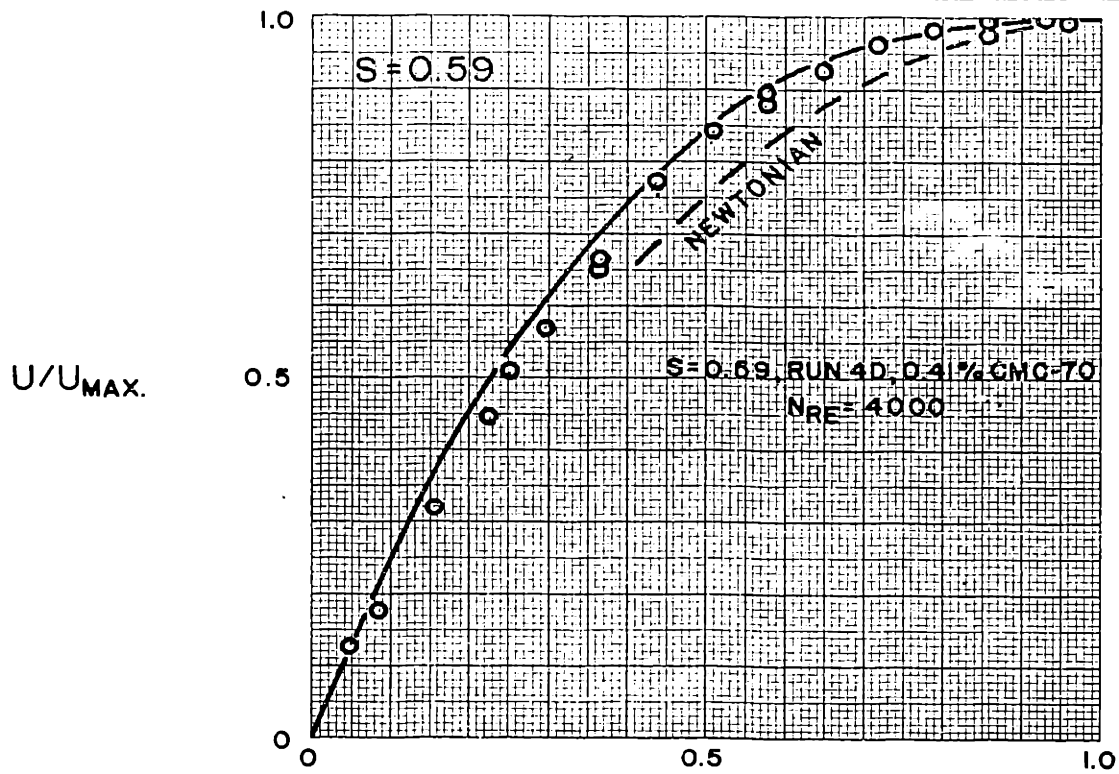


FIGURE 24
LAMINAR VELOCITY
PROFILES,
S = 0.59 & 0.60

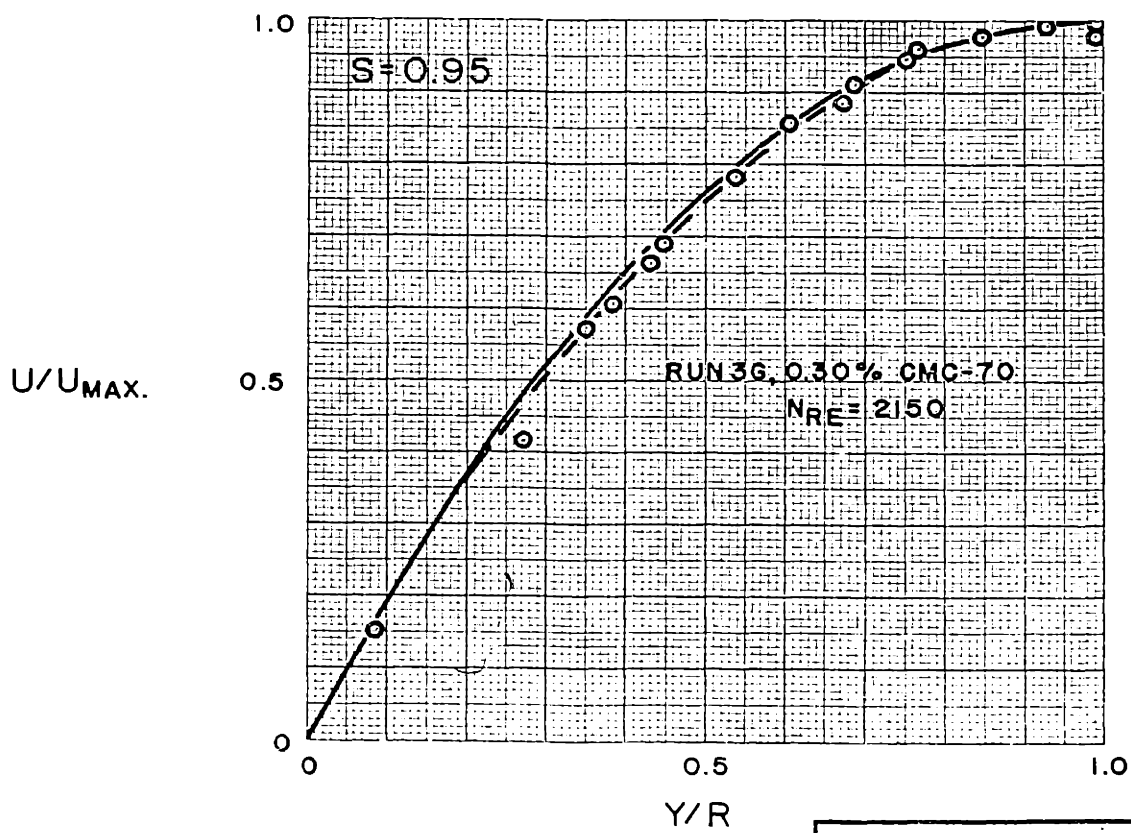
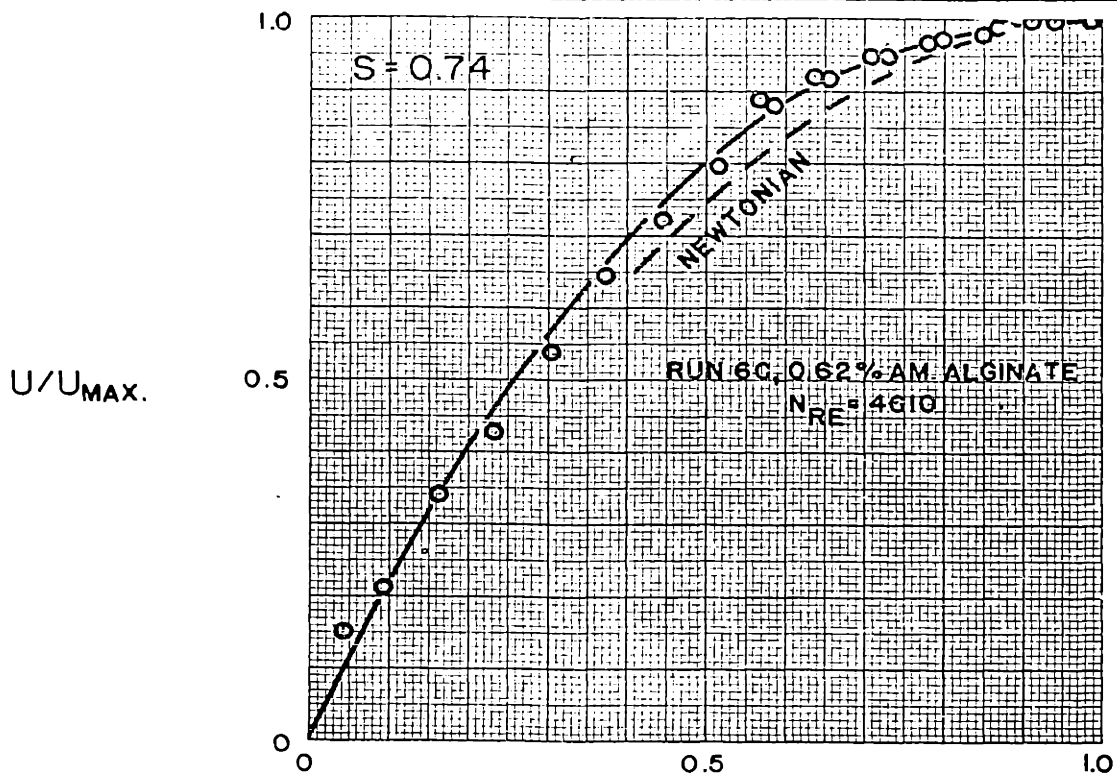


FIGURE 25
LAMINAR VELOCITY
PROFILES,
S = 0.74 & 0.95

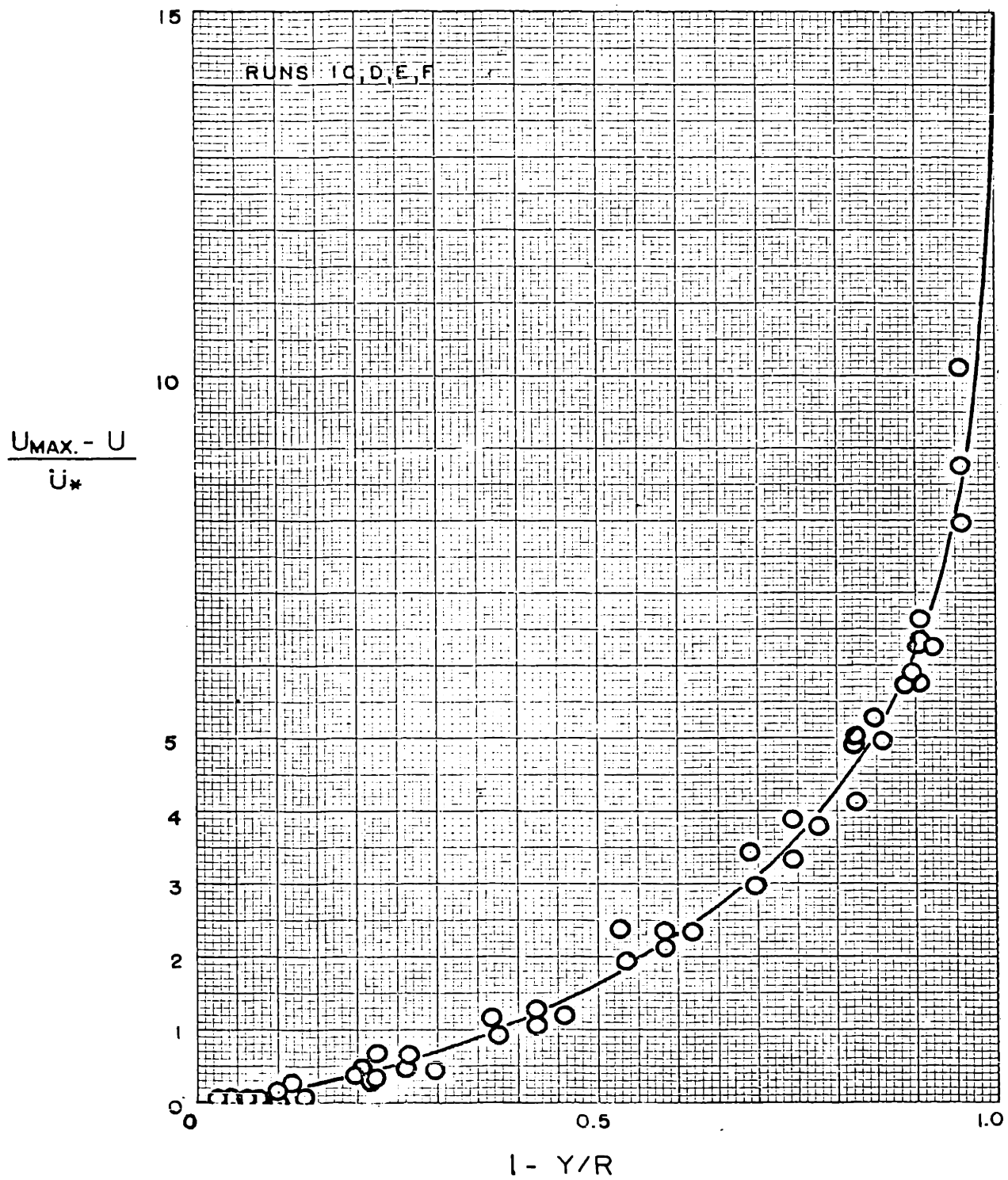


FIGURE 26
 NEWTONIAN VELOCITY
 DEFICIENCY CURVE

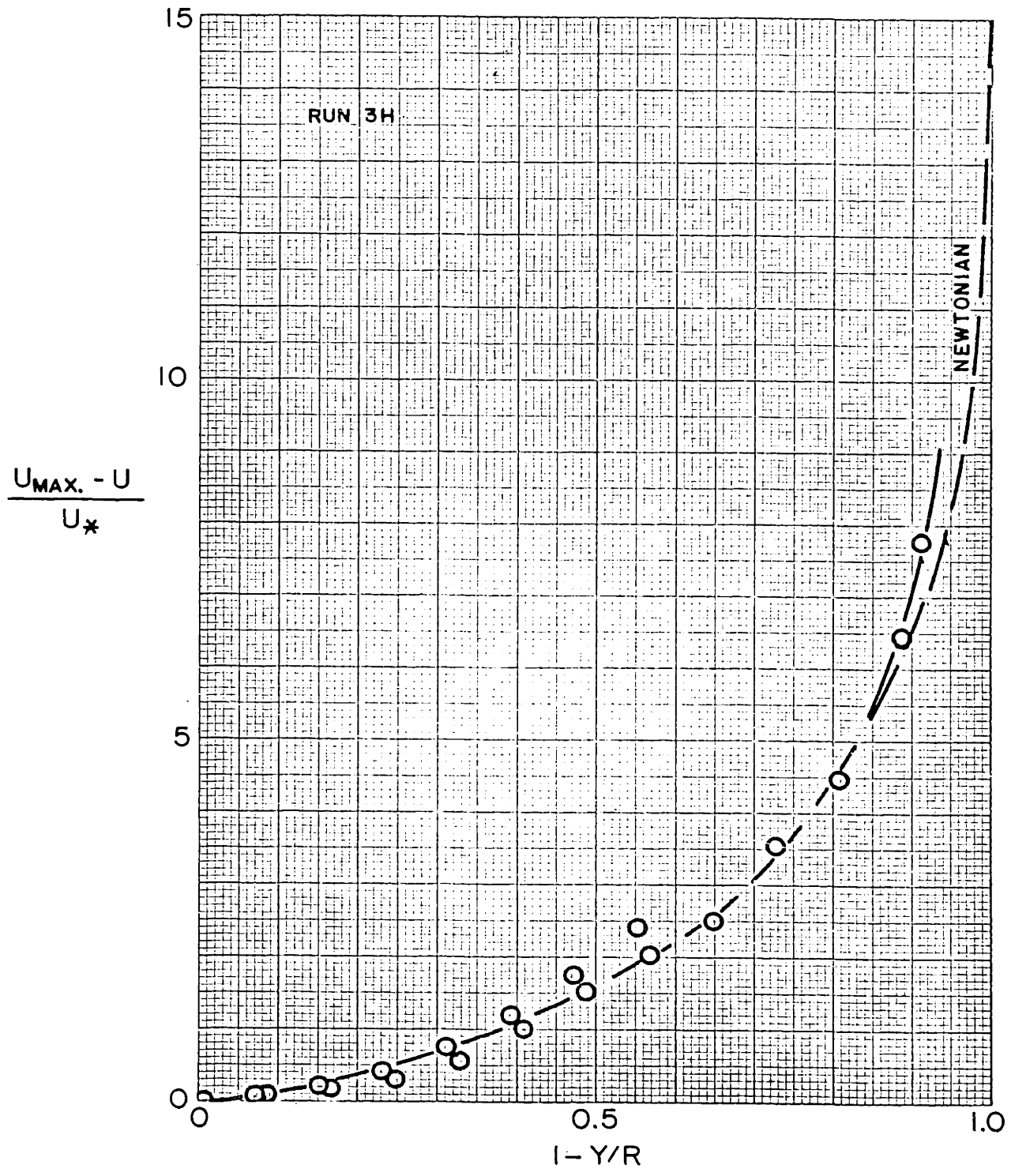


FIGURE 27
 PSEUDOPLASTIC (S=0.85)
 VELOCITY DEFICIENCY

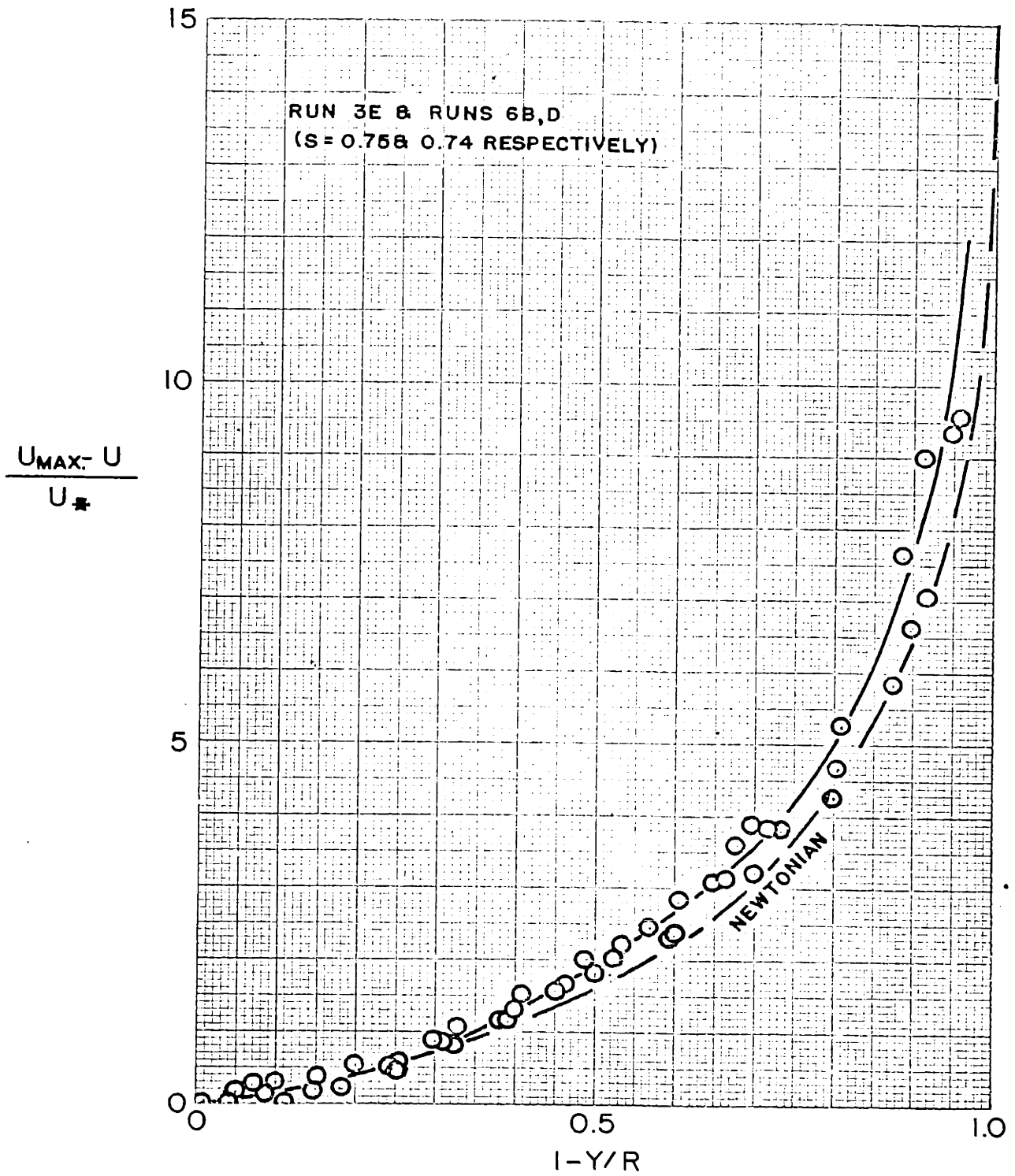


FIGURE 28
PSEUDOPLASTIC (S = 0.75)
VELOCITY DEFICIENCY

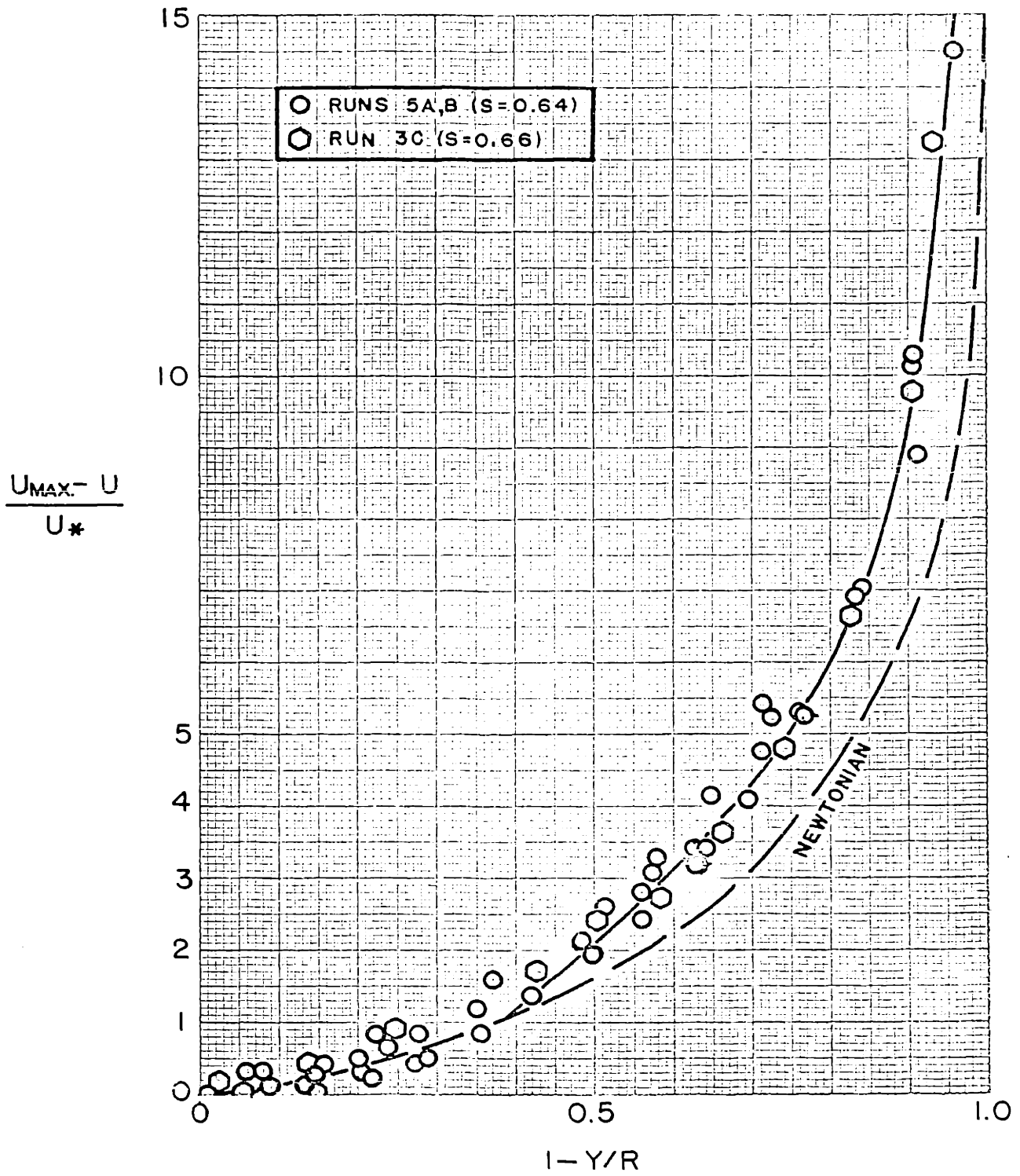


FIGURE 29
 PSEUDOPLASTIC (S=0.65)
 VELOCITY DEFICIENCY

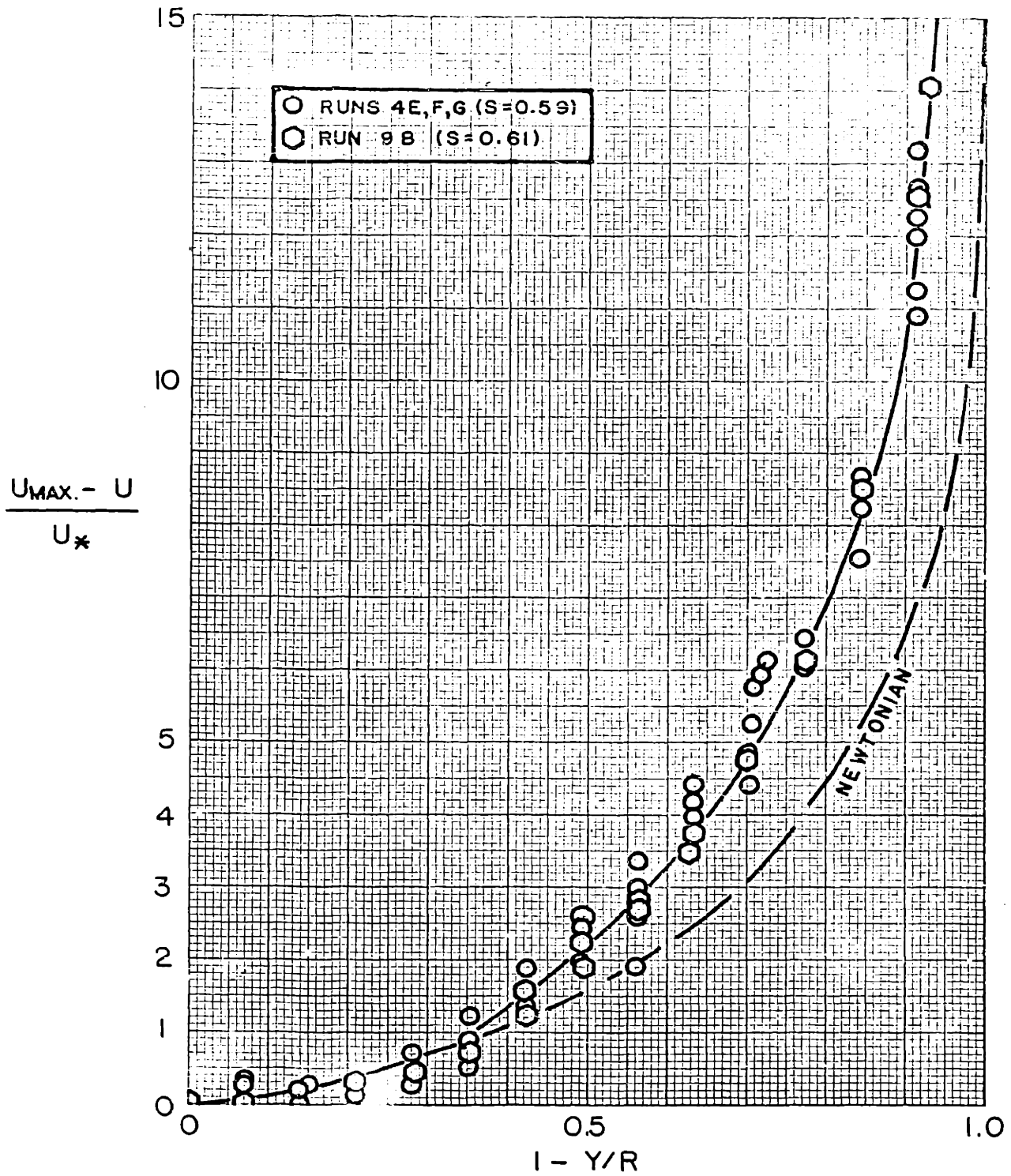


FIGURE 30
 PSEUDOPLASTIC (S=0.60)
 VELOCITY DEFICIENCY

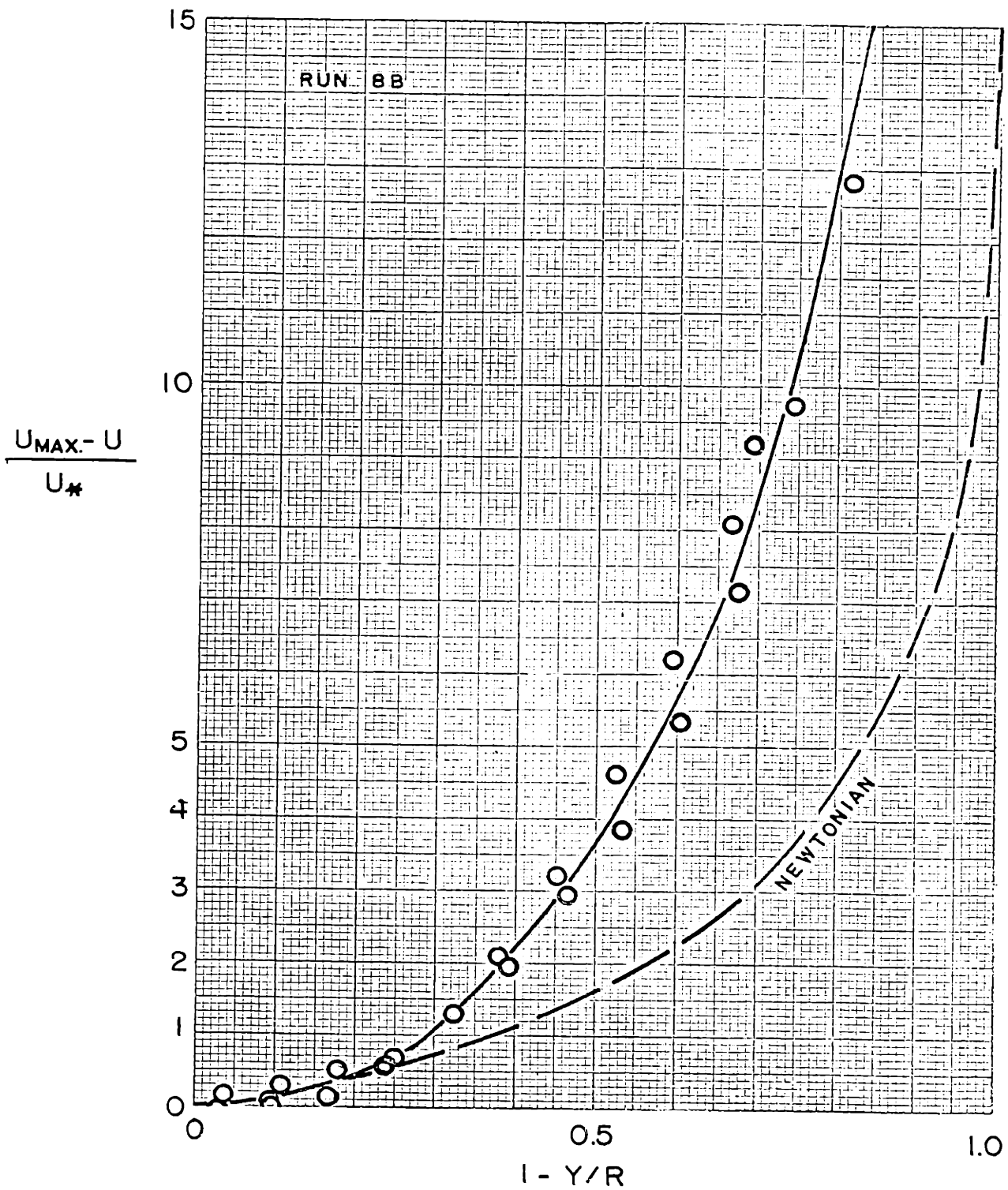
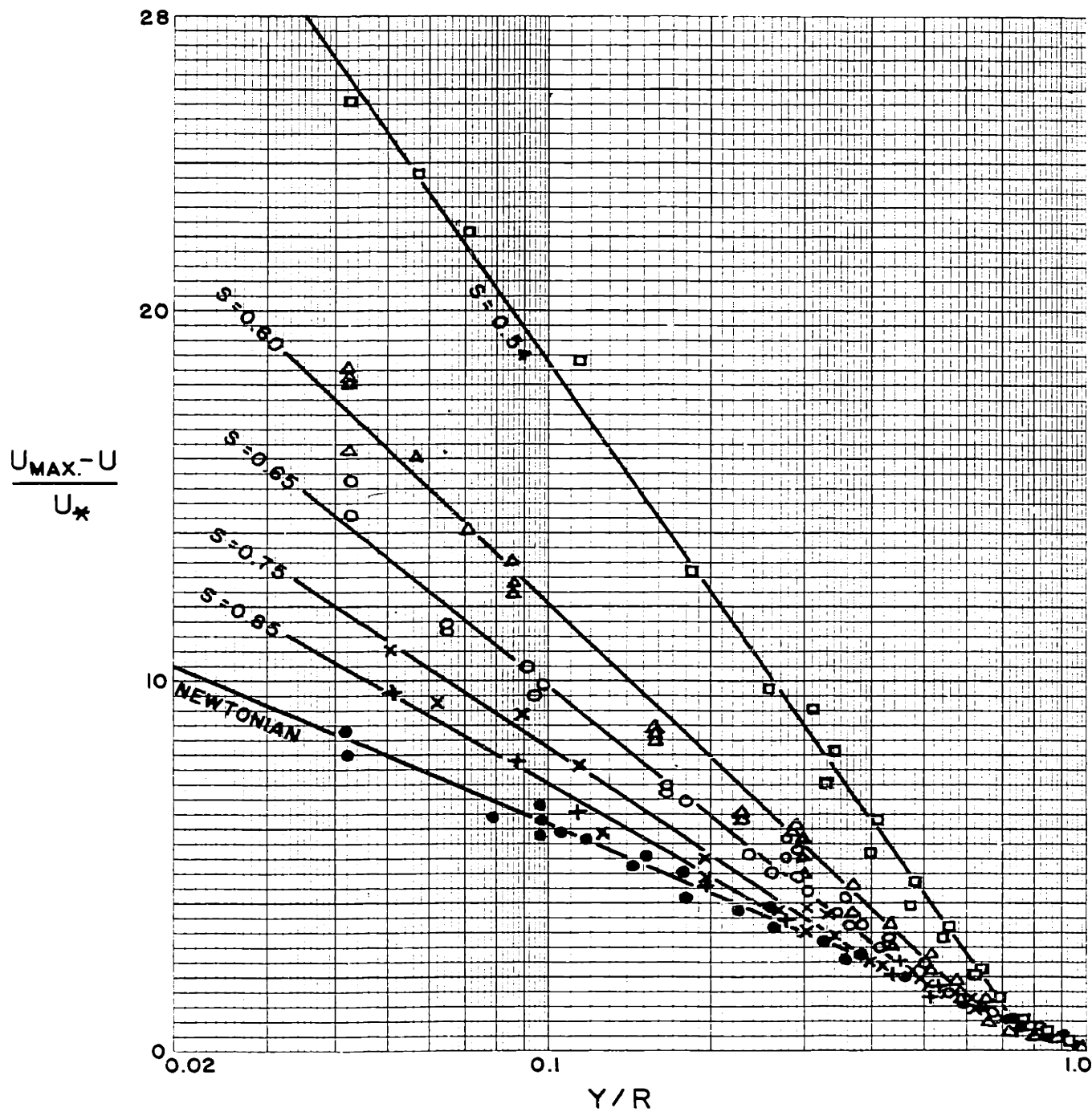


FIGURE 31
 PSEUDOPLASTIC (S=0.54)
 VELOCITY DEFICIENCY



WHERE $U_* = \sqrt{\tau_w/\rho}$

- \square - RUN 8B
- \triangle - RUNS 4E, F, G & 9B
- \circ - RUNS 5A, B & 3C
- \times - RUNS 3E & 6B, D
- $+$ - RUN 3H
- \bullet - RUNS 1C, D, E, F

FIGURE 32
LOGARITHMIC
DISTRIBUTION
OF
DEFICIENCIES

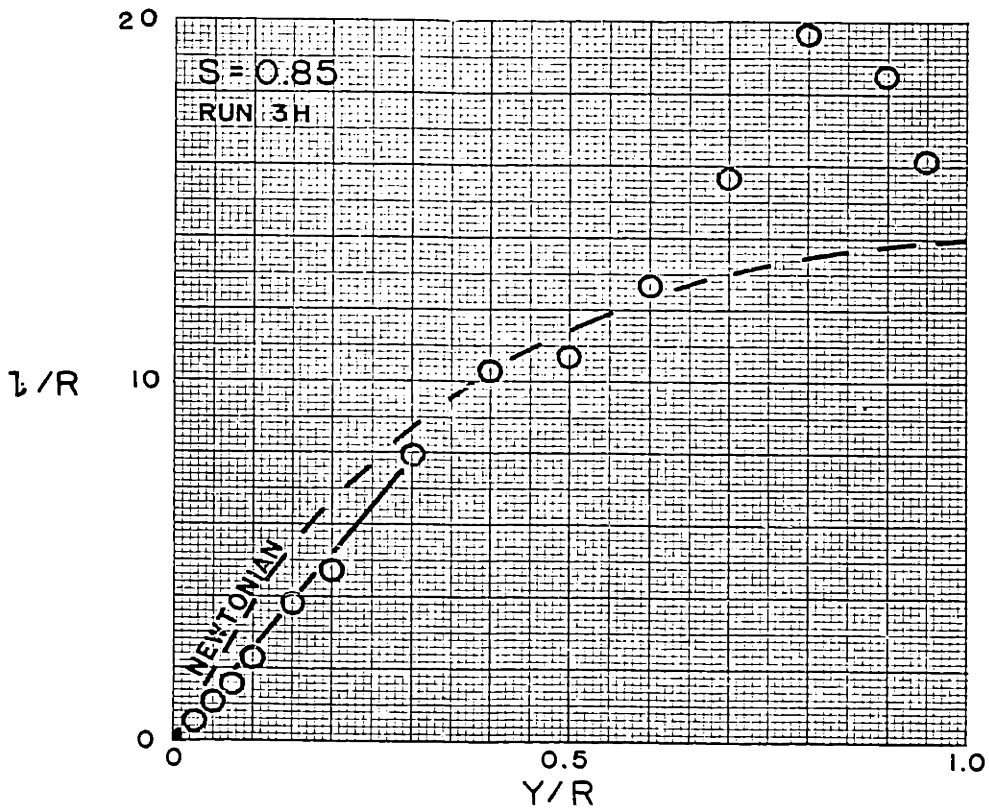
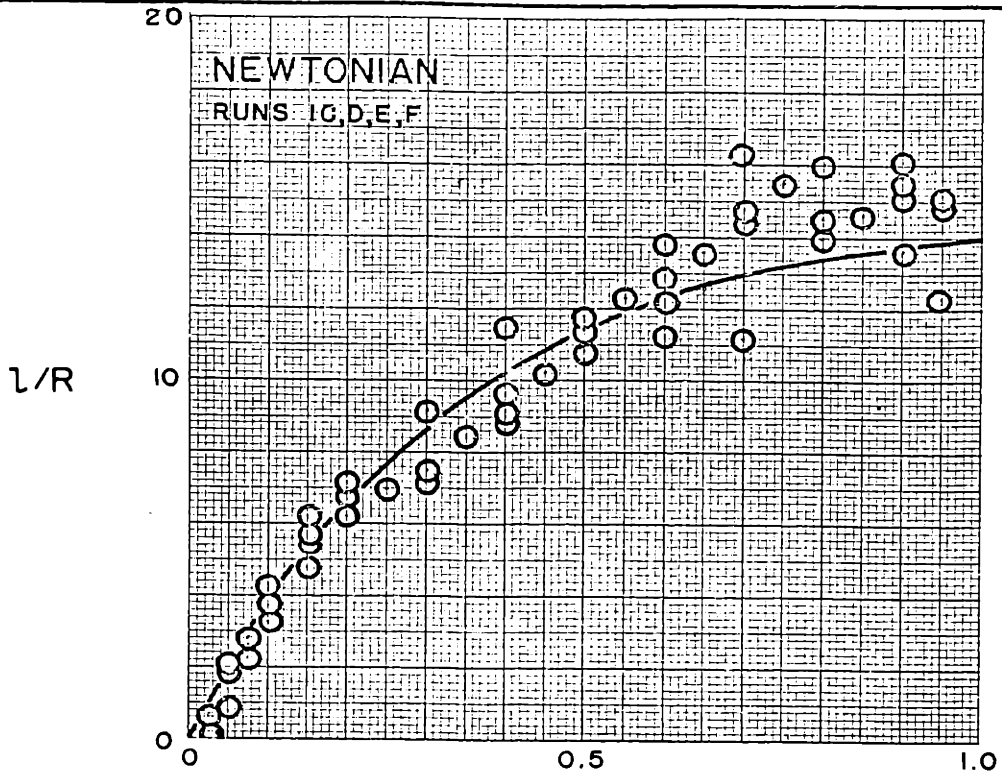


FIGURE 33
MIXING LENGTHS,
NEWTONIAN AND
 $S = 0.85$

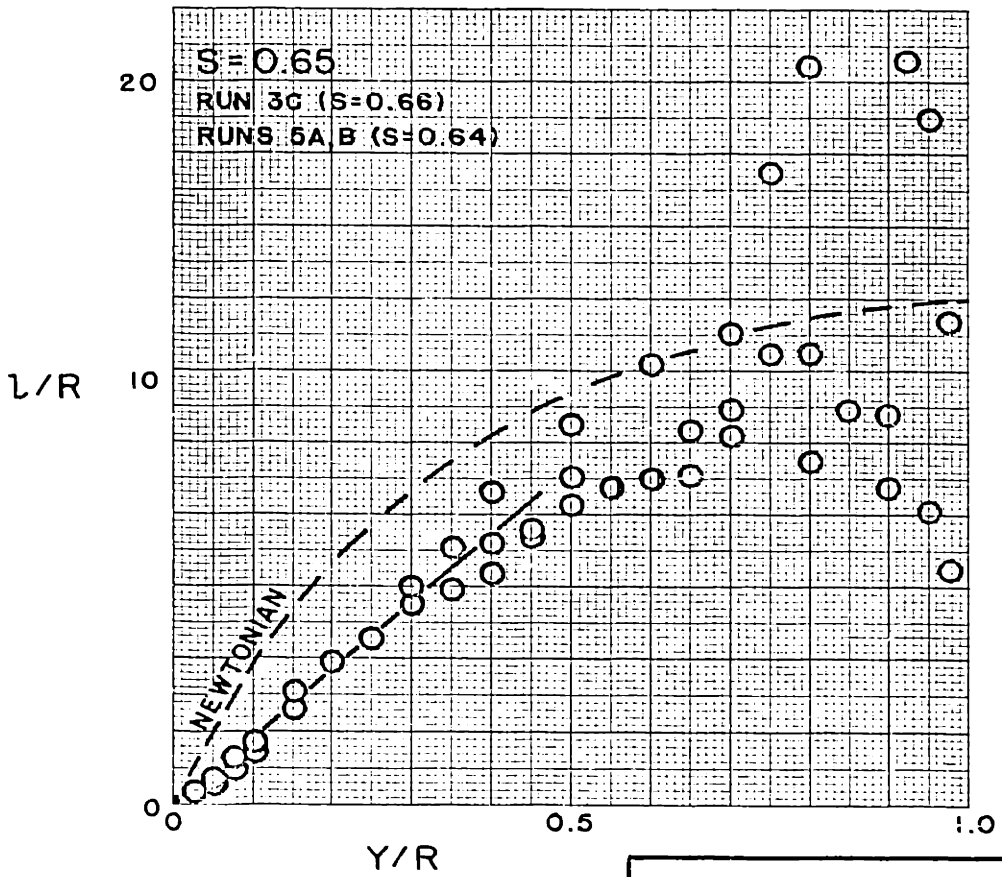
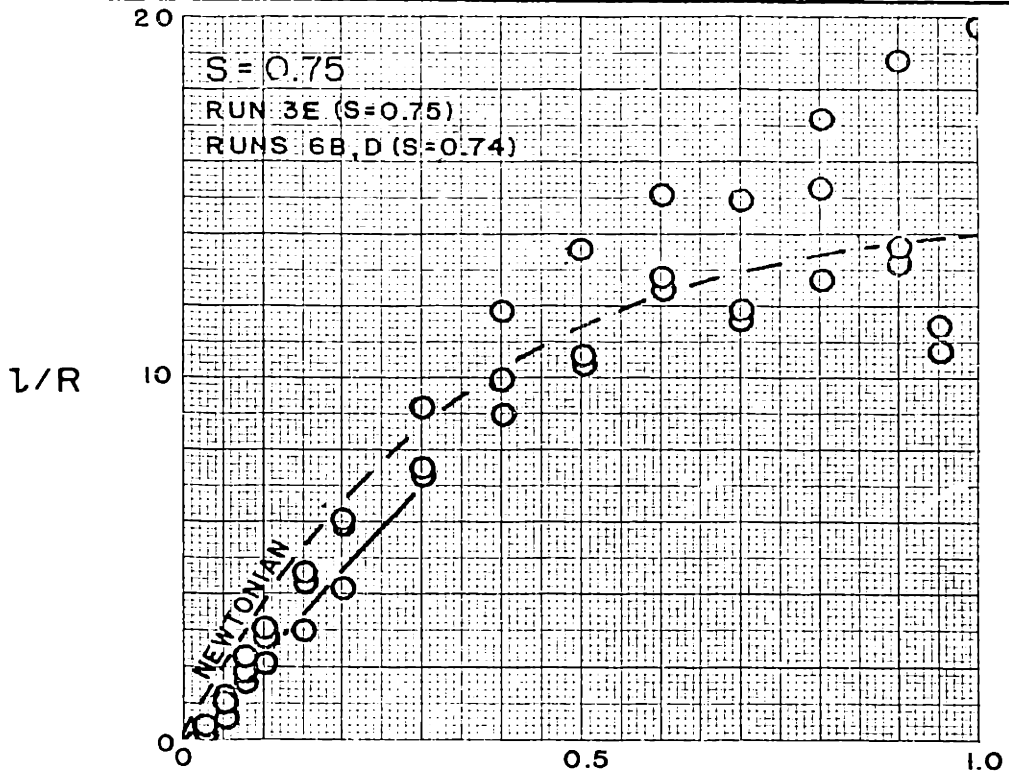


FIGURE 34
 MIXING LENGTHS,
 $S = 0.75$ AND 0.65

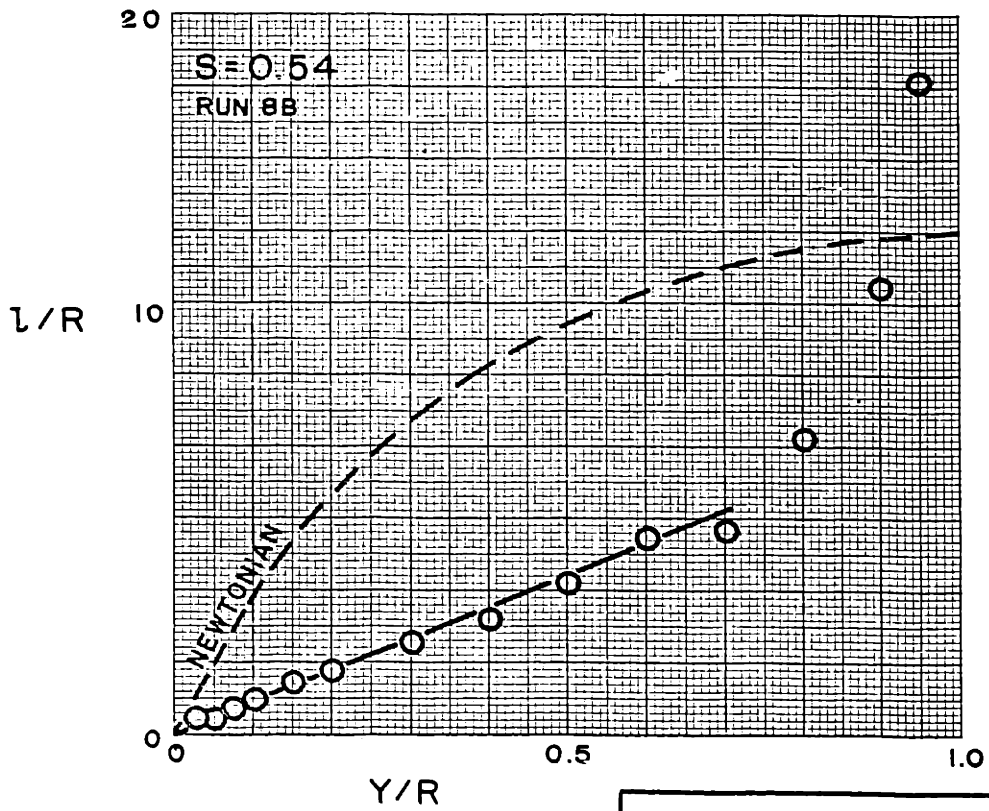
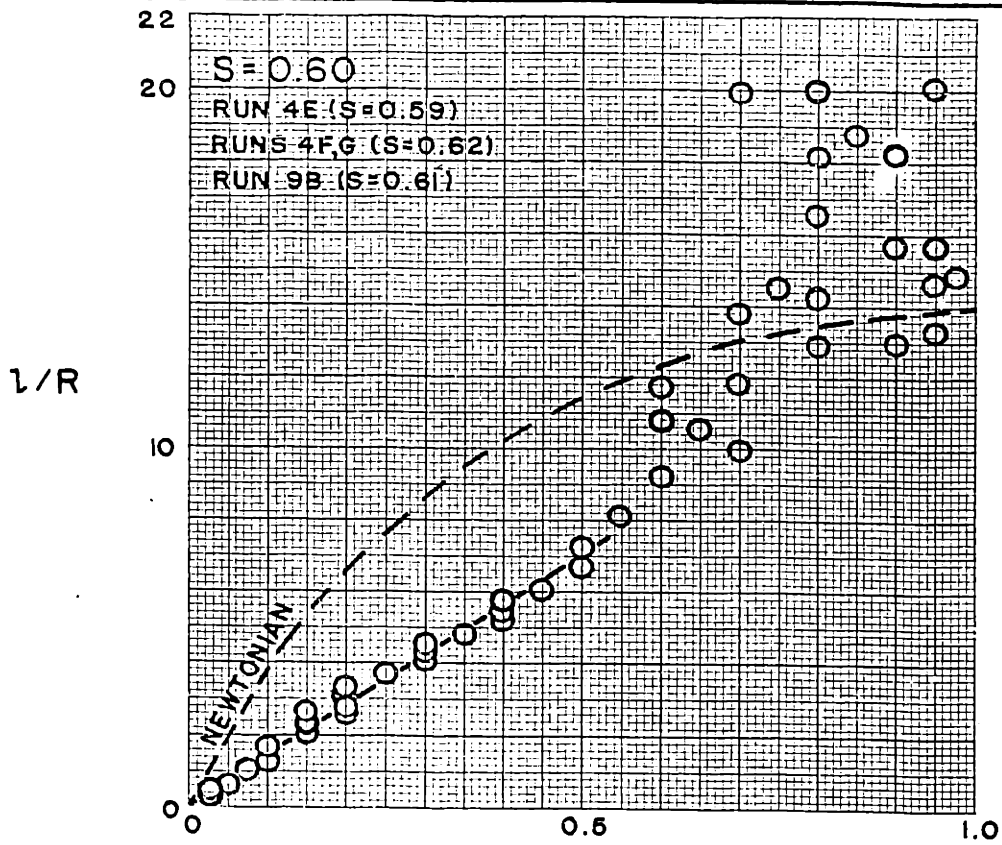


FIGURE 35
 MIXING LENGTHS,
 $S = 0.60$ AND 0.54

TABLE I: Mixing Length Constants (k)

s	Run No.	k	N_{Re}
1.00	1-C	0.40	82,600
"	1-D	0.35	9,600
"	1-E	0.38	19,700
"	1-F	0.37	176,000
0.85	3-H	0.25	17,000
0.75	3-E	0.21	10,500
0.74	6-B	0.27	7,540
"	6-D	0.30	9,680
0.68	3-D	0.17	9,500
0.66	3-C	0.15	14,600
0.64	5-A	0.16	8,800
"	5-B	0.18	12,700
0.62	4-F	0.14	8,400
"	4-G	0.16	14,300
0.61	9-B	0.14	11,300
0.59	4-E	0.14	12,200
0.54	8-B	0.09	8,780

Eddy Viscosity. Figure 36 presents a typical comparison of the eddy viscosity to molecular viscosity ratio for a highly pseudoplastic liquid and for a Newtonian one. The ratio was calculated by the relation:

$$\epsilon/\mu = \frac{\tau_w(1-y/R)}{\mu(du/dy)} - 1 \quad (36)$$

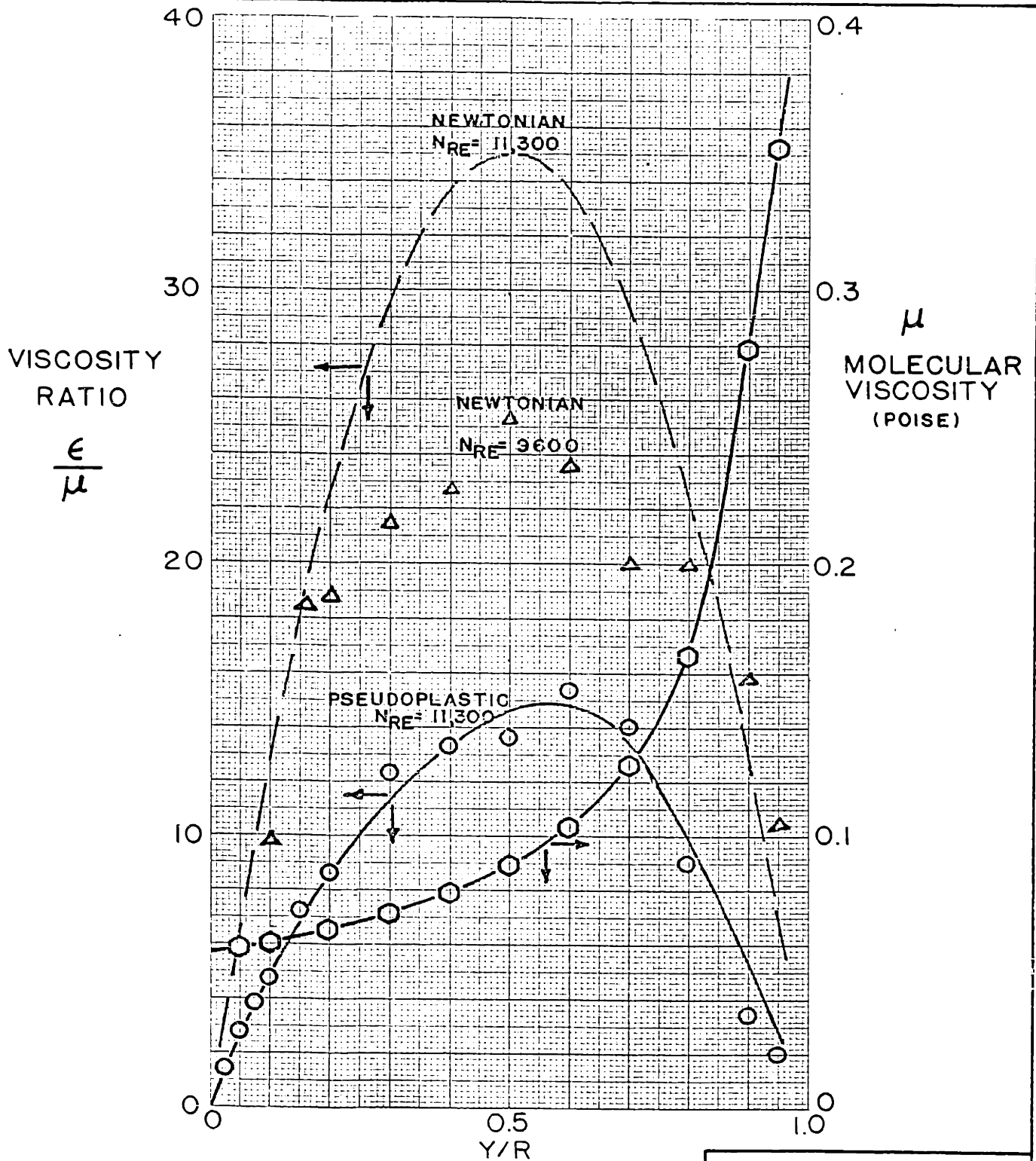
The viscosities for the pseudoplastic liquid were calculated by obtaining the shear stress locally:

$$\tau = \tau_w(1-y/R) \quad (37)$$

then reading the corresponding du/dy from the viscometric curve and dividing one by the other:

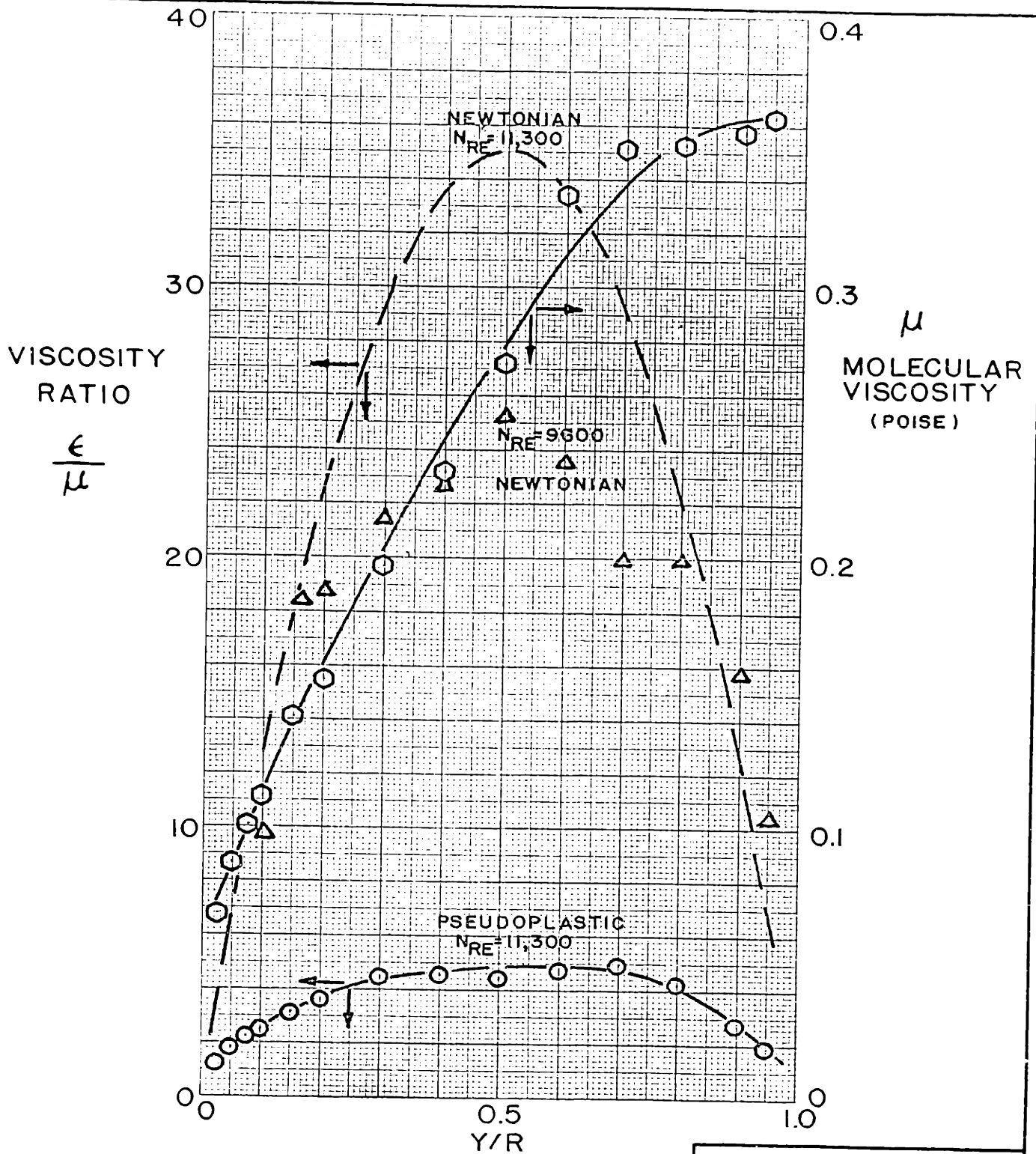
$$\mu = \tau/(du/dy) \quad (8)$$

Figure 37 presents the same information except that the pseudoplastic viscosities were calculated by taking the du/dy from the velocity profile and reading the corresponding τ from the viscometric curve. It is not all clear which of these two methods gives the more valid molecular viscosity at a point for a pseudoplastic in turbulent flow, and it is quite possible that neither is valid due to transient effects.



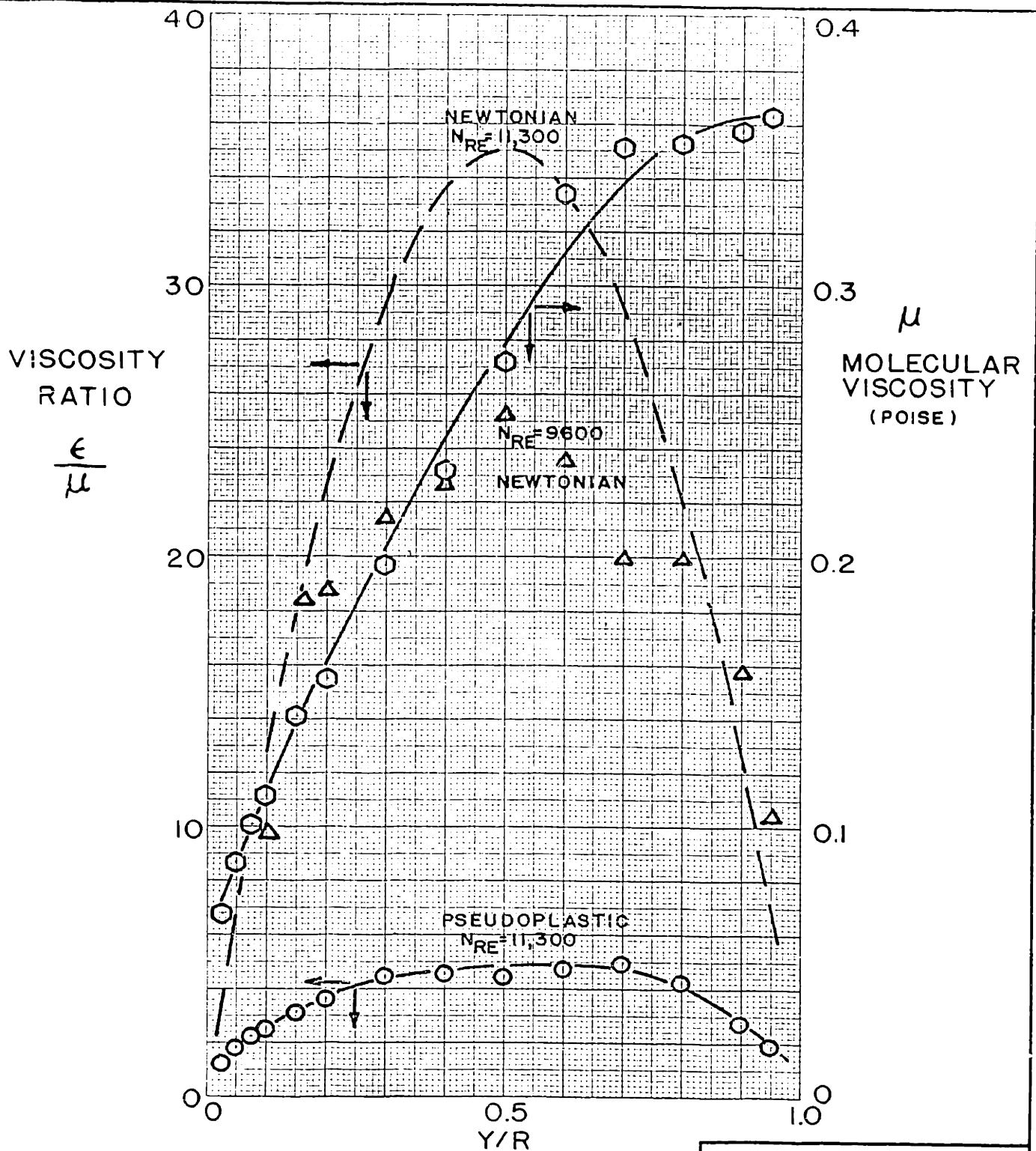
○ - RUN 9B, $N_{RE} = 11,300$, $S = 0.61$, $B = 2.22$
 Δ - RUN 10, $N_{RE} = 9600$, $\mu = 0.00905$ POISE, $S = 1.00$
 ○ - VISCOSITY FOR RUN 9B, BASED ON $\tau = \tau_w(1-Y/R)$ AND VISCOMETER DATA
 --- $\frac{\epsilon}{\mu} = N_{RE} \sqrt{f/2} \cdot K/2 \cdot (Y/R)(1-Y/R)$, WHERE $K = 0.4$ AND $N_{RE} = 11,300$

FIGURE 36
 COMPARISON OF
 NEWTONIAN AND
 PSEUDOPLASTIC
 EDDY VISCOSITIES
 AT CONSTANT N_{RE}
 - BASED ON τ



○ - RUN 9B, $N_{RE} = 11,300$, $S = 0.61$, $B = 2.22$
 △ - RUN 1D, $N_{RE} = 9600$, $\mu = 0.00905$ POISE, $S = 1.00$
 ○ - VISCOSITY FOR RUN 9B, BASED ON PROFILE μ/μ_R AND VISCOMETER DATA
 --- $\frac{\epsilon}{\mu} = N_{RE} \sqrt{Y/2} \cdot K/2 \cdot (Y/R)(1-Y/R)$, WHERE $K = 0.4$ AND $N_{RE} = 11,300$

FIGURE 37
 COMPARISON OF
 NEWTONIAN AND
 PSEUDOPLASTIC
 EDDY VISCOSITIES
 AT CONSTANT N_{RE}
 --- BASED ON μ/μ_R

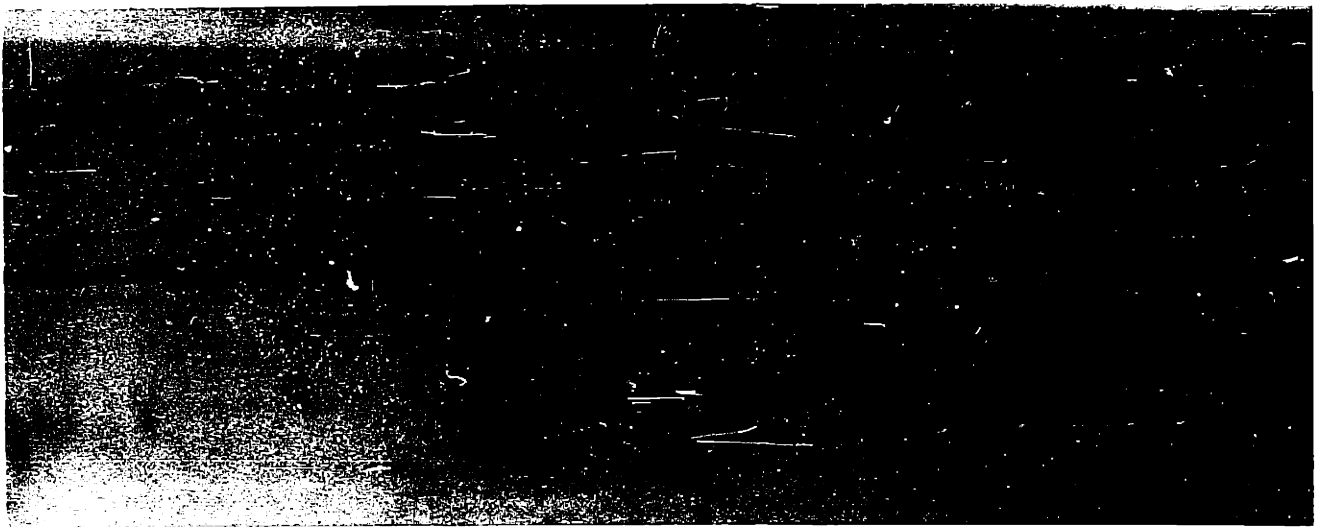


○ - RUN 9B, $N_{RE} = 11,300$, $S = 0.61$, $B = 2.22$
 △ - RUN 1D, $N_{RE} = 9600$, $\mu = 0.00905$ POISE, $S = 1.00$
 ○ - VISCOSITY FOR RUN 9B, BASED ON PROFILE μ/P AND VISCOMETER DATA
 --- $\frac{\epsilon}{\mu} = N_{RE}^{1/2} \cdot K/2 \cdot (Y/R)(1-Y/R)$, WHERE $K = 0.4$ AND $N_{RE} = 11,300$

FIGURE 37
 COMPARISON OF
 NEWTONIAN AND
 PSEUDOPLASTIC
 EDDY VISCOSITIES
 AT CONSTANT N_{RE}
 —BASED ON μ/P

Dye Injection. The Figures 38 to 44 contain the photographic results of the injection of pigmented solution in the flowing stream either at the center of the tube at its entrance or at the side of the tube from a wall tap. The liquids so studied were both water and sodium carboxymethylcellulose solutions. This was designed to give observations under the same generalized conditions of both Newtonian flow and pseudoplastic flow of almost the greatest degree of pseudoplasticity studied ($s = 0.54$). The alginate solutions were too dense optically to yield good photographs at a high degree of pseudoplasticity, the Carbopol solution was too small in volume and too unstable to stand recycling with addition of dye, and the polyisobutylene solution would affect the Lucite tube if it had been used for this type of experiment.

The exposure for all the photographs presented was 40 micro-seconds.



← FLOW

INJECTION 185 DIAMETERS UPSTREAM

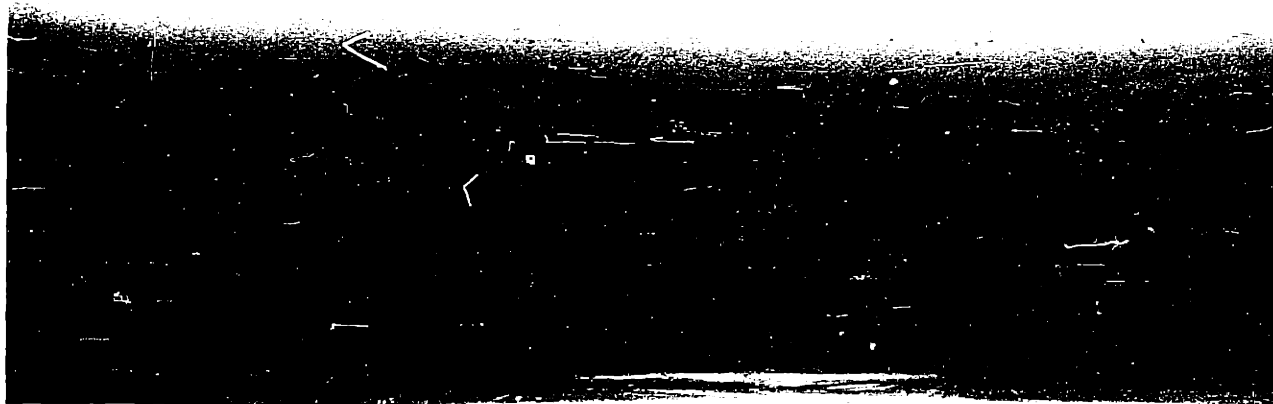
FIGURE 38
LAMINAR FLOW,
DYE INJECTION
AT TUBE CENTER



← FLOW

INJECTION 1/2 DIAMETER UPSTREAM OF
EDGE OF PHOTO

FIGURE 39
LAMINAR FLOW,
DYE INJECTION
AT TUBE WALL

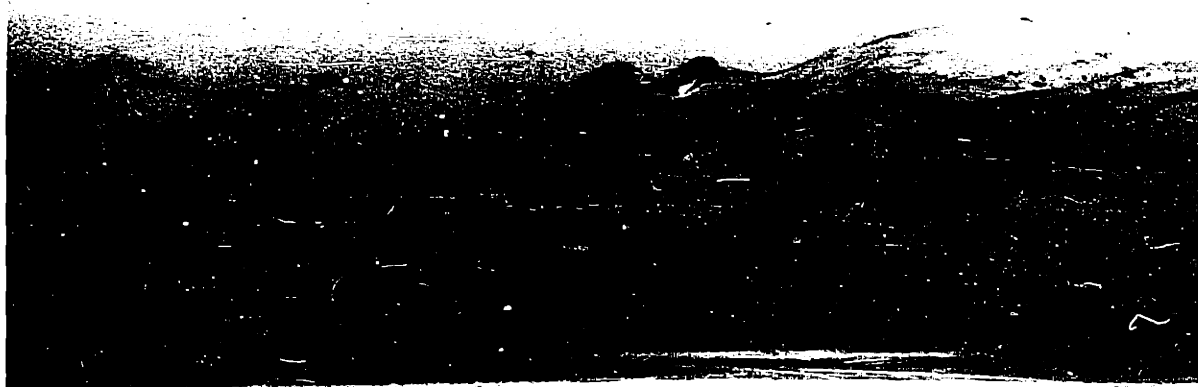


← FLOW

WATER, $N_{RE} = 3720$

INJECTION 185 DIAMETERS UPSTREAM

FIGURE 40
NEWTONIAN
TURBULENT FLOW,
DYE INJECTION AT
TUBE CENTER



← FLOW

0.25% CMC-70S, $N_{RE} = 8400$, $S = 0.61$

INJECTION 185 DIAMETERS UPSTREAM

FIGURE 41
PSEUDOPLASTIC
TURBULENT FLOW,
DYE INJECTION AT
TUBE CENTER

$N_{RE} = 10,600$



← FLOW

$N_{RE} = 12,800$



← FLOW

0.25% CMC-70S, $S = 0.61$

INJECTION 185 DIAMETERS UPSTREAM

FIGURE 42
PSEUDOPLASTIC
TURBULENT FLOW,
HIGHER N_{RE} ,
DYE INJECTION AT
TUBE CENTER



← FLOW

WATER, $N_{RE} = 3720$

INJECTION 1/2 DIAMETER UPSTREAM OF
EDGE OF PHOTO

FIGURE 43
NEWTONIAN
TURBULENT FLOW,
DYE INJECTION AT
TUBE WALL



← FLOW

0.25% CMC-70S, $N_{RE} = 12,800$, $S = 0.61$

INJECTION 1/2 DIAMETER UPSTREAM OF
EDGE OF PHOTO

FIGURE 44
PSEUDOPLASTIC
TURBULENT FLOW,
DYE INJECTION AT
TUBE WALL

Observations. During the course of the runs involving the more pseudoplastic liquids (s less than 0.7), it was noted that the manometers measuring the friction pressure drop would oscillate when the flow rate reached the transition range. This oscillation appeared to be roughly between values which would correspond to laminar flow extrapolated and turbulent flow extrapolated. Several calculations carried out on these extreme values generally confirmed this, although the manometer column would tend to "overshoot" under some conditions.

With fluids of intermediate degree of pseudoplasticity (about $s = 0.8$), this oscillation would be less pronounced and the extreme values often corresponded to friction factors between laminar and turbulent.

With fluids of Newtonian behavior or nearly so, it was noted that the manometers in this range would flutter slightly. Occasionally there was gross oscillation in this range with these fluids.

The magnitude of these oscillations seemed to be roughly inversely proportional to the difference in density between the liquid in the tube and the manometer liquid for a given flow condition. That is, depending on whether mercury or carbon tetrachloride were in the manometers, the oscillations would be less or greater, respectively.

Upon entering the turbulent region of flow, this oscillation or flutter would increase in frequency and decrease in magnitude until the manometers were completely quiet to the eye with fluids of Newtonian

behavior and with those of slightly or moderately pseudoplastic behavior. But with the highly pseudoplastic liquids tested (s less than 0.6), a very slight flutter would persist as far into the turbulent region as the experiment could be pushed. The magnitude of this flutter with a mercury manometer would be much less than 1 mm. The frequency of this turbulent range flutter was estimated to be about 10 cycles per second.

In the runs concerned with velocity profiles, the impact pressure manometer would be observed to undergo the same very slight flutter in turbulent flow of the very pseudoplastic liquids. This flutter would not occur under any other conditions except transition flow, in which no velocity profiles were made.

During the turbulent flow range in each run, the liquid in the test section could be heard to "gush" by placing the ear against the tube wall. This gushing noise was not present during the laminar flow of any liquid tested and tended to be relatively less for the highly pseudoplastic liquids than for any others, although no attempt was made to measure this quantitatively.

V. DISCUSSION OF RESULTS

A. Rheological Curves

It can be seen from the rheological curves of the fluids that were studied that they fit the pseudoplastic power model,

$$\tau = b(du/dy)^s \quad (7)$$

very well over rather large ranges of shear rate. However, with all fluids tested, there was a greater or lesser tendency for the curve to become more Newtonian toward low shear rates. Thus, for example, the 0.25% CMC-70S was highly pseudoplastic at high shear ($s = 0.61$), but was essentially Newtonian in the very low shear range. On the other extreme, the ammonium alginate solutions were shown to be moderately pseudoplastic in both shear rate regions, being somewhat more Newtonian in the lower range. Table 2 summarizes the differences between the pseudoplasticities at low and high shear rate and compares them.

The problem brought about by the change of the degree of pseudoplasticity, s , over a large range of shear rates is that of deciding which rheological constants, b and s , to use when computing the Reynolds Number for a given pipe-line condition. Since, in flow in a pipe, shear stress varies from a maximum at the wall to zero at the center of the pipe, there is actually an infinite range of shear conditions present.

Based on the pipe-line flow results in laminar flow, which will

TABLE 2: Summary of Differences in Pseudoplasticity between Low and High Shear Rate Ranges.

Liquid	High Range s	Low Range s	Δs	Pseudoplasticity Decrease
				$\frac{s_{low} - s_{high}}{1.00 - s_{high}}$
0.25% CMC-70S	0.61	1.00	0.39	100.0%
0.52% Vistanex	0.71	0.98	0.27	93.1%
0.18% CMC-70	0.60	0.86	0.26	65.0%
0.41% CMC-70	0.53	0.83	0.30	63.9%
0.12% Carbopol	0.78	0.85	0.07	31.8%
0.46% Alginate	0.82	0.86	0.04	22.2%
0.83% Alginate	0.73	0.78	0.05	18.5%

be discussed in the next section, it was decided to use the rheological constants in the shear range represented by the wall shear stress. This can be rationalized two ways: (1) the friction factors vs. Reynolds Numbers calculated this way follow the accepted $f = 16/N_{Re}$ with excellent precision in laminar flow (13,31,33) and (2) the amount of fluid undergoing shear of the order of magnitude of the wall shear stress is much greater than the amount of fluid undergoing shear of the order of magnitude of the stress at the center of the tube because the greater amount of material is present in the annular area near the wall than near the center.

It is not hard to rationalize why this effect of decreasing pseudoplasticity with decreasing shear rate occurs, if one bears in mind the power model

$$\tau = b(du/dy)^s \quad (7)$$

This expression predicts that a pseudoplastic liquid would have infinite viscosity at zero shear rate, since

$$\mu = \tau/(du/dy) = b(du/dy)^{s-1} \quad (38)$$

Since s is always less than 1 for a pseudoplastic liquid, $s-1$ is then always negative, and as du/dy becomes zero, μ goes to infinity mathematically. This does not seem reasonable, since infinite viscosity connotes a yield value.

Thus, if one rejects an infinite slope on the rheological curve

at zero shear rate, the only recourse left is a finite slope. This inevitably leads to increasingly Newtonian behavior (as decreasing) as zero shear rate is approached, an effect which has been verified experimentally (6). Therefore it appears that different pseudoplastic liquids differ in the "speed" with which they become Newtonian in approaching zero shear rate. By this it is meant that different pseudoplastic liquids begin to attain their pseudoplastic character at different ranges of shear rate. For example, ammonium alginate solutions appear to become pseudoplastic at much lower shear rate than CMC solutions.

The explanation for this phenomena lies in the field of the mechanics of macromolecules and is somewhat of a digression from the topic being presented. Therefore, this explanation is presented in APPENDIX A. Supplementary Details.

The Vistanex solution in cyclohexane was the only pseudoplastic liquid tested that irreversibly broke down noticeably under the shear in the pipe-line flow system. Figure 9 shows the effect of constant recycling of the Vistanex solution at constant temperature (77°F.), 25 GPM, and a system pressure drop of 15 psig. approximately. The rather alarming drop in both viscosity and pseudoplasticity was not recovered to any measurable extent upon standing, and it is to be presumed that polymer breakdown had occurred. This is in accord with the findings of Bestul and Belcher (8). Nevertheless, it was still possible to obtain a number of friction factor runs without appreciable change in rheological properties, but it was impossible to do so with

velocity profiles because of the much greater length of running time needed with them.

V . DISCUSSION OF RESULTS (Cont.), B. Pipe-line Flow

Friction Factors in Laminar Flow. The friction factors in laminar flow of the various liquids in the various tubes ranging from 1/4" copper tubing to 3/4" I.D. stainless steel tube were found to follow with a high degree of accuracy the $f = 16/N_{Re}$ accepted for Newtonian liquids (see Figure 14). This is in accord with the results of Metzner and Reed (33) and with those of Dakekian and Engelken (13), and substantiates the use of rheological constants obtained in the range of shear of the same order as the tube wall shear conditions. It should be noted here that the results obtained with ammonium alginate solutions do not depend on this assumption to a very large degree, since the variation of s between low and high shear rates was found to be small. The fact that the results obtained with CMC, whose variation in s is quite large, are just as close to the theoretical prediction as those obtained with ammonium alginate solutions demonstrates the validity of the assumption.

The fact that a good single-line correlation exists for pseudo-plastic friction factors in laminar flow is of great significance in the experiments that followed in turbulent flow. This means that any

frictional phenomena observed in pseudoplastic turbulent flow can be reasonably compared to laminar flow frictional phenomena, if one uses the Reynolds Number as presented and calculates the usual Fanning friction factor. Compared to the non-Newtonian laminar correlations that involve a series of parallel lines or family of curves, one can readily see that a much higher degree of order results from the proposed correlation, and any consequent study of the turbulent regime is therefore less likely to be unduly complex.

Friction Factors in Turbulent Flow. As can be seen in Figure 13 the friction factors in turbulent flow as a function of

$$N_{Re} = (D^s v^{2-s} \rho / b) \cdot \phi(s) \quad (22)$$

seem to be a function additionally of s only, giving a family of curves for differing values of s . The liquids included in this correlation are both ionic and non-ionic systems, and include behaviors from Newtonian to a pseudoplasticity of $s = 0.53$. With the apparatus used and the materials available, it was not possible to go beyond the laminar region with liquids of greater pseudoplasticity. The reason for this stems from the fact that to achieve a lower value of s , a greater concentration of polymer would have to be used with the resultant overall increase in viscosity. This had the effect of decreasing the maximum possible Reynolds Number the apparatus could be made to produce.

Empirical Correlation. Since the turbulent friction factors seem to be a function of N_{Re} and s only, and since the curves of f vs. N_{Re} form an

orderly family of curves, it seems possible to correlate them empirically by some mathematical expression of f , N_{Re} and s . It was found by extracting the slopes and intercepts of the curves that the following would fit the data well:

$$f = 0.079 / (s^5 \cdot N_{Re}^{\gamma}) \quad (39)$$

$$\text{where } \gamma = 2.63 / (10.5)^s \quad (40)$$

It should be noted that this expression when applied to Newtonian liquids ($s = 1.00$) reduces to the Blasius equation:

$$f = 0.079 / N_{Re}^{0.25} \quad (24)$$

When this empirical correlation was applied to the friction factor data in turbulent flow, it was found that most points fell within $\pm 12\%$. Figure 45 shows this graphically by plotting f vs. $s^5 \cdot N_{Re}^{\gamma}$. This expression is a very powerful function of the rheological constant, s , and therefore one might expect most of the deviation from the correlation to be due to inconsistencies in determining the rheological curves. However this is not meant to infer that this correlation constitutes an absolute test for the rheological behavior (or s value) of a pseudoplastic, since it is, after all, empirical. However, to the degree that one places faith in the correlation, one can determine the internal consistency of the data.

The limitations set on this correlation are: the fluids must be pseudoplastic or Newtonian, the Reynolds Number must be of the order of 100,000 or less and in turbulent regime, the values of s must be deter-

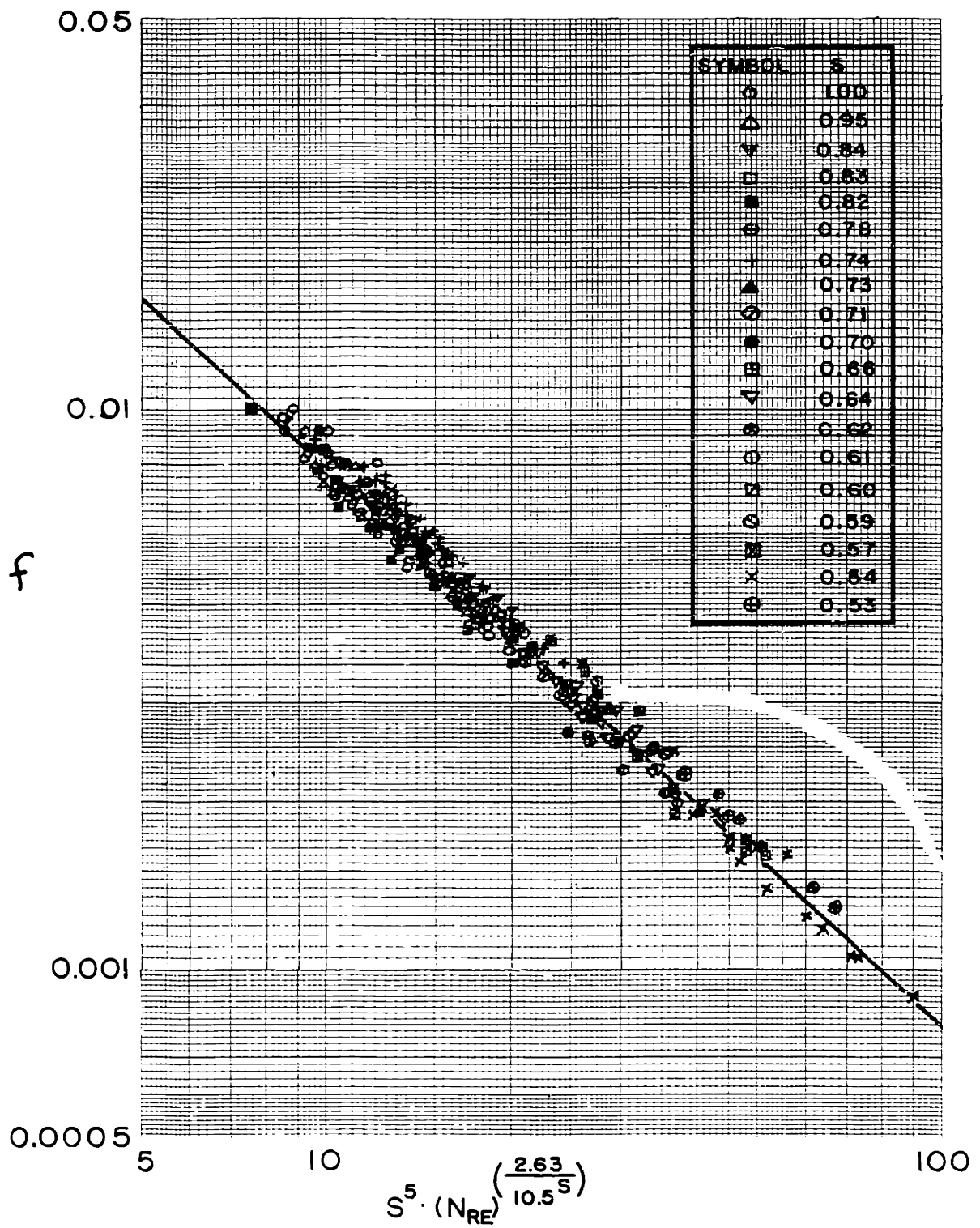


FIGURE 45
 CORRELATION OF
 PSEUDOPLASTIC
 FRICTION FACTORS IN
 TURBULENT FLOW

mined in the region of shear that is of the same order of magnitude as the shear conditions at the tube wall, and the value of s must not be less than 0.41 and preferably not less than 0.53. The latter conditions stem from the fact that if this correlation is applied to fluids having an s less than 0.41, the predicted log-log slope of the $f - N_{Re}$ curve would be more negative than -1. This is a logical absurdity since the laminar flow curve has such a slope of -1 and such a condition would predict turbulent friction factors lower than would be expected for laminar flow at the same Reynolds Number.

It is the feeling of the author that at s values of the order of 0.41 or less, turbulent flow resembles laminar flow very strongly and the laminar and turbulent friction factor curves merge. This argument will be substantiated with more facts later in this section.

Friction Factor Trends. The above correlation and the f vs. N_{Re} plot in turbulent flow show the following trends:

- (1) increasing Reynolds Number in turbulent flow at a given degree of pseudoplasticity decreases friction factors, and
- (2) increasing pseudoplasticity (decreasing s) decreases the friction factor at a given N_{Re} .

The striking practical implication of this is the possibility of decreasing pipe-line dynamic pressure drop through the judicious addition of a miscible high polymer. This is strikingly contrary to what one might imagine at first thought. Another practical implication is the in-

creasing insensitivity of pressure drop to increasing flow rate as pseudoplasticity is increased. That is, for a Newtonian liquid, pressure drop increases as slightly less than the square of flow rate, other conditions being constant, whereas a highly pseudoplastic liquid has a roughly first power dependence of pressure drop on flow rate.

Transition Flow. Inspection of the friction factor data makes the following facts evident concerning transition:

- (1) transition seems to occur at progressively higher Reynolds Numbers as pseudoplasticity is increased, and
- (2) transition is affected by the mechanical system in a manner unaccounted for in the Reynolds Number. That is, the Reynolds Number range of transition changed with tube diameter, and it was pushed to considerably lower Reynolds Numbers by the addition to the test section of a source of artificial disturbance, such as a restriction at the entrance.

Of course, these factors do not have any appreciable effect on fully laminar or turbulent flow, except as accounted for in the Reynolds Number.

The foregoing establishes the fundamental difference between transition and turbulent flow. Though both are regions of eddy formation and mixing across lamina, the turbulent region is much more highly ordered -- it is not appreciably affected by the physical details of the tube in which it is flowing, except as is expressed by the Reynolds Num-

ber. Transition flow is unstable; it can be forced into full turbulence by additional disturbance. .

Another interesting feature of transition flow, as brought out in the "Observations" presented in the Results section, is that of oscillation of the manometer columns. This oscillation seems to indicate a roughly periodic change between the laminar form and something resembling turbulence at a relatively low frequency. In order for the manometers to respond to such an oscillation in flow form, and hence in pressure drop, the frequency must be quite low because of the inertia of the system and the throttling at the wall taps. As the transition region is entered from the laminar side, this frequency is very low -- often several seconds -- but speeds up as the turbulent region is approached.

This effect of oscillation of the manometers has been observed by others -- see Prandtl and Tietjens (42), p. 38 -- and the effect attributed to intermittent turbulence. The production of a smooth friction factor curve in the transition region is therefore produced, usually, by the use of a manometer with very high damping. Short of this, the reading of the manometer leg in this region is difficult.

Laminar Velocity Profiles. Since laminar pseudoplastic flow follows the expression:

$$f = 16/N_{Re} \quad (21)$$

it is to be expected that the pseudoplastic velocity profiles in laminar flow would follow the predicted expression:

$$u/u_{\max.} = 1 - (1 - y/R)^{1/s + 1} \quad (15)$$

This is expected because both relations involve only one assumption, that of the power rheological model, and otherwise are rigorous mathematically. So if one relation works, the other should.

The only significant deviations in the laminar velocity profile data occur with the CMC solutions, with which the profile near the center of the tube more closely resembles the profile for a Newtonian liquid than that for the given degree of pseudoplasticity. But this can be reasonably explained if one bears in mind the tendency for the CMC rheological curves to become more Newtonian at lower shear conditions. Since the shear stress distributes itself in the tube according to the relation:

$$\tau = \tau_w (1 - y/R) \quad (37)$$

it is evident that the shear stress near the center of the tube is very small indeed. Therefore these velocity profiles are in accord with the rheological curves. Since the shear condition near the center of the tube has relatively little effect on the shear conditions near the tube wall, the pressure drop (energy dissipation) is, for all practical purposes, that predicted by a constant value of s determined at high shear rates.

An incidental result of the coincidence of the velocity profile data with the predicted curves is the refutation of the concept of "slip" at

the wall of the tube due to a layer of fluid deficient in polymer as proposed, and supposedly proved, by Toms (56). If this effect is at all present, it is of minor significance.

Turbulent Velocity Profiles. In the presentation of velocity profile data in turbulent flow there is considerable difficulty in managing to present the data with sufficient generality to permit comparison both among the various runs and with previous work. For example, a u/u_{\max} vs. y/R plot, while completely general in laminar flow at a given value of s , is not so general in turbulent flow. In Newtonian turbulent flow, such a correlation would vary with both Reynolds Number and wall roughness, even though there would be common points at $y/R = 0$ and 1.0 . The other common methods of presentation are the Nikuradse "universal velocity profile" and the velocity deficiency method, both giving a single curve in Newtonian turbulent flow at variable Reynolds Number and roughness.

The Nikuradse universal velocity profile involves the use of a distance Reynolds Number:

$$y^+ = yV \sqrt{f/2} \rho/\mu \quad (27)$$

In translating this, by analogy, to the pseudoplastic form the following is obtained:

$$y^+ = y^s u_*^{2-s} \rho/b \quad (41)$$

This expression has several obviously undesirable features, such as:

- (1) it is no longer a "distance" Reynolds Number, strictly speaking, since it carries y to the s power,
- (2) because of the exponents involved, it can no longer be readily visualized, and
- (3) there is an inordinate amount of calculational complexity involved in it.

This sort of correlation has been tried by the author for several runs and it was found to not give a curve coinciding with the accepted Newtonian curve, but rather differing widely for differing values of s . This fact, together with the excessive calculational complexity, leads the author to reject it as a practical means of correlating pseudoplastic turbulent velocity profiles.

The velocity deficiency method, proposed by von Karman (5), plots $(u_{\max} - u)/u_*$ as a function of $l-y/R$. Experiments show it to give a single curve for Newtonian fluids, and this was verified in this work by runs using water as the fluid. One great advantage of this method is that, calculationaly, it does not involve any concept of viscosity. That is, to calculate the data points all that need be known are the local velocities at the various radial points and the Fanning friction factor or wall shear stress. Therefore one does not get involved in the insuperable problem of deciding what the local viscosity at a given radial point may be under the irregular conditions prevailing locally in turbulent flow. Hence it was decided to present the pseudoplastic turbulent velocity profiles by this method.

Pseudoplastic Velocity Deficiencies. Examination of Figures 26 to 32 shows that the pseudoplastic turbulent velocity deficiency curves deviate progressively from the Newtonian curve as s decreases. However, at a given s value, the curve seems to be unique; it does not vary with the Reynolds Numbers studied. Therefore, this method seems to be an excellent one for comparing and contrasting the velocity distributions for Newtonian and pseudoplastic liquids in turbulent flow. Figure 46, in which the curves for the velocity deficiencies have been abstracted and replotted semi-logarithmically with y/R instead of $1-y/R$, shows this effect very clearly. Near the center of the tube, all the pseudoplastic velocity deficiencies lie on the Newtonian curve, but progressively toward the wall the pseudoplastic deficiencies deviate onto a family of curves that are a function of s .

In general one could say that the pseudoplastic turbulent velocity profiles are less blunt, progressively, than those for Newtonians under similar conditions of shear or at equal Reynolds Numbers. This is in accord with the previously observed fact that pseudoplastic turbulent friction factors are progressively lower than those for Newtonians. In addition, this serves to refute the contention of Oldroyd (38) that the abnormality in the pressure drop in turbulent flow of pseudoplastic liquids is due to an anisotropic layer at the wall of the tube, producing "slip" -- an abnormally high velocity gradient -- near the wall. If this were the case, the velocity profiles for pseudoplastic liquids would be inevitably more blunt than those for Newtonians. This would be due to the major portion of the velocity gradient being produced near

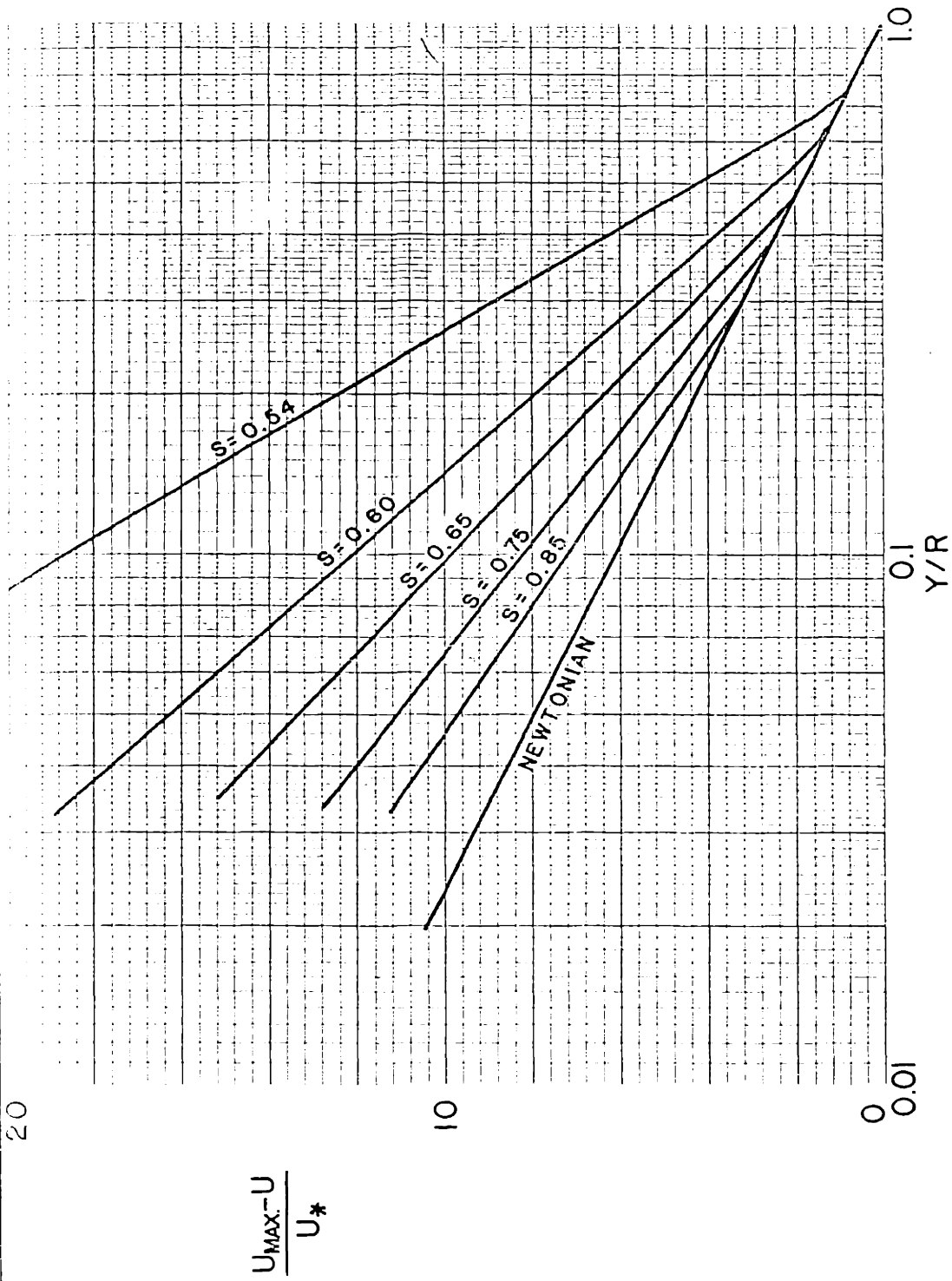


FIGURE 46
 COMPOSITE DIAGRAM OF
 TURBULENT VELOCITY
 DEFICIENCIES

SPAN OF REYNOLDS' NUMBERS OF DATA: S=0.54, 8780
 0.60, 8400 - 14,300
 0.65, 8800 - 14,600
 0.75, 7540 - 10,500
 0.85, 17,000

NEWTONIAN, 9600 - 176,000

the wall. Since this is in direct opposition to the facts, this concept must be rejected as a major consideration. Rather, it is evident that the lower pressure drop in pseudoplastic turbulent flow is due to the lower order of shear taking place in the tube as a whole.

An additional effect that may be seen in the plots is that the velocity deficiencies near the center of the tube coincide very closely with the classical Newtonian deficiencies. Progressively, this region of coincidence seems to decrease as pseudoplasticity is increased, until when $s = 0.54$ the similarity exists for only about 25% of the radial distance. Near the wall the deficiencies are greatly different.

Turbulent Mixing Lengths. Another one of the classical expressions of turbulent flow characteristics is that of the mixing length, which is a distance in the transverse direction through which a particle from one locality will travel before it completely equalizes momentum and merges with the surroundings. Mathematically it can be expressed:

$$l = u' / (du/dy) \quad (31)$$

where l is the mixing length and u' is the axial velocity component transported by the transverse movement. Reasoning that this "axial velocity component" is of the same order of magnitude as the pulsating transverse velocity component leads to the Prandtl equation:

$$\tau = \rho \cdot l^2 \cdot (du/dy)^2 \quad (32)$$

Data by Nikuradse (5, 21) indicates that this mixing length for New-

tonians distributes itself radially by increasing from zero at the wall to a maximum at the tube center. This is verified by the water profiles taken in this work.

Von Karman reasoned that the ratio of consecutive derivatives of the velocity should be proportional to this mixing length (5), leading to:

$$l = k(du/dy)/(d^2u/dy^2) \quad (34)$$

where k was considered to be a universal constant of about 0.4. In the region near the tube wall the above expression would reduce to:

$$l = ky \quad (35)$$

permitting one to determine the value of k as the slope of the mixing length curve at the wall.

Therefore, in order to compare and contrast the characteristics of Newtonian and pseudoplastic turbulence further, it was reasonable to see if pseudoplastic mixing lengths followed the same generalized curve as do Newtonian ones, and if not, to see if the constant, k , had also the same value for the pseudoplastics.

Pseudoplastic Mixing Lengths. Examination of the curves for the mixing lengths for the pseudoplastic liquids shows that neither do the curves coincide with that for Newtonians, nor are the values of k equal to about 0.4. Rather, it is apparent that the values of k progressively decrease from 0.4 as the pseudoplasticity is increased, and the curves de-

viate progressively. That is, the mixing lengths are considerably smaller toward the wall than are the Newtonian ones, but they increase to about the same magnitude or somewhat larger than the Newtonian ones near the tube center. This indicates that there is a progressively larger annular area toward the wall in which the intensity of turbulent agitation is considerably lower than in classical turbulence.

The rather large spread in the data points near the center of the tube is largely due to the fact that the reading of the very slight slope of the velocity curve there is subject to great intrinsic error, as is the original drawing of the curvature of the profile in that region.

Eddy Viscosities. If one writes an expression for resistance to flow in the turbulent regime that is analogous to that for viscous flow, it would be like the following:

$$\tau = \epsilon (du/dy) \quad (42)$$

where ϵ has the dimensions of viscosity, and is sometimes called the "eddy viscosity". Referring to equation (32), this eddy viscosity becomes:

$$\epsilon = \rho l^2 du/dy \quad (43)$$

Obviously, if physical significance is attributed to eddy viscosity, the conclusion is reached that part of the energy dissipation in turbulent flow is due to the effect of the eddies and part due to the effect of molecular viscosity, though for well-developed classical turbulence

the eddy effect would be much the greater.

Therefore one would expect the ratio of the eddy viscosity to the molecular viscosity, ϵ / μ , to be a good indication of the intensity of turbulent agitation.

In order to gain some insight into the parameters that may affect the viscosity ratio, the one assumption shall be made that Prandtl's equation for Newtonian turbulent flow (5) holds:

$$du/dy = u_*/(ky) \quad (44)$$

If this is combined with equation (42), the definition of Reynolds Number, and the distribution of shear stress:

$$\tau = \tau_w(1-y/R) \quad (37)$$

the following expression results for Newtonian turbulence:

$$\epsilon / \mu = N_{Re} \cdot \sqrt{f/2} \cdot k/2 \cdot y/R \cdot (1-y/R) \quad (45)$$

Since, for Newtonian flow, f is a function of N_{Re} and roughness only and k is a constant, one would be led to expect the eddy viscosity to molecular viscosity ratio to be a function only of N_{Re} , roughness and radial position. Therefore, it seems reasonable to compare plots of the viscosity ratio as a function of y/R at constant N_{Re} for the smooth tubes used in this experimentation for the Newtonian and the pseudoplastic situations.

This was done for a typical highly pseudoplastic velocity profile

run and plotted in Figures 36 and 37. The difference between the two plots lies in the assumptions used to determine the molecular viscosity locally at the various radial positions. In one the basis was shear stress as distributed linearly from τ_w at the wall to zero at the center and viscosities calculated from the viscometric curves at these values of shear stress. The other one was based on reading the slope (du/dy) of the velocity profile and calculating from the viscometric curve the viscosity at these values of shear rate. It is impossible to completely justify either method, and both are probably naive since the transient shear conditions in turbulent flow at a point can be quite different than the time-averaged conditions.

Nevertheless, comparison of the pseudoplastic viscosity ratios to the Newtonian ones, both the theoretical curve at the same N_{Re} and the points calculated from experiment at a slightly lower N_{Re} , shows that the pseudoplastic ratio is always less, and in this case much less. This reaffirms the contention that pseudoplastic turbulent flow has a lower degree of turbulence than classical Newtonian turbulent flow.

Dye Injection Studies. In order to try to visualize what was actually happening in the pseudoplastic liquid flowing in turbulent flow, a series of experiments were set up to inject pigmented liquid at various points in a transparent tube and to observe the action of the resultant dye stream photographically with high speed flash. The photographs presented in the Results section are the most pertinent ones of the group.

Finally, it became evident that the most information on the nature

of the turbulence could be obtained by injecting at two different points:

- (1) at the entrance of the test section in the center of the tube,
and
- (2) at a small, carefully drilled wall tap.

The first was intended to show the effect of turbulence on the liquid in the core of the tube and the second to show the effect on the fluid in layer near the wall. The first type of injection was at the portion of the system where the large feed pipe necked down to the smaller test section; hence the fluid there was being accelerated and there would be less tendency for flow separation and vortex formation to occur because of the presence of the hypodermic tubing probe.

Laminar Flow. As seen in Figure 38 the dye injected at the center of the tube in laminar flow retains its radial position and identity in both the Newtonian and the pseudoplastic cases, making a straight filament. This is as was expected. The presence of the hypodermic probe did not seem to disturb this configuration until very close to the transition region.

In the case of the dye injected at the wall, it can be seen that the resultant dye stream also retains its unity and becomes a straight filament against the tube wall.

Newtonian Turbulent Flow. The dye stream injected into the center of the tube into Newtonian turbulent flow as seen by the 40 microsecond flash 185 diameters downstream from the point of injection is completely dispersed across the diameter of the tube. There is no filamental quality

left to it, at least on the macroscopic scale.

This is in accord with the understanding of Newtonian turbulence as a very rapid, violent mixing action.

Where the dye was injected at the wall a very interesting effect showed up (see Figure 43). That is the appearance of loops of dyed liquid from the main body of the wall layer. This is in accord with the observations and calculations reported by Theodorsen (55) concerning "horseshoe" vortices formed in the vicinity of the wall and traveling toward the center under the influence of the main stream of flow going by it. The effect seen in the present experiments is the same as that he pictured, and it indicates that turbulent eddies form at or near the wall and travel radially away from it, thereby mixing fluid from the region of the wall with fluid in the core of the flow. The force that produces the movement toward the center is a "lift" force generated by the rotating mass intruding into the flowing stream. It exchanges momentum with the fluid through which it is passing by means of normal drag forces and finally loses its identity.

Pseudoplastic Turbulent Flow. When injected into a highly pseudoplastic turbulent flow at the center of the tube, the dye stream takes on a much different appearance 185 diameters downstream from the point of injection than it does in Newtonian turbulent flow (see Figures 41, 42). To a large extent the dye stream seems to be still intact, although it is highly distorted and grossly distributed across a large portion of the diameter of the tube. This reinforces the previous assertion that pseudo-

plastic turbulence is a lower degree of turbulence than Newtonian turbulence.

This effect also infers that the material originally at the center of the tube does not readily lose its identity, but rather is pushed aside by the turbulent vortices and does not become part of them. The action has been aptly described by T. K. Sherwood as a kneading action.

With respect to the wall injection study (Figure 44), it can be seen that the smoothly flowing layer near the wall is much thicker in pseudoplastic turbulence than in Newtonian turbulence and the horseshoe vortices leaving this layer are very few in number and not at all well-developed at this short distance from the point of injection.

On the basis of these observations it is concluded that the formation of horseshoe vortices is highly repressed in pseudoplastic turbulent flow leading to much lower energy dissipation. Also the core fluid tends to retain its identity, although highly distorted by the vortices that do penetrate it. This may be explained by the fact that the more slowly sheared fluid in the center of the tube has as a result a higher viscosity than the more highly sheared fluid near the wall and the fluid surrounding the core of a vortex, thereby resisting intermingling with the more rapidly moving fluid. This may be visualized by the analogy of mixing two liquids of widely differing viscosity, say water and heavy syrup. In this case one fluid will penetrate the other under the action of the mixing forces but there will be considerable retention of the unity of each of the two fluids, though highly distorted. Not until

considerable mixing has occurred will the liquids be dispersed in one another below the macroscopic level.

Fluctuations in Pressure Drop. The observed oscillations of the manometer columns during transition of most of the fluids tested gave the impression of periodic lapses into the turbulent form of flow from an obviously unstable laminar form. That is, the manometers often oscillated between values corresponding to laminar and turbulent forms at the particular Reynolds Number, so long as the frequency was slow enough for the manometer to respond and settle down. When the frequency was higher, the values tended to approximate the above conditions more and more poorly and averaged a value some where in the middle. When these oscillations occurred, they happened at all the consecutive manometers at very nearly the same moment. This indicated that whatever change had occurred in the flow had happened throughout the whole test section at nearly the same moment.

In view of the foregoing demonstration of the presence of horseshoe vortices, it seems probable that what is happening is the periodic formation of horseshoe vortices, with the consequent distortion of flow, at frequencies slow enough to be seen on the manometers.

Oscillations in the Low Turbulent Region. As the flow rate increases from the transition region into the turbulent region, the great oscillations in the manometers tended to increase in frequency and decrease in amplitude until a quite steady reading is present for all but the very pseudoplastic liquids (s less than 0.7). But for these materials

a flutter of very small magnitude (less than 1 mm.) and high frequency persisted for a long way into the turbulent region, often as far as the flow could be extended. The flutter was more noticeable progressively as more highly pseudoplastic liquids were tested.

These facts suggest that the periodic change between two forms of flow that was observed in the transition region persists into the turbulent region, only under stable and predictable conditions (in the sense that the friction factors and velocity profiles are reproducible in turbulent flow). However, the characteristics of this periodicity are such that it is not detectable by gross means (such as manometers) under Newtonian or slightly pseudoplastic conditions. As pseudoplasticity is increased, this effect becomes more gross, less "statistical", slower in frequency.

A possible explanation for the apparent decrease in the frequency of the formation of vortices is the viscosity gradient present across the radius of a tube flowing with a pseudoplastic fluid. Consider such a fluid flowing in laminar flow at a high Reynolds Number: the viscosity gradient in it would be defined by the linear shear stress distribution and the rheological curve of the material. The effect would be to have a minimum viscosity at the wall and a maximum viscosity at the center of the tube. Thus, a vortex formed at the wall of the tube in traveling inward toward the center penetrates layers of increasing viscosity. As a consequence of this, it seems reasonable to expect that there would be a damping effect on the vortex over and above that imposed by a Newtonian system.

By means of this concept of viscosity gradient two effects observed in pseudoplastic flow can be explained:

- (1) the persistence of stable laminar flow to abnormally low friction factors (high Reynolds Numbers), and
- (2) the relatively low frequency of formation of turbulent vortices in turbulent flow leading to lower friction factors than Newtonian and to flutter of manometer columns under certain conditions.

One could reasonably expect such a viscosity gradient to retard both the point of incipient formation of vortices and the frequency of their formation once this point has been passed.

Periodic Boundary Layers. In view of the foregoing it is interesting to consider concept of "periodic boundary layers" as proposed by Richardson (44). Reported experiments were conducted in a pipe fitted with a loose section that could be oscillated in a direction transverse to the flow. When a stable laminar flow was passed through the tube and the loose section oscillated, the resultant velocity profile was the steep logarithmic type of turbulent flow (44). The effect is ascribed to an alternation between the laminar form of flow and an "alternating" form whose profile has a peak near the wall. The "turbulent" profile is then the time-average between the two (see Figure 47).

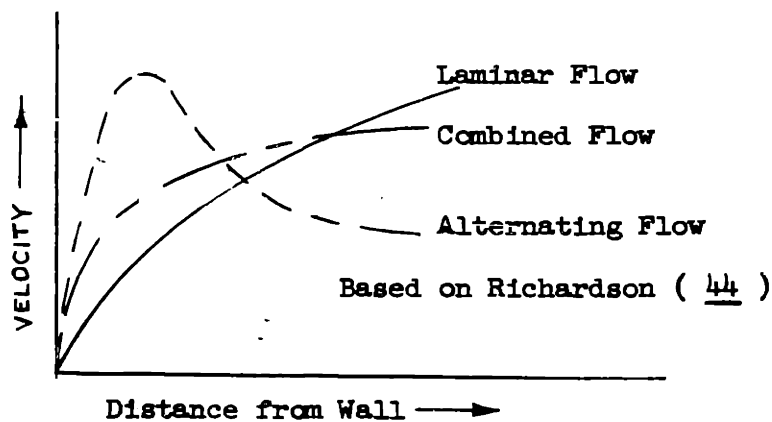


FIGURE 47. Conversion of Laminar to Turbulent Profiles.

This alternating form of flow is taken to be the hydrodynamic analogy of the "skin" effect shown by alternating current in a conductor.

If one ascribes the formation of turbulent flow to some process resembling the above artificial one, the decreasing bluntness of pseudoplastic turbulent profiles with increasing pseudoplasticity can be readily explained in the following manner. Given the laminar form of flow in an unstable region, the vortex formation causes the flow to distort to the "alternating" form, with a peak near the wall. However, the effect of pseudoplasticity, as deduced from other facts, is to reduce the frequency of occurrence of these vortices. Therefore, as pseudoplasticity is increased, progressively less of the alternating form is time-averaged with the laminar form resulting in progressively less blunt turbulent profiles and progressively lower friction factors. Since the laminar profiles become more blunt as pseudoplasticity is increased, it is apparent

that the decrease in frequency of alternation must be such as to more than compensate for this effect in the resultant profile.

Thus the advantage of this concept of the oscillation between two forms of flow in the turbulent region is that it reasonably explains all the main phenomena observed with pseudoplastic turbulence:

- (1) the decrease in friction factors at constant N_{Re} as pseudoplasticity is increased,
- (2) the progressively less blunt velocity profiles with increasing pseudoplasticity,
- (3) the flutter of the manometer columns in the turbulent region with the highly pseudoplastic liquids,
- (4) the relatively poor mixing of dye stream injected into the center of the tube, and
- (5) the thicker calm layer near the wall and fewer horse-shoe vortices as seen by wall dye injection.

VI. CONCLUSIONS

- (1) The degree of turbulent agitation in the turbulent flow region is progressively less at comparable Reynolds Numbers as pseudoplasticity is increased.
- (2) This is attributed to a progressively decreasing frequency of vortex formation at the tube wall.
- (3) The result of this is lower friction factors and less blunt velocity profiles in pseudoplastic turbulent flow than in Newtonian turbulent flow.
- (4) Pseudoplastic liquids become more Newtonian in the vicinity of zero shear rate (e.g. 0.1 to 10 sec.⁻¹).
- (5) There is considerable difference in the range of shear rate at which a pseudoplastic liquid changes from its highly pseudoplastic state at high shear rates to Newtonian at very low shear rates. For example, sodium carboxymethylcellulose solutions in water are Newtonian to considerably higher shear rates than are those of ammonium alginate.
- (6) Laminar pseudoplastic velocity profiles are progressively blunter than Newtonian ones, as is predicted by the power model of pseudoplastic rheology.
- (7) "Slip" of the fluid at the wall due to an anisotropic layer is not a factor of significance for true pseudoplastic fluids in both the laminar and turbulent regions. As a consequence there is no "plug flow" with these fluids in either of these two regions.

VII. RECOMMENDATIONS

- (1) The frequency of turbulent vortex formation in pseudoplastics should be studied quantitatively, perhaps by the use of some sort of hot wire anemometer.
- (2) A rheological study should be undertaken to determine whether a pseudoplastic solution of the type studied can possibly have a value of s less than about 0.4, in order to determine if $s = 0.4$ is a kind of natural limitation on the rheology of free-draining, non-associating molecules in solution.
- (3) The high Reynolds Number range (about 10,000) should be studied for strictly pseudoplastic fluids of s less than 0.5, and particularly s less than 0.4, if they exist. This would entail apparatus capable of very high flow rates and able to withstand pressures upwards of 150 psig.
- (4) The range of Reynolds Numbers above 100,000 should be studied for slightly and moderately pseudoplastic fluids. This would also entail high flow rates and high pressures.

APPENDIX

VIII. APPENDIXA. Supplementary Details

1. Change in Degree of Pseudoplasticity with Shear Rate. As was brought out in the DISCUSSION OF RESULTS Section, the degree of pseudoplasticity, expressed as the exponent s , was constant within the range of 1000 to 20,000 sec.^{-1} for the majority of pseudoplastic fluids used in this investigation. However, at the low shear rate range of the modified Brookfield Synchroelectric viscometer (0.1 to 42 sec.^{-1}) all the fluids tested were to a greater or lesser degree less pseudoplastic than at the higher range. That the fluids should become less pseudoplastic at very low shear rates follows directly from the contention that infinite slope of the shear stress - shear rate curve at zero shear rate is not possible for a truly pseudoplastic fluid (that is, a fluid with no yield value among other characteristics). Infinite slope of this curve is the mathematical necessity of differentiation of $\tau = b (du/dy)^s$ which would lead to $d\tau/d(du/dy) \rightarrow \infty$ as $du/dy \rightarrow 0$ when s is less than 1.00. This contention then precludes a value of s of less than 1.00 at zero shear rate. If this is so, then there must be a region of transition from the low values of s observed in the high shear rate region to an s of 1.00 at zero shear rate, and the experiments with the Modified Brookfield instrument confirmed that this exists.

However, beyond this there is the question as to why the various fluids apparently do not undergo this transition in the value of s at the same shear rates (see Table 1). For example, the solution of CMC-70S

had become very nearly Newtonian in the low range whereas the ammonium alginate solutions were still highly pseudoplastic.

As Beuche (9) explains, the change in viscous loss with change in shear rate with pseudoplastics takes place because of the change in phase between the applied force and the deformation of a segment of the polymer coil due to the "stiffness" of the coil. By analogy to a spring and dashpot system, there would be a characteristic frequency at which the change would be most pronounced. At higher frequencies the viscosity is rapidly decreasing, while at lower frequencies the viscosity approaches a maximum value. This theory is in accord with the experimental facts concerning the slow change in viscosity at low shear rates (nearly Newtonian behavior) and the rapid change in viscosity at high shear rates (pseudoplastic behavior) that were found to a greater or lesser extent with all the fluids used in this experimentation. Hence the Beuche analysis would also predict that differences in the shear rate range of the rapid transition from nearly Newtonian to highly pseudoplastic behavior would be a function of the stiffness of the molecular coil in question.

Therefore, by this analysis one would expect, with two solutions whose only difference were the stiffness of the molecular coils contained within, that the solution with the stiffer coils would exhibit its pseudoplastic behavior at lower shear rates than the solution with the less stiff coils. This then would lead one to expect the pseudoplastic behavior to be affected by such factors as affect the stiffness of a molecule -- such as presence of side groups with steric hindrance, bond angles, mul-

tiple bonds, ring structure, amount of solvating sheath, etc.

Considering the specific cases of the sodium carboxymethylcellulose solutions and the ammonium alginate solutions, the following analysis of the differences in their rheological behavior would follow from the foregoing type of analysis. Since the CMC solutions were much less pseudoplastic than the alginate solutions in the low shear rate range but considerably more pseudoplastic in the high shear rate region, it follows that the frequency (shear rate) at which the transition to highly pseudoplastic behavior occurs is higher with the CMC solutions than with the alginate solutions. Therefore the molecular coils in the CMC solutions must be less stiff than the ones in the alginate solutions. However the molecular structures of these two polymers are very similar -- both are based on the anhydroglucose chain (see Figure 48).

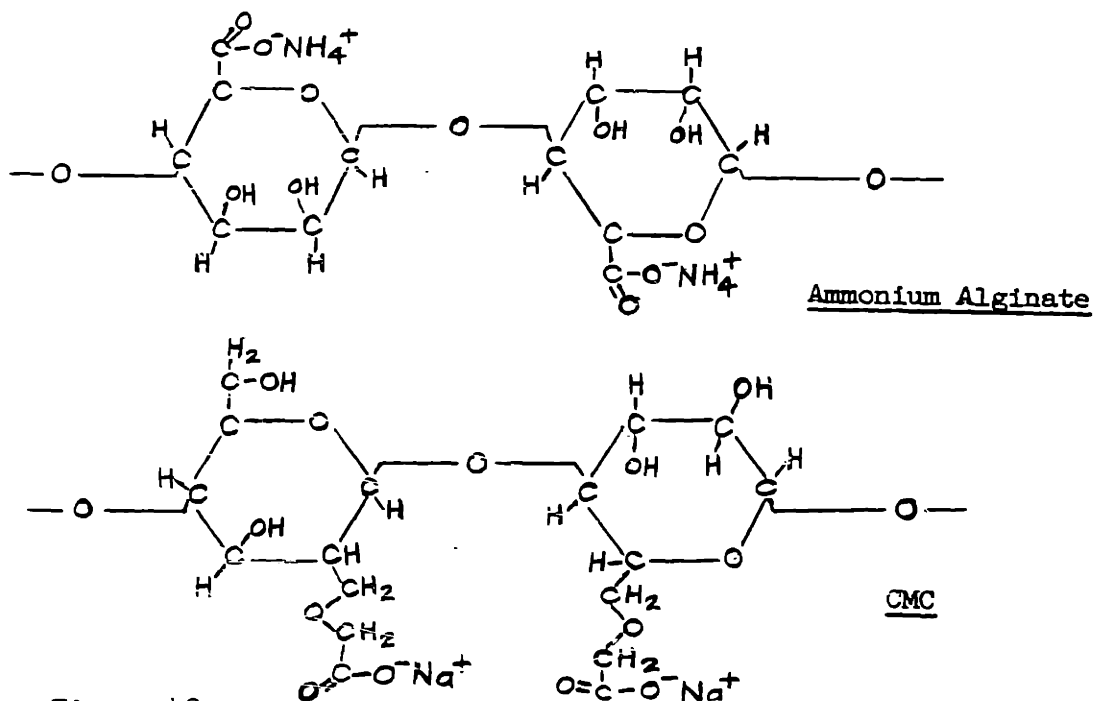


Figure 48. Molecular Structures of Ammonium Alginate and CMC.

There are two main structural differences in these two polymers; (1) the presence of longer side chains on the CMC molecule, and (2) the presence of ammonium ion with one and sodium ion with the other. Since the presence of the longer side chains on the CMC would predict a stiffer coil for the CMC, there must be some additional effect which overbalances this one and makes the alginate coil more stiff.

In a solution of the alginate there was an excess of ammonia over that ammonium ion tied up by the carboxy side groups. Therefore, there exists the possibility of hydrogen-bonding of the excess ammonium ion to the hydroxyl groups and to the carboxylic oxygens on the alginate structure which would in turn suggest a large amount of water in the solvating sheath surrounding the alginate molecule, held by the large number of ammonium ions at its surface. In the case of the CMC solution, any excess of sodium ions would not bond to the structure, so the solvating sheath on the CMC molecule ought to be less extensive than on the alginate molecule. If this is so, one could attribute the apparent greater stiffness of ammonium alginate coils to a greater amount of water of solvation -- a thicker "coat" of solvating molecules -- which merely by its presence as a tube around the molecule, makes it stiffer in effect.

A remarkable set of rheological experiments by Beerli (6) tends to confirm the above conclusion. In these experiments, solutions of CMC and CMC with a small amount of Gentian Violet added were studied at high and low shear rates. The Gentian Violet (hexamethylpararosaniline chloride), having a rather large organic cation, could exchange this

group for the sodium on the CMC, splitting off sodium chloride. One would expect the compound to be less soluble in water than the original sodium CMC. This has been demonstrated by the addition of considerable Gentian Violet solution to a solution of CMC which resulted in a precipitate. Therefore, a CMC molecule that had been reacted with Gentian Violet, but not to the point of precipitation, would be less highly solvated by water than the original CMC.

The rheological curves of these two types of CMC solutions -- sodium CMC and CMC reacted with Gentian Violet -- showed two remarkable effects: (1) above 6000 sec.^{-1} both solutions had similar rheology -- both were highly pseudoplastic --, and (2) directly below 6000 sec.^{-1} the CMC solution with Gentian Violet was essentially Newtonian whereas the unreacted CMC solution was still highly pseudoplastic. This is directly analogous to the case of the CMC vs. ammonium alginate, whereby the ammonium alginate was deduced to have a greater solvating sheath by rheological considerations. The CMC-Gentian Violet combination, which obviously has less solvation than pure CMC, when compared with the pure CMC rheologically showed a much higher shear rate range of transition from Newtonian to pseudoplastic behavior.

An alternative way of approaching this problem is to consider the following.

We know that pure cellulose is insoluble in water. It hydrogen-bonds intra and inter molecularly so strongly that the molecules can neither be relaxed nor separated from each other. Same is true for alginic acid -- totally insoluble (though swellable) unless reacted with (NaOH)

or (NH_4OH). Presumably the substitution of ionic side groups ($-\text{CH}_2-\text{O}-\text{CH}_2-\overset{\text{O}^-}{\underset{\text{O}}{\parallel}}{\text{C}}$ or $-\overset{\text{O}^-}{\underset{\text{O}}{\parallel}}{\text{C}}$) not only increases solvation of molecules by ion solvolysis but also means that when segments of the same or different molecules come together, they are ionically repelled, cannot H-bond. If one decreases the amount of Na^+ or NH_4^+ substitution in a given concentration of alginate or CMC, the viscosity level drops until finally precipitation occurs. This seems to mean that as the repulsive ionic sites are decreased in number the molecule can more and more successfully hydrogen-bond intramolecularly. This means that the molecule should not only be smaller in radius (\therefore lower viscosity) but more rigid. According to Bueche, if you have a completely rigid spherical molecule you had better use Einstein's equation, which predicts Newtonian flow. The addition of Gentian Violet probably accomplishes about the same result as the addition of HCl to CMC, conversion of the ionized carboxylic acid group to unionized, hydrogen-bonding $-\text{COOH}$. According to this picture then, the CMC molecule rotates as essentially a rigid sphere at low shear rates, owing to a small amount of internal tie-up by H-bonding. As the shear rate increases this limited internal H-bonding is disrupted and the molecule is free to flex -- giving the spring and dashpot system treated by Beuche. One must admit that the molecule under low shear rates must be lightly tied up in a much more voluminous sphere than in the other extreme case of high shear rates, in order to explain the very high Newtonian viscosity at low shear rates relative to the viscosity found, e.g., at $20,000 \text{ sec.}^{-1}$.

2. Merrill-Brookfield Viscometer Details. The Merrill-Brookfield viscometer is a rotational concentric-cylinder apparatus with a small, bottomless annulus capable of shear rates continuous between 0 and 20,000 sec.⁻¹. It provides cooling to both the rotor and stator to eliminate non-isothermal conditions. It automatically programs and records the shear information by means of electronic circuits.

Figure 49 presents a cross-section of the head of this viscometer and Figure 50 shows a schematic of the layout of the viscometer system.

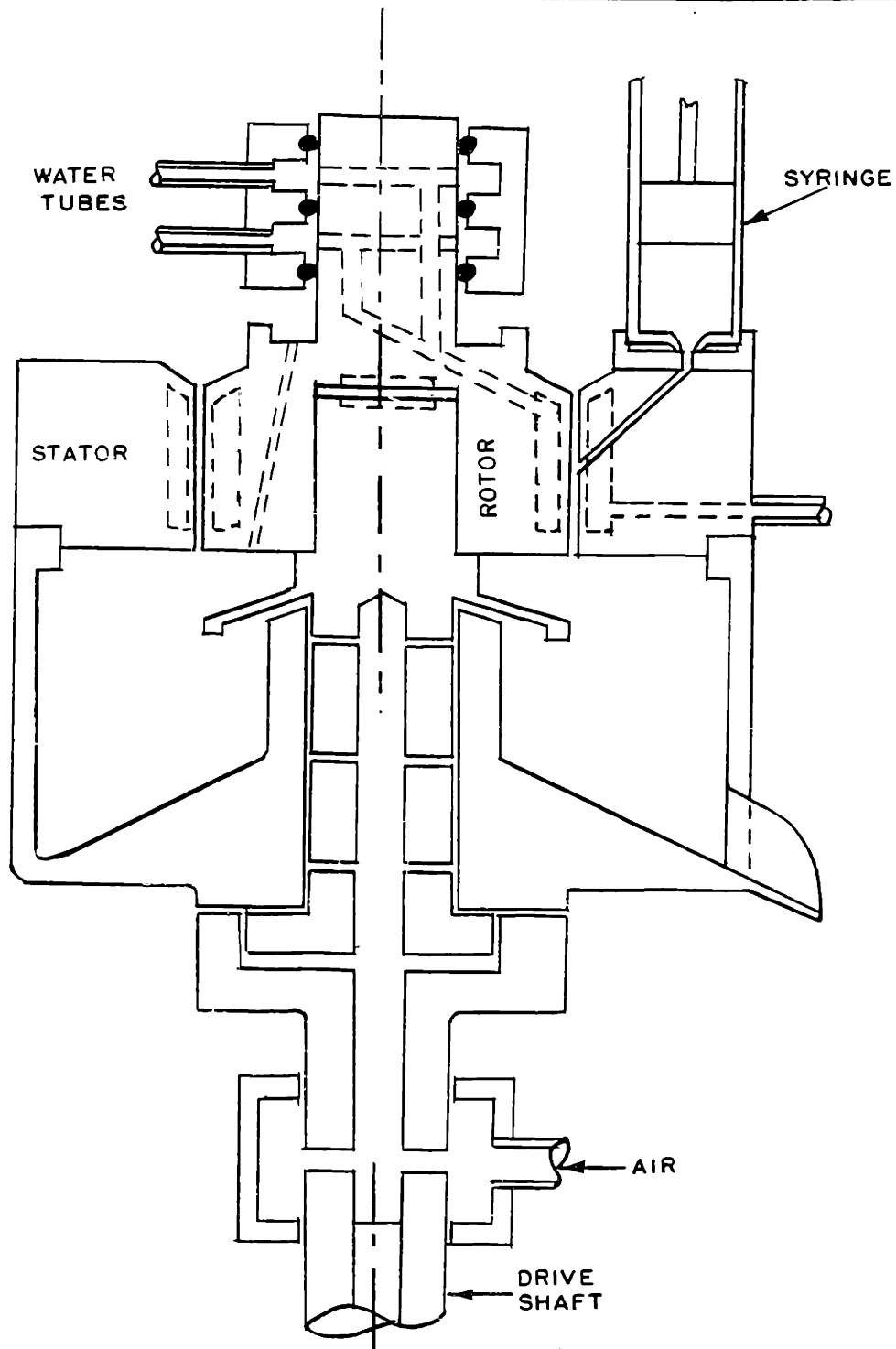


FIGURE 49
MERRILL
VISCOMETER
HEAD

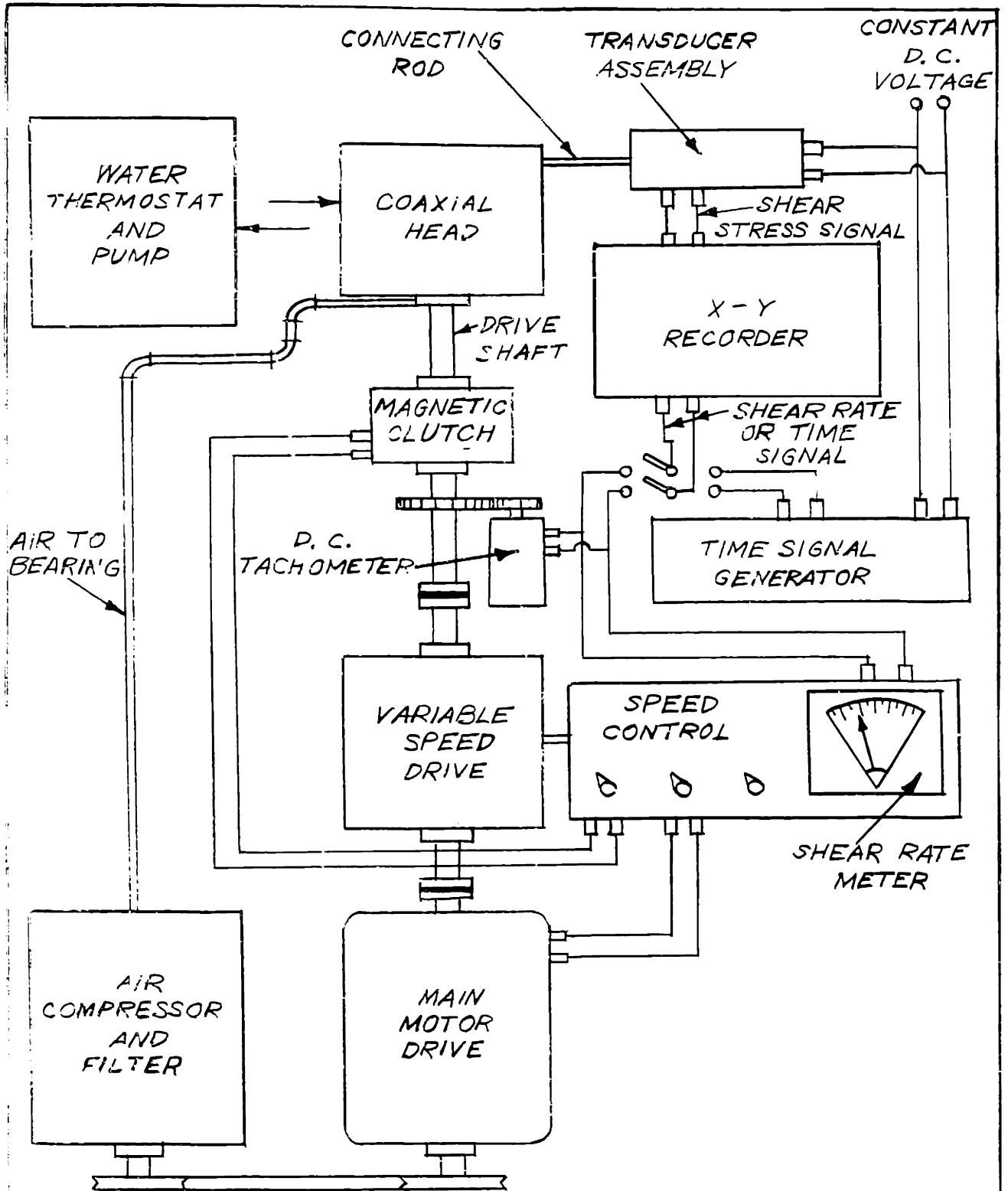


FIGURE 50
MERRILL
VISCOMETER
SYSTEM

3. Low Shear Rate Viscometer Details. The viscometer used for rheological studies at low shear rate consisted of the standard Brookfield Synchroelectric viscometer modified to minimize the variation in shear stress usually present with this type of instrument, and hence to make its measurements meaningful for pseudoplastic fluids. The modification consisted of a special rotor and stator (see Figure 51) with small annular width. The rotor was fastened to either an LVT or an RVF Synchroelectric head to provide the rotation and torque measurement.

The LVT head provided eight speeds: 20, 10, 4, 2, 1, 0.5, 0.2, and 0.1 RPM. Its full-scale torque was 673.7 dyne-centimeters.

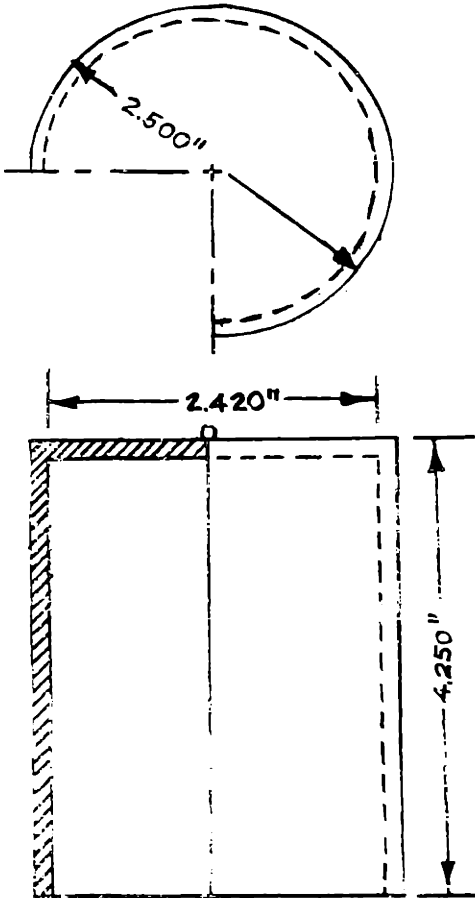
The RVF head provided four speeds: 20, 10, 4, and 2 RPM. Its full-scale torque was 7073 dyne-centimeters.

The scale factors for the two heads were: $0.00613 \text{ dynes/cm.}^2/\text{division}$ for the LVT and $0.0644 \text{ dynes/cm.}^2/\text{division}$ for the RVF.

In operation the rotor and stator assembly were fastened steady and level in a thermostatic bath and the proper Synchroelectric head fastened to the rotor and levelled.

The calibration of the rotor and stator assembly involved the factor: $2.10 \text{ sec.}^{-1}/\text{RPM}$.

ROTOR:



STATOR:

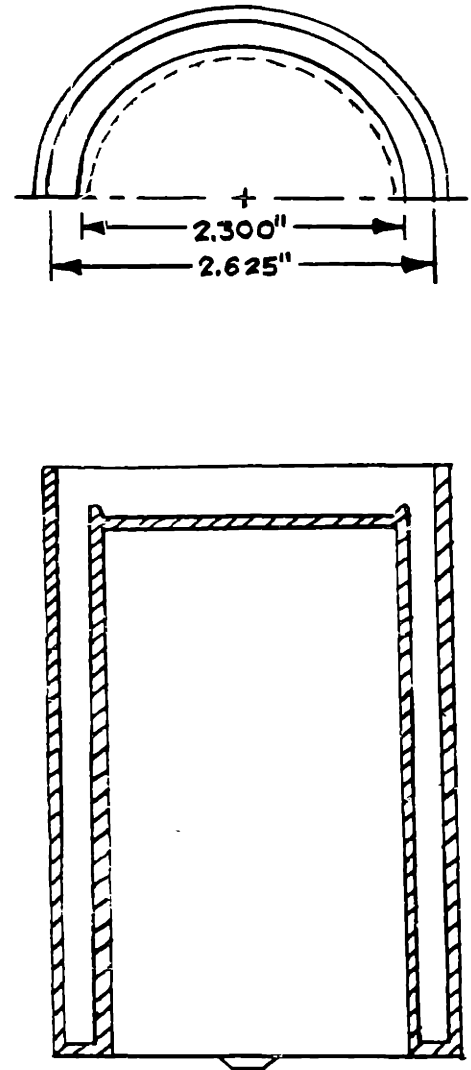


FIGURE 51

ROTOR AND STATOR
OF LOW SHEAR RATE
VISCOMETER
(BROOKFIELD ENG. CO.)

4. Details of Moyno Pumps. Positive, pulse-free flow in the pipeline system was provided by two Robbins and Myers "Moyno" pumps mounted in parallel. These pumps were substantially positive displacement in the range of pressures encountered.

⊙
For high flow rates, a 6M4 Moyno pump was used with rated performance of 2.02 GPM/100 RPM and maximum rated pressure of 600 psi. See Figure 52 for the experimentally determined performance curves for this pump. The rotor on this pump was chromed steel and the stator neoprene rubber,

For low flow rates, a 3L2 Moyno pump was used with rated performance of 0.26 GPM/100 RPM and a maximum rated pressure of 225 psi. See Figure 53 for the performance curve of this pump determined experimentally. This pump, too, had a rubber stator and chromed steel rotor.

The 6M4 unit was driven by a 7.5 HP DC motor with shunt field control and the 3L2 unit by a U.S. Varidrive No. 4500 3/4 HP. The result was a complete control of flow rates, variable from very low rates to 40 GPM, with displacement known from voltage signals delivered from DC tachometer generators driven from the pump shafts.

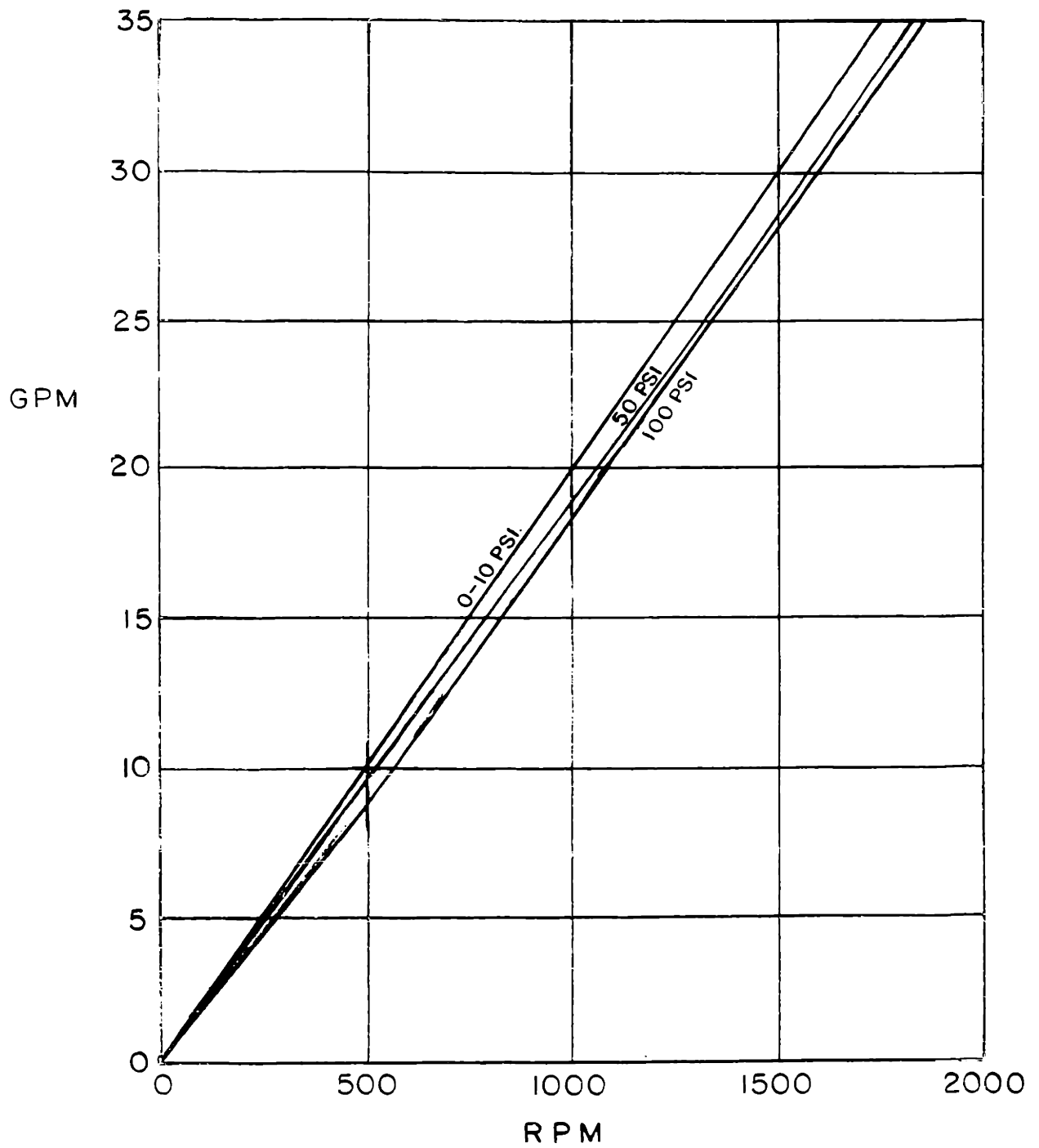


FIGURE 52
GM4 MOYNO
PUMP CURVES

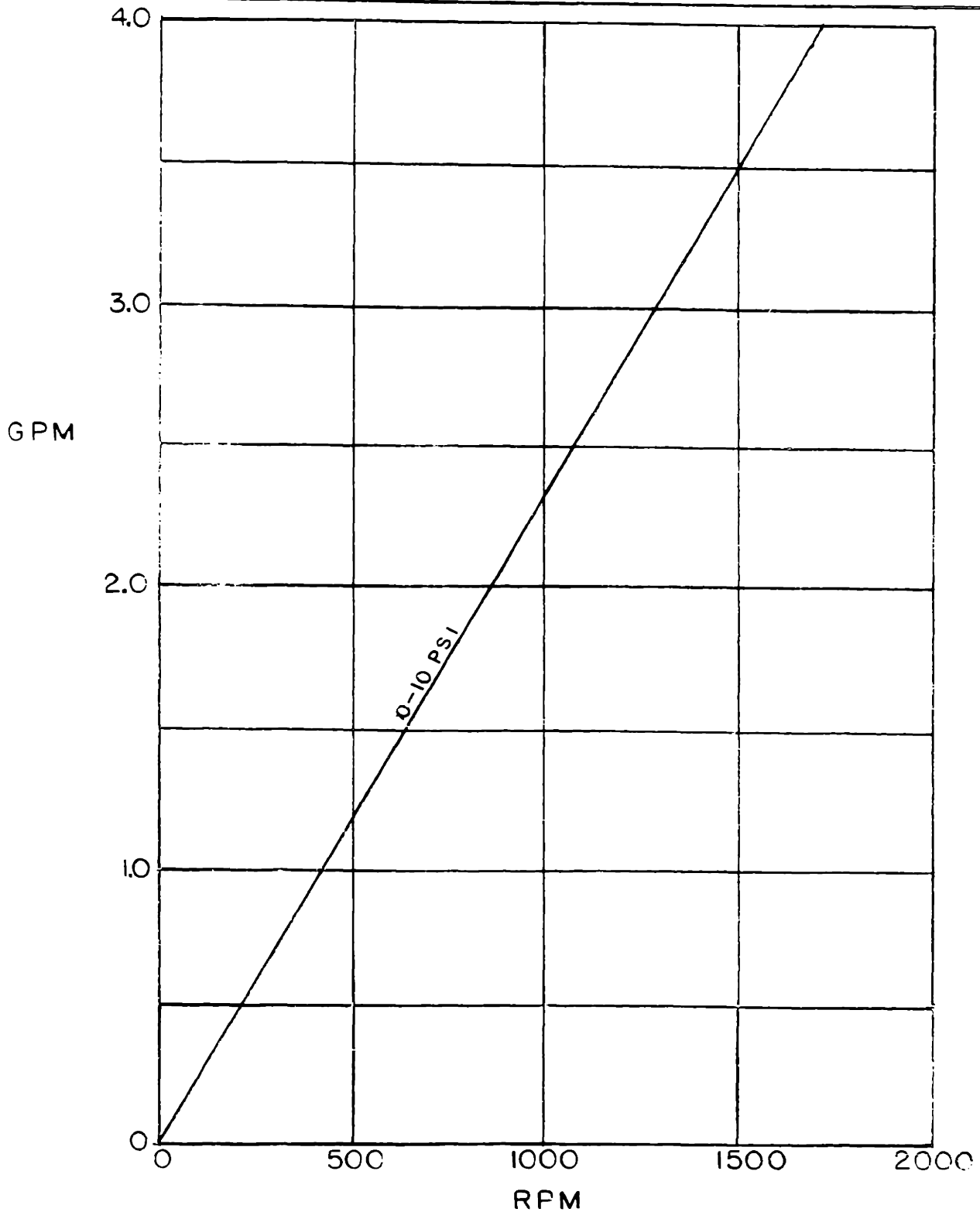


FIGURE 53
3 L 2 MOYNO
PUMP CURVE

5. Details of Traversing Impact Probe. The traversing impact probe was designed and built by the author to be fitted onto any of the stainless-steel tube test sections. Details of the design were influenced by designs for traversing probes intended for use in air flow (23, 37, 58).

The salient characteristics of this probe were:

- (1) positive traversing and location of the probe tip by means of a micrometer,
- (2) positive location of the wall relative to the probe tip by means of an electric circuit and an insulated probe,
- (3) minimum disturbance of flow by means of a very small probe tip (0.025 in. OD) and location of the static pressure tap at the tube wall, and
- (4) good structural rigidity of the probe by means of stacking short lengths of successively smaller diameter hypodermic tubing.

Figure 54 shows the physical arrangement of the components of this mechanism.

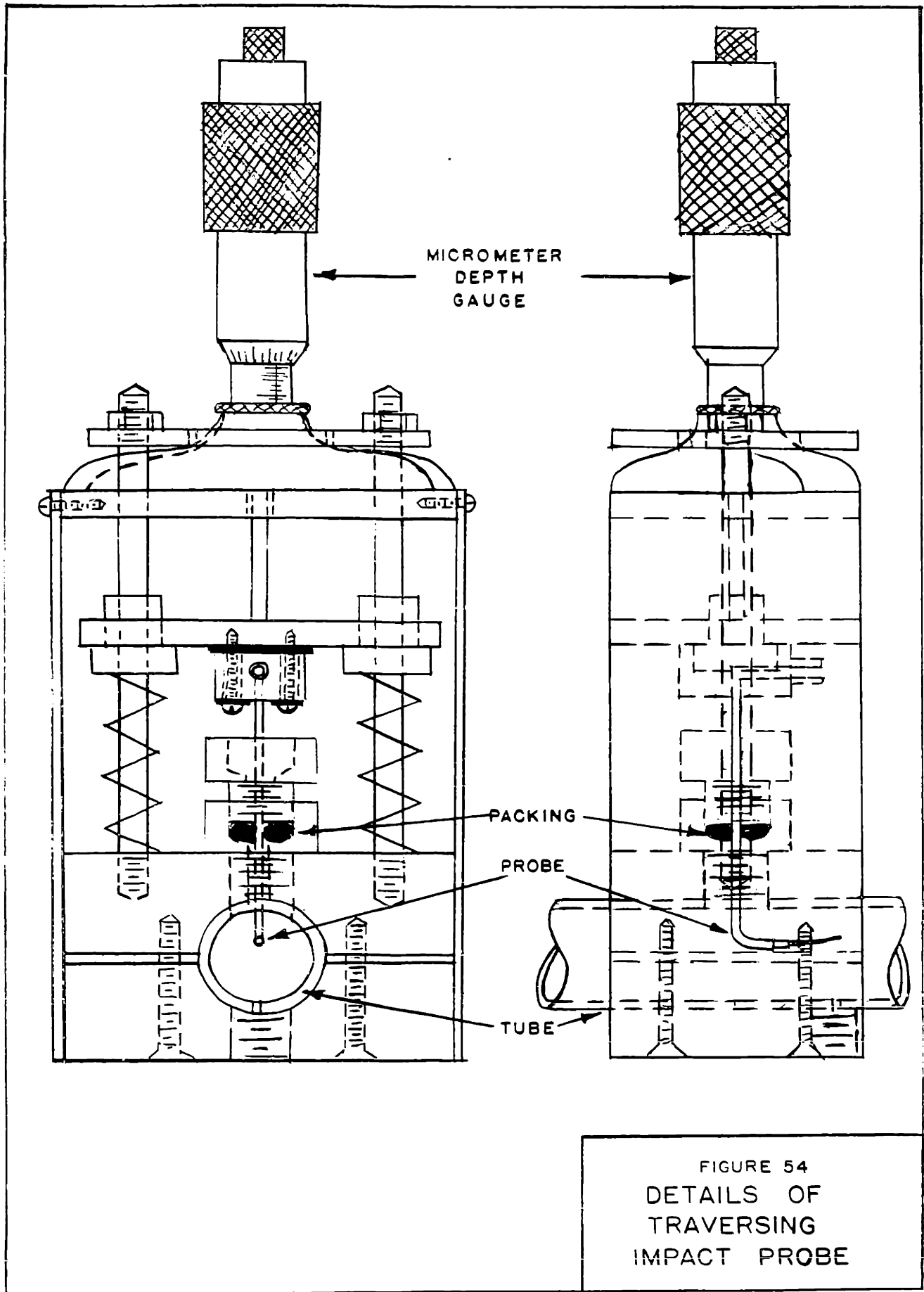


FIGURE 54
DETAILS OF
TRAVERSING
IMPACT PROBE

VIII. APPENDIX (Cont.), B. Sample Calculations

1. Calculation of Fanning friction factor.

$$f = (\Delta h \cdot \Delta \rho \cdot g \cdot R) / (\rho \cdot v^2 \cdot L) \quad (46)$$

For Run No. J-2, first point:

Manometer leg	$\Delta h = 21.5 \pm 0.1 \text{ cm. (Hg-H}_2\text{O)}$
Density Diff.	$\Delta \rho = 12.55 \pm 0.05 \text{ gm./cc.}$
Grav. const.	$g = 980 \text{ cm./sec.}^2$
Radius of tube	$R = 0.231 \pm 0.005 \text{ cm.}$
Fluid density	$\rho = 1.00 \pm 0.01 \text{ gm./cc.}$
Av. velocity	$V = 471 \pm 7 \text{ cm./sec.}$
Length	$L = 30.5 \pm 0.1 \text{ cm.}$

$$f = \frac{(21.5 \pm 0.5\%)(12.55 \pm 0.4\%)(980)(0.231 \pm 2.2\%)}{(1.00 \pm 1.0\%)(471 \pm 1.5\%)^2(30.5 \pm 0.3\%)}$$

$$f = 0.00700 \pm 0.00052$$

2. Calculation of Reynolds' Number.

$$N_{Re} = (D^s v^{2-s} \rho / b) \cdot \phi(s) \quad (22)$$

For Run No. J-1, first point:

Diameter of tube	$D = 1.80 \pm 0.01$ cm.
Av. velocity	$V = 2.99 \pm 0.045$ cm./sec.
Fluid density	$\rho = 1.00 \pm 0.01$ gm./cc.
Exponent	$s = 0.82$ (assume no error, put all error in b)
Rheological const.	$b = 0.422 \pm 0.021$ dyne-sec. $^{0.82}$ /cm. 2
s function	$\phi(s) = 1.39$

$$N_{Re} = \frac{(1.80 \pm 0.6\%)^{0.82} (2.99 \pm 1.5\%)^{1.18} (1.00 \pm 1.0\%) (1.39)}{0.422 \pm 5.0\%}$$

$$N_{Re} = 1100 \pm 91$$

3. Calculation of wall shear stress.

$$\tau_w = (\Delta h \cdot \Delta \rho \cdot g \cdot R) / 2L \quad (47)$$

For Run No. J-2, first point:

Manometer leg	$\Delta h = 21.5 \pm 0.1$ cm. (Hg-H ₂ O)
Density Diff.	$\Delta \rho = 12.55 \pm 0.05$ gm./cc.
Grav. const.	$g = 980$ cm./sec. 2
Tube radius	$R = 0.231 \pm 0.005$ cm.
Length	$L = 30.5 \pm 0.1$ cm.

$$\tau_w = \frac{(21.5 \pm 0.5\%)(12.55 \pm 0.4\%)(980)(0.231 \pm 2.2\%)}{(2)(30.5 \pm 0.3\%)}$$

$$\tau_w = 1000 \pm 34 \text{ dynes/cm.}^2$$

4. Calculation of local velocity

$$u = \sqrt{2 \cdot \Delta h \cdot \Delta \rho \cdot g / \rho} \quad (48)$$

For Run No. 9-B, first point:

Manometer leg	$\Delta h = 30.00 \pm 0.03$ cm. (Hg-H ₂ O)
Density diff.	$\Delta \rho = 12.55 \pm 0.05$ gm/cc.
Grav. constant	$g = 980$ cm./sec. ²
Fluid density	$\rho = 1.00 \pm 0.02$ gm./cc.

$$u = \sqrt{(2)(30.00 \pm 0.1\%)(12.55 \pm 0.4\%)(980)/(1.00 \pm 2.0\%)}$$

$$u = 861 \pm 11 \text{ cm./sec.} = 28.25 \pm 0.35 \text{ ft./sec.}$$

5. Calculation of average velocity

$$V = \text{GPM} \cdot (\text{conversion factor}) / (\pi R^2) \quad (49)$$

For Run No. F-2, first point:

Pump output	GPM = 3.69 ± 0.04 gal./min.
Conversion factor	= $0.320 \frac{(\text{in.}^2)(\text{min.})(\text{ft.})}{(\text{sec.})(\text{gal.})}$
Tube radius	$R = 0.3545 \pm 0.001$ in.

$$V = \frac{(3.69 \pm 1.1\%)(0.320)}{(\pi)(0.3545 \pm 0.3\%)^2}$$

$$V = 2.99 \pm 0.05 \text{ ft./sec.}$$

6. Calculation of friction velocity

$$u_* = V \sqrt{f/2} \quad (50)$$

For Run No. 9-B:

Av. velocity	$V = 22.1 \pm 0.4 \text{ ft./sec.}$
--------------	-------------------------------------

Friction factor	$f = 0.00394 \pm 0.00030$
-----------------	---------------------------

$$u_* = (22.1 \pm 1.7\%) \sqrt{(0.00394 \pm 7.5\%)/2}$$

$$u_* = 0.847 \pm 0.030 \text{ ft./sec.}$$

7. Calculation of relative mixing length.

$$1/R = (u_* \cdot \sqrt{1-y/R}) / (du/dy \cdot R) \quad (33)$$

For Run No. 9-B, first mixing length point:

Friction velocity	$u_* = 0.847 \pm 0.030 \text{ ft./sec.}$
-------------------	--

Distance from wall	$y/R = 0.025 \text{ (not experimental)}$
--------------------	--

Tube radius	$R = 0.3545 \pm 0.001 \text{ in.}$
-------------	------------------------------------

Velocity gradient	$du/dy = 630 \pm 63 \text{ ft./sec./in.}$
-------------------	---

$$1/R = \frac{(0.847 \pm 3.5\%)(1-0.025)}{(630 \pm 10.0\%)(0.3545 \pm 0.3\%)}$$

$$1/R = 0.0037 \pm 0.0005$$

VIII. APPENDIX (Cont.), C. Summary of Data and Calculated Values

Friction Factor Run No. A-1

$s = 1.00$

$b = 0.00941$ poise

Material: Water

5/8" s.s. Tube

GPM	f	N_{Re}	$s^5 N_{Re}^{\delta}$	T_w (dynes/cm ²)	Condition of Manometers
20.0	0.00454	103,500	17.9	865	steady
23.9	0.00423	123,000	18.6	1140	steady

Friction Factor Run No. A-2

$s = 1.00$

$b = 0.00890$ poise

Material: Water

5/8" s.s. Tube

12.4	0.00493	67,600	16.1	360	steady
11.2	0.00536	61,200	15.7	320	steady
13.4	0.00485	80,800	16.8	414	steady
15.2	0.00472	91,000	17.3	510	steady
17.8	0.00451	107,000	18.1	675	steady
21.0	0.00440	126,000	18.8	917	steady
23.3	0.00433	140,000	19.3	1100	steady
27.2	0.00416	163,000	20.0	1450	steady

Friction Factor Run No. A-3

$s = 1.00$

$b = 0.00885$ poise

Material: Water

5/8" s.s. Tube

10.4	0.00489	57,000	15.4	268	steady
14.2	0.00441	77,700	16.7	470	steady
16.6	0.00423	90,100	17.3	609	steady
20.4	0.00415	111,000	18.2	870	steady
22.9	0.00397	127,000	18.8	1070	steady
26.3	0.00380	148,500	19.6	1365	steady
28.8	0.00419	162,300	20.0	1595	steady
34.3	0.00405	197,000	21.0	2140	steady
3.77	0.00595	21,700	12.1	50.4	steady
2.52	0.00675	14,500	11.0	23.0	steady
1.20	0.00820	7,000	9.22	6.2	steady

Friction Factor Run No. A-4

$s = 1.00$

$b = 0.00942$ poise

Material: Water

0.182" Copper Tube

0.926	0.00691	17,100	11.4	552	steady
0.294	0.00925	5,340	8.53	72.2	steady
0.832	0.00929	15,400	11.1	454	steady
0.776	0.00935	14,240	10.9	398	steady

Friction Factor Run No. A-4 (cont.)

GPM	f	N_{Re}	$s^5 N_{Re}^8$	T_w (dynes/cm ²)	Condition of Manometers
0.681	0.00955	12,600	10.5	315	steady
0.545	0.0101	10,070	10.0	212	steady
0.418	0.00841	7,730	9.35	138	steady
1.187	0.00785	21,850	12.1	779	steady
2.065	0.00778	38,100	13.9	2340	steady
2.67	0.00747	49,300	14.9	3770	steady

Friction Factor Run No. A-5

s = 1.00

b = 0.0106 poise

Material: Water

3/8" s.s. Tube

13.6	0.00408	109,000	18.3	3040	steady
11.97	0.00422	95,700	17.6	2430	steady
11.13	0.00430	89,200	17.3	2155	steady
9.67	0.00450	77,500	16.7	1700	steady
7.62	0.00482	61,000	15.7	1125	steady
6.61	0.00499	53,000	15.2	877	steady
3.685	0.00596	29,600	13.1	334	steady
2.58	0.00640	20,650	12.0	177	steady
1.195	0.00760	9,570	9.90	44.0	steady

Friction Factor Run No. A-6

s = 1.00

b = 0.00995 poise

Material: Water

3/8" s.s. Tube

13.2	0.00423	113,000	18.3	2980	steady
11.67	0.00438	99,500	17.8	2400	steady
10.44	0.00450	89,300	17.3	1975	steady
8.50	0.00484	72,600	16.4	1405	steady
6.89	0.00501	58,900	15.6	959	steady
3.685	0.00619	31,500	13.3	339	steady
2.48	0.00700	21,200	12.1	173	steady
1.195	0.00927	10,200	10.1	67.1	steady

Friction Factor Run No. A-7

s = 1.00

b = 0.0105 poise

Material: Water

3/4" s.s. Tube

6.65	0.00585	28,300	13.0	79.2	steady
8.14	0.00518	34,600	13.6	105	steady
10.25	0.00530	43,600	14.4	170	steady
12.50	0.00499	53,100	15.2	238	steady
14.50	0.00498	61,600	15.8	319	steady
17.00	0.00487	72,300	16.4	429	steady
21.3	0.00469	90,600	17.4	653	steady

Friction Factor Run No. A-7 (cont.)

GPM	f	N_{Re}	$s^5 N_{Re}^\delta$	τ_w ($\frac{\text{dynes}}{\text{cm}^2}$)	Condition of Manometers
25.3	0.00453	107,500	18.1	884	steady
32.5	0.00433	138,300	19.2	1395	steady
36.09	0.00418	153,300	19.9	1660	steady
3.685	0.00703	15,670	11.2	29.0	steady
3.685	0.00705	15,670	11.2	28.9	steady
1.19	0.00975	5,060	8.48	3.93	fluctuations (1/2 cm.)
1.72	0.00917	7,310	9.25	7.97	steady
1.43	0.01005	6,080	8.85	5.99	steady
2.58	0.00797	11,000	10.2	15.9	steady
0.923	0.00436	3,920	--	0.855	steady
0.298	0.0114	1,270	--	0.062	steady

Friction Factor Run No. B-1

s = 1.00
b = 0.0254

Material: 1.5% Polyvinyl
Alcohol
5/8" s.s. Tube

11.1	0.00660	21,300	12.1	388	steady
13.3	0.00660	25,500	12.7	556	steady
16.2	0.00625	31,100	13.3	780	steady
21.5	0.00578	41,300	14.2	1265	steady
28.9	0.00538	55,400	15.4	2120	steady
31.4	0.00556	60,100	15.7	2585	steady
11.2	0.00687	21,600	12.2	410	steady
1.88	0.00485	3,610	--	9.10	steady
1.21	0.00700	2,330	--	5.46	steady
3.75	0.0910	7,200	9.20	68.0	steady
3.05	0.0772	5,860	--	38.3	fluctuations (1/2 cm.)
2.50	0.00402	4,800	--	13.3	steady
2.72	0.00375	5,210	--	14.7	steady

Friction Factor Run No. C-1

s = 0.60
b = 2.09

Material: 0.178% CMC-70
5/8" s.s. Tube

10.5	0.00372	4,300	--	196	steady
12.0	0.00316	5,180	--	217	slight fluctuation
16.0	0.00234	7,740	--	284	fluctuation (1/2 mm.)
19.2	0.00199	9,950	--	348	fluctuation (1 mm.)

Friction Factor Run No. C-1 (cont.)

GPM	f	N_{Re}	$s^5 N_{Re}^8$	T_w ($\frac{\text{dynes}}{\text{cm}^2}$)	Condition of Manometers
23.6	0.00178	13,300	--	505	fluctuation (1 cm.)
25.8	0.00188	14,900	36.6	623	fluctuation (1 cm.)
34.9	0.00163	23,000	48.1	972	almost steady
3.77	0.0104	1,020	--	84.1	steady
1.22	0.0816	211	--	32.3	steady

Friction Factor Run No. D-1

s = 0.54

b = 4.80

Material: 0.30% CMC-70

5/8" s.s. Tube

10.52	0.00638	2,730	--	330	steady
13.2	0.00473	3,820	--	385	fluctuation (1 mm.)
16.66	0.00353	5,400	26.0	458	fluctuation (1 mm.)
22.50	0.00247	8,380	36.7	583	slight fluctuation
33.2	0.00160	15,000	56.0	828	slight fluctuation
3.79	0.0223	695	--	168	steady
2.93	0.0326	495	--	148	steady
2.15	0.0494	320	--	120	steady
1.23	0.105	114	--	84.1	steady

Friction Factor Run No. D-2

s = 0.66

b = 1.27

Material: 0.30% CMC-70

5/8" s.s. Tube

1.24	0.0520	291	--	41.9	steady
1.63	0.0398	406	--	55.5	steady
1.95	0.0318	509	--	63.6	steady
2.50	0.0238	688	--	78.2	steady
2.98	0.0190	853	--	88.8	steady
3.44	0.0158	1,024	--	98.3	steady
3.86	0.0136	1,180	--	106	steady
1.24	0.00525	291	--	42.5	steady
1.94	0.00318	505	--	63.1	steady

Friction Factor Run No. D-3
 $s = 0.66$
 $b = 1.27$

Material 0.30% CMC-70

5/8" s.s. Tube

GPM	f	N_{Re}	$s^5 N_{Re}^8$	T_w ($\frac{\text{dynes}}{\text{cm}^2}$)	Condition of Manometers
6.57	0.00770	2,270	--	155	steady
8.16	0.00550	2,950	--	171	steady
9.54	0.00456	3,580	--	194	fluctuation (1 mm.)
11.16	0.00382	4,330	--	221	fluctuation (2 mm.)
13.80	0.00531	5,640	--	560	fluctuation (5 mm.)
28.30	0.00323	13,600	24.5	1245	fluctuation (1 mm.)
21.50	0.00414	9,780	20.5	893	fluctuation (1 mm.)
17.45	0.00481	7,550	17.8	685	fluctuation (1 mm.)
33.40	0.00313	16,700	27.5	1625	almost steady

Friction Factor Run No. D-4
 $s = 0.66$
 $b = 1.27$

Material: 0.30% CMC-70

5/8" s.s. Tube

10.4	0.00356	4,500	--	164	steady
11.4	0.00314	5,100	--	173	steady
12.3	0.00288	5,630	--	185	slight fluctuation
12.65	0.00284	5,830	--	192	fluctuation (1 mm.)
13.35	0.00271	6,310	--	204	fluctuation (3 cm.)
13.9	0.00258	6,620	--	212	fluctuation (5 cm.)
14.55	0.00367	7,020	--	329	fluctuation (4 cm.)
15.4	0.00372	7,600	--	376	fluctuation (3 cm.)
16.9	0.00437	8,700	19.2	532	fluctuation (3 mm.)
18.2	0.00412	9,530	20.1	580	slight fluctuation
19.95	0.00383	10,800	21.6	648	almost steady
22.0	0.00390	12,300	23.2	800	almost steady
26.3	0.00340	15,600	26.3	997	steady
34.0	0.00293	22,100	32.1	1443	steady

Friction Factor Run No. D-5

$s = 0.74$
 $b = 0.505$

Material 0.30% CMC-70

5/8" s.s. Tube

GPM	f	N_{Re}	$s^5 N_{Re}^{\delta}$	T_w ($\frac{\text{dynes}}{\text{cm}^2}$)	Condition of Manometers
32.4	0.00352	26,800	24.2	1720	steady
22.6	0.00441	17,000	20.0	1054	steady
16.5	0.00535	11,500	16.7	681	steady
14.35	0.00590	9,590	15.3	566	steady
13.7	0.00610	9,030	14.9	533	slight fluctuation
12.73	0.00642	8,260	14.3	483	slight fluctuation
11.55	0.00682	7,300	13.5	425	slight fluctuation
10.85	0.00700	6,760	13.0	385	fluctuation (1 mm.)
10.31	0.00724	6,340	12.6	359	fluctuation (2 cm.)
10.2	0.00726	6,280	12.6	352	fluctuation (2 cm.)
6.64	0.00487	3,630	--	100	steady
3.79	0.00884	1,800	--	66.6	steady
2.89	0.0126	1,280	--	55.2	steady
2.18	0.0160	865	--	40.0	steady
1.240	0.0295	439	--	23.7	steady

Friction Factor Run No. D-6

$s = 0.74$
 $b = 0.505$

Material: 0.30% CMC-70

5/8" s.s. Tube

6.00	0.00931	3,360	--	157	steady
7.92	0.00823	4,690	--	241	steady
8.81	0.00710	5,200	--	257	fluctuation (3 cm.)
9.70	0.00750	5,850	12.0	330	fluctuation (1 mm.)
12.00	0.00650	7,450	13.5	436	steady
6.28	0.00560	3,560	--	104	steady
8.21	0.00381	4,810	--	120	steady
9.41	0.00462	5,630	--	191	fluctuation (3 cm.)
10.3	0.00741	6,230	12.4	367	fluctuation (2 mm.)
10.8	0.00705	6,620	12.9	383	fluctuation (1 mm.)
31.7	0.00374	22,600	22.6	1760	steady

Friction Factor Run No. D-7

$s = 0.74$
 $b = 0.505$

Material: 0.30% CMC-70

5/8" s.s. Tube w/ Turbulence Promoter

GPM	f	N_{Re}	$s^5 N_{Re}^8$	τ_w ($\frac{\text{dynes}}{\text{cm}^2}$)	Condition of Manometers
6.93	0.00910	3,830	10.0	204	slight fluctuation
8.71	0.00790	5,110	11.4	279	steady
10.7	0.00708	6,640	12.8	378	steady
10.95	0.00708	6,740	12.9	378	steady
13.85	0.00602	8,500	16.6	538	steady
33.3	0.00369	21,000	21.8	1920	steady
3.83	0.00821	2,010	--	63.2	steady
3.00	0.0108	1,520	--	51.0	steady
2.14	0.0157	1,030	--	37.6	steady
1.24	0.0290	552	--	23.4	steady

Friction Factor Run No. D-8

$s = 0.85$
 $b = 0.1195$

Material: 0.30% CMC-70

5/8" s.s. Tube

3.83	0.00700	2,220	--	54.0	steady
3.16	0.00858	1,735	--	44.9	steady
2.16	0.0122	1,318	--	29.8	steady
1.24	0.0217	649	--	17.5	steady
3.83	0.00680	2,220	--	52.4	steady
3.83	0.00543	3,030	--	41.7	steady
1.24	0.0176	925	--	14.2	steady
2.16	0.00955	1,660	--	23.4	steady
3.16	0.00649	2,465	--	33.9	steady

Friction Factor Run No. D-9

$s = 0.85$
 $b = 0.1195$

Material: 0.30% CMC-70

5/8" s.s. Tube

9.90	0.00752	7,050	10.4	344	steady
11.93	0.00720	9,900	11.7	480	steady
14.25	0.00655	12,900	12.9	619	steady
17.1	0.00555	15,870	13.8	760	steady
21.8	0.00483	22,750	15.8	1070	steady
24.9	0.00448	27,700	17.0	1297	steady
26.3	0.00458	31,100	17.7	1480	steady
31.3	0.00404	39,700	19.3	1850	steady
6.40	0.00964	4,180	8.60	184	fluctuation (1 cm.)
8.05	0.00860	5,280	9.38	260	steady
1.24	0.0206	771	--	16.6	steady

Friction Factor Run No. D-9 (cont.)

GFM	f	N_{Re}	$s^5 N_{Re}^8$	τ_w ($\frac{\text{dynes}}{\text{cm}^2}$)	Condition of Manometers
3.85	0.00647	2,470	--	50.1	steady
3.16	0.00800	2,020	--	41.7	steady
2.16	0.0118	1,366	--	28.7	steady

Friction Factor Run No. E-1

s = 0.53

b = 9.20

Material: 0.41% CMC-70

5/8" s.s. Tube

10.32	0.0107	1,490	--	533	steady
12.61	0.00803	1,980	--	597	steady
15.2	0.00621	2,580	--	670	steady
18.4	0.00470	3,390	--	743	steady
22.3	0.00368	4,450	--	853	steady
6.78	0.0197	818	--	423	steady
8.52	0.0141	1,135	--	476	steady
10.35	0.0107	1,490	--	531	steady
25.43	0.00308	5,430	--	935	slight fluctuation
32.2	0.00237	8,530	--	1146	slight fluctuation

Friction Factor Run No. E-2

s = 0.53

b = 9.20

Material: 0.41% CMC-70

5/8" s.s. Tube w/ Turbulence Promoter

10.18	0.00950	1,650	--	500	steady
11.8	0.00766	2,050	--	540	steady
13.18	0.00658	2,410	--	579	steady
14.81	0.00545	2,850	--	619	steady
18.57	0.00400	3,970	--	715	steady
21.77	0.00328	5,000	--	808	steady
25.2	0.00276	6,200	--	911	steady
32.2	0.00205	8,920	--	1100	slight fluctuation
34.1	0.00207	9,730	43.2	1170	slight fluctuation
35.3	0.00186	10,250	45.8	1203	fluctuation (1 mm.)
3.85	0.0362	394	--	279	steady

Friction Factor Run No. E-3

 $\epsilon = 0.53$ $b = 9.20$

Material: 0.41% CMC-70

3/8" s.s. Tube

GPM	f	N_{Re}	$s^5 N_{Re}^{\delta}$	$T_w \left(\frac{\text{dynes}}{\text{cm}^2} \right)$	Condition of Manometers
1.24	0.0584	260	--	333	steady
2.02	0.0288	535	--	433	steady
2.40	0.02215	686	--	474	steady
3.12	0.0142	1,010	--	546	steady
3.85	0.0111	1,440	--	609	steady
10.1	0.00307	5,590	--	1160	slight fluctuation
11.64	0.00259	6,830	--	1300	slight fluctuation
13.21	0.00223	8,300	38.2	1440	slight fluctuation
15.44	0.00188	10,350	45.0	1660	almost steady
17.26	0.00166	12,300	50.9	1820	almost steady
20.5	0.00139	15,700	61.7	2165	almost steady
22.2	0.00129	17,700	67.1	2355	almost steady
6.50	0.00535	2,920	--	838	steady
8.30	0.00385	4,210	--	983	steady

Friction Factor Run No. E-4

 $\epsilon = 0.57$ $b = 5.59$

Material: 0.41% CMC-70

3/8" s.s. Tube

1.24	0.0505	314	--	288	steady
2.04	0.0249	640	--	385	steady
2.88	0.0153	1,046	--	469	steady
3.85	0.00992	1,580	--	545	steady
6.32	0.00503	3,200	--	745	steady
7.44	0.00406	4,040	--	832	steady
8.51	0.00336	4,900	--	902	fluctuation (1 mm.)
9.51	0.00286	5,720	--	956	fluctuation (3 mm.)
9.80	0.00284	6,000	--	1010	fluctuation (3 mm.)
10.60	0.00276	6,650	--	1145	fluctuation (5 mm.)
13.10	0.00239	9,050	32.2	1525	fluctuation (2 mm.)
15.10	0.00211	11,240	36.6	1780	fluctuation (1 mm.)
20.00	0.00170	16,500	48.0	2510	almost steady
21.8	0.00160	18,600	51.8	2815	almost steady
1.24	0.00500	314	--	284	steady

Friction Factor Run No. E-5
 $s = 0.59$
 $b = 4.01$

Material: 0.41% CMC-70
 3/4" s.s. Tube

GPM	f	N_{Re}	$s^5 N_{Re}^\delta$	τ_w ($\frac{\text{dynes}}{\text{cm}^2}$)	Condition of Manometers
10.06	0.00985	1,800	--	305	steady
12.32	0.00734	2,380	--	341	steady
13.77	0.00627	2,790	--	363	steady
14.80	0.00570	3,080	--	381	steady
18.58	0.00420	4,270	--	442	steady
20.74	0.00363	5,000	--	479	steady
23.3	0.00320	5,870	--	533	slight fluctuation
25.5	0.00283	6,640	--	564	fluctuation (1 mm.)
27.0	0.00268	7,260	--	600	fluctuation (2 mm.)
28.5	0.00252	7,780	--	624	fluctuation (5 mm.)
29.8	0.00239	8,280	--	650	fluctuation (1 cm.)
31.8	0.00293	9,050	28.7	904	fluctuation (5 mm.)
35.1	0.00261	10,300	31.1	982	fluctuation (2 mm.)
12.30	0.00745	2,380	--	345	steady
37.95	0.00252	11,630	33.9	1110	almost steady

Friction Factor Run No. E-7
 $s = 0.62$
 $b = 2.70$

Material: 0.41% CMC-70
 3/4" s.s. Tube w/ turbulence promoter

GPM	f	N_{Re}	$s^5 N_{Re}^\delta$	$\frac{\text{dynes}}{\text{cm}^2}$	Condition of Manometers
10.31	0.00703	2,300	--	229	steady
12.03	0.00571	2,830	--	254	steady
15.95	0.00391	4,090	--	305	steady
20.4	0.00287	5,700	--	365	slight fluctuation
21.66	0.00293	6,180	--	421	fluctuation (1 cm.)
24.03	0.00355	7,200	21.1	630	fluctuation (1 cm.)
28.5	0.00311	9,120	24.1	772	almost steady
32.6	0.00281	11,000	27.1	914	steady
36.45	0.00254	12,900	29.6	1040	steady
3.685	0.0271	585	--	113	steady

Friction Factor Run No. E-6

s = 0.59

b = 4.01

Material: 0.4% CMC-70

3/4" s.s. Tube w/ Turbulence
Promoter

GPM	f	N _{Re}	s ⁵ · N _{Re} ⁸	T _w ($\frac{\text{dynes}}{\text{cm}^2}$)	Condition of Manometers
10.20	0.00905	1,820	--	285	steady
12.69	0.00664	2,510	--	323	steady
15.6	0.00507	3,310	--	374	steady
19.15	0.00386	4,390	--	428	steady
22.2	0.00319	5,410	--	475	slight fluctuation
24.1	0.00284	6,100	--	500	fluctuation (4 mm.)
26.05	0.00265	6,800	--	544	fluctuation (5 mm.)
27.5	0.00267	7,360	--	610	fluctuation (1 cm.)
30.1	0.00303	8,340	27.0	831	fluctuation (1.5 cm.)
30.55	0.00327	8,570	27.5	922	fluctuation (2 mm.)
37.45	0.00245	11,400	33.4	1035	almost steady
40.35	0.00243	12,600	35.4	1195	almost steady
9.80	0.00956	1,730	--	278	steady

Friction Factor Run No. F-1

s = 0.64

b = 2.22

Material: 0.35% CMC-70

3/4" s.s. Tube

3.685	0.0242	665	--	101	steady
10.48	0.00640	2,460	--	214	steady
12.25	0.00523	3,060	--	240	steady
14.31	0.00431	3,760	--	270	steady
17.5	0.00337	4,960	--	316	steady
19.9	0.00291	5,900	--	354	fluctuation (1 mm.)
20.8	0.00450	6,280	17.8	600	fluctuation (1 cm.)
23.2	0.00415	7,240	19.3	685	fluctuation (1 cm.)
24.1	0.00401	7,680	19.9	715	fluctuation (1 cm.)
26.8	0.00369	8,850	21.5	811	almost steady
29.6	0.00346	9,510	22.5	931	almost steady
32.9	0.00308	11,650	25.2	1023	almost steady
37.05	0.00291	13,800	27.8	1230	steady
3.685	0.0235	665	--	99	steady

Friction Factor Run No. F-2

s = 0.64

b = 2.22

Material: 0.35% CMC-70

3/4" s.s. Tube

GPM	f	N_{Re}	$s^5 \cdot N_{Re}^8$	T_w (dynes/cm ²)	Condition of Manometers
3.685	0.0234	665	--	96.1	steady
9.76	0.00668	2,240	--	195	steady
12.48	0.00489	3,120	--	232	steady
17.3	0.00328	4,860	--	302	slight fluctuation
19.35	0.00297	5,660	--	341	fluctuation (5 mm.)
20.9	0.00443	6,340	17.7	594	fluctuation (5 mm.)
23.6	0.00404	7,480	19.5	691	fluctuation (3 mm.)
26.0	0.00370	8,380	20.8	772	steady
30.1	0.00329	10,300	23.6	920	steady
31.9	0.00315	11,400	24.8	985	steady
36.0	0.00286	13,200	27.1	1136	steady
39.75	0.00262	14,100	28.2	1270	steady
3.685	0.0230	665	--	94.8	steady
14.16	0.00412	3,700	--	254	steady

Friction Factor Run No. F-3

s = 0.64

b = 2.22

Material: 0.35% CMC-70

1/2" s.s. Tube

3.685	0.01215	1,230	--	206	steady
1.195	0.0501	267	--	89.2	steady
10.25	0.00323	4,940	--	423	steady
11.9	0.00275	6,040	--	483	steady
12.64	0.00260	6,600	--	515	steady
13.73	0.00303	7,300	--	710	fluctuation (1 cm.)
15.44	0.00259	8,650	--	767	fluctuation (1 cm.)
18.7	0.00298	11,200	24.8	1297	fluctuation (2 cm.)
20.1	0.00294	12,400	26.1	1470	fluctuation (2 mm.)
21.8	0.00275	13,700	27.9	1623	almost steady
26.0	0.00241	17,600	31.9	2025	almost steady
31.35	0.00204	22,600	37.1	2610	steady
35.0	0.00198	26,200	40.7	3000	steady
38.50	0.00187	30,000	44.1	3430	steady

Friction Factor Run No. F-4

s = 0.64

b = 2.22

Material: 0.35% CMC-70

3/8" s.s. Tube

GPM	f	N_{Re}	$s^5 \cdot N_{Re}^8$	τ_w (dynes/cm ²)	Condition of Manometers
3.685	0.00685	2,270	--	377	steady
1.195	0.0299	494	--	175	steady
6.10	0.00353	4,510	--	531	steady
8.02	0.00260	6,550	--	673	fluctuation (1 mm.)
8.54	0.00240	7,100	--	709	fluctuation (2 mm.)
9.02	0.00222	7,610	--	730	fluctuation (2 cm.)
9.52	0.00275	8,270	--	1006	fluctuation (4 cm.)
11.67	0.00301	10,900	24.4	1656	fluctuation (1 cm.)
12.78	0.00282	12,300	26.0	1870	fluctuation (2 mm.)
14.33	0.00258	14,400	28.6	2150	almost steady
16.85	0.00228	17,800	32.3	2620	steady
17.76	0.00224	19,200	33.6	2860	steady
3.685	0.00685	2,270	--	376	steady
1.195	0.0300	500	--	175	steady

Friction Factor Run No. F-5

s = 0.64

b = 2.22

Material: 0.35% CMC-70

5/8" s.s. Tube

1.195	0.0704	216	--	51.0	steady
3.685	0.0180	889	--	128	steady
10.1	0.00509	3,070	--	263	steady
12.27	0.00400	4,030	--	304	steady
14.09	0.00336	4,800	--	338	fluctuation (1 mm.)
16.31	0.00283	5,950	--	381	fluctuation (2 cm.)
19.2	0.00421	7,380	19.4	789	fluctuation (3 cm.)
22.53	0.00372	9,170	22.1	957	steady
26.85	0.00324	11,700	25.3	1185	steady
32.15	0.00290	14,900	29.0	1517	steady
35.6	0.00270	17,100	31.8	1725	steady
39.24	0.00248	19,600	34.0	1960	steady
3.685	0.0180	889	--	128	steady
1.195	0.0699	216	--	50.7	steady

Friction Factor Run No. G-1
 $s = 0.70$
 $b = 3.47$

Material: 1.0% Ammonium
 Alginate
 1/2" s.s. Tube

GPM	f	N_{Re}	$s^5 \cdot N_{Re}^8$	T_w ($\frac{\text{dynes}}{\text{cm}^2}$)	Condition of Manometers
10.60	0.00751	2,040	--	1060	steady
12.53	0.00610	2,550	--	1200	steady
16.19	0.00440	3,490	--	1444	steady
20.05	0.00336	4,580	--	1700	steady
23.83	0.00274	5,710	--	1944	steady
24.55	0.00379	5,930	--	2860	fluctuation (5 cm.)
26.50	0.00550	6,770	14.7	4840	fluctuation (5 mm.)
26.80	0.00558	6,890	14.8	5020	fluctuation (1 mm.)
31.23	0.00496	8,450	16.5	6010	steady
36.58	0.00455	10,300	18.3	7630	steady
3.685	0.0301	522	--	510	steady

Friction Factor Run No. H-1
 $s = 0.73$
 $b = 2.15$

Material: 0.83% Ammonium
 Alginate
 1/2" s.s. Tube

3.685	0.0234	685	--	398	steady
10.62	0.00611	2,640	--	865	steady
12.54	0.00492	3,240	--	970	steady
16.13	0.00360	4,470	--	1180	steady
19.53	0.00430	5,720	--	2050	fluctuation (2 cm.)
22.60	0.00593	6,860	13.4	3790	fluctuation (2 mm.)
25.15	0.00555	7,810	14.2	4400	steady
29.40	0.00504	9,610	15.9	5470	steady
33.75	0.00465	11,350	17.0	6640	steady
36.90	0.00431	12,800	18.0	7390	steady

Friction Factor Run No. I-1
 $s = 0.74$
 $b = 1.38$

Material: 0.62% Ammonium
 Alginate
 1/2" s.s. Tube

7.79	0.00601	2,550	--	476	steady
6.71	0.00769	2,110	--	433	steady
10.22	0.00851	3,590	9.77	1110	steady
9.36	0.00702	3,220	--	770	fluctuation (1 cm.)
11.07	0.00820	4,000	10.2	1260	steady

Friction Factor Run No. I-1 (cont.)

GPM	f	N_{Re}	$s^5 \cdot N_{Re}^{\delta}$	τ_w ($\frac{\text{dynes}}{\text{cm}^2}$)	Condition of Manometers
12.50	0.00536	4,650	--	1050	fluctuation (2 cm.)
13.63	0.00730	5,150	11.3	1700	fluctuation (1 mm.)
15.86	0.00675	6,290	12.6	2120	fluctuation (1 mm.)
20.16	0.00591	8,480	14.5	3000	steady
28.80	0.00484	13,300	17.9	5010	steady
31.23	0.00460	14,700	18.7	5670	steady
35.08	0.00422	17,000	20.0	6500	steady
3.85	0.0143	1,000	--	244	steady

Friction Factor Run No. I-1A

s = 0.74

b = 1.38

Material: 0.62% Ammonium Alginate

1/2" s.s. Tube

3.685	0.0154	1,000	--	263	steady
1.195	0.0573	240	--	102	steady
6.05	0.00834	1,860	--	383	steady
7.09	0.00690	2,270	--	433	steady
8.31	0.00544	2,780	--	497	steady
11.14	0.00407	4,010	--	630	steady
12.88	0.00337	4,850	--	699	fluctuation (2 cm.)
15.05	0.00485	5,870	--	1375	fluctuation (5 cm.)
16.92	0.00659	6,800	13.1	2360	fluctuation (1 mm.)
23.23	0.00542	10,150	15.9	3660	steady

Friction Factor Run No. I-2

s = 0.74

b = 1.38

Material: 0.62% Ammonium Alginate

0.182" Copper Tube

1.196	0.0133	1,450	--	1346	steady
3.70	0.00765	6,020	12.4	7470	steady
0.925	0.0165	1,050	--	1010	steady
0.299	0.0610	253	--	387	steady
0.592	0.0274	597	--	687	steady
1.85	0.0929	2,530	--	2270	fluctuation (1 mm.)
1.39	0.0119	1,760	--	1616	steady
2.37	0.00883	3,430	9.55	3520	fluctuation (2 mm.)
1.915	0.0919	2,630	--	2420	fluctuation (2 mm.)
1.545	0.0107	2,000	--	1810	steady

Friction Factor Run No. I-3

$s = 0.74$

$b = 1.38$

Material: 0.62% Ammonium
Alginate

3/4" s.s. Tube

GPM	f	N_{Re}	$s^5 \cdot N_{Re}^{\delta}$	T_w ($\frac{\text{dynes}}{\text{cm}^2}$)	Condition of Manometers
10.45	0.00793	2,000	--	265	steady
13.27	0.00605	2,690	--	326	steady
15.48	0.00513	3,230	--	377	steady
18.41	0.00422	4,050	--	438	fluctuation (1 mm.)
21.25	0.00562	4,910	--	797	fluctuation (2 cm.)
25.00	0.00702	5,940	12.3	1340	fluctuation (2 mm.)
27.20	0.00680	6,590	12.9	1540	almost steady
33.05	0.00607	8,450	14.4	2030	steady
36.40	0.00578	9,530	15.2	2340	steady
40.05	0.00549	10,600	16.0	2690	steady
6.68	0.0133	1,050	--	182	steady
8.28	0.0104	1,480	--	218	steady
3.685	0.0261	535	--	109	steady

Friction Factor Run No. I-4

$s = 0.74$

$b = 1.38$

Material: 0.62% Ammonium
Alginate

3/4" s.s. Tube

10.06	.00819	1,900	--	254	steady
12.04	.00643	2,380	--	287	steady
15.52	.00600	3,270	--	442	slight fluctuation
3.685	.0253	535	--	105	steady
21.45	.00741	4,910	11.3	1045	fluctuation (1 cm.)
24.00	.00705	5,680	12.0	1250	slight fluctuation
32.75	.00598	8,400	14.4	1970	steady
36.45	.00565	9,610	15.3	2300	steady

Friction Factor Run No. J-1

$s = 0.82$

$b = 0.422$

Material: 0.46% Ammonium
Alginate

3/4" s.s. Tube

3.685	0.0157	1,100	--	65.5	steady
6.89	0.00773	2,080	--	113	steady
8.80	0.00595	2,780	--	142	steady
14.26	0.00349	4,910	--	218	fluctuation (2 cm.)

Friction Factor Run No. J-1 (cont.)

GPM	f	N_{Re}	$s^5 \cdot N_{Re}^{\delta}$	$T_w \left(\frac{\text{dynes}}{\text{cm}^2} \right)$	Condition of Manometers
14.98	0.00632	5,200	--	437	fluctuation (2 cm.)
16.83	0.00752	6,010	10.3	655	fluctuation (1 mm.)
25.10	0.00621	9,630	12.2	1203	steady
35.05	0.00530	14,100	14.3	2000	steady
38.90	0.00501	16,100	15.0	2330	steady
18.23	0.00715	6,580	10.6	730	steady

Friction Factor Run No. J-2

s = 0.82

b = 0.422

Material: 0.46% Ammonium Alginate

0.182" Copper Tube

1.245	0.00700	2,770	--	1002	steady
1.58	0.00684	3,960	--	1547	fluctuation (2 mm.)
1.78	0.00680	4,200	--	1960	slight fluctuation
2.20	0.00628	5,320	--	2760	fluctuation (2 mm.)
2.495	0.00669	6,250	10.4	3780	steady
3.18	0.00615	8,330	11.7	5620	steady
3.85	0.00538	10,500	12.7	7270	steady
0.310	0.0288	535	--	241	steady
0.965	0.00940	2,050	--	796	steady

Friction Factor Run No. K-1

s = 0.95

b = 0.0302

Material: 0.10% Ammonium Alginate

3/4" s.s. Tube

9.86	0.00660	20,400	12.7	196	steady
12.80	0.00580	26,700	13.7	291	steady
15.2	0.00550	31,800	14.4	385	steady
21.0	0.00489	44,900	15.9	661	steady
25.2	0.00459	54,500	16.7	894	steady
31.9	0.00440	69,900	17.9	1365	steady
34.70	0.00427	76,200	18.4	1570	steady
3.85	0.00853	7,600	9.60	38.6	fluctuation (1 mm.)
1.245	0.00758	2,330	--	3.6	fluctuation (1 mm.)

Friction Factor Run No. K-2

$s = 0.95$
 $b = 0.0302$

Material: 0.10% Ammonium
 Alginate
 3/4" s.s. Tube

GPM	f	N_{Re}	$s^5 \cdot N_{Re}^{\delta}$	$\tau_w \left(\frac{\text{dynes}}{\text{cm}^2} \right)$	Condition of Manometers
10.0	0.00634	20,600	12.7	195	steady
7.54	0.00705	15,400	11.8	124	steady
6.25	0.00790	12,650	11.1	98.8	steady
3.85	0.00800	7,600	9.60	36.6	fluctuation (1 mm.)
1.245	0.00795	2,330	--	4.10	steady
0.963	0.00965	1,770	--	3.08	steady
0.311	0.0289	540	--	1.20	steady
11.96	0.00605	24,900	13.4	265	steady
3.29	0.00820	6,450	--	27.6	steady
2.76	0.00845	5,360	--	20.0	steady
2.195	0.00454	4,200	--	6.84	steady
1.875	0.00516	3,590	--	5.71	steady
1.50	0.00631	2,820	--	4.51	steady

Friction Factor Run No. K-3

$s = 0.95$
 $b = 0.0302$

Material: 0.10% Ammonium
 Alginate
 3/8" s.s. Tube

0.3115	0.0143	1,135	--	5.90	steady
0.505	0.00905	1,885	--	9.62	steady
0.633	0.00727	2,400	--	12.1	steady
0.774	0.00600	2,950	--	14.8	steady
0.918	0.00505	3,540	--	17.5	steady
0.962	0.00514	3,700	--	19.4	fluctuation (1 cm.)
1.245	0.00382	4,860	--	24.2	steady
1.625	0.00307	6,430	--	33.0	fluctuation (2 cm.)
2.117	0.00734	8,480	9.90	8.15	fluctuation (5 cm.)
1.245	0.00396	4,860	--	1.16	fluctuation (3 mm.)
2.415	0.00730	9,760	10.3	8.05	steady
2.89	0.00693	11,750	10.8	10.9	steady
3.39	0.00643	13,900	11.4	14.3	steady
3.85	0.00630	15,900	11.8	17.6	steady
6.47	0.00578	27,500	13.8	45.8	steady
7.29	0.00532	31,200	14.3	53.3	steady
8.15	0.00510	34,900	14.8	64.0	steady
9.32	0.00488	40,100	15.4	80.1	steady
10.53	0.00469	45,900	16.0	98.1	steady
13.00	0.00435	57,200	17.0	139	steady

Friction Factor Run No. L-1

$s = 0.84$
 $b = 0.119$

Material: 0.20% Ammonium
 Alginate
 3/8" s.s. Tube

GPM	f	N_{Re}	$s^5 \cdot N_{Re}^8$	τ_w ($\frac{\text{dynes}}{\text{cm}^2}$)	Condition of Manometers
13.25	0.00442	40,000	20.0	3110	steady
11.90	0.00466	34,000	18.9	2660	steady
10.80	0.00480	31,100	18.2	2260	steady
9.36	0.00512	26,600	17.2	1800	steady
7.54	0.00558	20,600	15.6	1280	steady
6.41	0.00595	17,100	14.6	984	steady
3.85	0.00680	9,490	11.8	405	steady
3.18	0.00725	7,580	10.9	295	slight fluctuation
2.835	0.00707	6,660	--	228	fluctuation (1 cm.)
3.85	0.00680	9,490	--	406	steady
2.01	0.00375	4,460	--	61	steady
2.01	0.00360	4,460	--	59	steady
1.555	0.00474	3,310	--	46	steady
1.243	0.00590	2,560	--	37	steady
0.964	0.00770	1,900	--	29	steady
0.821	0.00905	1,580	--	21	steady
0.687	0.0108	1,280	--	18	steady
0.517	0.0146	923	--	16	steady
0.311	0.0244	513	9.6	10	steady

Friction Factor Run No. M-1

$s = 0.83$
 $b = 0.189$

Material: 0.30% Ammonium
 Alginate
 3/8" s.s. Tube

0.964	0.0123	1,270	--	46.1	steady
0.311	0.0401	341	--	15.8	steady
1.243	0.00910	1,710	--	56.9	steady
2.60	0.00420	4,050	--	115.	steady
3.85	0.00726	6,410	10.4	164.	steady
6.28	0.00661	11,350	13.0	1045	fluctuation (1 cm.)
7.45	0.00604	13,900	13.8	1350	steady
9.86	0.00535	19,100	15.8	2100	steady
11.14	0.00504	22,200	16.5	2530	steady
12.57	0.00479	25,700	17.5	3040	steady

Friction Factor Run No. N-1
 $s = 0.54$
 $b = 7.05$

Material: 0.50% CMC-70s

3/8" s.s. Tube

GPM	f	N_{Re}	$s^5 \cdot N_{Re}^{\delta}$	$\tau_w \left(\frac{\text{dynes}}{\text{cm}^2} \right)$	Condition of Manometers
3.85	0.0165	1,530	--	629	steady
2.60	0.0192	873	--	523	steady
1.245	0.0587	302	--	361	steady
6.61	0.00494	3,340	--	868	steady
8.25	0.00361	4,600	--	982	steady
10.10	0.00268	6,300	--	1110	slight fluctuation
11.66	0.00224	7,710	--	1240	fluctuation (2 mm.)
13.23	0.00188	9,170	39.2	1325	fluctuation (2 mm.)
14.9	0.00164	11,000	45.0	1480	fluctuation (1 mm.)
17.57	0.00139	13,700	51.8	1750	slight fluctuation
19.85	0.00124	16,500	60.1	2000	slight fluctuation
23.65	0.00105	21,100	73.0	2410	fluctuation (2 mm.)
28.9	0.000897	28,300	90.0	3040	fluctuation (2 mm.)

Friction Factor Run No. N-2
 $s = 0.54$
 $b = 7.05$

Material: 0.50% CMC-70s

1/2" s.s. Tube

10.28	0.00498	3,270	--	668	steady
11.55	0.00425	3,880	--	716	steady
13.52	0.00331	4,860 _q	--	788	steady
15.18	0.00291	5,780	--	836	slight fluctuation
17.5	0.00225	7,000	---	862	fluctuation (2 mm.)
21.5	0.00193	9,500	40.4	1190	fluctuation (2 mm.)
24.8	0.00156	11,700	46.8	1240	fluctuation (1 mm.)
32.9	0.00118	17,500	63.8	1655	fluctuation (1 mm.)
36.60	0.00106	20,500	71.1	1815	fluctuation (1 mm.)
6.50	0.00985	1,690	--	525	steady
7.80	0.00750	2,200	--	579	steady
3.85	0.0214	794	--	403	steady
2.56	0.0396	444	--	329	steady
1.245	0.113	157	--	222	steady

Friction Factor Run No. N-3
 $s = 0.54$
 $b = 7.05$

Material: 0.50% CMC-70s
 5/8" s.s. Tube

GPM	f	N_{Re}	$s^5 \cdot N_{Re}^{\delta}$	$\tau_w \left(\frac{\text{dynes}}{\text{cm}^2} \right)$	Condition of Manometers
10.25	0.00855	1,960	--	471	steady
12.4	0.00646	2,580	--	516	steady
15.05	0.00491	3,400	--	579	steady
17.4	0.00402	4,150	-	638	steady
20.37	0.00324	5,260	--	703	slight fluctuation
23.97	0.00261	6,660	--	785	fluctuation (2 mm.)
34.1	0.00172	11,000	45.0	1048	fluctuation (2 mm.)
37.85	0.00167	12,800	50.0	1210	fluctuation (2 mm.)
6.64	0.0164	1,040	--	376	steady
3.85	0.0362	476	--	278	steady
1.245	0.184	93.9	--	147	steady

Friction Factor Run No. N-4
 $s = 0.54$
 $b = 7.05$

Material: 0.50% CMC-70s
 3/4" s.s. Tube

38.00	0.00206	9,400	35.0	930	fluctuation (3 mm.)
34.45	0.00206	8,200	--	698	fluctuation (2 mm.)
28.55	0.00270	6,250	--	672	slight fluctuation
25.4	0.00318	5,280	--	629	nearly steady
22.4	0.00377	4,420	--	578	nearly steady
19.0	0.00473	3,470	--	520	nearly steady
15.08	0.00665	2,500	--	458	steady
12.1	0.00923	1,750	--	411	steady
10.56	0.0113	1,490	--	382	steady
3.85	0.0483	349	--	216	steady
1.245	0.240	68.6	--	111	steady
40.45	0.00191	10,300	43.1	951	fluctuation (1 mm.)

Friction Factor Run No. O-1
 $s = 0.61$
 $b = 2.22$

Material: 0.25% CMC-70s
 3/4" s.s. Tube

13.9	0.00329	4,440	--	194	steady
15.18	0.00296	5,000	--	207	slight fluctuation

Friction Factor Run No. O-1 (cont.)

GPM	f	N_{Re}	$s^5 \cdot N_{Re}^{\delta}$	$\tau_w \left(\frac{\text{dynes}}{\text{cm}^2} \right)$	Condition of Manometers
17.12	0.00260	5,940	--	222	fluctuation (3 mm.)
19.95	0.00263	7,320	--	305	fluctuation (1 cm.)
22.55	0.00266	8,670	24.8	370	slight fluctuation
24.6	0.00255	9,760	26.7	436	slight fluctuation
28.0	0.00226	11,700	30.1	494	slight fluctuation
33.7	0.00210	15,200	35.3	708	slight fluctuation
36.45	0.00194	16,600	37.1	756	slight fluctuation
40.04	0.00190	19,200	40.5	926	slight fluctuation
10.54	0.00456	3,020	--	154	steady
3.685	0.0189	700	--	39.6	steady

Friction Factor Run No. P-1

s = 0.78
b = 0.710

Material: 0.12% Carbopol 934

3/4" s.s. Tube

6.90	0.00805	1,770	--	117	steady
7.76	0.00725	2,050	--	120	steady
9.20	0.00595	2,520	--	138	steady
10.7	0.00503	3,040	--	160	almost steady
11.8	0.00435	3,420	--	167	fluctuation (5 mm.)
13.3	0.00531	3,960	--	290	fluctuation (1 cm.)
14.2	0.00507	4,290	--	290	fluctuation (2 cm.)
16.3	0.00702	5,080	10.3	203	fluctuation (5 mm.)
18.6	0.00690	5,960	11.0	573	almost steady
22.7	0.00630	7,550	12.2	1000	steady
24.8	0.00640	8,470	12.8	1180	steady
32.5	0.00565	11,700	14.5	1815	steady
25.5	0.00610	8,750	13.0	1200	steady
28.6	0.00583	10,050	13.9	1470	steady
22.8	0.00625	7,660	12.2	997	steady
19.8	0.00653	6,430	11.3	796	steady
15.2	0.00856	4,650	9.90	603	fluctuation (2 mm.)
10.8	0.00442	3,060	--	162	steady

Friction Factor Run No. Q-2

$s = 0.71$
 $b = 0.644$

Material: 0.515% PIB

3/4" s.s. Tube

GPM	f	N_{Re}	$s^5 \cdot N_{Re}$	$\tau_w \left(\frac{\text{dynes}}{\text{cm}^2} \right)$	Condition of Manometers
3.685	0.0102	1,370	--	33.0	almost steady
1.156	0.0352	494	--	11.2	steady
1.307	0.0403	560	--	15.5	steady
2.21	0.0161	996	--	17.9	steady
2.755	0.0131	938	--	22.8	steady
3.34	0.0117	1,200	--	30.3	steady
3.73	0.0128	1,390	--	41.8	fluctuation (1 mm.)
1.17	0.0349	496	--	11.4	steady
1.343	0.0388	577	--	15.9	steady
6.60	0.00439	2,890	--	44.8	steady
6.50	0.00380	3,400	--	50.8	steady
8.45	0.00630	3,980	--	107	fluctuation (1 cm.)

Friction Factor Run No. Q-3

$s = 0.71$
 $b = 0.644$

Material: 0.515% PIB

3/4" s.s. Tube

33.90	0.00261	23,900	26.5	710	almost steady
28.20	0.00308	18,900	23.8	583	almost steady
25.90	0.00334	16,900	22.6	532	almost steady
23.20	0.00364	14,600	21.0	466	almost steady
20.65	0.00400	12,600	19.7	406	steady
18.90	0.00431	11,200	18.5	366	steady
16.85	0.00481	9,730	17.2	325	steady
14.60	0.00541	8,080	15.7	273	steady
11.95	0.00634	6,190	13.7	215	steady
10.36	0.00712	5,180	12.6	182	steady
9.16	0.00743	4,410	11.6	148	steady
8.12	0.00803	3,780	10.7	126	steady
7.46	0.00838	3,390	10.1	111	steady
6.88	0.00920	3,050	9.75	104	steady

Friction Factor Run No. Q-4

$s = 0.82$
 $b = 0.133$

Material: 0.515% PIB

3/4" s.s. Tube

23.5	0.00460	22,500	17.0	630	steady
32.6	0.00390	34,900	20.1	1010	steady
15.2	0.00586	14,300	14.2	345	steady
11.6	0.00622	10,450	12.7	222	steady
6.42	0.00779	5,150	9.66	99.0	steady
7.70	0.00720	6,400	10.5	125	steady

Friction Factor Run No. Q-4 (cont.)

GPM	f	N_{Re}	$s^5 \cdot \frac{N}{Re} \delta$	$\tau_w \left(\frac{\text{dynes}}{\text{cm}^2} \right)$	Condition of Manometers
3.685	0.0101	2,680	7.55	32.6	slight fluctuation
10.3	0.00660	9,050	12.0	167	steady
12.8	0.00562	11,700	13.2	219	steady
16.8	0.00486	16,100	15.0	326	steady
20.5	0.00448	20,000	16.3	439	steady
23.8	0.00405	22,800	17.0	544	steady
32.6	0.00351	34,900	20.1	885	steady

Friction Factor Run No. R-1

s = 1.00

b = 0.0108 poise

Material: Impure Cyclohexane

3/4" s.s. Tube

10.9	0.00538	34,800	13.7	152	steady
12.4	0.00527	39,700	14.1	192	steady
14.8	0.00502	47,300	14.7	261	steady
17.2	0.00497	54,600	15.3	344	steady
21.2	0.00463	67,900	16.1	495	steady
24.4	0.00446	78,000	16.7	629	steady
27.0	0.00427	86,300	17.1	738	steady
29.5	0.00422	94,400	17.5	875	steady
31.9	0.00415	102,000	17.9	1003	steady
35.5	0.00397	113,500	18.3	1185	steady
38.80	0.00372	153,000	19.8	1330	steady
6.70	0.00812	21,400	12.1	86.7	steady
8.57	0.00700	27,400	12.8	122	steady
3.70	0.00800	11,800	10.4	26.0	steady

Turbulent Velocity Profile Run No. 1-C
 $s = 1.00$
 $b = 0.00931$ poise
 $N_{Re} = 82,600$

Material: Water
 5/8" s.s. Tube
 $u_* = 0.775$ ft./sec.

y (in.)	u (ft./sec.)	$\frac{u_{max} - u}{u_*}$	y/R	du/dr (ft./sec/in)	$1/R$
0.024	14.2	6.22	0.025	1230	0.002
0.044	15.2	4.94	0.050	114	0.021
0.069	16.1	3.77	0.075	85.4	0.028
0.094	16.7	2.97	0.100	55.5	0.043
0.119	17.2	2.33	0.150	40.5	0.057
0.144	17.5	1.95	0.200	33.0	0.068
0.169	18.1	1.18	0.300	27.8	0.075
0.194	18.3	0.93	0.400	20.0	0.097
0.219	18.7	0.42	0.500	15.5	0.114
0.244	18.8	0.29	0.600	13.0	0.122
0.269	19.0	0.04	0.700	9.2	0.148
0.294	19.0	0.04	0.800	8.0	0.140
0.302	19.0	0.04	0.900	5.2	0.151
0.287	19.0	0.04	0.950	3.7	0.151

Turbulent Velocity Profile Run No. 1-D
 $s = 1.00$
 $b = 0.00905$ poise
 $N_{Re} = 9,600$

Material: Water
 5/8" s.s. Tube
 $u_* = 0.1141$ ft./sec.

y (in.)	u (ft./sec.)	$\frac{u_{max} - u}{u_*}$	y/R	du/dr (ft./sec/in)	$1/R$
0.030	1.69	6.24	0.025	52.5	0.0069
0.032	1.73	5.89	0.050	41.0	0.0088
0.036	1.75	5.71	0.075	15.6	0.0226
0.047	1.80	5.27	0.100	10.5	0.0332
0.097	2.01	3.43	0.150	5.5	0.0626
0.147	2.13	2.38	0.200	5.1	0.0645
0.197	2.27	1.16	0.300	4.3	0.0715
0.247	2.35	0.46	0.400	3.2	0.0891
0.297	2.40	0.02	0.500	2.4	0.108
0.274	2.37	0.28	0.600	2.05	0.113
0.249	2.36	0.37	0.700	1.80	0.112
0.013	1.25	10.10	0.800	1.20	0.137
0.0295	1.68	6.32	0.900	0.75	0.155
0.0545	1.83	5.01	0.950	0.55	0.149

Turbulent Velocity Profile Run No. 1-E

 $s = 1.00$ $b = 0.00950$ poise $N_{Re} = 19,700$

Material: Water

5/8" s.s. Tube

 $u_* = 0.222$ ft./sec.

y (in.)	u (ft./sec.)	$\frac{u_{max}-u}{u_*}$
0.0130	2.84	8.74
0.0295	3.31	6.62
0.0545	3.70	4.87
0.0795	3.92	3.87
0.1295	4.26	2.34
0.1795	4.50	1.26
0.2295	4.64	0.63
0.2795	4.75	0.14
0.2915	4.76	0.09
0.2415	4.71	0.32

y/R	du/dr (ft/sec/in)	$1/R$
0.025	110	0.0065
0.050	38.0	0.0184
0.075	26.4	0.0260
0.100	18.3	0.0371
0.150	13.8	0.0478
0.200	10.3	0.0621
0.250	8.9	0.0696
0.300	8.0	0.0747
0.350	6.8	0.0846
0.400	6.1	0.0910
0.450	5.2	0.102
0.500	4.4	0.115
0.550	3.9	0.123
0.600	3.5	0.129
0.650	3.1	0.136
0.700	2.7	0.145
0.750	2.3	0.155
0.800	2.0	0.160
0.850	1.9	0.146
0.900	1.6	0.136
0.950	1.3	0.123

Turbulent Velocity Profile Run No. 1-F

 $s = 1.00$ $b = 0.00950$ $N_{Re} = 176,000$

Material: Water

5/8" s.s. Tube

 $u_* = 1.66$ ft./sec.

y (in.)	u (ft./sec.)	$\frac{u_{max}-u}{u_*}$
0.0130	30.2	7.95
0.0295	33.9	5.72
0.0545	36.6	4.10
0.0795	37.9	3.31
0.1295	39.9	2.11
0.1795	41.7	1.02
0.2295	42.6	0.48
0.2795	43.4	0.
0.2195	43.3	0.06
0.2415	42.3	0.66

y/R	du/dr (ft/sec/in)	$1/R$
0.025	3360	0.0016
0.050	263	0.0198
0.075	195	0.0263
0.100	149	0.0340
0.150	88.5	0.0557
0.200	65.0	0.0720
0.300	50.5	0.0916
0.400	36.0	0.115
0.500	32.0	0.118
0.600	24.5	0.138
0.700	17.9	0.163
0.800	16.5	0.145
0.900	10.5	0.161
0.950	7.5	0.159

Laminar Velocity Profile Run No. 2-A

$s = 0.60$
 $b = 2.09$
 $N_{Re} = 5880$

Material: 0.178% CMC-70

5/8" s.s. Tube

<u>y (in.)</u>	<u>u (ft./sec.)</u>	<u>y/R</u>	<u>u/u_{max.}</u>
0.019	4.51	0.061	0.217
0.044	7.91	0.141	0.381
0.069	10.62	0.221	0.512
0.094	13.18	0.301	0.635
0.119	15.10	0.381	0.728
0.144	16.13	0.461	0.779
0.169	17.32	0.541	0.835
0.219	18.95	0.701	0.913
0.269	19.25	0.861	0.928
0.319	19.94	0.979	0.961
0.357	20.19	0.857	0.972

Laminar Velocity Profile Run No. 3-A

$s = 0.54$
 $b = 4.80$
 $N_{Re} = 3930$

Material: 0.3% CMC-70

5/8" s.s. Tube

<u>y (in.)</u>	<u>u (ft./sec.)</u>	<u>y/R</u>	<u>u/u_{max.}</u>
0.019	4.10	0.061	0.202
0.034	5.65	0.109	0.279
0.059	9.14	0.189	0.450
0.084	11.87	0.269	0.585
0.109	13.64	0.349	0.673
0.134	15.18	0.429	0.748
0.159	16.45	0.509	0.811
0.184	17.49	0.589	0.862
0.234	19.01	0.749	0.936
0.284	19.96	0.909	0.984
0.309	20.27	0.989	0.999
0.291	20.14	0.931	0.992
0.241	19.35	0.771	0.954

Laminar Velocity Profile Run No. 3-B

$s = 0.54$
 $b = 4.80$
 $N_{Re} = 664$

Material: 0.3% CMC-70

5/8" s.s. Tube

y (in.)	u (ft./sec.)	y/R	u/u_{max}
0.020	1.46	0.064	0.247
0.020	1.42	0.064	0.241
0.035	2.05	0.112	0.348
0.035	1.84	0.112	0.312
0.035	1.68	0.112	0.285
0.085	2.91	0.272	0.494
0.135	4.31	0.432	0.730
0.185	4.96	0.592	0.841
0.235	5.54	0.752	0.940
0.235	5.68	0.752	0.963
0.310	5.90	0.992	1.000
0.310	5.88	0.992	0.997

Turbulent Velocity Profile Run No. 3-C

$s = 0.66$
 $b = 1.27$
 $N_{Re} = 14,600$

Material: 0.3% CMC-70

5/8" s.s. Tube

 $u_{max} = 0.995$ ft./sec.

y (in.)	u (ft./sec.)	$\frac{u_{max}-u}{u_{max}}$	y/R	du/dr (ft./sec/in)	$1/R$
0.020	16.3	13.25	0.025	940	0.0035
0.030	20.09	9.77	0.050	430	0.0072
0.055	23.2	6.64	0.075	329	0.0094
0.080	25.05	4.78	0.100	205	0.0148
0.105	26.18	3.64	0.150	111	0.0265
0.130	27.1	2.72	0.200	79.0	0.0361
0.155	27.4	2.42	0.300	45.5	0.0606
0.180	28.1	1.71	0.400	28.5	0.0868
0.205	28.2	1.61	0.500	21.5	0.105
0.230	28.9	0.91	0.600	16.5	0.122
0.255	29.1	0.70	0.700	16.0	0.109
0.280	29.2	0.60	0.800	15.0	0.0950
0.305	29.6	0.20	0.900	11.5	0.0875
0.295	29.8	0.	0.950	9.0	0.0795
0.270	29.4	0.40			
0.245	28.8	1.01			
0.220	28.5	1.31			

Turbulent Velocity Profile Run No. 3-D

$s = 0.68$
 $b = 1.05$
 $N_{Re} = 9500$

Material: 0.3% CMC-70

5/8" s.s. Tube
 $u_* = 0.837$ ft./sec.

y (in.)	u (ft./sec.)	$\frac{u_{max}-u}{u_*}$	y/R	du/dr (ft/sec/in)	$1/R$
0.020	11.9	11.50	0.025	830	0.00318
0.045	16.1	5.32	0.050	335	0.00780
0.070	17.7	4.60	0.075	195	0.0132
0.095	18.6	3.53	0.100	148	0.0172
0.120	19.5	2.45	0.150	99.0	0.0249
0.145	20.0	1.85	0.200	56.5	0.0424
0.170	20.5	1.25	0.300	34.5	0.0672
0.195	20.8	0.90	0.400	26.4	0.0786
0.220	21.1	0.54	0.500	19.5	0.103
0.245	21.4	0.18	0.600	13.8	0.123
0.270	21.5	0.06	0.700	8.8	0.166
			0.800	6.2	0.193
			0.900	4.0	0.211
			0.950	2.5	0.239

Turbulent Velocity Profile Run No. 3-E

$s = 0.75$
 $b = 0.505$
 $N_{Re} = 10,500$

Material: 0.3% CMC-70

5/8" s.s. Tube
 $u_* = 0.800$ ft./sec.

y (in.)	u (ft./sec.)	$\frac{u_{max}-u}{u_*}$	y/R	du/dr (ft/sec/in)	$1/R$
0.027	11.4	9.00	0.025	660	0.0038
0.035	12.5	7.62	0.050	400	0.0063
0.060	14.4	5.25	0.075	160	0.0154
0.085	15.55	3.81	0.100	116	0.0209
0.110	16.15	3.06	0.150	78.0	0.0303
0.135	16.65	2.44	0.200	55.0	0.0416
0.160	17.0	2.00	0.300	29.0	0.0755
0.185	17.4	1.50	0.400	20.0	0.0993
0.210	17.75	1.06	0.500	17.0	0.106
0.235	18.18	0.53	0.600	13.0	0.124
0.260	18.45	0.19	0.700	12.0	0.117
0.285	18.5	0.13	0.800	9.0	0.127
0.310	18.68	0.	0.900	5.9	0.137
0.290	18.4	0.25	0.950	5.0	0.115
0.265	18.3	0.37			

Laminar Velocity Profile Run No. 3-F, Asymmetric

Material: 0.3% CMC-70

 $s = 0.75$ $b = 0.505$ $N_{Re} = 1850$

5/8" s.s. Tube

<u>y (in.)</u>	<u>u (ft./sec.)</u>
0.027	1.18
0.027	1.42
0.029	1.58
0.035	1.66
0.060	2.18
0.085	2.88
0.110	3.49
0.135	4.01
0.160	4.54
0.185	4.98
0.210	5.35
0.210	5.44
0.235	5.66
0.235	5.77
0.260	5.94
0.285	6.06
0.310	6.36
0.310	6.48
0.310	6.27
0.290	6.50
0.290	6.62
0.265	6.55
0.265	6.65
0.240	6.50
0.165	5.75
0.121	4.815

Laminar Velocity Profile Run No. 3-G

$s = 0.95$
 $b = 1.20$
 $N_{Re} = 2150$

Material: 0.3% CMC-70

5/8" s.s. Tube

y (in.)	u (ft./sec.)	y/R	u/u_{max}
0.121	4.13	0.387	0.607
0.140	4.70	0.448	0.691
0.165	5.31	0.528	0.781
0.190	5.84	0.608	0.859
0.215	6.19	0.689	0.910
0.240	6.54	0.768	0.961
0.265	6.65	0.848	0.978
0.290	6.75	0.928	0.993
0.310	7.48	0.992	--
0.310	6.65	0.992	0.978
0.310	6.76	0.992	0.994
0.285	7.23	0.913	--
0.260	6.99	0.833	--
0.235	6.46	0.752	0.947
0.210	6.01	0.673	0.884
0.135	4.51	0.432	0.663
0.110	3.90	0.352	0.574
0.085	2.82	0.272	0.415
0.027	1.03	0.087	0.152

Turbulent Velocity Profile Run No. 3-H

$s = 0.85$
 $b = 0.1195$
 $N_{Re} = 17,000$

Material: 0.3% CMC-70

5/8" s.s. Tube
 $u_* = 1.165$ ft./sec.

y (in.)	u (ft./sec.)	$\frac{u_{max} - u}{u_*}$	y/R	du/dr (ft/sec/in)	$1/R$
			0.025	685	0.0054
			0.050	335	0.0109
0.027	19.87	7.75	0.075	229	0.0157
0.035	21.4	6.44	0.100	151.5	0.0233
0.060	23.7	4.46	0.150	90.0	0.0382
0.085	24.8	3.52	0.200	70.0	0.0476
0.110	26.0	2.49	0.300	40.5	0.0796
0.135	26.55	2.02	0.400	28.0	0.103
0.160	27.15	1.50	0.500	24.5	0.107
0.185	27.75	0.99	0.600	18.5	0.127
0.210	28.25	0.56	0.700	13.0	0.157
0.235	28.55	0.30	0.800	8.5	0.197
0.260	28.7	0.17	0.900	6.4	0.185
0.285	28.8	0.09	0.950	5.2	0.162
0.310	28.9	0.			
0.290	28.8	0.09			
0.265	28.65	0.21			
0.240	28.4	0.43			
0.215	28.0	0.77			
0.190	27.5	1.20			
0.165	26.85	1.76			
0.140	26.1	2.40			

Laminar Velocity Profile Run No. 4-A

$s = 0.53$
 $b = 9.20$
 $N_{Re} = 4180$

Material: 0.41% CMC-70

5/8" s.s. Tube

<u>y (in.)</u>	<u>u (ft./sec.)</u>	<u>y/R</u>	<u>u/u_{max.}</u>
0.017	5.48	0.055	0.203
0.025	6.19	0.081	0.229
0.050	11.4	0.161	0.422
0.075	15.2	0.242	0.563
0.100	17.9	0.322	0.663
0.125	20.3	0.402	0.752
0.125	20.1	0.402	0.744
0.150	21.6	0.483	0.800
0.175	23.1	0.564	0.855
0.200	24.65	0.644	0.913
0.225	25.35	0.725	0.939
0.250	25.8	0.805	0.956
0.275	26.55	0.885	0.983
0.300	27.0	0.966	1.000
0.296	27.2	0.953	1.006
0.271	27.1	0.872	1.003
0.246	26.7	0.792	0.989
0.221	25.9	0.711	0.960
0.196	24.95	0.631	0.924
0.171	23.75	0.550	0.878
0.146	22.2	0.470	0.821
0.128	20.5	0.412	0.759

Laminar Velocity Profile Run No. 4-C, Asymmetric

$s = 0.53$
 $b = 9.20$
 $N_{Re} = 6000$

Material: 0.4% CMC-70

3/8" s.s. Tube

<u>y (in.)</u>	<u>u (ft./sec.)</u>
0.027	21.3
0.027	20.3
0.037	26.7
0.037	25.25
0.047	31.8
0.047	30.8
0.057	34.8
0.067	37.0
0.072	38.7
0.072	37.8
0.097	44.5
0.122	46.9
0.147	47.8
0.175	47.9
0.178	47.6
0.153	46.4
0.153	46.0
0.128	43.6
0.105	40.5

Laminar Velocity Profile Run No. 4-D

 $s = 0.59$ $b = 4.01$ $N_{Re} = 4000$

Material: 0.41% CMC-70

3/4" s.s. Tube

<u>y (in.)</u>	<u>u (ft./sec.)</u>	<u>y/R</u>	<u>u/u_{max.}</u>
0.017	3.19	0.048	0.130
0.030	4.39	0.085	0.179
0.055	7.85	0.155	0.320
0.080	10.88	0.226	0.444
0.105	13.99	0.296	0.570
0.130	16.29	0.366	0.665
0.155	18.44	0.437	0.753
0.180	20.55	0.508	0.839
0.205	22.00	0.578	0.898
0.230	22.70	0.649	0.926
0.255	23.60	0.720	0.963
0.280	24.10	0.790	0.984
0.305	24.35	0.860	0.994
0.330	24.35	0.930	0.994
0.340	24.35	0.960	0.994
0.329	24.25	0.928	0.990
0.329	24.30	0.928	0.992
0.304	23.85	0.858	0.973
0.304	23.95	0.858	0.976
0.279	23.85	0.788	0.973
0.254	23.55	0.716	0.960
0.229	22.50	0.646	0.919
0.204	21.50	0.575	0.877
0.179	20.20	0.505	0.824
0.154	18.90	0.434	0.770
0.129	15.80	0.364	0.645
0.104	13.63	0.293	0.556
0.089	12.40	0.251	0.506

Turbulent Velocity Profile Run No. 4-E
 $s = 0.59$
 $b = 4.01$
 $N_{Re} = 12,200$

Material: 0.4% CMC-70

3/4" s.s. Tube
 $u_* = 1.115$ ft./sec.

y (in.)	u (ft./sec.)	$\frac{u_{max}-u}{u_*}$	y/R	du/dr (ft./sec/in)	$1/R$
0.015	16.14	18.4	0.025	675	0.0046
0.030	22.6	13.2	0.050	485	0.0063
0.055	27.75	8.67	0.075	320	0.0095
0.080	30.6	6.40	0.100	254	0.012
0.105	32.4	4.73	0.150	140	0.021
0.130	33.7	3.59	0.200	102	0.028
0.155	34.5	2.62	0.250	74.5	0.037
0.180	34.8	1.93	0.300	63.5	0.041
0.205	35.4	1.31	0.350	53	0.048
0.230	36.4	0.88	0.400	45	0.054
0.255	36.8	0.70	0.450	38	0.061
0.280	37.2	0.35	0.500	33	0.067
0.305	37.3	0.22	0.550	25.8	0.082
0.330	37.5	0.09	0.600	21.5	0.093
0.354	37.4		0.650	17.5	0.106
0.329	37.6		0.700	14.5	0.119
0.329	37.6		0.750	10.8	0.146
0.304	37.4		0.800	8.5	0.166
0.279	37.1		0.850	6.5	0.188
0.254	37.0		0.900	4.33	0.230
0.229	36.6		0.925	3.77	0.228
0.204	36.2		0.950	3.5	0.201
0.179	35.4		0.975	3.33	0.149
0.154	33.5				
0.129	33.3				
0.104	31.3				
0.100	30.8				

Turbulent Velocity Profile Run No. 4-F

 $s = 0.62$ $b = 3.03$ $N_{Re} = 8400$

Material: 0.4% CMC-70

3/4" s.s. Tube

 $u_* = 0.920$ ft./sec.

y (in.)	u (ft./sec.)	$\frac{u_{max} - u}{u_*}$	y/R	du/dr (ft/sec/in)	$1/R$
0.015	10.1	18.10	0.025	540	0.0048
0.015	10.7	17.55	0.050	390	0.0065
0.030	15.08	12.64	0.075	252	0.0099
0.030	15.56	12.27	0.100	172	0.0143
0.055	18.86	8.62	0.150	102	0.0234
0.055	18.96	8.62	0.200	75.0	0.0309
0.080	20.8	6.09	0.300	51.5	0.0437
0.105	22.5	4.40	0.400	38.0	0.0530
0.130	23.0	4.18	0.500	27.3	0.0672
0.155	24.8	1.90	0.600	17.8	0.0922
0.180	25.6	1.09	0.700	12.0	0.188
0.205	25.9	0.60	0.800	5.8	0.200
0.230	25.8	0.49	0.900	4.5	0.182
0.255	26.5	0.27	0.950	3.7	0.157
0.280	26.7	0.11			
0.305	26.7	0.			
0.330	26.65	0.			
0.354	26.8	0.			
0.329	27.5	0.			
0.329	26.4	0.33			
0.304	26.3	0.82			
0.279	25.9	1.20			
0.254	25.6	1.58			
0.229	25.4	1.74			
0.204	25.1	2.12			
0.179	24.5	2.45			
0.154	24.3	2.99			
0.129	23.45	3.97			
0.104	22.4	5.27			
0.100	21.75	5.93			

Turbulent Velocity Profile Run No. 4-G

$s = 0.62$
 $b = 3.03$
 $N_{Re} = 14,300$

Material: 0.4% CMC-70

3/4" s.s. Tube
 $u_* = 1.095$ ft./sec.

y (in.)	u (ft./sec.)	$\frac{u_{max} - u}{u_*}$	y/R	du/dr (ft./sec./in)	$1/R$
0.015	19.77	16.00	0.025	900	0.0034
0.015	19.57	15.20	0.050	465	0.0065
0.030	25.0	11.23	0.075	268	0.0111
0.030	25.4	10.88	0.100	174	0.0168
0.055	28.3	8.22	0.150	105.0	0.0270
0.055	29.05	7.54	0.200	83.0	0.0338
0.080	30.7	6.03	0.300	58.5	0.0457
0.105	32.05	4.80	0.400	43.0	0.0558
0.130	33.1	3.84	0.500	29.8	0.0732
0.155	34.1	2.92	0.600	21.2	0.0921
0.180	34.75	2.33	0.700	16.8	0.100
0.205	35.45	1.69	0.800	10.7	0.129
0.230	35.95	1.23	0.900	6.3	0.155
0.255	36.5	0.73	0.950	4.7	0.147
0.280	36.8	0.46			
0.305	37.1	0.18			
0.330	37.3	0.			
0.354	37.3	0.			
0.329	37.3	0.			
0.329	36.9	0.37			
0.304	37.0	0.27			
0.279	36.8	0.46			
0.254	36.45	0.78			
0.229	35.9	1.28			
0.204	35.25	1.87			
0.179	34.45	2.60			
0.154	33.6	3.38			
0.129	32.45	4.43			
0.104	31.0	5.75			
0.101	30.6	6.11			

Turbulent Velocity Profile Run No. 5-A

$s = 0.64$
 $b = 2.22$
 $N_{Re} = 8800$

Material: 0.35% CMC-70

3/4" s.s. Tube
 $u_* = 0.933 \text{ ft./sec.}$

$y \text{ (in.)}$	$u \text{ (ft./sec.)}$	$\frac{u_{\max} - u}{u_*}$	y/R	$du/dr \text{ (ft/sec/in)}$	$1/R$
0.015	11.88	15.46	0.025	630	0.0041
0.015	11.88	15.46	0.050	410	0.0063
0.032	16.7	10.32	0.075	255	0.0099
0.032	16.88	10.12	0.100	145	0.0172
0.057	19.80	7.02	0.150	85	0.0285
0.082	21.47	5.25	0.200	65	0.0361
0.107	22.55	4.10	0.250	50	0.0454
0.132	23.42	3.17	0.300	40	0.0550
0.157	24.15	2.40	0.350	36.	0.0590
0.182	24.75	1.76	0.400	32	0.0638
0.207	25.15	1.33	0.450	26	0.0750
0.232	--	--	0.500	22.5	0.0826
0.257	26.0	0.43	0.550	21.	0.0838
0.282	26.15	0.27	0.600	18.5	0.0900
0.307	26.3	0.11	0.650	15	0.1038
0.332	26.3	0.11	0.700	11	0.1310
0.352	26.4	0.	0.750	7.5	0.1755
0.327	26.3	0.11	0.800	5.75	0.2045
0.327	26.56	0.	0.850	4.0	0.2540
0.302	26.45	0.	0.900	3.67	0.2270
0.277	26.2	0.21	0.925	3.5	0.2060
0.152	25.95	0.48	0.950	3.1	0.1900
0.227	25.6	0.85	0.975	3.1	0.1340
0.202	25.2	1.28			
0.177	24.6	1.92			
0.152	23.5	3.09			
0.127	23.2	3.40			
0.102	21.93	4.75			
0.097	21.5	5.21			

Turbulent Velocity Profile Run No. 5-B

 $s = 0.64$ $b = 2.22$ $N_{Re} = 12,700$

Material: 0.35% CMC-70

 $3/4''$ s.s. Tube $u_* = 1.092$ ft./sec.

y (in.)	u (ft./sec.)	$\frac{u_{max}-u}{u_*}$	y/R	du/dr (ft/sec/in)	$1/R$
0.015	18.3	14.5	0.025	765	0.00398
0.033	23.8	9.60	0.050	440	0.00683
0.058	26.8	6.90	0.075	228	0.0128
0.083	26.8	5.30	0.100	173	0.0169
0.108	29.75	4.26	0.150	92	0.0309
0.133	30.7	3.41	0.200	70.5	0.0391
0.158	31.4	2.78	0.300	43	0.0598
0.183	32.1	2.15	0.400	33	0.0722
0.208	32.7	1.62	0.500	24	0.0906
0.233	33.2	1.17	0.600	21.5	0.0906
0.258	33.6	0.81	0.700	16.5	0.1022
0.283	34.0	0.45	0.800	11	0.1253
0.308	34.15	0.31	0.900	9	0.1083
0.333	34.15	0.31	0.950	8.5	0.0810
0.351	34.5	0	0.975	7.5	0.0648
0.326	34.3	0.18	0.850	10	0.1093
0.326	34.15	0.31	0.750	12.3	0.1250
0.301	34.05	0.40	0.650	20	0.0911
0.276	33.6	0.81	0.550	23.5	0.0880
0.251	33.25	1.12	0.450	30	0.0761
0.226	32.75	1.57	0.350	35	0.0710
0.201	32.2	2.06			
0.176	31.7	2.60			
0.151	30.9	3.32			
0.126	29.9	4.12			
0.101	28.45	5.43			
0.098	28.1	5.75			

Turbulent Velocity Profile Run No. 6-B
 $s = 0.74$
 $b = 1.38$
 $N_{Re} = 7540$

Material: 0.62% Ammonium
 Alginate
 3/4" s.s. Tube

y (in.)	u (ft./sec.)	$\frac{u_{max} - u}{u_*}$
0.319	29.50	0.29
0.284	29.20	0.51
0.248	28.70	0.88
0.213	28.15	1.29
0.177	27.45	1.80
0.142	26.60	2.35
0.106	25.55	3.20
0.071	24.10	4.26
0.035	20.90	6.61
0.018	17.20	9.34
0.337	29.70	0.15
0.136	26.35	--
0.111	25.65	--
0.086	24.80	--
0.061	23.70	--
0.036	22.30	--
0.015	17.00	--
0.351	29.85	--
0.233	28.40	--
0.208	28.00	--
0.183	27.40	--
0.158	25.95	--
0.133	25.20	--
0.108	24.80	--
0.083	24.40	--
0.058	23.10	--
0.033	20.80	--
0.015	12.58	--
0.326	29.60	--
0.301	29.40	--
0.276	29.10	--
0.251	28.70	--
0.226	28.20	--
0.201	27.65	--
0.176	27.00	--
0.151	26.20	--
0.126	25.35	--
0.113	24.80	--
0.023	18.95	--
0.133	26.40	--

y/R	du/dr (ft/sec/in)	$1/R$
0.025	900	0.0042
0.050	375	0.0100
0.075	197	0.0187
0.100	130	0.0280
0.150	83.0	0.0425
0.200	56.5	0.0606
0.300	36.0	0.0923
0.400	25.0	0.119
0.500	20.0	0.136
0.600	16.0	0.151
0.700	14.0	0.150
0.800	10.0	0.172

Laminar Velocity Profile Run No. 6-C

$s = 0.74$
 $b = 1.38$
 $N_{Re} = 4610$

Material: 0.62% Ammonium
 Alginate
 3/4" s.s. Tube

<u>y (in.)</u>	<u>u (ft./sec.)</u>	<u>y/R</u>	<u>u/u_{max}</u>
0.351	23.85	0.990	1.000
0.258	22.65	0.728	0.950
0.251	22.65	0.708	0.950
0.226	22.00	0.637	0.921
0.201	21.25	0.567	0.890
0.176	20.45	0.496	0.857
0.151	19.25	0.426	0.806
0.126	17.70	0.356	0.742
0.111	16.20	0.313	0.679
0.333	23.80	0.940	0.997
0.308	23.60	0.869	0.989
0.283	23.25	0.978	0.975
0.258	22.70	0.728	0.951
0.233	21.90	0.657	0.918
0.208	20.80	0.586	0.871
0.183	18.95	0.516	0.794
0.158	17.15	0.446	0.719
0.133	15.40	0.375	0.645
0.108	12.75	0.305	0.534
0.083	10.20	0.234	0.427
0.058	8.12	0.164	0.340
0.033	5.15	0.093	0.216
0.015	3.64	0.042	0.153
0.326	23.80	0.920	0.997
0.301	23.40	0.849	0.980
0.276	23.10	0.779	0.968

Turbulent Velocity Profile Run No. 6-D

 $s = 0.74$
 $b = 1.38$
 $N_{Re} = 9680$

 Material: 0.62% Ammonium
 Alginate
 3/4" s.s. Tube
 $u_* = 1.575$ ft./sec.

y (in.)	u (ft./sec.)	$\frac{u_{max}-u}{u_*}$	y/R	du/dr (ft/sec/in)	$1/R$
0.269	36.30	0.445	0.025	1860	0.0023
0.244	35.70	0.825	0.050	395	0.0110
0.219	35.20	1.142	0.075	184	0.0232
0.194	34.55	1.556	0.100	139	0.0303
0.169	33.85	2.00	0.150	90.0	0.0455
0.144	33.40	2.285	0.200	65.0	0.0610
0.119	32.10	3.11	0.300	51.8	0.0743
0.094	31.00	3.81	0.400	38.5	0.0895
0.069	29.70	4.64	0.500	30.4	0.103
0.044	27.85	5.81	0.600	22.0	0.128
0.015	21.95	9.55	0.700	20.5	0.119
0.340	37.05	0.	0.800	13.0	0.153
0.315	37.00	0.	0.900	7.5	0.188
0.290	36.70	0.191	0.950	4.8	0.207
0.265	36.30	0.445			
0.240	35.75	0.793			
0.215	35.20	1.142			
0.190	34.40	1.65			
0.165	33.50	2.22			
0.140	32.55	2.825			
0.115	31.35	3.59			
0.107	30.90	3.87			
0.029	25.95	7.01			

Laminar Velocity Profile Run No. 8-A
 $s = 0.54$
 $b = 7.05$
 $N_{Re} = 2600$

Material: 0.50% CMC-70s

3/4" s.s. Tube

<u>y (in.)</u>	<u>u (ft./sec.)</u>	<u>y/R</u>	<u>u/u_{max.}</u>
0.319	21.70	0.900	--
0.344	19.90	0.970	0.055
0.315	21.80	0.889	--
0.290	20.95	0.819	0.005
0.265	21.45	0.748	--
0.240	20.60	0.677	0.022
0.215	20.55	0.606	0.025
0.190	19.35	0.536	0.081
0.165	15.68	0.465	0.255
0.140	15.90	0.395	0.245
0.115	14.65	0.324	0.305
0.090	13.35	0.254	0.366
0.065	11.75	0.183	0.442
0.040	10.25	0.113	0.514
0.015	9.22	0.0423	0.562
0.319	21.70	0.900	--
0.294	21.50	0.830	--
0.269	21.25	0.759	--
0.244	20.36	0.689	0.034
0.219	19.96	0.618	0.052
0.194	19.23	0.547	0.087
0.169	18.20	0.476	0.135
0.144	16.90	0.406	0.197
0.119	15.50	0.336	0.265
0.105	14.50	0.308	0.312
0.344	21.35	0.970	--
0.340	21.10	0.954	--
0.265	20.70	0.748	0.017
0.240	20.22	0.677	0.040
0.215	19.60	0.606	0.070
0.015	7.55	0.0423	0.642
0.020	7.66	0.0565	0.636
0.025	8.02	0.0705	0.619
0.315	20.40	0.889	0.031
0.319	20.60	0.900	0.022
0.340	20.80	0.954	0.012
0.215	19.43	0.606	0.077
0.265	20.20	0.748	0.040

Turbulent Velocity Profile Run No. 8-B

s = 0.54

b = 7.05

 $N_{Re} = 8780$

Material: 0.50% CMC-70s

3/4" s.s. Tube

 $u_* = 1.01$ ft./sec.

y (in.)	u (ft./sec.)	$\frac{u_{\max} - u}{u_*}$	y/R	du/dr (ft/sec/in)	$1/R$
0.319	39.45	0.05	0.025	650	0.0043
0.344	39.75	0	0.050	610	0.0044
0.340	39.30	0.20	0.075	377	0.0073
0.315	39.20	0.30	0.100	288	0.0094
0.290	38.95	0.54	0.150	182	0.0144
0.265	38.80	0.69	0.200	142	0.0179
0.240	38.15	1.33	0.300	97.0	0.0254
0.215	37.50	1.98	0.400	68.5	0.0322
0.190	36.50	2.97	0.500	48.0	0.0420
0.165	35.60	3.86	0.600	33.0	0.0546
0.140	34.10	5.35	0.700	27.5	0.0567
0.115	32.25	7.18	0.800	15.5	0.0824
0.090	29.65	9.75	0.900	7.2	0.125
0.065	26.50	12.87	0.950	3.5	0.182
0.040	20.65	18.65			
0.025	16.45	22.10			
0.020	15.08	23.70			
0.015	13.53	25.70			
0.319	39.70	0.			
0.294	39.35	0.15			
0.269	38.90	0.59			
0.244	38.15	1.33			
0.219	37.30	2.18			
0.194	36.20	3.27			
0.169	34.80	4.65			
0.144	33.20	6.23			
0.119	31.30	8.12			
0.109	30.20	9.21			

Laminar Velocity Profile Run No. 9-A

 $s = 0.61$ $b = 2.22$ $N_{Re} = 3960$

Material: 0.25% CMC-70s

3/4" s.s. Tube

<u>y (in.)</u>	<u>u (ft./sec.)</u>	<u>y/R</u>	<u>u/u_{max.}</u>
0.354	19.15	0.999	1.003
0.330	18.90	0.930	0.990
0.305	18.55	0.860	0.971
0.280	18.13	0.790	0.950
0.255	17.31	0.720	0.906
0.230	16.30	0.649	0.854
0.205	15.80	0.579	0.827
0.180	15.23	0.508	0.797
0.155	14.47	0.437	0.757
0.130	13.17	0.367	0.689
0.105	11.19	0.296	0.585
0.080	9.58	0.226	0.501
0.055	8.15	0.155	0.427
0.030	7.39	0.0846	0.387
0.015	6.82	0.0423	0.357
0.354	18.75	0.999	0.981
0.329	18.15	0.929	0.969
0.304	18.50	0.858	0.969
0.297	18.50	0.787	0.969
0.254	18.20	0.716	0.953
0.229	17.50	0.646	0.915

Laminar Velocity Profile Run No. 9-A-1

 $s = 0.61$ $b = 2.22$ $N_{Re} = 3960$

Material: 0.25% CMC-70s

3/4" s.s. Tube

<u>y (in.)</u>	<u>u (ft./sec.)</u>	<u>y/R</u>	<u>u/u_{max.}</u>
0.354	17.40	0.999	0.983
0.330	17.35	0.931	0.980
0.305	17.55	0.860	0.9915
0.280	17.30	0.790	0.978
0.255	16.78	0.720	0.948
0.230	16.18	0.649	0.914
0.205	15.55	0.539	0.879
0.180	14.60	0.508	0.825
0.155	13.37	0.437	0.755
0.130	11.10	0.367	0.627
0.105	9.28	0.295	0.525
0.080	7.23	0.225	0.409
0.055	5.23	0.155	0.296
0.030	3.02	0.085	0.171
0.015	2.45	0.042	0.139
0.354	17.70	0.999	1.000
0.329	17.60	0.928	0.994
0.304	17.47	0.858	0.986
0.279	16.85	0.776	0.952
0.254	17.00	0.714	0.960
0.229	16.50	0.646	0.932
0.204	15.83	0.575	0.895
0.179	14.90	0.505	0.842
0.154	14.02	0.434	0.792
0.133	12.72	0.375	0.719
0.330	17.48	0.931	0.987

Turbulent Velocity Profile Run No. 9-B
 $s = 0.61$
 $b = 2.22$
 $N_{Re} = 11,300$

Material: 0.25% CMC-70s

3/4" s.s. Tube
 $u_* = 0.847$ ft./sec.

y (in.)	u (ft./sec.)	$\frac{u_{max}-u}{u_*}$
0.330	28.25	0
0.305	27.20	0.71
0.280	27.55	0.30
0.255	27.75	1.24
0.230	26.55	1.47
0.205	26.45	1.59
0.180	25.90	2.24
0.155	25.40	2.83
0.130	24.65	3.72
0.105	23.80	4.72
0.080	22.60	6.14
0.055	20.60	8.50
0.030	17.15	12.56
0.025	15.90	14.05
0.020	14.27	15.97
0.015	12.57	17.98
0.354	27.85	0
0.329	27.94	0
0.304	27.25	0.65
0.279	27.50	0.35
0.254	27.45	0.41
0.229	27.20	0.71
0.204	26.75	1.24
0.179	26.20	1.89
0.154	25.50	2.72
0.132	24.85	3.48

y/R	du/dr (ft/sec/in)	$1/R$
0.025	630	0.0037
0.050	334	0.0070
0.075	230	0.0100
0.100	179	0.0127
0.150	99.0	0.0216
0.200	79.0	0.0270
0.300	47.5	0.0435
0.400	32.0	0.0580
0.500	23.0	0.0734
0.600	14.0	0.108
0.700	9.5	0.138
0.800	7.5	0.143
0.900	5.8	0.130
0.950	4.0	0.133

Low Shear Rate Rheology

Material: 0.18% CMC-70

Temperature °F.	Viscometer Head	du/dr (sec. ⁻¹)	τ (dynes/cm. ²)
72.0	LVT	0.210	0.101
72.0	LVT	0.420	0.175
72.0	LVT	1.05	0.387
72.0	LVT	0.420	0.172
72.0	LVT	0.210	0.0975

Material: 0.41% CMC-70

72.2	LVT	0.21	0.312
72.2	LVT	0.42	0.559
72.2	LVT	0.21	0.310
72.2	LVT	0.42	0.556

Material: 0.83% Ammonium Alginate

71.2	RVF	4.20	3.70
71.2	RVF	8.40	6.23
71.2	RVF	21.0	13.28
71.2	RVF	21.0	13.30
71.2	RVF	8.40	6.44
71.1	RVF	4.20	3.96
71.1	LVT	1.05	1.25

Material: 0.46% Ammonium Alginate

71.3	RVF	4.20	1.27
71.3	RVF	8.40	2.57
71.3	RVF	21.0	6.29
71.1	RVF	42.0	11.85
71.1	RVF	21.0	6.22
71.1	RVF	8.40	2.84
71.1	RVF	4.20	1.51

Low Shear Rate Rheology

Material: 0.25% CMC-70s

Temperature °F.	Viscometer Head	du/dr (sec. ⁻¹)	τ (dynes/cm. ²)
74.9	RVF	4.20	0.991
74.9	RVF	8.40	2.08
74.9	RVF	21.0	5.26
74.9	RVF	8.40	2.01
74.9	RVF	4.20	0.944
75.0	RVF	4.20	1.19
75.0	RVF	8.40	2.27
75.0	RVF	21.0	5.50
75.0	RVF	8.40	2.19
75.0	RVF	4.20	0.992

Material: 0.12% Carbopol 934

70.4	RVF	4.20	1.55
70.5	RVF	8.40	2.67
70.5	RVF	21.0	6.00
70.7	RVF	8.40	2.75
70.2	RVF	4.20	1.53
70.5	LVT	2.10	off scale
69.8	LVT	1.05	0.458
72.5	LVT	0.420	0.184
67.0	LVT	0.210	0.101
70.2	LVT	0.210	0.098

Material: 0.52% Vistanex
in Cyclohexane

77.4	LVT	8.40	off scale
77.4	LVT	4.20	0.400
77.5	LVT	2.10	0.194
77.6	LVT	1.05	0.107
77.7	LVT	2.10	0.185
77.4	LVT	4.20	0.376
77.4	RVF	4.20	0.438
77.4	RVF	8.40	0.759
77.4	RVF	21.0	1.94
77.5	RVF	42.0	3.83
77.5	RVF	21.0	1.91
77.6	RVF	8.40	0.759
77.6	RVF	4.20	0.450

Low Shear Rate Rheology

Material: Cyclohexane (Impure)

<u>Temperature</u> <u>°F.</u>	<u>Viscometer</u> <u>Head</u>	<u>du/dr (sec.⁻¹)</u>	<u>τ (dynes/cm.²)</u>
77.5	LVT	42.0	0.445
77.5	LVT	21.0	0.228
77.5	LVT	8.40	0.0963
77.5	LVT	4.20	0.0442
77.5	LVT	42.0	0.452
77.5	LVT	2.10	0.0301
77.5	LVT	4.20	0.0515
77.5	LVT	8.40	0.102
77.5	LVT	21.0	0.227
77.5	LVT	42.0	0.449
77.3	LVT	21.0	0.232
77.5	LVT	8.40	0.0957
77.5	LVT	4.20	0.0476
77.5	LVT	2.10	0.0245
77.5	LVT	1.05	0.0129
77.5	LVT	0.420	0.00613
78.5	LVT	0.210	0.00430

VIII. APPENDIX (Cont.), D. Location of Original Data

The original data for this thesis are located in laboratory notebooks numbered 1 and 2 under the name of the author. These notebooks are located in the files of Professor E. W. Merrill of the Chemical Engineering Department of the Massachusetts Institute of Technology.

VIII. APPENDIX (Cont.), E. Nomenclature

b	pseudoplastic rheological constant	(dyne)(sec.) ³ /cm. ²
d	differential operator	- - - -
D	tube diameter	in., cm.
f	Fanning friction factor	- - - -
ξ_c	conversion factor	ft.lb./lb. force/sec. ²
k	mixing length constant	- - - -
l	turbulent mixing length	in., cm.
L	length	ft., cm.
N_{Re}	Reynold's No., $DV\rho/\mu$, $\frac{D^3V^2-s_e}{b} \phi(s)$	- - - -
P	pressure	lb/ft. ² , dynes/cm. ²
Q	volumetric flow rate	cu.ft./min.
r	radius	in., cm.
R	tube radius	in., cm.
s	pseudoplastic rheological exponent	- - - -
u	local velocity	ft./sec., cm./sec.
u_*	friction velocity	ft./sec., cm./sec.
V	average velocity	ft./sec., cm./sec.
w	wall	- - - -
y	distance from wall	in., cm.
γ	exponent to N_{Re} in correlation	- - - -
ϵ	eddy viscosity	(dyne)(sec.)/cm. ²
μ	molecular viscosity	poises
ρ	density	gm./cm. ³
τ	shear stress	dynes/cm. ²
τ_w	wall shear stress	dynes/cm. ²
$\phi(s)$	$s \cdot \left[\frac{1}{2(3+1/s)} \right] s$	- - - -

VIII. APPENDIX (Cont.), F. Literature Citations

- (1) Agoston, G.A., Harte, W.H., et al., "Flow of Gasoline Thickened by Napalm", Industrial and Engineering Chemistry, 46, 1017-1019 (1954).
- (2) Aitken, G. and Miller, R.J., Jr., "An Investigation of the Viscosity Characteristics of a Non-Newtonian Fluid", S.B. Thesis, Dept. of Chem. Eng., M.I.T., 1954.
- (3) Alfrey, T., "Mechanical Behavior of High Polymers", 33, New York, Interscience Publishers, 1948.
- (4) Alves, G.E., Boucher, D.F. and Pigford, R.L., "Pipe-Line Design for Non-Newtonian Solutions and Suspensions", Chemical Engineering Progress, 48, No. 8, 385-393 (1952).
- (5) Bakhmeteff, B.A., "The Mechanics of Turbulent Flow", Princeton, Princeton University Press, 1936.
- (6) Beerli, G.J., "Study of the Viscosity of Pseudoplastic Fluids Under High and Low Rates of Shear", S.B. Thesis, Dept. of Chem. Eng. M.I.T., 1957.
- (7) Bergen, J.T. and Patterson, W., Jr., "Anomalous Viscous Flow at Very Low Rate of Shear and Small Shearing Stress", Journal of Applied Physics, 24, No. 6, 712-719 (1953).
- (8) Bestul, A.B. and Belcher, H.V., "Degradation of Polyisobutylenes on Shearing in Solution", Journal of Applied Physics, 24, No. 8, 1011-1014 (1953).
- (9) Beuche, F., "Influence of Rate of Shear on the Apparent Viscosity of A-- Dilute Polymer Solutions, and B-- Bulk Polymers", Journal of Chemical Physics, 22, 1570 (1954).
- (10) Bird, R.B., "Correlation of Friction Factors in Non-Newtonian Flow", A.I.Ch.E. Journal, 2, No. 2, 428-8S (1956).
- (11) Charm, S.E., "Heat Transfer Coefficients in Straight Tubes for Pseudoplastic Food Materials in Streamline Flow", Sc.D. Thesis, Dept. of Food Technology, M.I.T., 1957.
- (12) Chu, J.C., Brown, F. and Burrige, K.G., "Heat Transfer Coefficients of Pseudo-Plastic Fluids", Industrial and Engineering Chemistry, 45, 1686-1696 (1953).
- (13) Dadekian, Z.A. and Engelken, R.C., "Boundary Effects on Laminar Flow of a Non-Newtonian Fluid", S.B. Thesis, Dept. of Chem. Eng., M.I.T. 1955.
- (14) DeButts, E.H., Hudy, J.A. and Elliott, J.H., "Rheology of Sodium Carboxymethylcellulose Solutions", Industrial and Engineering Chemistry, 49, 94-98 (1957).

- (15) Drew, T.B. and Hooper, J.W., Jr., editors, "Advances in Chemical Engineering", Vol. I, New York, Academic Press, 1956.
- (16) Farquhar, J., "Investigation of a Pitot-Impact Tube for Velocity Measurement in Gas Streams Containing Finely Divided Solids", S.B. Thesis, Dept. of Chemical Engineering, M.I.T., 1954.
- (17) Ferry, J., et al., Journal of Colloid Science, 6, 377 (1951).
- (18) Glasstone, S., et al., "The Theory of Rate Processes", New York, McGraw-Hill Book Company, Inc., 1941.
- (19) Goodeve, C.F., "A General Theory of Thixotropy and Viscosity", Transactions of the Faraday Society, 35, 342-358 (1939).
- (20) Green, H., "Industrial Rheology and Rheological Structures", New York, John Wiley and Sons, Inc., 1949.
- (21) Hunsaker, J.C. and Rightmire, B.G., "Engineering Applications of Fluid Mechanics", New York, McGraw-Hill Book Co., Inc., 1947.
- (22) Ippen, A.T., Tankin, R.S. and Raichlen, F., "Turbulence Measurements in Free Surface Flow with an Impact Tube-Pressure Transducer Combination", Technical Report No. 20, Hydrodynamics Laboratory, M.I.T., July 1955.
- (23) Kaye, J., Brown, G.A., Dieckmann, J.J. and Sziklas, E.A., "Experimental Velocity Profiles for Supersonic Flow of Air in a Tube with and without Heat Transfer", Proceedings of the Second U.S. National Congress of Applied Mechanics, New York, The American Society of Mechanical Engineers, 784-792 (1954).
- (24) Lewis, W.K., Squires, L. and Broughton, G., "Industrial Chemistry of Colloidal and Amorphous Materials", 164-169, New York, The Macmillan Co., 1943.
- (25) Lindquist, C.G. and Sierichs, W.C., "The Measurement of the Flow Properties of a Pseudoplastic with a Concentric Cylinder Viscometer", Journal of Colloid Science, 6, 33-41 (1951).
- (26) Lyche and Bird, "The Graetz-Nusselt Problem for a Power-Law Non-Newtonian Fluid", Chemical Engineering Science, 6, 35 (1956).
- (27) Mark, H. and Tobolsky, A.V., "Physical Chemistry of High Polymeric Systems", New York, Interscience Publishers, Inc., 1950, Ch. IX.

- (28) Merrill, E.W., "A Coaxial Cylinder Viscometer for the Study of Fluids Under High Velocity Gradients", Journal of Colloid Science, 9, No. 1, 7-19 (1954).
- (29) Merrill, E.W., "Basic Problems in the Viscometry of Non-Newtonian Fluids", ISA Journal, 2, 462-465 (1955).
- (30) Merrill, E.W., "A Coaxial-Cylinder Viscometer for Non-Newtonian Fluids", ISA Journal, 3, No. 4, 462 (1956).
- (31) Merrill, E.W., "Pseudoplastic Flow: Viscometry, Correlations of Shear Stress vs. Shear Rate, and Prediction of Laminar Flow in Tubes", Journal of Colloid Science, 11, 1-14 (1956).
- (32) Metzner, A.B., "Pipe-Line Design for Non-Newtonian Fluids", Chemical Engineering Progress, 50, No. 1, 27-34 (1954).
- (33) Metzner, A.B. and Reed, J.C., "Flow of Non-Newtonian Fluids -- Correlation of the Laminar, Transition, and Turbulent-flow Regions", A.I.Ch.E. Journal, 1, No. 4, 434-440 (1955).
- (34) Metzner, A.B. and Otto, R.E., "Agitation of Non-Newtonian Fluids", A.I.Ch.E. Journal, 3, No. 1, 3-10 (1957).
- (35) Metzner, A.B., Vaughn, R.D. and Houghton, G.L., "Heat Transfer to Non-Newtonian Fluids", A.I.Ch.E. Journal, 3, No. 1, 92-100 (1957).
- (36) Mooney, M., "Explicit Formulas for Slip and Fluidity", Journal of Rheology, 2, No. 2, 210 (1931).
- (37) Nagengast, P., "Design, Construction and Testing of a Velocity Impact Probe, etc." S.M. Thesis, Mechanical Engineering Dept., M.I.T., 1952.
- (38) Oldroyd, J.G., "A Suggested Method of Detecting Wall-Effects in Turbulent Flow through Tubes", Proceedings of the International Congress on Rheology, Holland, 1948, Amsterdam, North-Holland Publishing Co., Section C, II 130-141 (1949).
- (39) Ott, E. and Elliott, J.H., "Observations on the Thixotropy and Structural Characteristics of Sodium Carboxymethylcellulose", Die Makromolekulare Chemie, 18/19, 352-366 (1956).
- (40) Peebles, F.N., Garber, H.J. and Jury, S.H., "Preliminary Studies of Flow Phenomena Utilizing a Doubly Refractive Liquid", Proceedings of the Third Midwestern Conference on Fluid Mechanics, Minneapolis, The University of Minnesota, 441-453.
- (41) Peterlin, A. and Copic, M., "Gradient Dependence of the Intrinsic Viscosity of Linear Macromolecules", Journal of Applied Physics, 27, No. 5, 434-438 (1956).
- (42) Prandtl, L., "Applied Hydro- and Aeromechanics", New York, McGraw-Hill Book Co., Inc., 1934.
- (43) Ree, T. and Eyring, H., "Theory of Non-Newtonian Flow. I and II.", Journal of Applied Physics, 26, No. 7, 793-808 (1955).

- (44) Richardson, E.G., "Dynamics of Real Fluids", London, Edward Arnold and Co., 1950.
- (45) Richardson, R.J., Sc.D. Thesis, Dept. of Chemical Engineering, M.I.T., 1954.
- (46) Rothfus, R.R., Monrad, C.C. and Senecal, V.E., "Velocity Distribution and Fluid Friction in Smooth Concentric Annuli", Industrial and Engineering Chemistry, 42, 2511 (1950).
- (47) Rothfus, R.R. and Prengle, R.S., "Laminar--Turbulent Transition in Smooth Tubes", Industrial and Engineering Chemistry, 44, 1683-1688 (1952).
- (48) Salt, D.L., Ryan, N.W. and Christiansen, E.B., "The Rheology of Carboxymethylcellulose Dispersions in Water", Journal of Colloid Science, 6, 146-154 (1951).
- (49) Schmidt, A.X. and Marlies, C.A., "Principles of High-Polymer Theory and Practice", Ch. 7, New York, McGraw-Hill Book Co., Inc., 1948.
- (50) Schnurmann, R., "Critical Reynolds Numbers of Solutions of Large Molecules", Proceedings of the International Congress on Rheology, Holland 1948, Section C, Amsterdam, North-Holland Publishing Co., II 142-151 (1949).
- (51) Senecal, V.E. and Rothfus, R.R., "Transition Flow of Fluids in Smooth Tubes", Chemical Engineering Progress, 49, No. 10, 533-538 (1953).
- (52) Shaver, R.G., "A Study of the Solubility Relations of Buna-S in Various Solvent and Non-Solvent Combinations", S.B. Thesis, Dept. of Chemical Engineering, M.I.T., 1952.
- (53) Staudinger, H., "Die Hochmolekularen Organischen Verbindungen", Berlin, Springer, 1932
- (54) Storey, B.T., "The Rheology of Starch Solutions", S.M. Thesis, Dept. of Chemical Engineering, M.I.T., 1955.
- (55) Theodorsen, T., "The Structure of Turbulence", 50 Jahre Grenzschichtforschung, H. Gortler and W. Tollmien, ed.
- (56) Toms, B.A., "Detection of a Wall Effect in Laminar Flow of Solutions of a Linear Polymer", Journal of Colloid Science, 4, 511-521 (1949).
- (57) Townsend, A.A., "The Structure of Turbulent Shear Flow", Cambridge, The University Press, 1956.
- (58) Warner, J.L., "Design, Construction and Testing of a Velocity Probe Traversing Mechanism", S.B. Thesis, Mechanical Engineering Dept., M.I.T., 1952.
- (59) Weltmann, R.N. and Kuhns, P.W., "An Automatic Viscosimeter for Non-Newtonian Materials", National Advisory Committee for Aeronautics, Technical Note 3510, August 1955.

- (60) Weltmann, R.N., "Friction Factors for Flow of Non-Newtonian Materials in Pipelines", Industrial and Engineering Chemistry, 48, No. 3, 386-387 (1957).
- (61) Winding, C.C., Baumann, G.P. and Kranich, W.L., "Flow Properties of Pseudoplastic Fluids -- Part I", Chemical Engineering Progress, 43, No. 10, 527-536 (1947).
- (62) Winding, C.C., Baumann, G.P. and Kranich, W.L., "Flow Properties of Pseudoplastic Fluids -- Part II", Chemical Engineering Progress, 43, No. 11, 613-622 (1947).